NUREG/CR-4561
LA-10678-M

FIRAC User's Manual: A Computer Code to Simulate Fire Accidents in Nuclear Facilities

Prepared by B. D. Nichols, W. S. Gregory

Los Alamos National Laboratory

Prepared for
U.S. Nuclear Regulatory
Commission

NUREG/CR-4561
LA-10678-M

FIRAC User's Manual: A Computer Code to Simulate Fire Accidents in Nuclear Facilities

Manuscript Completed: February 1986
Date Published: April 1986

Prepared by
B. D. Nichols, W. S. Gregory

Los Alamos National Laboratory
Los Alamos, NM 87545

Prepared for
Division of Fuel Cycle and Material Safety
Office of Nuclear Material Safety and Safeguards
U.S. Nuclear Regulatory Commission
Washington, D.C. 20555
NRC FIN A7152

CONTENTS

NOMENCLATURE

T_{in}	Duct inlet gas temperature
T_{out}	Duct outlet gas temperature
T_g	Average gas temperature in duct
T_N	Duct wall temperature on outside surface
T_i	Duct wall temperature on inside surface
T_j	Duct wall temperature at node j
T_o	Air temperature outside duct
Q_i	Net amount of energy transfer from the gas to the duct inside surface because of forced convection and radiation heat transfer
Q_{ci}	Net amount of energy transfer from the gas to the duct inside surface because of forced convection heat transfer
Q_{ri}	Net amount of energy transfer from the gas to the duct inside surface because of radiation heat transfer
Q_o	Net amount of energy transfer from the duct outside surface to the environment because of natural convection and radiation heat transfer
Q_{co}	Net amount of energy transfer from the duct outside surface to the environment because of natural convection heat transfer
Q_{ro}	Net amount of energy transfer from the duct outside surface to the environment because of radiation heat transfer
A	Neat transfer area of wall
D	Duct equivalent diameter (four times the cross-sectional area divided by the perimeter)
I_g	Radiation intensity factor evaluated at the average gas temperature
I_w	Radiation intensity factor evaluated at the inside wall temperature
Re	Reynolds number
Pr	Prandtl number
Gr	Grashof number
C_p	Gas specific heat at constant pressure
C_{pw}	Wall specific heat at constant pressure
$\dot{m}$	Duct mass flow rate
k	Gas or air thermal conductivity
k_w	Duct wall thermal conductivity
h	Heat transfer coefficient (natural or forced convection)

ρ	Duct wall density
t	Time
Δt	Time-step size
Δx	Thickness of each wall node
σ	Stephan-Boltzman constant
ϵ_i	Emissivity of duct inside surface
ϵ	Emissivity of duct outside surface evaluated at the outside duct wall temperature
α	Absorptivity of the duct outside surface evaluated at the outside air temperature

FIRAC USER'S MANUAL

A COMPUTER CODE TO SIMULATE FIRE ACCIDENTS IN NUCLEAR FACILITIES

by

B. D. Nichols and W. S. Gregory

ABSTRACT

This user's manual supports the fire accident analysis computer code FIRAC. FIRAC is designed to estimate radioactive and nonradioactive source terms and to predict fire-induced flows and thermal and material transport within the ventilation systems of nuclear fuel cycle facilities. FIRAC has been expanded and modified to include the capabilities of the zone-type compartment fire model computer code FIRIN developed by Battelle Pacific Northwest Laboratories. The two codes have been coupled to provide an improved simulation of a fire-induced transient within a facility. The basic material transport capability of FIRAC has been retained and includes estimates of entrainment, convection, deposition, and filtration of material. Also, the interrelated effects of filter plugging, heat transfer, gas dynamics, material transport, and fire and radioactive source terms are simulated.

This report summarizes the physical models that describe the gas dynamic, material transport, heat transfer, and source term processes and illustrates how a typical facility is modeled using the code. The modifications required to couple the code to FIRIN also are presented. Finally, the input and code-calculated output for several sample problems that illustrate some of the capabilities of the code are described.

I. INTRODUCTION

This user's manual supports an expanded and modified version of the computer code FIRAC. The expanded version is designed to predict the radioactive and nonradioactive source terms that lead to gas dynamic, material transport, and heat transfer transients in a nuclear facility when it is subjected to a fire. The code's capabilities are directed toward nuclear fuel cycle facilities and the primary release pathway—the ventilation system. However, the code is applicable to other facilities and can be used to model other airflow pathways within a structure.

This is one in a family of codes designed to provide improved safety analysis methods for the nuclear industry. Its predecessors include

- TVENT (a code to analyze tornado-induced gas dynamics[1]),
- TORAC (a code to analyze tornado-induced gas dynamics and material transport[2]), and
- EXPAC (a code to analyze explosion-induced gas dynamics and material transport[3]).

The FIRAC computer code now includes the capabilities of the zone-type compartment fire model FIRIN,[4] which was developed by Battelle Pacific Northwest Laboratories (PNL). The two codes have been coupled to allow an improved simulation of a fire-induced transient within a facility.

The physical models used in the code may be divided into four principal categories.

- Gas dynamics models
- Material transport models
- Heat transfer models
- FIRIN fire and radioactive source term models

These models are summarized in Sec. II, and a detailed description of the models (except for the FIRIN fire and radioactive source terms[4]) is presented in the appendixes. Setting up a computer model to simulate a given system's response to a fire transient is discussed in Sec. III. Modeling strategies and examples for several flow networks are given.

Translating the computer model to the actual deck that the code uses as input is discussed in Sec. IV. The data deck organization and input card specifications are presented, and the output from the computer code also is discussed. This includes both expected results and diagnostic messages that may be returned in case of program abort. Also, several system-dependent features of the code are discussed in Sec. IV. Information concerning installing the code on a computing system, computer storage requirements, file requirements, and system-dependent subprograms is presented.

An illustration of the modeling strategies for several flow networks is discussed in Sec. V. Also, the initial inputs needed to run the selected sample problems are discussed, and the data (input) deck required to run the sample problems is provided. Finally, typical selected output results are presented and discussed.

II. PHYSICAL MODELS

A. Gas Dynamics Models

A system is modeled using a flow network. The flow network consists of two distinct types of components: nodes and branches. A node can be either a boundary node, where the conditions (pressure and temperature) are known as a function of time, or a room node, where the laws of conservation of mass and energy are applied. Branches connect any two nodes, and branch models are provided to represent

- ducts,
- dampers or valves,
- filters, and
- blowers or fans.

The physical models representing these components are quite varied and are summarized below. The equations used and the numerical solution method for the resulting equations are detailed in Appendix A.

1. Ducts. Ducts are modeled using a momentum equation that includes the effects of inertia, friction, heat transfer, and gravity (buoyancy). In the case of high flow rates, the momentum equation is replaced by a choking condition. A distinguishing characteristic of the duct model is the nonlinear steady-state pressure drop relationship:

$$\Delta p = R \rho v^2 ,$$

where Δp is the pressure drop across the duct, ρ is the density, v is the gas velocity, and R is a constant resistance coefficient. The code will calculate the value of the resistance coefficient based on input values of pressure drop and flow. A user-specified resistance coefficient also may be used. The resistance coefficients are used to obtain both the steady-state and transient results.

Because a lumped-parameter formulation is used in this code (Appendix A), no spatial distribution of parameters along the length of the duct is calculated. However, the user may obtain more spatial detail by dividing the duct into a number of smaller sections. For example, a 100-ft-long (30.48 m) duct could be treated as 10 10-ft (3.05-m)-long ducts in series. This method is illustrated in one of the sample problems in Sec. V.

Heat transfer effects along the length of the duct will be calculated if requested by the user; otherwise, they are ignored. More details on the available heat transfer models are given in Sec. II.C and Appendix B.

2. Filters. Filters are modeled as elements that exhibit only resistance to flow (that is, no inertia, buoyancy, or heat transfer). The fundamental aspects of filter behavior are reviewed in Appendix C. In general, the pressure drop across a clean filter consists of a sum of linear and quadratic dependencies on the flow rate. The equation is of the form

$$\Delta p_0 = aQ + b\rho Q^2 \quad , \tag{1}$$

where Δp_0 is the filter pressure drop, Q is the volumetric flow rate, ρ is the gas density, and a and b are constants. In general, only the linear part of the curve (b = o) is applicable to fire situations. In this case, the code will calculate the value of the resistance coefficient, a, based on input values of pressures and flow rates. If necessary, the complete equation may be specified, which requires additional user input.

A filter plugging model is provided that modifies Eq. (1) when there is material accumulation on the filter. This model is derived in Appendix C. The net result is that a filter with material accumulated on it is modeled by a relation of the form

$$\frac{\Delta p}{\Delta p_o} = 1 + \alpha M_a ,$$

where Δp_o is the pressure drop for a clean filter (at the same flow rate), Δp is the pressure drop for the dirty filter, M_a is the material mass on the filter, and α is the filter plugging factor dependent on filter and material properties and has units of the reciprocal of mass. The resistance for dirty filters usually is estimated as 2 to 5 times that for clean filters.

3. Dampers and Valves. Dampers and valves are modeled as elements that exhibit only resistance to flow. The pressure drop across these elements is modeled as a quadratic dependence on the flow rate,

$$\Delta p = RQ^2 .$$

The resistance coefficient, R, may be calculated by the code or entered by the user (similar to the input for ducts).

4. Blowers and Fans. The model of a blower or fan is discussed in Appendix D. The model essentially depends on the performance curve of the blower obtained at standard conditions. The model then adjusts these data to predict the blower performance at off-design conditions. The blower head/flow characteristic curve is input as a number of points on the curve obtained from the manufacturers' data and measured at standard conditions [ρ = 0.075 lb/ft^3 (1.20 kg/m^3)]. The curve then is approximated by a number of straight-line segments as shown in Fig. 1. As discussed in Appendix D, all the segments should have a negative slope.

A fire event usually will not lead to blower performance in the outrunning (ΔP negative) or backflow (Q negative) regions. If this is the case, points on the curve in these regions need not be entered. However, estimates must be made if it is necessary to enter data in these regions because there is little manufacturer data for these regions. The Los Alamos National Laboratory has obtained blower data in the outrunning and backflow regions from which such estimates can be obtained. An example of these data is shown in Fig. 2. This information is preliminary, and more data are needed before the blowers can be modeled accurately in the abnormal flow regions. However, this information can be used as a

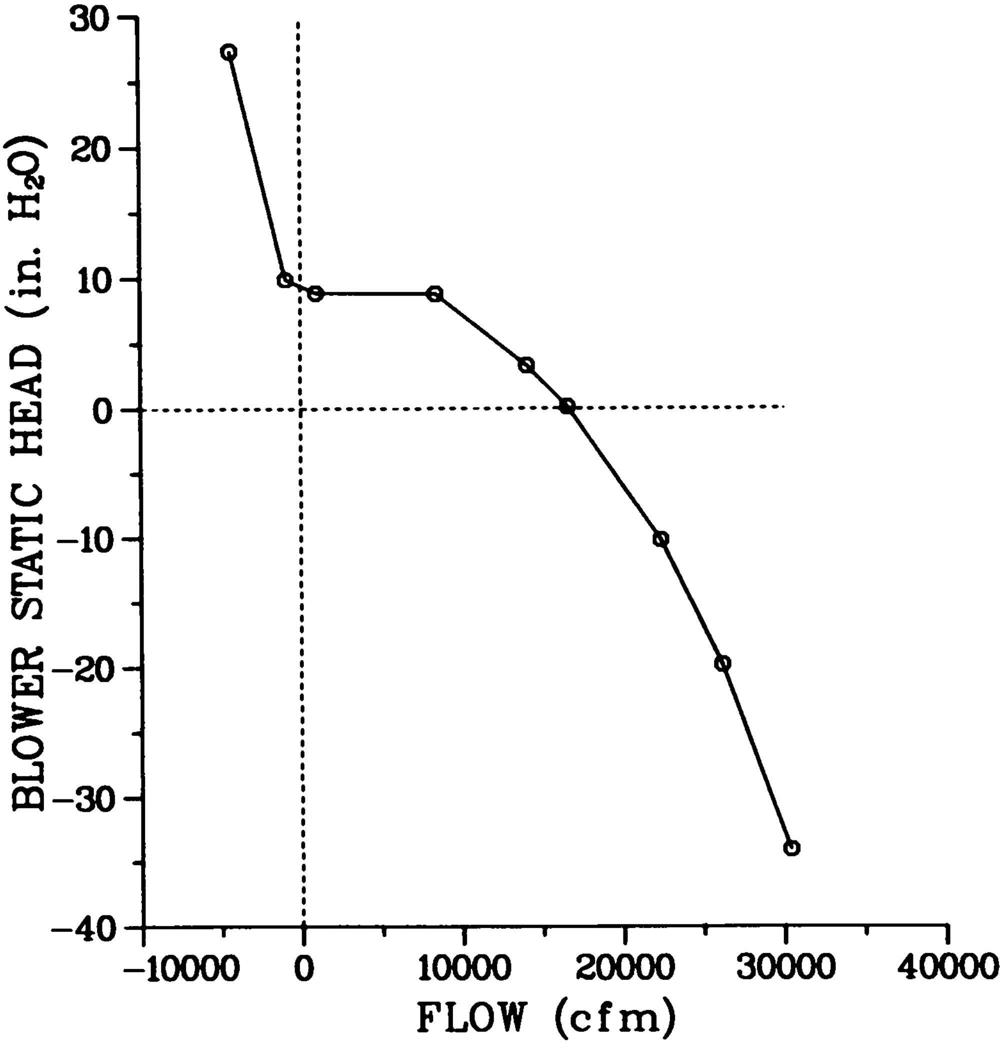

Fig. 1.
Computer model representation of a typical blower characteristic curve.

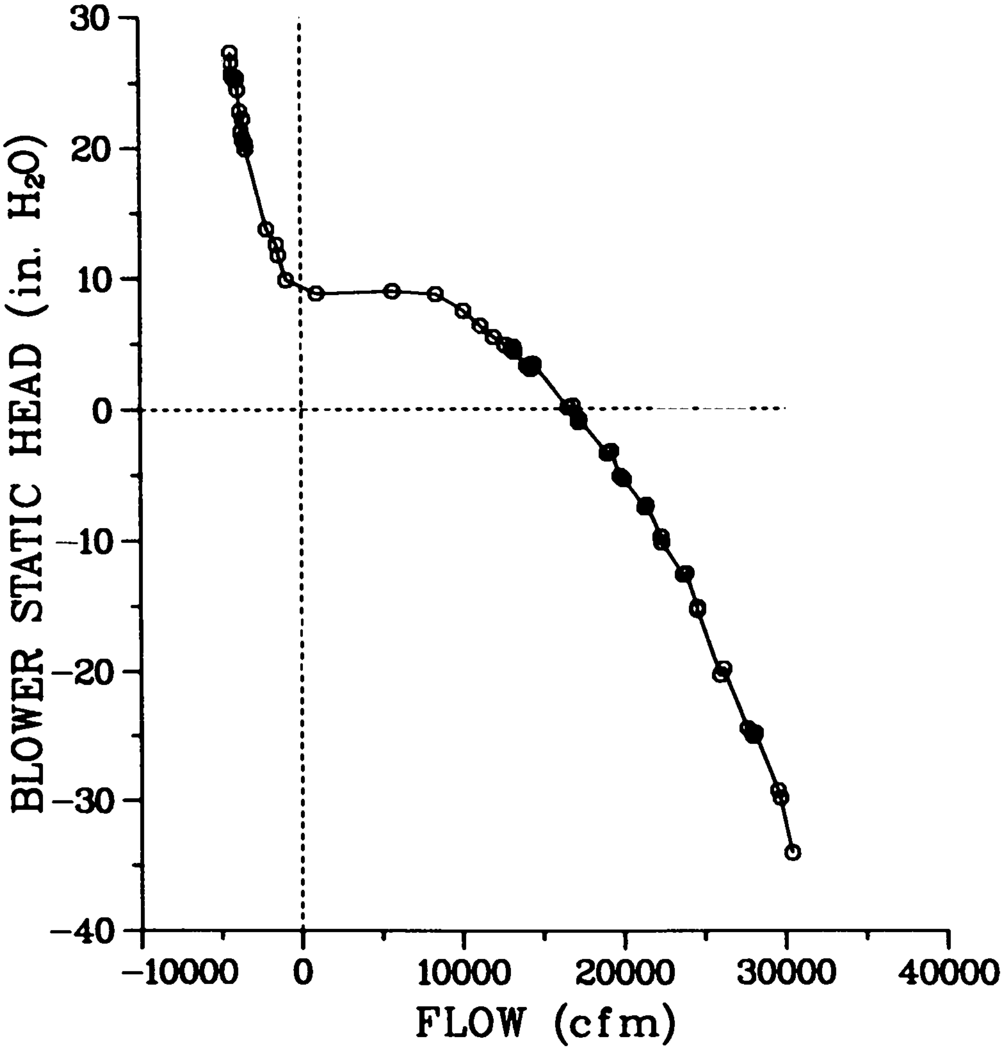

Fig. 2.
Quasi-steady-state characteristic curve
for a 24-in. (0.61-m) centrifugal blower.

guideline for estimating the blower performance in these regions. As an approximation, we use the same slope in the backflow quadrant as that to the right of the typical operating point in our blower model inputs.

5. Rooms, Cells, or Plenums. Components that have a finite volume (such as rooms, gloveboxes, plenums, and cells) are modeled using capacitance nodes or room nodes. The capacitance of the node is represented by its volume. Duct volume should be taken into account by including its volume in an adjacent room(s). (See Sample Problem 1 in Sec. V for an example of this concept.) Mass and energy storage at these nodes is taken into account by using the conservation of mass and energy equations. The conservation equations are applied to the room nodes using a lumped-parameter formulation assuming a homogeneous mixture and thermodynamic equilibrium. Therefore, spatial details within the nodes are not predicted.

An ideal gas (air) equation of state is assumed in the conservation equations. In the room nodes, the user may specify various combinations of pressure and temperature transient values along with various combinations of energy and mass sources. If the quantities are not specified, they are calculated by the code.

6. Boundary Nodes. Any node for which the pressure and temperature can be specified is considered a boundary node. An example is the supply and exhaust openings from a ventilation system to the atmosphere. The computer model of a system must have at least two boundary nodes. These nodes serve as boundary conditions for the remainder of the system. Both pressure and temperature must be specified for any boundary nodes contained in the computer model. The values of these quantities may be held constant for the transient, or they may be varied by a user-defined time function.

In addition to the standard boundary node described above, the coupled version of the code requires that the model of the system under study have at least two internal boundary nodes if FIRIN is used to simulate the fire-induced transient. The internal boundary nodes are necessary to represent the fire compartment within the network. An internal boundary node should not be confused with an internal node representing a room (volume). The internal boundary node is not treated as a capacitance node but is treated like a standard boundary node within the FIRAC computational formulation. The details and importance of the internal boundary node will be discussed and explained in Sec. II.D.

7. Leakage. Leakage paths from the system to the atmosphere may be approximated in the model by using a boundary node and a fictitious duct. The initial specified duct flow rate is the desired leak rate. During the course of a transient, the leak rate will vary, depending on the calculated system pressure response.

B. Material Transport Models

1. Introduction. The material transport portion of the code estimates the movement of material (aerosol or gas) in an interconnected network of ventilation system components representing a given fuel cycle facility. Using this capability, the code can calculate material concentrations and material mass flow rates at any location in the network. Furthermore, the code will perform these transport calculations for various gas dynamic transients. The code solves the entire network for transient flow and in so doing takes into account system interactions.

A generalized treatment of material transport under fire-induced accident conditions could become very complex. Several different types of materials could be transported, and more than one phase could be involved, including solids, liquids, and gases with phase transitions. Chemical reactions could occur during transport that lead to the formation of new species. Further, for each type of material there will be a size distribution that varies with time and position depending on the relative importance of effects such as homogeneous nucleation, coagulation (material interaction), diffusion (both by Brownian motion and by turbulence), and gravitational sedimentation. We know of no codes that can model transient-flow-induced material transport in a network system subject to the possibility of all of these complications. The transport portion of the code does not include this level of generality either. However, this version of the code does provide a simple material transport capability.

The material transport components of this code are

1. material characteristics,
2. transport initiation,
3. convective transport,
4. aerosol depletion, and
5. filtration.

Material characteristics and transport initiation are areas that must be considered by the user as he begins to set up the code to solve a given problem. Calculations of convective transport, aerosol depletion, and filtration are performed automatically by the code. Items 2--5 are actually separate subroutines or modules within the code. Item 3, convective transport, is a key subroutine that calls on items 2, 4, and 5 as needed during the course of the calculation. Each of the components listed above is subject to certain limitations and assumptions that will be brought out below or in Appendix C. We also will specify the required user inputs and provide appropriate references for the theory in each case.

2. Material Characteristics. The material transport models have some limitations with regard to the physical and chemical characteristics of the material. The pneumatically transportable contaminant material can consist of any number of aerosol or gaseous species. However, no phase transitions or chemical reactions are allowed. For example, condensation and gas-to-particle conversion are not permitted. If the contaminant is an aerosol (solid particles or liquid droplets suspended in air), a size distribution can be simulated. In this case, within each size range, the material will be treated as monodisperse (equal-sized), homogeneous (uniform density), spherical particles or droplets during a given code run. Both the size and density of each specie must be specified by the user. If the contaminant is a gas, then it is assumed to be inert. User guidance in the area of aerosol and gas characteristics is provided in Appendix C. Some suggestions are made for describing fuel-grade plutonium and uranium oxide powders.

3. Transport Initiation. To calculate material transport using the code, the analyst must determine or assume the location, distribution, and total quantity of contaminant material. This material can be located or generated in rooms, internal boundary nodes representing the fire compartment, cells, gloveboxes, corridors, or rectangular ductwork. (An assumption about material distribution is only necessary when the user wishes to exercise the calculated aerodynamic entrainment of dry powder from thick beds option discussed below.) A total quantity (mass of material) must be known or assumed.

There are three options for material transport initiation: user-specified, calculated aerodynamic entrainment, and FIRIN-calculated material generation. The user-specified option allows the analyst considerable flexibility but requires engineering judgment to specify input to the code. This option involves preparing a table or graph of material generation rate or mass injection rate (kilogram per second) vs time. The data are supplied to the code on the input deck TIME FUNCTION DEFINITION DATA CARDS.

For example, a given cell can have a given quantity of fuel-grade uranium or plutonium powder injected at a specified rate. The injected material also could be a gas. This user-specified option may be selected to calculate the consequences of a hypothetical aerosol or gaseous release and is recommended for the case of reentrainment from thin beds (dirty cells or ductwork). The code was developed assuming that off-design flows are the primary cause of source term initiation. Los Alamos is developing other codes specifically to assess the consequences of tornados and explosions. For accidents that do not disrupt the normal ventilation system flow significantly, such as pressurized release, spills, and equipment failures, a general purpose utility code may be used. Guidance for the user to estimate source terms may be found in Appendix C.

The user may wish to specify a material generation rate vs time. This procedure is exactly the same as that discussed above. That is, a table or graph of mass injection rate can be specified to simulate the injection of material associated with the event.

The calculated entrainment option specifically refers to a subroutine designed to calculate aerodynamic entrainment of dry powder from thick beds. This subroutine can be useful for analyzing material transport initiation. It uses a new semi-empirical analytical approach for calculating entrainment that takes advantage of detailed flow information produced by the gas dynamics module. To arrive at our estimate of mass of material entrained at each time step of calculation, this subroutine calculates when the surface particles will begin to move. To do this, particle, surface, and flow characteristics are taken into account. It also accounts for the aerodynamic, interparticle (cohesion), and surface to particle (adhesion) forces that may be acting. This procedure was used previously (Ref. 5) and is discussed more fully in Appendix C. The calculated entrainment option may be used whenever powder beds are known or assumed to be present. The code must be provided with particle size and density (Appendix C), total mass of contaminant, and the floor area of the (assumed duct) surface over which the powder is uniformly distributed.

The FIRIN module (subroutine) calculates various particulate and gaseous specie generation rates and concentrations for the fire compartment. If the user selects the FIRIN models to simulate the release of particulate material, up to 13 particulate and 3 gaseous species can be transported by the FIRAC material transport models. The first two particulate species (nspecie = 1 and nspecie = 2) are the total smoke and total radioactive particulates, respectively. The total radioactive particulate mass released as a result of the fire has been divided into 11 particle size distributions. These particle size distributions are generated within the FIRIN radioactive source term subroutines and are transported as the remaining 11 particulate species (nspecie = 3 through nspecie = 13). The particle size distributions are shown in Table I.

TABLE I

FIRIN-GENERATED SPECIES AND SPECIE IDENTIFICATION

Particulate	Specie Identification Number
Smoke particulate	nspecie* = 1
Total radioactive particulate	nspecie = 2
Radioactive particulate < 0.1 μm	nspecie = 3
Radioactive particulate between 0.1 and 0.3 μm	nspecie* = 4
Radioactive particulate between 0.3 and 0.5 μm	nspecie = 5
Radioactive particulate between 0.5 and 0.7 μm	nspecie = 6
Radioactive particulate between 0.7 and 0.9 μm	nspecie = 7
Radioactive particulate between 0.9 and 1.1 μm	nspecie = 8
Radioactive particulate between 1.1 and 2 μm	nspecie = 9
Radioactive particulate between 2 and 6 μm	nspecie = 10
Radioactive particulate between 6 and 10 μm	nspecie = 11
Radioactive particulate between 10 and 20 μm	nspecie = 12
Radioactive particulate > 20.0 μm	nspecie = 13

Gaseous Species	Specie Identification
Oxygen	ngspecie* = 1
Carbon dioxide	ngspecie = 2
Carbon monoxide	ngspecie = 3

*See input specifications for RUN CONTROL CARD II.

The sum of the material apportioned within particulate species 3 through 13 is equivalent to the total radioactive particulate material (mass) represented by nspecie = 2.

The user has two options to transport radioactive particulate generated by FIRIN. The user can transport all 11 radioactive particle sizes or only the total radioactive particulate (nspecie = 2). If the distribution of material is to be transported, the code will restrict the transport of the total particulate quantity automatically. The system would contain twice the amount of radioactive material actually available if nspecie = 2 through nspecie = 13 were transported. The transport of only the total radioactive particulate requires that the user set the number of particulate species (input parameter nspecies) equal to 2 and select a representative particle diameter and density. The transport of material does contribute to the total time (cost) for a fire-induced flow simulation. (See Sec. IV.J.) In some cases it may be possible for the user to reduce the number of species (using the option described above) and thus reduce the running time (cost) for a calculation without losing detail.

4. Convective Transport. The code includes a simple material transport model with the capability of predicting airborne material distribution in a flow network and its release to the environment. Accidental release to the environment from a fire is a major concern in nuclear facilities because the airborne material could be radioactive or chemically toxic. The model is based on the assumptions that the particle size is small and its mass fraction is small relative to the gas mass in the same volume. This allows us to assume that the material and the gas form a homogeneous mixture and that they are in dynamic equilibrium. In this case, the gas dynamic aspect of the problem is not affected by the presence of the airborne material, and the particulate or material velocity is the same as the gas velocity at any location and time. Accordingly, the only relation needed to describe the motion of the material is the continuity equation. This modeling and the underlying assumptions are presented in more detail in Appendix C.

5. Material Depletion. Once the user has chosen to exercise material transport, he can calculate aerosol losses caused by gravitational sedimentation in horizontal, rectangular, or round ducts. Aerosol depletion may be calculated throughout the network during transient flow. The theory is based on quasi-steady-state settling with the terminal settling velocity corrected by the Cunningham slip factor. The flow in ducts and rooms is assumed to be well-mixed so that the aerosol concentration is uniform within the volume. The user must supply the aerosol diameter, density, and duct height to this model. The aerosol may consist of solid particles or liquid droplets. (More detail and references may be found in Appendix C.)

6. Filter Loading. A phenomenological approach to filter loading is presented. The filter gas dynamic performance can be changed by the accumulation of airborne material on the filter, which in turn causes an increase in resistance. A linear model is used in which the increase in resistance is linearly proportional to the amount of material on the filter. The proportionality constant is a function of the fuel source and filter properties. The user supplies the filter efficiency and plugging factor. Some information on the filter plugging factor is given in Appendix C.

C. Duct Heat Transfer Model

The purpose of the duct heat transfer model is to predict how the combustion gas in the system heats up or cools down as it flows throughout the ducts in the ventilating system. The model predicts the exit gas temperature for any section of the duct if the inlet temperature and gas properties are known. An ancillary result of the calculation is the duct wall temperature. A heat transfer calculation is performed for a duct component. Furthermore, the calculation is performed in a given duct only if that branch has been flagged in the input deck. Experience in using the code has shown that duct heat transfer calculations can increase the computer running time by a factor of 2. Therefore, we advise that duct heat transfer calculations be performed only where needed. Generally, the main region of interest and concern is those ducts downstream from the fire compartment and especially between the fire compartment and any filters downstream from it.

The overall model is composed of five distinct sub-models of heat transfer processes along with a numerical solution procedure to evaluate them. The following heat transfer processes are modeled.

- Forced-convection heat transfer between the combustion gas and the inside duct walls
- Radiation heat transfer between the combustion gas and the inside duct walls
- Heat conduction through the duct wall
- Natural convection heat transfer from the outside duct walls to the surroundings
- Radiation heat transfer from the outside duct walls to the atmosphere

Details concerning the physical assumptions and simplifications as well as the heat transfer correlations and their ranges of applicability are given in Appendix B. There it is shown that the total amount of energy removed from the gas as it flows through the duct is the solution of a set of four nonlinear algebraic equations. The solution procedure used to solve these equations also is presented in Appendix B.

The user inputs required to execute the duct heat transfer model include the following duct properties.

- Equivalent diameter and heat transfer area
- Outside wall emissivity and absorptivity
- Wall density, thermal conductivity, specific heat, and thickness

A typical application of the duct heat transfer model is shown in one of the sample problems presented in Sec. V. The actual code inputs are shown, and typical output results are discussed for a full-scale (but simple) system.

D. FIRIN Fire and Radioactive Source Term Simulation

1. Summary. Fire-generated radioactive and nonradioactive source terms are estimated in the FIRIN module of the FIRAC code. The FIRIN code, which was developed by PNL under the sponsorship of the Division of Risk Analysis of the US Nuclear Regulatory Commission, uses a zone-type compartment fire model. A zone-type fire compartment assumes that the gas in the room is divided into two homogeneous regions, or layers, during a fire. One layer (the hot layer) develops near the ceiling and contains the hot combustion products released from the burning material. The cold layer, which is between the hot layer and the floor, contains fresh air. FIRIN predicts the fire source mass loss rate, energy generation rate, and fire room conditions (temperatures of the two layers and room pressure) as a function of time. It also calculates the mass

generation rate and particle size distributions for radioactive and nonradioactive particles that can become airborne for a given fire accident scenario. The radioactive release factors incorporated within the FIRIN module are primarily those developed in experimental work at PNL, and the combustion product data were developed from a literature search of combustibles that commonly are found in nuclear facilities.[4] More information on the fire and radioactive source term models and FIRIN code assumptions is available in Ref. 4.

2. FIRAC/FIRIN Integration.

a. Introduction. The coupling scheme chosen for integrating FIRAC and FIRIN uses internal boundary nodes to represent the fire compartment within the network. Internal boundary nodes are boundary nodes that are located within the network. Typically, boundary nodes are used to define the conditions at the inlet and outlet of the network. The use of internal boundary nodes within a system required that FIRAC and FIRIN be modified to produce an interactive code version.

An interactive version of the code was obtained by requiring that FIRIN calculate the fire compartment thermodynamic conditions (pressure and temperature for each layer) and the particulate and gaseous releases (in the form of concentrations) at each time step. This FIRIN-supplied information is transferred to FIRAC through the internal boundary node scheme. The internal boundary nodes that represent the fire compartment are assigned the FIRIN-calculated pressures, temperatures, particulate, and gaseous species concentrations at each time step. Within the computational formulation of FIRAC, the internal boundary nodes are treated as standard boundary nodes; that is, the internal boundary nodes can have pressures and temperatures specified as a function of time. Because boundary nodes are zero-capacitance nodes, several modifications to the material transport subroutines were made to permit material concentrations to be assigned at the internal boundary nodes. When the FIRIN-calculated fire compartment conditions for that time step have been transferred to FIRAC (as boundary node conditions), the network response (system flows, material transport, and heat transfer) can be determined by FIRAC. The FIRAC-calculated total inlet and outlet volumetric flow rates for the fire compartment (based on the current fire compartment conditions) are transferred to FIRIN to complete one computational cycle. A schematic of the coupling scheme is presented in Fig. 3.

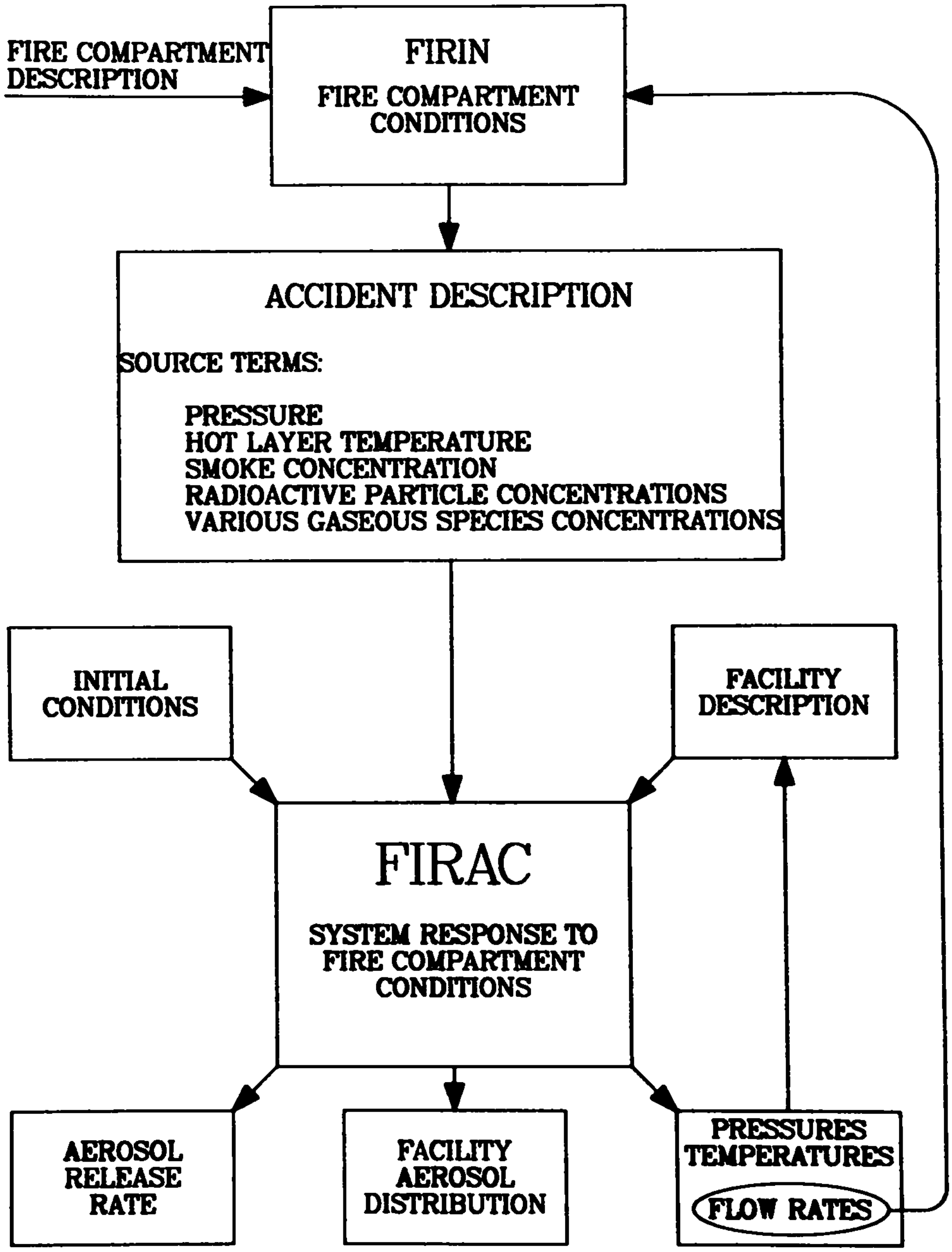

Fig. 3.
Schematic of FIRAC/FIRIN coupling.

At least two internal boundary nodes are required to represent the fire compartment because the FIRIN zone-type model requires an inflow and outflow condition for the compartment. Three internal boundary nodes can be used to extend the fire compartment model. The additional internal boundary node is not required but could be used to simulate a potential leak path or an additional compartment flow condition. For example, if there were several inflow/outflow conditions that needed to be modeled, it could be beneficial to use the third internal boundary node instead of lumping the flow conditions into a major inflow/outflow condition. (See Sec. III.C.)

b. FIRAC Input Changes. The input specifications for FIRAC requires several values in addition to the necessary FIRIN input data. These additional input values assist in the transfer of information between the FIRIN module and the FIRAC subroutines. The FIRIN input and the new input variables that assist in the coupling of the two codes are incorporated within the input specifications section of the manual. (See Sec. IV.C.)

c. Internal Boundary Node Pressures and Temperatures. The FIRIN two-layer fire compartment model calculates a pressure, a cold-layer temperature, and a hot-layer temperature for the compartment. The two internal boundary nodes are assigned the FIRIN-calculated compartment pressure at each time step. Based on the user-specified duct elevation and diameter of the inlet or outlet of the fire compartment and the position of the hot layer, the internal boundary nodes are assigned a value of the FIRIN-calculated cold layer, hot layer, or an averaged temperature value. If the hot layer is positioned above the duct centerline elevation plus one-half the duct diameter, the internal boundary node representing the fire compartment inlet or outlet would be assigned a temperature value equal to the FIRIN cold-layer temperature. Similarly, if the hot layer is positioned below the duct centerline elevation minus one-half the duct diameter, the internal boundary node is assigned the value of the FIRIN hot-layer temperature. When the hot layer is positioned within the region of the flow boundary, the internal boundary node is assigned a temperature value that is a function of the hot- and cold-layer temperatures and the position of the hot layer with respect to the flow boundary centerline elevation. The user must enter the duct elevations and diameters for the internal boundary nodes in the fire compartment initial conditions and noding data cards.

d. Internal Boundary Node Material Transport. The improved FIRAC code version is capable of transporting 13 particulate species and 3 gaseous species generated by FIRIN. Eleven of the thirteen particulate species are radioactive particles ranging in size from less than 0.1 μm in diameter to greater than 20 μm in diameter. The remaining particulate species are the total smoke and radioactive particulate generated by the fire. The three gaseous species that can be transported are the hot-layer combustion products (oxygen, carbon dioxide, and carbon monoxide). The values of the smoke, radioactive particles, oxygen, carbon dioxide, and carbon monoxide concentrations calculated by the FIRIN subroutine are transferred to FIRAC at each time step. Based on the user-specified physical properties of the species, the FIRAC material transport models (convection, deposition, entrainment, and so on) are used to determine the time-dependent transport characteristics and concentration of the particulate and gaseous species throughout the system.

III. SYSTEM MODELING STRATEGIES FOR FIRE-INDUCED TRANSIENTS

A. General

FIRAC is designed to predict airflows in an arbitrarily connected network system. In a nuclear facility, this network system could include process cells, canyons, laboratories, offices, corridors, and offgas systems. In addition, an integral part of this network is the ventilation system. The ventilation system is used to move air into, through, and out of the facility. Therefore, the code must be capable of predicting flow through a network system that also includes ventilation system components such as filters, dampers, ducts, and blowers. These ventilation system components are connected to the rooms and corridors of the facility to form a complete network for moving air through the structure and perhaps maintaining pressure levels in certain areas.

B. Fire Accident System Modeling

1. Model Set Up. The first and most critical step is setting up a model of the air pathways in a nuclear facility, which requires a schematic showing the system components and their interconnections. Drawings, specifications, material lists, safety analysis reports, and existing schematics are sources that can be used in deriving a system description. A physical inspection of the facility and consultations with the designer(s) before and after the schematic is drawn may be necessary to verify that it is correct. Frequently, there is a lack of needed data at this step. Although there is no substitute

for accurate data, certain assumptions, averaging, or conservative estimates can be used to make the problem manageable. Figures 4 and 5 show how a simple ventilation system within a facility structure can be transformed into a network schematic. We will illustrate the system modeling concepts in the next section and then provide additional detail for the flow and material transport modeling.

2. System Definitions. Three terms are used to describe the construction of a model and are used extensively in the remainder of this report.

- System - A network of components (branches) joined together at points called nodes.
- Branch - A connecting member between upstream and downstream nodal points. A branch contains one component such as a duct, valve, damper, filter, or blower. Gas flow, pressure differential, and material flow are associated with branches.
- Node - A connection point or junction for one or more branches. Volume elements such as rooms, gloveboxes, and plenums are defined as capacitance nodes. Even a long duct or slow pathway is divided into a series of volume nodes. Compressibility of the system fluid is taken into account at these capacitance nodes. Boundary points also are defined at nodes; gas pressure, density, temperature, material concentration, and mass fraction are specified at nodes. The improved FIRAC code version has a third type of junction or point, the internal boundary node. As mentioned earlier (Sec. II.D.2), internal boundary nodes are required to represent the fire if the FIRIN fire compartment effects subroutine (module) is selected.

3. Fire Compartment Modeling Options. The organization of the ventilation system components that will form the complete network will depend on the user-specified fire simulation option. Two options are available in FIRAC to simulate a fire within a ventilation system. One is to use the FIRIN fire compartment model that has been integrated within FIRAC. The second is to apply the user-specified time function capability. This option enables the user to simulate a fire in a capacitance node by inputting an energy release rate (to simulate heat addition to the room) and particulate and gaseous species generation rates (to simulate combustion particles and gases and radioactive particle releases) for that volume.

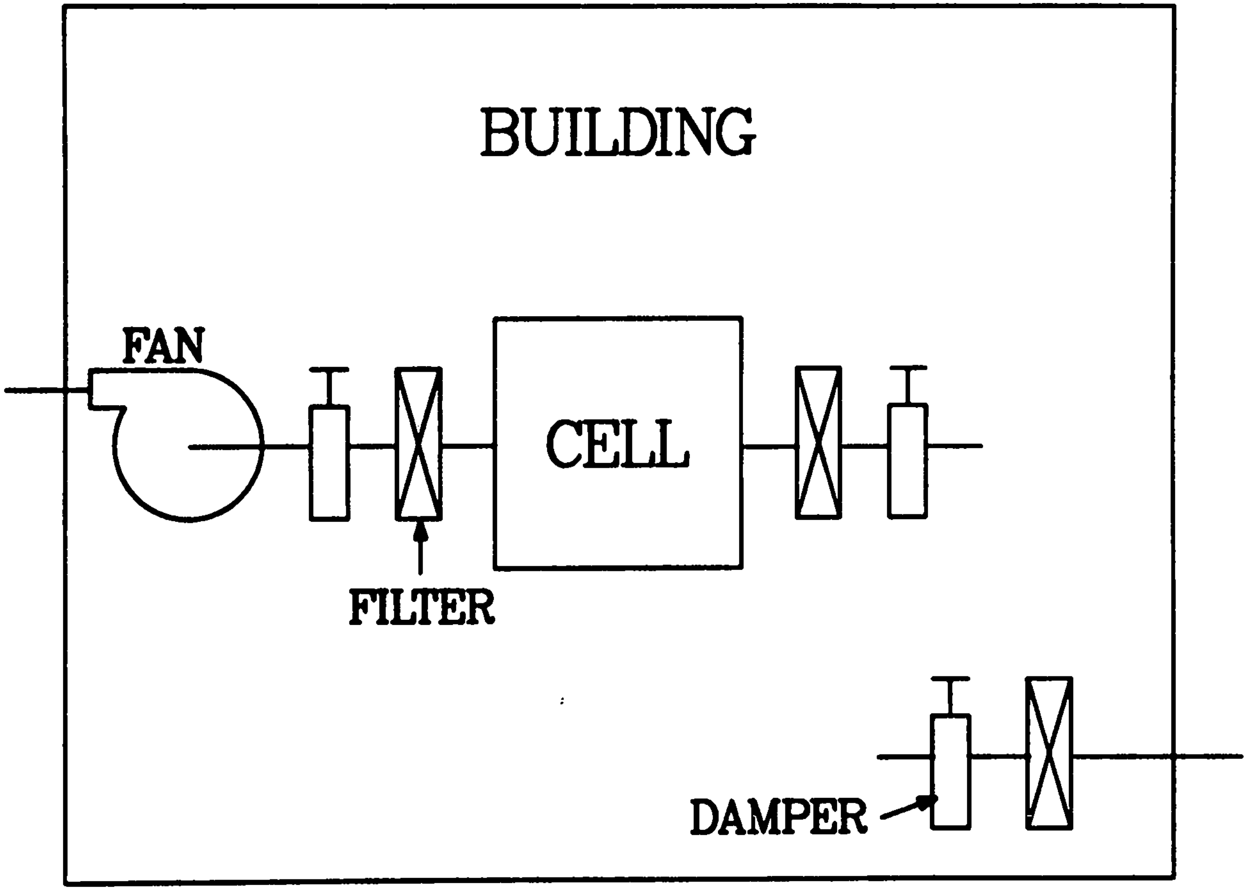

Fig. 4.
Example of a simple facility with a ventilation system.

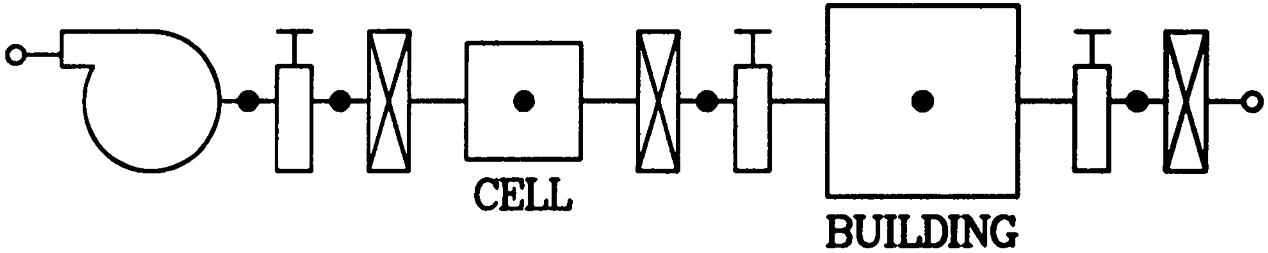

Fig. 5.
Network schematic of a simple facility with a ventilation system.

If the user selects the FIRIN fire compartment module, internal boundary nodes must be used to represent the fire compartment (room). The remainder of the system can be modeled with the more conventional components (branches and capacitance and boundary nodes). If the user-specified time function option is selected, the system model requires the use of conventional components only. Internal boundary nodes should be used only if the user plans to enable the FIRIN module.

Typically, the user would select one of the two possible options to simulate a fire. However, both options could be used simultaneously to simulate several fires in a facility. The FIRIN module can be used to simulate a fire in only one location of the facility network; however, the user-specified time function option could be used to represent additional fires in other capacitance nodes.

C. System Modeling Examples

Network systems for airflow through a nuclear facility may be constructed using a building block approach. The building blocks that are used to construct fire network analysis systems are shown in Fig. 6 and can be arranged as shown in Figs. 7(a) and 7(b) to form arbitrary systems. These building block symbols will be used throughout this report. An example showing how the building block schematic corresponds to a simple network system for the user-specified time function fire simulation option is presented in Fig. 8(a). Nodes 1 and 11 in Fig. 8(a) are boundary nodes. A capacitance node (node 4) represents the sampling room where the fire is postulated to occur. Branches are shown in Fig. 8(a) at the tips of arrows. The branch numbers are enclosed in parentheses adjacent to their corresponding branches. Note that branch 3 is connected on the upstream side by node 3 and on the downstream side by node 4.

Figure 8(b) illustrates how the example shown in Fig. 8(a) would be modified to accomodate the FIRIN option for a postulated fire in node 4. The nodes representing the intake and exhaust conditions (nodes 1 and 12) are boundary nodes. The sampling room and postulated fire location that was represented by a capacitance node (node 4) in Fig. 8(a) is replaced with two internal boundary

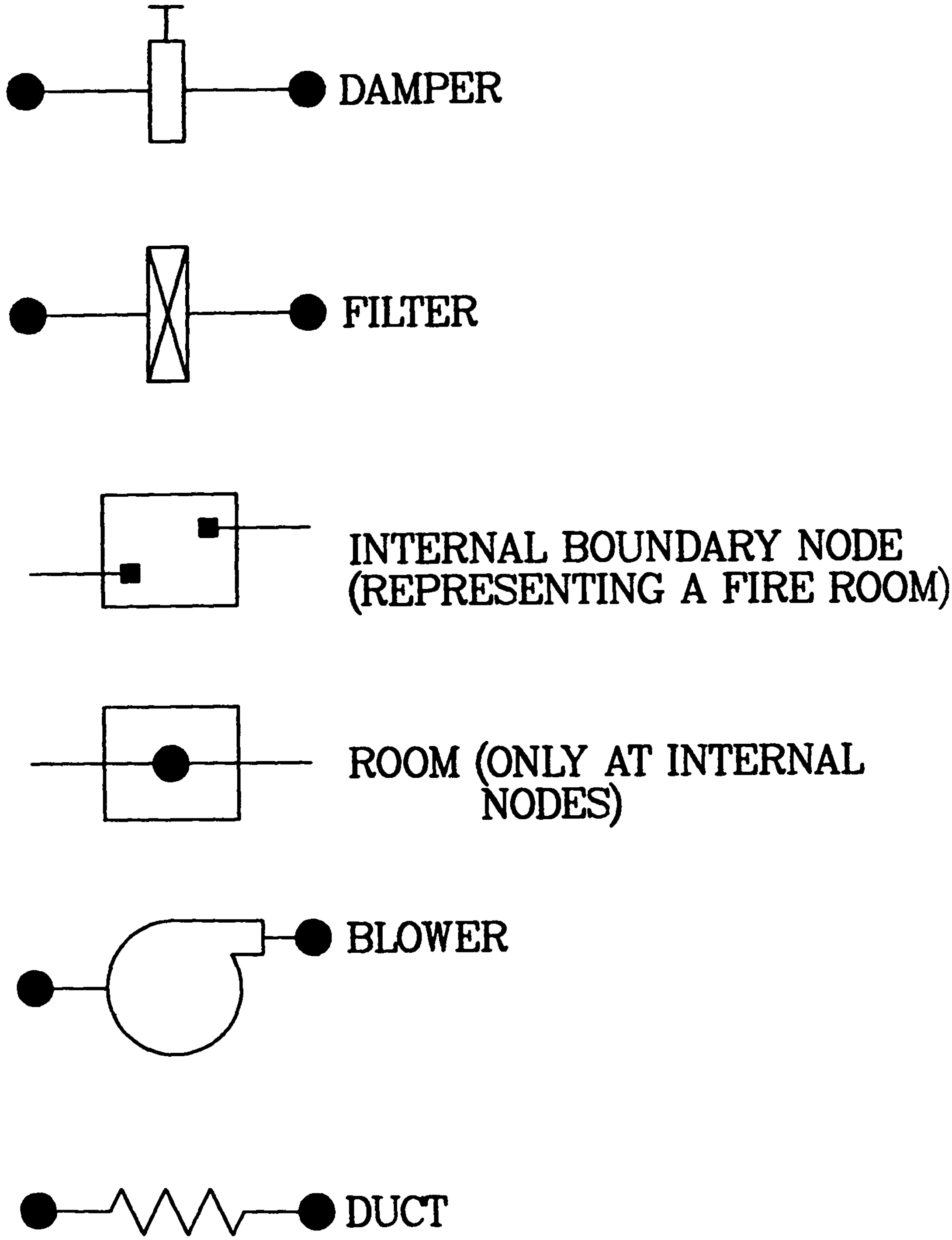

Fig. 6.
Fire network analysis building blocks.

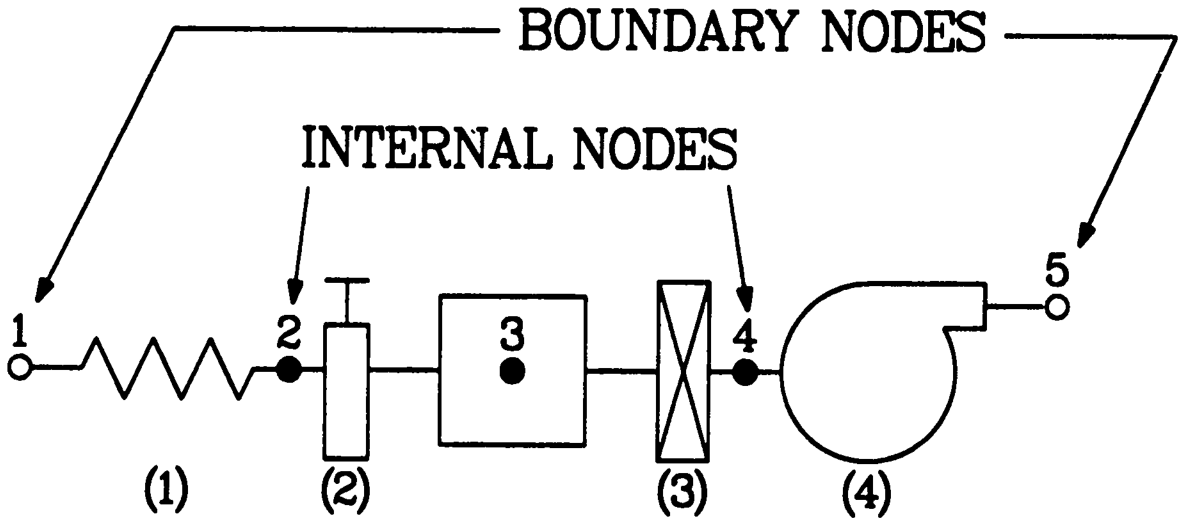

Fig. 7(a).
Arbitrary system using capacitance nodes.

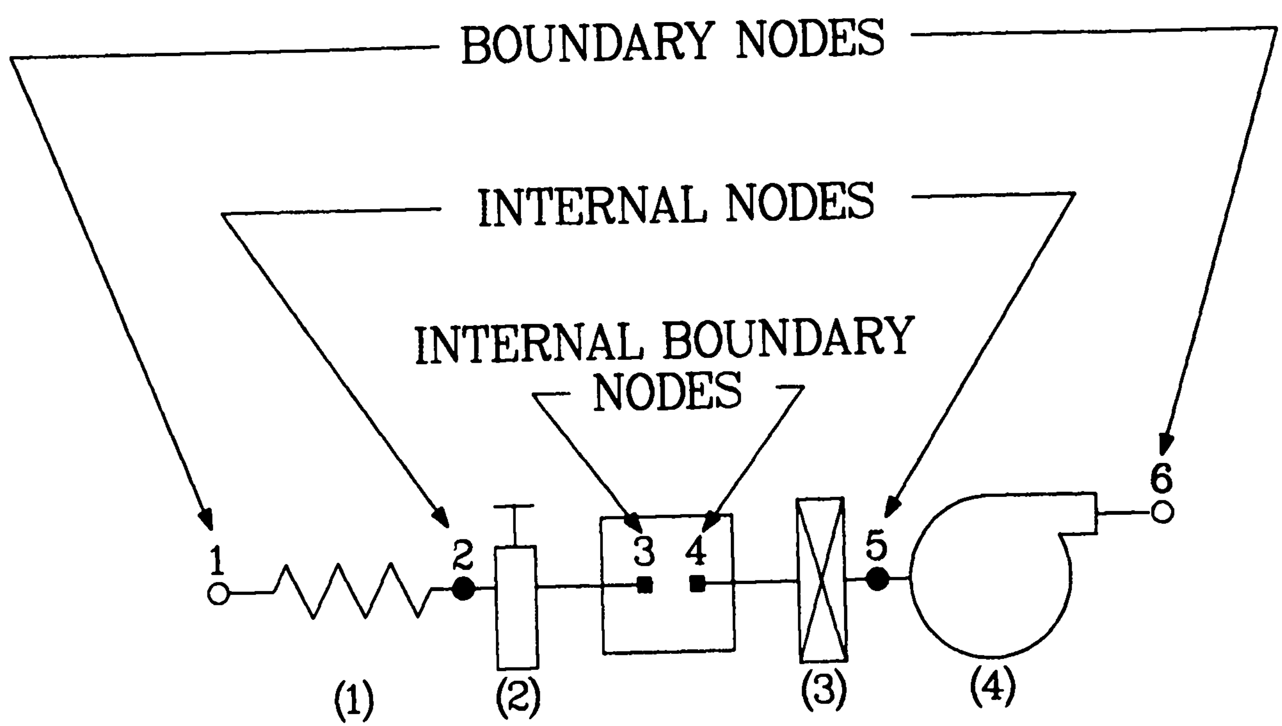

Fig. 7(b).
Arbitrary system using capacitance and internal boundary nodes.

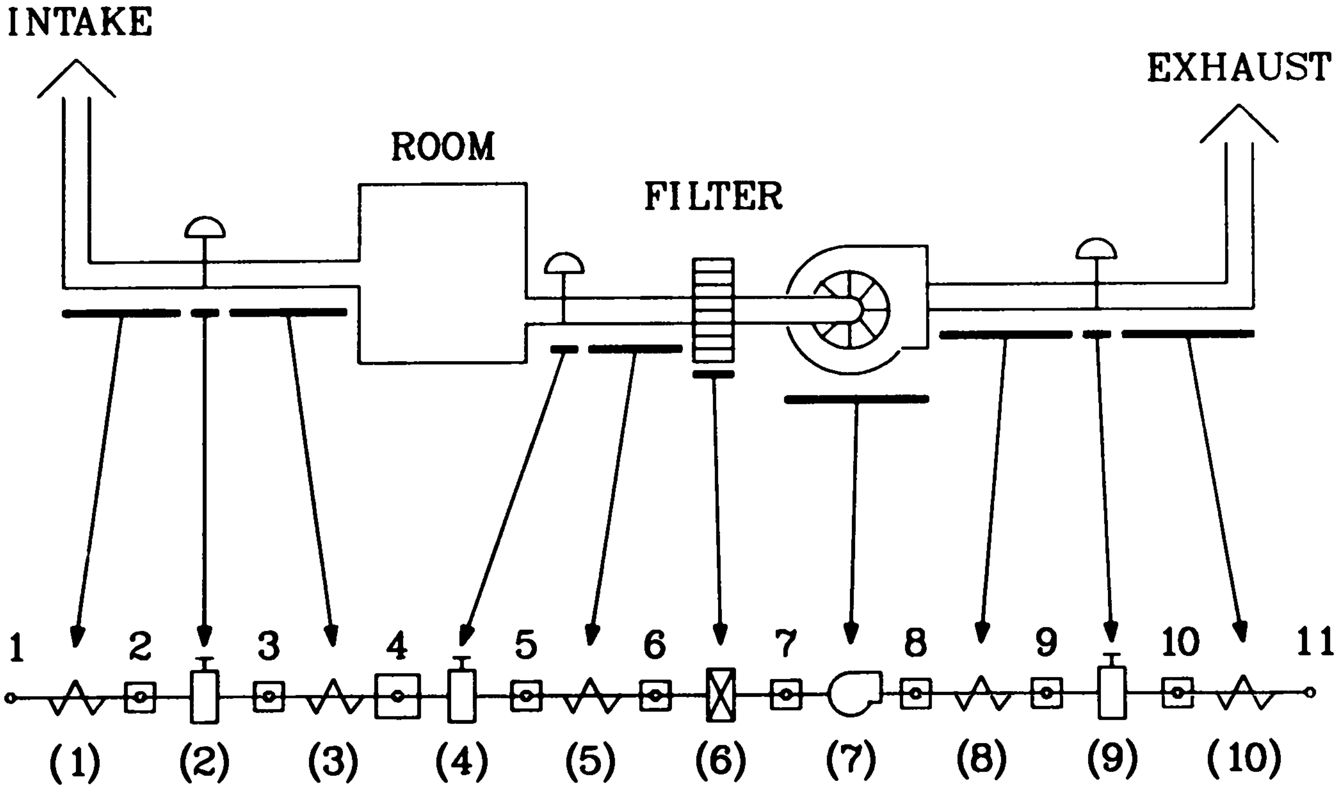

Fig. 8(a).
Building block correspondence with standard noding.

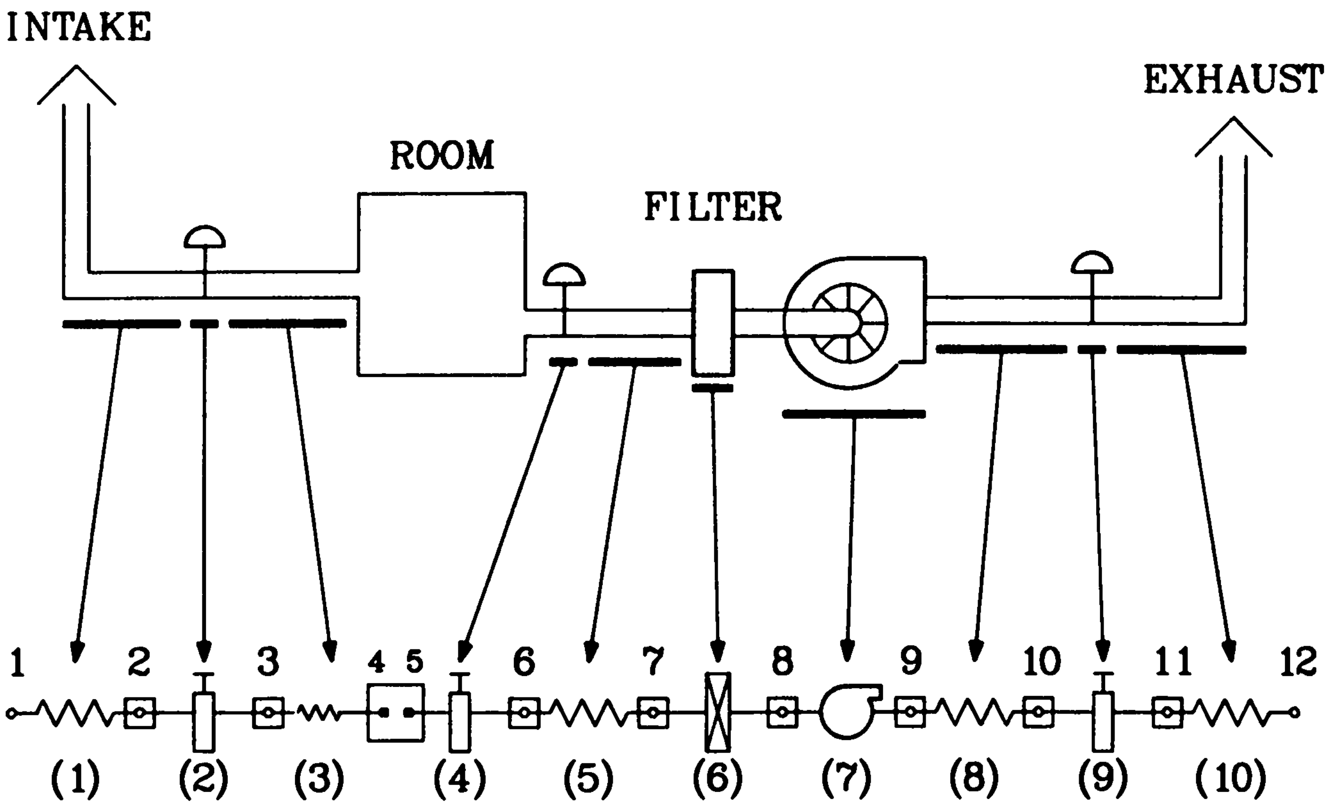

Fig. 8(b).
Building block correspondence with internal boundary noding.

nodes (nodes 4 and 5) as shown in Fig. 8(b). Two internal boundary nodes are required to model the room's intake and exhaust. In the input deck, the user will specify the fire room intake and exhaust branch identification parameters, duct elevations and diameters, the two internal boundary node identification parameters, and other information that will enable the FIRIN compartment model and the FIRAC systems code to be interactive.

We have illustrated extremely simple network systems. A slightly more complex system is shown in Fig. 9, and the corresponding schematics are shown in Figs. 10(a) and 10(b). The conventionally modeled system shown in Fig. 10(a) illustrates a room (node 2) with three connected branches (1, 2, and 3), and a leakage path around the cell (node 3) access hatch also is modeled using branch 5 and node 5. If a fire were postulated to occur in the cell, the user could specify the necessary time function data for node 3 (energy release rate, particulate and gaseous species release rates, and so on) to simulate the fire accident. If the user selected the FIRIN model option, the flow network computer schematic shown in Fig. 10(b) presents an example of one possible noding arrangement for this option. The cell can be represented by three internal boundary nodes. Internal boundary nodes 3 and 4 model the intake and exhaust to the cell, and internal boundary node 5 models the potential leak path (access hatch). FIRAC can model three main connections (requiring three internal boundary nodes) to a FIRIN fire compartment (Sec. II.D.2). If more than three inflow/outflow conditions are specified for the room that will represent the fire compartment, several approximations may be required. The selection of the inflow/outflow approximations is an important consideration because the flow conditions influence the mass and energy balance in the fire compartment. For example, if the fire compartment had the inflow/outflow conditions as shown in Fig. 11(a), two feasible modeling options are possible [Figs. 11(b) and 11(c)]. The first option would be to combine the inflow conditions of intakes 2 and 3 because these intakes represent a fraction of the total inflow condition and are located at the same room elevation. Another possibility would be to combine all three intakes [Fig. 11(c)]. This arrangement would require an average inflow room elevation and duct diameter (required fire compartment input parameters) based on the three intakes.

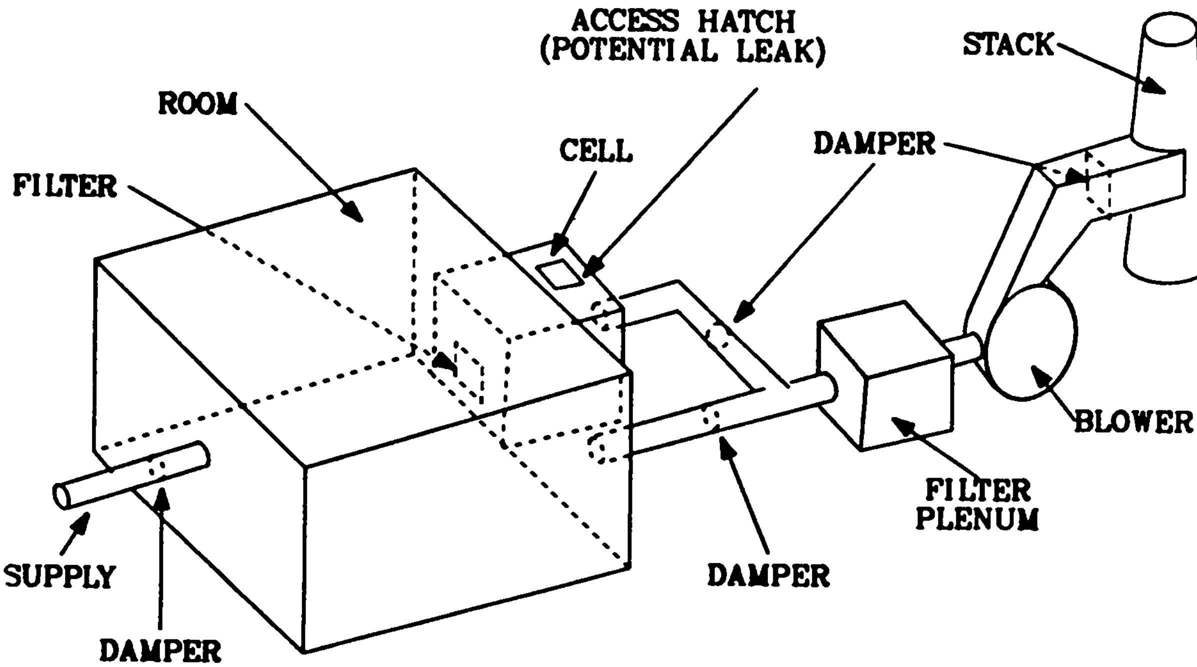

Fig. 9.
Simple flow network with leak path.

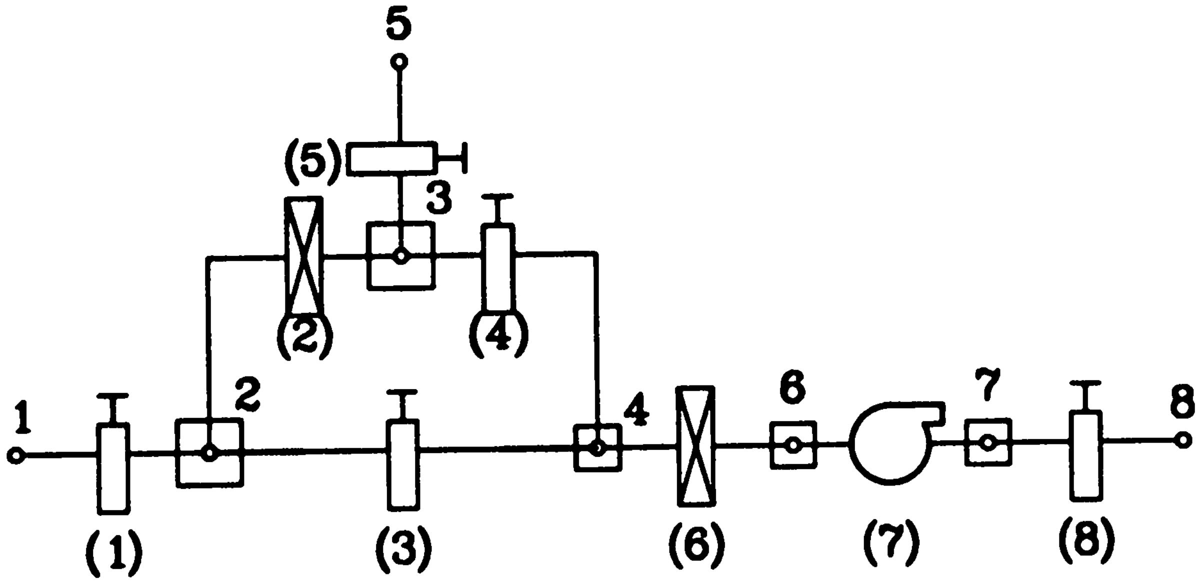

Fig. 10(a).
FIRAC model of the simple flow network
with leak path using standard noding.

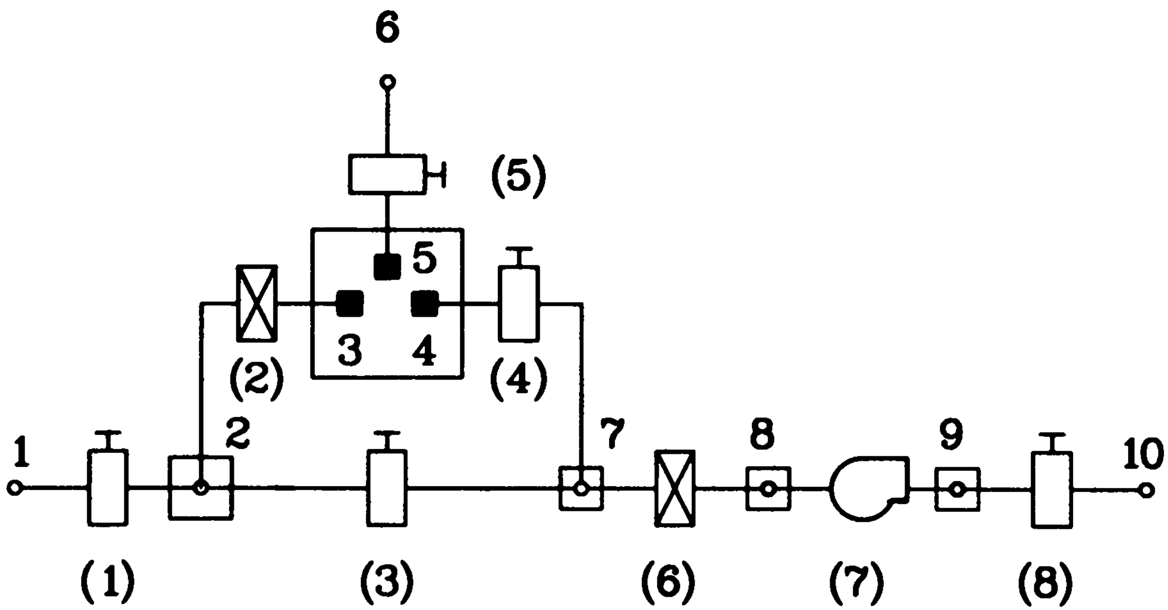

Fig. 10(b).
FIRAC model of the single flow network with
leak path using internal boundary noding.

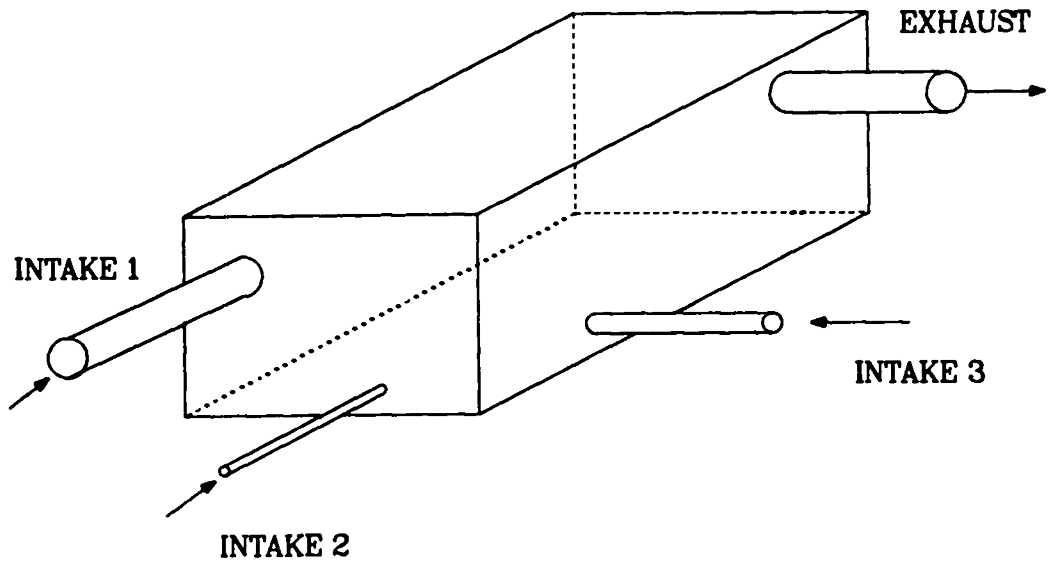

Fig. 11(a).
Fire compartment example with several inflow ventilators.

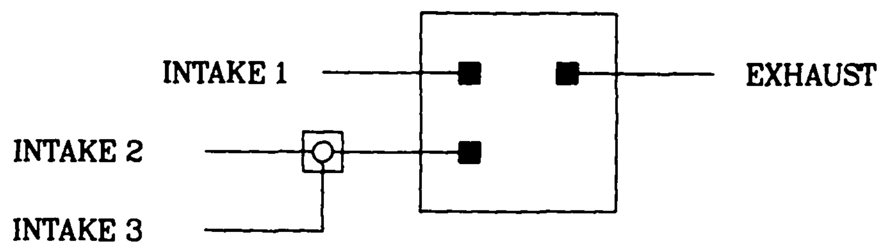

Fig. 11(b).
Fire compartment representation with three internal boundary nodes.

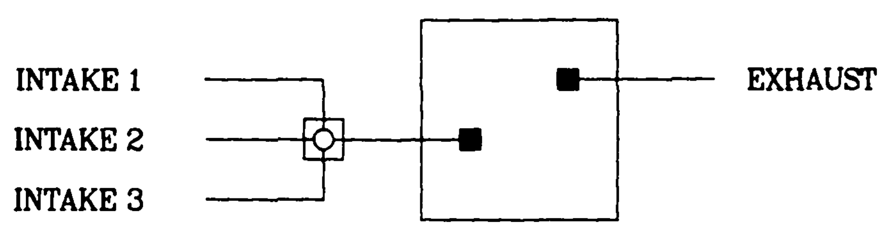

Fig. 11(c).
Fire compartment representation with two internal boundary nodes.

This configuration would not be as accurate because of the engineering approximations for the inflow elevation and duct diameter. In some cases the user may be confronted with using approximations and may need to perform a sensitivity study to determine the importance of the approximations selected.

IV. USER INFORMATION AND PROGRAMMING DETAILS

A. Input Organization

The improved FIRAC input deck is divided into 10 sections: problem control, branch geometry, specie description, boundary node, time function, capacitance node, component, initial conditions, FIRIN module, and time-step. These blocks of data are read in the order shown in Fig. 12 and compose the FIRAC input file FIN. The problem control data cards contain general problem control information including title cards for problem identification, output and plotting package control, steady-state or transient run options, iteration convergence criteria, and geometry, component, FIRIN simulation option and time function control options. The branch geometry data blocks specify the branch general geometric characteristics (branch identifier, adjacent nodes, length, flow area, and so on) and branch heat transfer characteristics if the heat transfer option is enabled.

The boundary node data block section contains initial values for the boundary node, pressure, and/or temperature time function identifiers and the boundary node type. Internal boundary nodes are required if the FIRIN simulation option is selected. (See Secs. II and III.)

If particulate and gaseous species are present and indicated in the problem control data block, the data for the species selected will follow the branch geometry input. For particulate species, the user must specify the particle identifier, diameter, and density and can input initial mass fractions and initial wall mass if desired. For the gaseous species, the user must specify the gaseous species identifier and can select initial volume fractions. The selection of particulate and gaseous specie identifiers is restricted by internal modifications made to FIRAC to accomodate FIRIN. These restrictions are discussed in Sec. II B.3 and only apply if FIRIN is selected to simulate the transient.

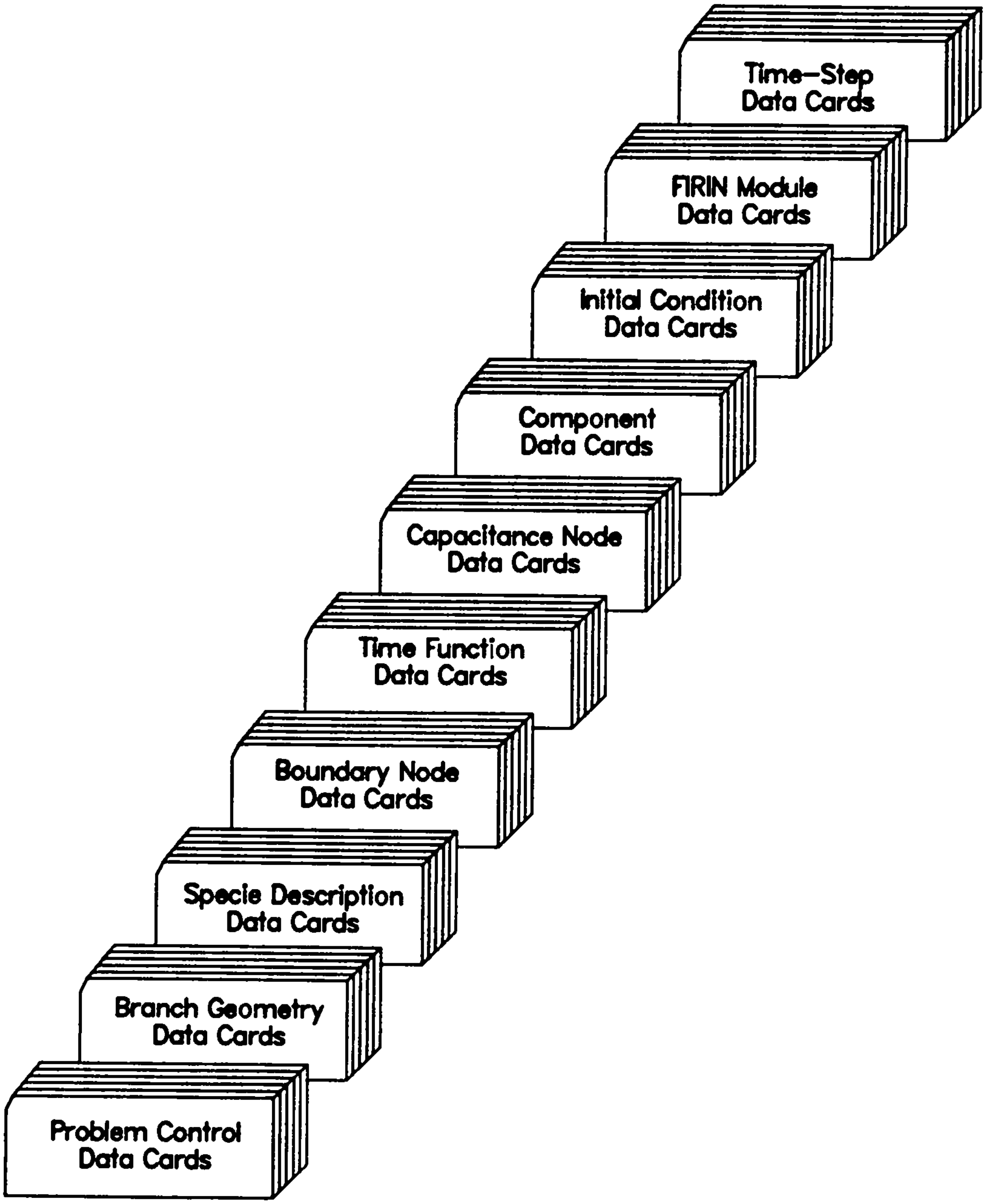

Fig. 12.
Improved FIRAC input deck organization.

The time function data contain time-dependent data for boundary nodes and capacitance nodes. Pressure and temperature time functions can be defined for boundary and capacitance (room) nodes, and energy addition, mass addition, particulate, and gaseous species sources also can be defined for room nodes. The required room data block that follows the time function information specifies the room node identifier, room volume, cross-sectional area, elevation, and time function identifiers.

Component data cards define the input parameters for the blower and filter components of the system. An identifier and performance curve are required input for the blower. The filter data card specifies the filter identifier, efficiency, and plugging factor.

Initial pressure and/or temperature conditions can be defined for each system node if desired. The pressure and/or temperature control parameter in the problem control data block must be enabled for this optional input.

If the user selects the FIRIN module to simulate the nonradioactive and/or radioactive releases caused by fire, the user must define the fire growth concept; the type, quantity, and burn area of the fuel; output control parameters that specify the edit frequency for the FIRIN-generated data; the dimensional and material characteristics of the burn room; and the type and amount of radioactive contaminant and the release mechanisms associated with that contaminant. Also, the user can specify additional flow path connections to the fire compartment, potential equipment heat sinks, and pressurized vessel failures if desired.

The last set of input information is the time step cards that control the calculation. The problem transient time can be divided into time domains. Each time domain can have different time-step sizes and output edit intervals.

B. Input Format

The FIRAC input specifications (Sec. IV.C) give the organization of the input deck (FIN) that must be followed. If the FIN fixed formats are not followed (the location of card information is prescribed), the program will attempt to read data from an adjacent column or from the next line of input and probably will abort with a format error. Input diagnostic messages have been incorporated within the input processor to help the user debug improperly formatted input.

There are three types of input data in FIRAC: (a) A/N, alphanumeric data (any combination of letters and numbers); (b) FP, floating point data; and (c) I, integer data. Alphanumeric data should be left-justified with respect to the first column of the field definition (data should start in the first column of the field). Integer data should be right-justified in the data field (the last data character should appear in the right-most column of the field). For example, the integer 6 placed in column 4 of the first branch description card would be interpreted as branch 60 because the field definition encompasses columns 1 through 5. If branch 6 were to be specified, it should be placed in column 5. Floating point data also are right-justified. Only large or small floating point numbers require the form ±nnnE±mm where n and m are integers. Intermediate floating point numbers may be specified as ±nn—.nnnn-- with the decimal point given. Values of data occurring under the heading "Default Value" are used if the input data field is left blank.

C. Improved FIRAC Input Specifications

In the FIRAC input deck (Table II), the sets of information are separated by data separator cards. These cards must be included in the positions indicated in the specifications (Table III) and should be used to identify the data that will follow. The sets of information that form the input deck data cards. Each data card description has four parts: data card descriptor, card comments, data type, format and variables, and data description. The data type, format, and variables follow the data card comments. The data type (alphanumeric, floating point, or integer) is indicated by the actual format used in the code. The variables are presented in the order they occur on the data card. The data description section contains a brief description of the data, the variable name associated with the data, the card location (column) of that variable, the variable default value, and the variable's maximum value. User-oriented comments pertaining to that particular data card are presented after the data descriptor and occasionally following the data description section.

TABLE II

FIRAC INPUT DECK ORGANIZATION

Card Identification	General Information
Data separator	
TITLE	User-specified problem identification
Data separator	
RUN CONTROL I	Run option, initial output time, time step for output, last output time, and special output times
Data separator	
PRINT/PLOT CONTROL, CARD 1	Units for output lists and plots, additional output times, number of plot frames of each type
PRINT/PLOT CONTROL, CARD 2	Number of plots of various information for each specie
Data separator	
PLOT FRAME	Number of curves on each frame and identification number of node or branch
Data separator	
RUN CONTROL II	Maximum iterations, convergence criterion, calculated deposition and entrainment options, relaxation parameter, initial pressure input option, initial temperature input option, initial particulate species mass fraction option, initial gaseous species volume fraction option, number of gaseous species, number of particulate species, natural convection option, and fire simulation options
Data separator	
BOUNDARY CONTROL	Number of boundary nodes, atmospheric pressure and temperature, and total number of each time function (pressure, temperature, energy, mass, particulate species, and gaseous species)
Data separator	

TABLE II (CONT)

Card Identification	General Information
GEOMETRY AND COMPONENT CONTROL	Total number of branches, nodes, rooms, blower function types, filter types, and control dampers
Data separator	
BRANCH DESCRIPTION DATA, CARD 1	Branch number, upstream node, downstream node, initial flow estimate, flow area, duct length, component type, differential pressure, and blower function identification
BRANCH DESCRIPTION DATA, CARD 2	Forward and backward resistance coefficients, filter type duct height, duct floor area, and heat transfer option
BRANCH DESCRIPTION DATA, CARD 3	Duct equivalent diameter, heat transfer area, wall thickness, emissivity, absorptivity, thermal conductivity, density, specific heat, initial wall temperature, and number of wall heat transfer nodes
Data separator	
PARTICULATE SPECIES DATA, CARD 1	Particulate species identification, diameter, and particle density
PARTICULATE SPECIES DATA, CARD 2	Initial particulate species mass fraction at each node
PARTICULATE SPECIES DATA, CARD 3	Initial particulate species wall mass
Data separator	
GASEOUS SPECIES DATA, CARD 1	Gaseous species identification
GASEOUS SPECIES DATA, CARD 2	Initial gaseous species volume fraction at each node
Data separator	
BOUNDARY NODE DATA	Node number, node type, initial pressure, pressure time function number, initial temperature, temperature time function number, and elevation
Data separator	
PRESSURE TIME FUNCTION DATA CONTROL	Function identification number and number of sets of points
PRESSURE/TIME DATA	Coordinates - value of time and pressure

TABLE II (CONT)

Card Identification	General Information
Data separator	
TEMPERATURE TIME FUNCTION DATA CONTROL	Function identification number and number of sets
TEMPERATURE/TIME DATA	Coordinates - value of time and temperature
Data separator	
ENERGY TIME FUNCTION DATA CONTROL	Function identification number and number of sets
ENERGY/TIME DATA	Coordinates - value of time and energy rate
Data separator	
MASS TIME FUNCTION DATA CONTROL	Function identification number, number of sets, and temperature function associated with injected mass
MASS/TIME DATA	Coordinates - value of time and mass rate
Data separator	
PARTICULATE SPECIES-TIME FUNCTION DATA CONTROL	Function identification number and number of sets
PARTICULATE-SPECIES/TIME DATA	Coordinates - value of time and mass rate
Data separator	
GASEOUS SPECIES TIME FUNCTION DATA CONTROL	Function identification number and number of sets
GASEOUS-SPECIES/TIME DATA	Coordinates - value of time and mass rate
Data separator	
ROOM DATA, CARD 1	Node number, volume, energy, mass, pressure, and temperature time function identification numbers, and initial values of energy, mass, pressure, and temperature
ROOM DATA, CARD 2	Cross-sectional area of room, number of particulate species time functions, number of gaseous species time functions, and elevation

TABLE II (CONT)

Card Identification	General Information
ROOM DATA, CARD 3	Particulate species number corresponding to source function, time function number, and initial value of the source function
ROOM DATA, CARD 4	Gaseous species number corresponding to source function, time function number, and initial value of source function
Data separator	
CONTROL DAMPER	Controlled node, branch number, damper type, pressure range, initial damper angle, rate of damper angle change
Data separator	
BLOWER CURVE CONTROL	Function identification number and number of points
BLOWER CURVE DATA	Coordinates - flow and head
Data separator	
FILTER DATA	Filter identification number, filter efficiency, filter plugging factor, number of species, and turbulent and laminar coefficients
Data separator	
PRESSURE INPUT	Initial value of pressure at each node
Data separator	
TEMPERATURE INPUT	Initial value of temperature at each node
Data separator	
SCENARIO CONTROL SPECIFICATIONS, CARD 1	Fire duration, output frequency, and fire growth option
SCENARIO CONTROL SPECIFICATIONS, CARD 2	Fire growth option, number of additional flow paths, number of pieces of equipment and vessels, and third fire compartment node identifier
Data separator	
INITIAL CONDITIONS	Initial compartment temperature and pressure
INFLOW SPECIFICATIONS	Inflow branch number, inflow node number, and height and diameter of inlet ventilator

TABLE II (CONT)

Card Identification	General Information
OUTFLOW SPECIFICATIONS	Outflow branch number, outflow node number, and height and diameter of outlet ventilator
THIRD COMPARTMENT NODE SPECIFICATIONS	Third node branch number, third node number, and height and diameter of extra ventilator
Data separator	
FUEL MASS DATA	Mass of fuels
FUEL SURFACE AREA DATA	Surface area of fuels
Data separator	
FIRE COMPARTMENT GEOMETRY	Length, width, and height of compartment; thickness of ceiling, wall, and floor; and height of flame base
Data Separator	
FIRE COMPARTMENT MATERIALS	Ceiling, wall, and floor construction materials
COMBUSTIBLES IDENTIFICATION	Identification of combustibles
Data separator	
EQUIPMENT/VESSEL IDENTIFIER	Identification of equipment and vessels at risk
EQUIPMENT/VESSEL GEOMETRY	Width, length, and height of equipment/ vessels; construction materials; and weight
EQUIPMENT/VESSEL CONTENT	Volume of contents, moisture content, initial surface temperature, initial inside temperature, and failure (rupture) pressure of equipment/vessel
Data separator	
ADDITIONAL FLOW PATH DATA	Failure times of additional flow paths, heights of paths, pressures at outlets, and diameters of paths
Data separator	
RADIOACTIVE SOURCE IDENTIFIER	Number of radioactive source terms
CONTAMINATED COMBUSTIBLE SOLID IDENTIFIER	Form of radioactive contaminant, material identification, tracking number, and burning order

TABLE II (CONT)

Card Identification	General Information
CONTAMINATED COMBUSTIBLE SOLID MASS	Mass of radioactive material
CONTAMINATED COMBUSTIBLE LIQUID IDENTIFIER	Form of radioactive contaminant, material identification, tracking number, and burning order
CONTAMINATED COMBUSTIBLE LIQUID MASS	Mass of radioactive material
CONTAMINATED SURFACE	Tracking number and mass of radioactive material
UNPRESSURIZED RADIOACTIVE LIQUID	Identification number, tracking number, and mass of radioactive material
PRESSURIZED RADIOACTIVE POWDER	Identification number, tracking number, and mass of radioactive material
PRESSURIZED RADIOACTIVE LIQUID	Identification number, tracking number, and mass of radioactive material
RADIOACTIVE PYROPHONIC SOLID	Tracking number, burning order, mass of radioactive material, and size of metal
TIME STEP CARDS	Time step size, end of time domain, and print edit interval

TABLE III

FIRAC INPUT DATA DECK

DATA SEPARATOR CARDS

Col.(s)	Data Description
1-80	These cards may be left blank or may contain alphanumeric data. These cards are used to separate different types of data cards. The contents of these cards are not used by the FIRAC.

Only one data separator card is shown here, but these cards should be placed in the input deck in the positions indicated in Table II.

TITLE CARD

Col.(s)	Data Description
1-80	Eighty columns of alphanumeric data are available to the user. This title is used for headings on output lists and user identification of the problem.

RUN CONTROL I CARD

(FORMAT 3X, A2, 2F5.0, E10.0, I5, 5F5.0) RUNT, TINIT, DTI, TOT, NSPOUT,
SOUT(I), (I = 1,5)

Col.(s)	Variable	Data Description	Default Value	Maximum Value
4-5	RUNT	Run option SS - steady-state solution only ST - steady-state plus transient	ST	
6-10	TINIT	First output time(s)	0.0	
11-15	DTI	Time between outputs(s)	0.01	
16-25	TOT	Last output time(s)	1.0	
30	NSPOUT	Number of special outputs	0	5
31-35	SOUT (1)	First special output time(s)	0.0	
36-40	SOUT (2)	Second special output time(s)	0.0	
41-45	SOUT (3)	Third special output time(s)	0.0	
46-50	SOUT (4)	Fourth special output time(s)	0.0	
51-55	SOUT (5)	Fifth special output time(s)	0.0	

Transient values of pressure, temperature, mass, and volume flows are saved for listing and plotting. These values are spaced uniformly between the first output time and the last output time. Additionally, up to five special output times may be requested.

PRINT/PLOT CONTROL CARD

(FORMAT A2, A3, 6I5) LUNITS, PLTOPT, NPFRMS, NQFRMS, NMFRMS, NAFRMS, NTFRMS, NSPECC

Col.(s)	Variable	Data Description	Default Value	Maximum Value
1-2	LUNITS	Units for output lists and plots. SI specified here yields pressures (kPa), flows (m^3/s), and temperatures (K).	(BLANK) yields pressures (in. w.g. at 60°F), flows (cfm), and temperatures (°F).	
3-5	PLTOPT	Entering the letters "ALL" produces lists of pressures, flows, temperatures, and differential pressures at every output time (including special outputs).	(BLANK) Lists produced only at start time, total run time, and special output times.	
6-10	NPFRMS	Number of pressure plot frames	0	10
11-15	NQFRMS	Number of volumetric flow rate plot frames	0	10
16-20	NMFRMS	Number of mass flow rate plot frames	0	10
21-25	NTFRMS	Number of temperature plot frames	0	10
26-30	NAFRMS	Number of damper blade angle frames.	0	10
31-35	NSPECC	Number of particulate species for which plots will be requested (next set of data cards)	0	5

The maximum number of plot frames that can be requested is 25; therefore, the sum of pressure frames, volumetric flow rate frames, mass flow rate frames, temperature frames, and particulate species frames must not exceed 25. These entries may be left blank if printer plots are not desired.

PRINT/PLOT CONTROL CARD

(Second Card -- Particulate Species Specification Card)

These cards are provided only if NSPECC is > 0. This quantity is specified in Cols. 36--40 of the first PRINT/PLOT control card. NSPECC cards must be provided.

(FORMAT 7I5) KNDSPC(I) NFLXFR(I), NPMOFR(I), NWMAFR(I), NSRCFR(I), NSINFR(I), NYFRMS(I), (I = 1, NSPECC)

Col.(s)	Variable	Data Description	Default Value	Maximum Value
1-5	KNDSPC	Particulate species number	0	
6-10	NFLXFR	Number of particulate flow rate plots for this particulate species number	0	10
11-15	NPMOFR	Number of integrated particulate flow rate through branch plots for this particulate species number	0	10
16-20	NWMAFR	Number of particulate mass on duct wall plots for this particulate species number	0	10
21-25	NSRCFR	Number of entrainment rate plots for this particulate species number	0	10
26-30	NSINFR	Number of deposition rate plots for this particulate species number	0	10
31-35	NYFRMS	Number of mass fraction plots for this particulate species number	0	10

PLOT FRAME CARD

(FORMAT 5I5, F10.0) NCRVS(K), NCID(1,K), NCID(2,K), NCID(3,K) NCID(4,K), XSCL(K), (K = 1, NFMT)

Col.(s)	Variable	Data Description	Default Value	Maximum Value
1-5	NCRVS	Total number of curves this frame	0	4
6-10	NCID	Node/branch number for first curve	0	100
11-15	NCID	Node/branch number for second curve	0	100
16-20	NCID	Node/branch number for third curve	0	100
21-25	NCID	Node/branch number for fourth curve	0	100
26-35	XSCL	Scale limit for frame	BLANK	

Pressures, temperatures, and mass fraction quantities are available for plotting at each node. Volumetric flow rate and mass flow rate are available for plotting at each branch. Particulate flow rate, integrated particulate flow rate, particulate mass on duct wall, entrainment rate, and deposition rate are available for plotting for each duct type branch. This card identifies how many and which nodes or branches are to appear as curves on the print/plot frame. Different quantities cannot be mixed on the same frame. There is one plot-frame card for each frame. These cards may be omitted if plot frames are not requested on the print/plot control card. A scale limit may be specified for the frame; otherwise the plot routine finds the maximum value of all the pressures, flows, or temperatures on the frame and uses this value as 100% of full scale.

RUN CONTROL II CARD

(FORMAT I5, F10.0, 4X, I1, 4X, I1, 4X, A1, 4X, A1, 2I5, 5X, I5, 5X, 3I5) MAXIT,
CONVRG, IDEP, IENT
PINP,TINP, IAINP,
IGINP, IFIRIN,
NGSPECE,NSPECES, INC

Col.(s)	Variable	Data Description	Default Value	Maximum Value
1-5	MAXIT	Maximum iterations permitted per time step. The program will abort if convergence (discussed in App. A) has not been achieved for this number of iterations. Ten times this number is permitted for steady-state calculations.	1000	
6-15	CONVRG	Criterion for iteration convergence (App. A).	0.0001	
20	IDEP	Calculated particulate deposition option. If IDEP = 1, deposition is calculated.	0	
25	IENT	Calculated particulate entrainment option. If IENT = 1, entrainment is calculated.	0	
30	PINP	Initial pressure input option. Insert the letter "P" in this column if pressures at nodal points are to be supplied.	(BLANK) no input pressures supplied	
35	TINP	Initial temperature input option. Insert the letter "T" in this column if temperatures at nodal points are to be supplied.	(BLANK) implies all ambient values	

RUN CONTROL II CARD (CONT)

(FORMAT I5, F10.0, 4X, I1, 4X, I1, 4X, A1, 4X, A1, 2I5, 5X, I5, 5X, 3I5) MAXIT,
CONVRG, PINIP,
TINP, IAINP, IGINP,
IFIRIN, NGSPECE,
NSPECES, INC

Col.(s)	Variable	Data Description	Default Value	Maximum Value
40	IAINP	1 if initial particulate specie mass fractions are to be input.	0	
45	IGINP	1 if initial gas species volume fractions are to be input.	0	
55	IFIRIN	1 if time functions are to be used to simulate the fire 0 if the FIRIN module is to simulate the fire.* See Sec. III on modeling strategies.	0	
61-65	NGSPECE	Number of gaseous species	0	5
66-70	NSPECES	Number of particulate species	0	5
75	INC	1 if buoyancy term in Eq. (A-3) is to be included. [(BLANK) (recommended) results in neglecting this term.]	(BLANK)	

*If the FIRIN module simulates the fire, the fire accident will not begin until the problem time equals 2.0 s.

BOUNDARY CONTROL CARD

(FORMAT 2I5, 2F10.0, 5I5) NPFN, NBNODS, PZERO, TAMB, NTFN, NEFN, NMFN, NCFN, NGFN

Col.(s)	Variable	Data Description	Default Value	Maximum Value
1-5	NPFN	Total number of pressure-time functions	0	5
6-10	NBNODS	Total number of boundary nodes	0	10
11-20	PZERO	Value for atmospheric pressure (psia)	14.7	
21-30	TAMB	Value for atmospheric temperature (°F)	60	
35	NTFN	Total number of temperature-time functions	0	5
40	NEFN	Total number of energy-time functions	0	5
45	NMFN	Total number of mass-time functions	0	5
50	NCFN	Total number of particulate species addition time functions	0	5
55	NGFN	Total number of gaseous species addition time functions	0	5

The code is limited to handle a maximum of 10 boundary nodes and a maximum of 5 time functions of each type.

GEOMETRY AND COMPONENT CONTROL CARD

(FORMAT 2I5, 5X, 3I5) NBRCH, NNODES, NROOMS, NBLFNS, NFILRS

Col.(s)	Variable	Data Description	Default Value	Maximum Value
1-5	NBRCH	Number of branch description data card sets	0	100
6-10	NNODES	Number of nodes defined for problem (includes boundary nodes)	0	100
16-20	NROOMS	Total number of rooms	0	100
21-25	NBLFNS	Total number of blower characteristic functions	0	15
26-30	NFILRS	Total number of special filter types	0	20
31-35	NCDAMP	Total number of control dampers	0	100

Values of these parameters control the reading of input data and should not exceed maximum values.

BRANCH DESCRIPTION DATA, CARD 1

(FORMAT 3I5, 3F10.0, A1, 4X, F10.2, 10X, I2) IBRN, INDU(IBRN), INDD(IBRN), Q(IBRN), FA(IBRN), XL(IBRN), ICPTYP(IBRN), DP(IBRN), IBCN

Col.(s)	Variable	Data Description	Default Value	Maximum Value
1-5	IBRN	Branch number	0	100
6-10	INDU	Upstream node number	0	100
11-15	INDD	Downstream node number	0	100
16-25	Q	Initial estimate of flow (cfm). This value is used to calculate damper, filter, and duct resistance coefficients.	(0.1 x FA)	
26-35	FA	Flow area (ft^2)	1.0	
36-45	XL	Duct length (ft)	$(FA)^{.5}/2$	
46	ICPTYP	Component type V ..... Damper F ..... Filter B ..... Blower D ..... Duct	0	
51-60	DP	Branch pressure differential (in. w.g. at 60°F)	0.0	
71-72	IBCN	Blower curve identification Identifies which blower curve to use for component type B.	0	15

BRANCH DESCRIPTION DATA, CARD 2

(FORMAT 2E10.0, I10, 20X, 2E10.0, 9X, I1) FZ, RZ, NFE, HEIGHT(IBRN), FLAREA(IBRN), IHNT(IBRN)

Col.(s)	Variable	Data Description	Default Value	Maximum Value
1-10	FZ	Forward resistance coefficient for branch. If > 0, this value overrides that calculated by the code from pressure differential and initial flow.	Code-calculated value	
11-20	RZ	Rear resistance coefficient for branch. If > 0, this value overrides that calculated by the code from pressure differential and initial flow.	Code-calculated value	
21-30	NFE	Filter type.	0	
51-60	HEIGHT	Duct height (use h = 2D for round duct) (ft).	0	
61-70	FLAREA	Duct floor area (ft^2).	0	
80	IHNT	Heat transfer option = 1 if heat transfer calculation is to be performed for this branch.	0	

Two cards are required per branch. The branch pressure differential is used with the initial estimate of branch flow to calculate a resistance coefficient. The differential pressures also are used to calculate initial starting point system pressures if these pressures are not input separately.

The BRANCH DESCRIPTION CARDS need not be ordered in the input deck (branch 10 might precede branch 5). However, the number of cards should agree with that specified in Cols. 1—5 of the GEOMETRY AND COMPONENT CONTROL card.

The blower curve identification refers to the blower curve number identifier specified later on the BLOWER CURVE CONTROL CARD.

The filter type refers to special type filters for which a plugging calculation is to be performed. The filter types are specified on the FILTER DATA CARD(S). The filter type may be left blank if a plugging calculation (detailed in App. C) is not requested.

BRANCH DESCRIPTION DATA, CARD 3

This card is read only if duct heat transfer is requested on the second branch description data card (Col. 80).

(FORMAT 2E8.0, I8, 7E8.0) DIA, HTAREA, NODES, THICK, EMISS, ABST, KWALL, RHOW, CPW, TWALL

Col.(s)	Variable	Data Description	Default Value	Maximum Value
1-8	DIA	Duct equivalent diameter (ft)	0.0	
9-16	HTAREA	Duct heat transfer area (ft^2)	0.0	
17-24	NODES	Number of heat transfer nodes in wall	1	
25-32	THICK	Duct wall thickness (in.)	0.0	
33-40	EMISS	Duct emissivity (outside)	0.0	
41-48	ABST	Duct absorptivity (outside)	0.0	
49-56	KWALL	Wall thermal conductivity (Btu/h/ft-°F)	0.0	
57-64	RHOW	Wall density (lbm/ft^3)	0.0	
65-72	CPW	Wall specific heat (Btu/lb-°F)	0.0	
73-80	TWALL	Initial wall temperature (°F)	0.0	

PARTICULATE SPECIES DATA, CARD 1

These cards are read only if NSPECIES is > 0. This quantity is in Cols. 66—70 of RUN CONTROL CARD II. Provide NSPECIES sets of these cards. (One for each particulate specie.)

(FORMAT I10, 2X, A8, 2E10.0) ISPEC, IDSPEC, DIAP, RHOP

Col.(s)	Variable	Data Description	Default Value	Maximum Value
1-10	ISPEC	Species Number	0	NSPECIES
13-20	IDSPEC	Identification of this species (up to eight characters)	BLANK	
21-30	DIAP	Particle diameter (μm)	0.0	
31-40	RHOP	Particle density (g/cm^3)	0.0	

PARTICULATE SPECIES DATA, CARD 2

Initial Particulate Species Wall Mass

The following card should be present only if RUN CONTROL CARD II (Col. 40) indicates that initial particulate specie quantities are to be input. The default for these quantities is zero. Use as many cards as necessary to define the initial particulate specie mass fraction at all nodes. The number of quantities to be provided should be the same as specified in Cols. 6—10 of the GEOMETRY AND COMPONENT CONTROL CARD. Values that are left blank are assumed to be zero.

(Format 5E15.0)

Col.(s)	Data Description	Default Value	Maximum Value
1-15	Mass fraction in the first node	0.0	
16-30	Mass fraction in the second node	0.0	
31-45	Mass fraction in the third node	0.0	
46-60	Mass fraction in the fourth node	0.0	
61-75	Mass fraction in the fifth node	0.0	

PARTICULATE SPECIES, DATA CARD 3

Initial Particulate Specie Wall Mass

The following card should be present only if RUN CONTROL CARD II (Col. 40) indicates that initial particulate specie quantities are to be input. The default for these quantities is zero. Use as many cards as necessary to define the initial particulate specie mass contained on the walls of each branch. The number of quantities to be provided should be the same as specified in Cols. 1--5 of the GEOMETRY AND COMPONENT CONTROL CARD. Values that are left blank are assumed to be zero.

(FORMAT 5E15.0)

Col.(s)	Data Description	Default Value	Maximum Value
1-15	Wall mass in the first branch	0.0	
16-30	Wall mass in the second branch	0.0	
31-45	Wall mass in the third branch	0.0	
46-60	Wall mass in the fourth branch	0.0	
61-75	Wall mass in the fifth branch	0.0	

GASEOUS SPECIES DATA, CARD 1

These cards are read only if NGSPECIES is > 0. This quantity is in Cols. 61—65 of RUN CONTROL CARD II. Provide NGSPECIES sets of these cards (one for each gaseous specie).

(FORMAT I10, 2X, A8) ISPEC, IDSPEC

Col.(s)	Variable	Data Description	Default Value	Maximum Value
1-10	ISPEC	Species No. 1 < ISPEC < NGSPECIES	0	
13-20	IDSPEC	Identification of this species (Up to eight characters)	BLANK	

GASEOUS SPECIES DATA, CARD 2

Initial Gaseous Species Volume Fraction

The following card should be present only if RUN CONTROL CARD II (Col. 45) indicates that initial gaseous specie quantities are to be input. The default for these quantities is zero. Use as many cards as necessary to define the initial volume fraction of this specie at all nodes. The number of quantities provided should be the same as specified in Cols. 6--10 of the GEOMETRY AND COMPONENT CONTROL CARD.

(FORMAT 5E15.0)

Col.(s)	Data Description	Default Value	Maximum Value
1-15	Volume fraction in the first node	0.0	
16-30	Volume fraction in the second node	0.0	
31-45	Volume fraction in the third node	0.0	
46-60	Volume fraction in the fourth node	0.0	
61-75	Volume fraction in the fifth node	0.0	

BOUNDARY NODE DATA CARD

(FORMAT I5, I2, F11.0, F10.0, I5, F10.0) IBNNR(I), ITYPBN(I), PB(I), IBPFN(I), TBI(I), IBTFN(I), ELEV[IBNNR(I)], [I = 1, NBNODS]

Col.(s)	Variable	Data Description	Default Value	Maximum Value
1-5	IBNNR	Boundary node number	0	10
6-7	ITYPBN	Boundary node type (ITYPBN = 1 denotes an internal boundary node)	0	
8-18	PB	Initial value of pressure at node (in. w.g. at 60°F)	atmospheric	
19-22	IBPFN	Identification number of pressure-time function at the boundary node (See Time Function Data card.)	0 (Steady value of pressure)	5
23-32	TBI	Initial value of temperature (°F)	atmospheric	
33-37	IBTFN	Identification of temperature-time function number at this boundary node	0	5
38-47	ELEV	Elevation (ft)	0	

TIME FUNCTION DATA CONTROL CARD

(FORMAT 2I5, 3X, I2) IFN, NP(IFN), ITEM(IFN)

Col.(s)	Variable	Data Description	Default Value	Maximum Value
1-5	IFN	Time function identifier.	0	5
6-10	NP	Number of data points in time function definition. A data point is defined as an ordered pair of values of time and function of time.	0	20
14-15	ITEM	Temperature function number for mass injection.	0	5

This card controls the reading of subsequent TIME FUNCTION DEFINITION cards and should precede each time function definition. The TIME FUNCTION DATA CONTROL card is followed by one or more TIME FUNCTION DEFINITION data cards. This set of cards may be present, but it is not required for steady-state runs.

TIME FUNCTION DEFINITION DATA CARD

(Format 3(2F10.0)) T(I,IFN), FT(I,IFN), (I = 1, INP) REPEATED

Col.(s)	Variable	Data Description	Default Value	Maximum Value
1-10	T	Value of time for first time function data point.	0.0	
11-20	FT	Value of variable for first time function data point.	0.0	
21-30	T	Value of time for second time function data point.	0.0	
31-40	FT	Value of variable for second time function data point.	0.0	
41-50	T	Value of time for third time function data point.	0.0	
51-60	FT	Value of variable for third time function data point.	0.0	

Insert as many TIME FUNCTION DEFINITION cards as needed to define all the data points. The TIME FUNCTION data card sets are used to define all the time-dependent user-specified data for the problem. This includes time-dependent data for both boundary nodes and capacitance nodes (rooms). Each <u>type</u> of time function must be preceded by a data separator card.

Use as many TIME FUNCTION DATA CARD DESCRIPTION and TIME FUNCTION DEFINITION DATA CARD DESCRIPTION sets as necessary to define all the time function sets required by the problem. The card sets must be in the following order and in the quantities provided in the indicated units.

- Pressure (psig)
- Temperature (°F)
- Energy (kW)
- Mass (lbm/h)
- Particulate species (g/s)
- Gaseous species (cfm)

The defining times must be in ascending order.

ROOM DATA, CARD 1

(FORMAT I5, F10.0, 4I5, 4F10.0) IND(K), VOL(K), NOE(K), NOM(K), NOP(K), NOT(K), REDOT(K), RMDOT(K), RP(K), RT(K), (K =1, NROOMS)

Col.(s)	Variable	Data Description	Default Value	Maximum Value
1-5	IND	Node number for room	0	100
6-15	VOL	Room volume (ft^3)	0.0	
20	NOE	Energy time function number	0	5
25	NOM	Mass addition time function number	0	5
30	NOP	Pressure time function number	0	5
35	NOT	Temperature time function number	0	5
36-45	REDOT	Initial value of energy (kW)	0.0	
46-55	RMDOT	Initial value of mass (lbm/h)	0.0	
56-65	RP	Initial value of pressure (in. w.g. at 60°F)	0.0	
66-75	RT	Initial value of temperature (°F)	atmospheric	

Two cards are required per room. The volume dimension is used in the calculation of capacitance coefficients, and zero volume is not permitted. Room volumes are required input for steady-state runs. Duct volume (if significant) must be input as a pseudo-room requiring an additional node. Rooms cannot be located at boundary nodes. The ROOM DATA cards need not be in numerical order.

ROOM DATA, CARD 2

(FORMAT E10.0, 2I10, 10X, E10.0) RFA(K), (K = 1, NROOMS), NOPFNS, NOGFNS, ELEV(IND(K))

Col.(s)	Variable	Data Description	Default Value	Maximum Value
1-10	RFA	Room area (ft^2) (flow area)	0.0	
11-20	NOPFNS	No. of particulate species source time functions for this room	0	
21-30	NOGFNS	No. of gaseous species source time functions for this room	0	
41-50	ELEV	Elevation (ft)	0.0	

ROOM DATA, CARD 3

Particulate Species Source Specification Card

These cards are present only if there are particulate specie sources in this room (Cols. 11—20 on the second room data card). There is one card for each particulate time function requested for this room. The total number of cards must be the same as the number of particulate sources specified in Cols. 11—20 of the second room data card.

(FORMAT 2I10, E10.0) ISPEC, IPTFNO, PCDOT

Col.(s)	Variable	Data Description	Default Value	Maximum Value
1-10	ISPEC	Species number for this source must agree with that stated on the particulate species data cards)	0	
11-20	IPTFNO	Time function number describing this source	0	
21-30	PCDOT	Initial value of the particulate source (kg/s)	0.0	

ROOM DATA, CARD 4

(Gaseous Species Source Specification Cards)

These cards are present only if there are gaseous specie sources in this room (Cols. 21—30 on the second room data card). There is one card for each gaseous species time function requested for this room. The total number of cards must be the same as the number of gaseous species sources specified in Cols. 21—30 of the second ROOM DATA CARD.

(FORMAT 2I10, E10.0) ISPEC, IGTFNO, GCDOT

Col.(s)	Variable	Data Description	Default Value	Maximum Value
1-10	ISPEC	Species number for this source (must agree with that stated on the gaseous species data cards)	0	
11-20	IGTFNO	Time function number describing this source	0	
21-30	GCDOT	Initial value of the gaseous specie source (cfm)	0.0	

CONTROL DAMPER CARD

Format (3I5, 5F 10.0) CTLNODE, DAMPNUM, TYPE, PMIN, PMAX, THETA, dTHETA, tDELAY

Col.(s)	Variable	Data Description	Default Value	Maximum Value
1-5	CTLNODE	The node at which a pressure is being maintained.		100
6-10	DAMPNUM	The branch number of the controlling damper.		100
11-15	TYPE	The damper type. 1 - opposed-blade medium duty 2 - opposed-blade light duty 3 - parrallel-blade light duty	1	3
16-25	PMIN	The minimum pressure allowed at the controlled node (in. wg.).	0	
26-35	PMAX	The maximum pressure allowed at the controlled node (in. wg.).	0	
36-45	THETA	The initial angle of the damper blade. 90° - open 0° - closed	0°	90°
46-55	DTHETA	The number of degrees that the blower opens if the pressure is above PMAX or closes if the pressure is below PMIN (negative if the damper closes at high pressures).	0°	90°
56-65	TDELAY	The time that the pressure must remain above or below the limits before the damper will respond (s).	0°	

The control damper model can be used to model fixed dampers by setting THETA to the blade angle of the damper and dTHETA to 0°. Additional damper types can be added to FIRAC by the procedure explained in Appendix E. Control dampers respond by closing or opening DTHETA degrees after the pressure has been outside of the specified range for TDELAY seconds. After the damper responds, it will wait another TDELAY seconds before responding again. To obtain "continous" opening or closing of a damper use a TDELAY equal to the timestop and a DTHETA to match.

BLOWER CURVE CONTROL CARD

(FORMAT 2I5) JB, NPBC(JB)

Col.(s)	Variable	Data Description	Default Value	Maximum Value
1-5	JB	Blower curve number identifier.	0	15
6-10	NPBC	Number of points defining this blower curve. A point is defined as an ordered pair of values of flow (cfm) and head (in. w.g. at 60°F).	0	20

The blower curve data are ordered in the same way as time function data--a curve input control card is followed by one or more curve description cards. One curve control card is required for each blower type. The order of the blower curves is unimportant (curve 3 might precede curve 1); however, this card is used in reading the following blower curve data points and must appear just before the appropriate curve description card(s).

BLOWER CURVE DATA CARD

(FORMAT 3(2F10.0)) XB(I, JB), FXB(I, JB), [I = 1, NPBC(JB)] REPEATED

Col.(s)	Variable	Data Description	Default Value	Maximum Value
1-10	XB	Flow (cfm) for the first point	0.0	
11-20	FXB	Blower head (in. w.g. at 60°F) for the first point	0.0	
21-30	XB	Flow for the second point	0.0	
31-40	FXB	Blower head for the second point	0.0	
41-50	XB	Flow for the third point		
51-60	FXB	Blower head for the third point	0.0	

FILTER DATA CARD(S)

(FORMAT I10, 4F10.2) NFE, FEF(NFE), ALF1(NFE), AKL(NFE), AKT(NFE)

Col.(s)	Variable	Data Description	Default Value	Maximum Value
1-10	NFE	Filter type number (required)	0	NFILRS
11-20	FEF	Filterefficiency (required)	0.0	
21-30	ALF1	Filter plugging factor (1/kg) (optional)	0.0	
31-40	AKL	Laminar filter factor K_L	0.0	
41-50	AKT	Turbulent filter factor K_T	0.0	

One card for each special filter type specified in Cols. 26—30 of the GEOMETRY AND COMPONENT CONTROL CARD. Special filter types refer to filters for which a plugging calculation is to be performed. The definition of the filter plugging factor is given in Eq. (C-42). The laminar and turbulent filter factors are defined by Eqs. (C-39) and (C-40).

PRESSURE INPUT CARD

(FORMAT 5E15.0) P(I), (I = 1, NNODES) (Five entries per card)

Col.(s)	Variable	Data Description	Default Value	Maximum Value
1-15	P	Pressure (in. w.g. at 60°F) at the first node	0.0	
16-30		Pressure at the second node	0.0	
31-45		Pressure at the third node	0.0	
46-60		Pressure at the fourth node	0.0	
61-75		Pressure at the fifth node	0.0	

These cards are required only if Col. 30 of the RUN CONTROL II CARD is set to P. The values of pressure for boundary nodes may be left blank because these values are supplied on the BOUNDARY NODE DATA cards. Use as many cards as required to define all the system pressures.

TEMPERATURE INPUT CARD

(FORMAT 5E15.0) T(I), (I= 1, NNODES) Five entries per card

Col.(s)	Variable	Data Description	Default Value	Maximum Value
1-15	T	Temperature (°F) at the first node	0.0	
16-30		Temperature at the second node	0.0	
31-45		Temperature at the third node	0.0	
46-60		Temperature at the fourth node	0.0	
61-75		Temperature at the fifth node	0.0	

These cards are required only if Col. 35 of the RUN CONTROL II CARD is set to T. The values of temperature for boundary nodes may be left blank because these values are supplied on the BOUNDARY NODE DATA cards. Use as many cards as required to define all the system temperatures.

SCENARIO CONTROL SPECIFICATIONS, CARD 1

(FORMAT F10.2, 2I10) TSPEC, IPRNT, MIBO

Col.(s)	Variable	Data Description	Default Value	Maximum Value
1-10	TSPEC	User-specified fire duration in real-time seconds (used only in FIRIN module).	0.0	
11-20	IPRNT	User-specified frequency of time step intervals for which the computed data are printed into the output unit files. For example, if the time-step interval (DTMAX) is 0.1 s and the user wishes to obtain computed data every 10 s in real time of the fire, IPRNT = 100 should be specified.	0	
2-30	MIBO	One way to approximate fire growth with the FIRIN module; users must estimate the orders of fuel consumption (burning order) in the fire if more than one combustible material is specified at risk in the compartment. MIBO is the maximum number of burning orders, and it governs the number of physical card requirements for FIRE SOURCE TERM DATA CARDS.	0	5

SCENARIO CONTROL SPECIFICATIONS, CARD 2

(FORMAT I10, F10.1, I10, F10.1, 2I10) IGNITE, PFLOW, NFP, EQUIP, MJE, IFLOW3

Col.(s)	Variable	Data Description	Default Value	Maximum Value
1-10	IGNITE	A less conservative way to approximate fire growth with the FIRIN module is using the ignition energy concept. This approximation allows auto-ignition of combustibles at risk if the heat flux levels generated by the initial burning combustibles in the compartment are sufficient. The ignition energy levels required for auto-ignition of the combustibles depend on material properties, and they are stored in the program. To use this concept for approximation, IGNITE = 1 must be input; otherwise, IGNITE = 0 must be specified. When this concept is applied, MIBO = 2 must be specified where the first burning order (IBO = 1), the fuel quantity, and the surface area are input for initial burning materials, and for second burning order (IBO = 2), the quantity and surface area of combustibles at risk (because of possible auto-ignition) are specified.	0	

SCENARIO CONTROL SPECIFICATIONS, CARD 2 (CONT)

Col.(s)	Variable	Data Description	Default Value	Maximum Value
11-20	PFLOW	Numeric identifier for additional flow paths to/from the fire compartment. FLOW = 1.0 (additional flow paths), or FLOW = 0.0 (no additional flow paths). If FLOW = 0.0 is specified, no input data are required for additional FLOW PATH DATA CARDS.	0.0	
21-30	NFP	Number of additional flow paths to/from the fire compartment. A glovebox is an example of a compartment that has glove ports as its additional flow paths where the gloves attached to it have burnt off. The value selected for NFP governs the number of physical card requirements for additional FLOW PATH DATA CARDS. If NFP = 0, no data input is required for these cards.	0	50
31-40	EQUIP	Numeric identifier for equipment and vessels at risk in the fire compartment. EQUIP = 1.0 (equipment and vessels) EQUIP = 0.0 (no equipment or vessels)	0.0	

Col.(s)	Variable	Data Description	Default Value	Maximum Value
		If EQUIP = 0.0 is specified, no input data are required for EQUIPMENT/VESSEL GEOMETRY CARDS or EQUIPMENT/VESSEL CONTENT DATA CARDS.		
41-50	MJE	Number of pieces of equipment and vessels at risk inside the fire compartment. The number assigned for MJE is the number required for each type of EQUIPMENT/VESSEL GEOMETRY CARDS.	0	10
51-60	IFLOW3	Numeric identifier for third fire compartment node. IFLOW3 = 1 Third node contributes to inflow at steady-state conditions. IFLOW3 = 0 No third node. IFLOW3 = -1 Third node contributes to outflow at steady-state conditions.	0	

INITIAL CONDITIONS CARD

(FORMAT F10.2, F10.6) TENIT, PINIT

Col.(s)	Variable	Data Description	Default Value	Maximum Value
1-10	TENIT	Initial temperature (°F) of the fire compartment	0.0	
11-20	PINIT	Initial pressure (in. w.g.) inside the fire compartment	0.0	

INFLOW SPECIFICATIONS CARD

(FORMAT 2I10, 2F10.2) IBRCHI, IFCND1, ZIF, DIF

Col.(s)	Variable	Data Description	Default Value	Maximum Value
1-10	IBRCHI	Fire compartment inflow branch number	0	
11-20	IFCND1	Fire compartment inflow node number	0	
21-30	ZIF	Height of elevation (ft) of the center plane of inlet ventilator from the floor level in the compartment	0.0	
31-40	DIF	Diameter (ft) of inlet ventilator	0.0	

OUTFLOW SPECIFICATIONS CARD

(FORMAT 2I10, 2F10.2) IBRCHO, IFCND2, ZOF, DOF

Col.(s)	Variable	Data Description	Default Value	Maximum Value
1-10	IBRCHO	Fire compartment outflow branch number	0	
11-20	IFCND2	Fire compartment outflow node number	0	
21-30	ZOF	Height of elevation (ft) of the center plane of outlet ventilator from the floor level in the compartment	0.0	
31-40	DOF	Diameter (ft) of outlet ventilator	0.0	

THIRD COMPARTMENT NODE SPECIFICATIONS CARD

This card is not required if IFLOW3 = 0 (SCENARIO CONTROL SPECIFICATIONS CARD 2).

(FORMAT 2I10, 2F10.2) IBRCH3, IFCND3, ZIOF3, DIOF3

Col.(s)	Variable	Data Description	Default Value	Maximum Value
1-10	IBRCH3	Third compartment node branch number	0	
11-20	IFCND3	Third compartment node number	0	
21-30	ZIOF3	Height of elevation (ft) of the center plane of extra ventilator (option of either inflow or out flow) from the floor level in the compartment	0.0	
31-40	DIOF3	Diameter (ft) of extra ventilator	0.0	

FUEL SOURCE TERMS DATA CARDS

The number of sets of the following two card types is governed by the number of burning orders, MIBO (SCENARIO CONTROL SPECIFICATIONS CARD 1). MIBO sets must be entered in sequence, and all FUEL MASS DATA CARDS must be entered before any FUEL SURFACE AREA DATA CARDS

FUEL MASS DATA CARDS

(FORMAT 9F8.2) FUEL (I, IBO), (I = 1, 9; IBO = 1, MIBO)

Col.(s)	Variable	Data Description	Default Value	Maximum Value
1-8 9-16 17-24 25-32 33-40 41-48 49-56 57-64 65-72	FUEL	Mass (pounds) of nine different types of combustible fuel materials (I = 1, 9) commonly found in fuel cycle facilities and possibly present in the fire compartment. I is the numeric identifier for types of fuels, which are described in Table IV*. IBO is the burning order (that is, first, second, third, fourth, and so on) of fuels specified by the user. Put 0.0 in the corresponding columns of each physical card where that particular fuel is not involved in the fire. Currently, up to nine combustible materials can be burning all at once, and burning orders can be up to MIBO = 5.	0.0	

*Table IV follows the completion of Table III on p. 110.

FUEL SURFACE AREA DATA CARDS

(FORMAT 9F8.2) AREC (I, IBO), I = 1, 9; IBO = 1, MIBO

Col.(s)	Variable	Data Description	Default Value	Maximum Value
1-8	AREC	Surface area (ft^2) of	0.0	
9-16		fuels for nine different types of		
17-24		combustible materials (I = 1, 9).		
25-32		A value of 0.0 should be entered		
33-40		in the corresponding columns of		
41-48		each physical card when that		
49-56		particular fuel is not involved		
57-64		in the fire. A total of nine values		
65-72		should be filled for for each		
		physical card as in FUEL (I, IBO).		

FIRE COMPARTMENT GEOMETRY CARD

(FORMAT 7F10.3) RL, WR, ZR, XCEIL, XWALL, XFLOOR, ZFIRE

Col.(s)	Variable	Data Description	Default Value	Maximum Value
1-10	RL	Length (ft) of fire compartment.	0.0	
11-20	WR	Width (ft) of fire compartment.	0.0	
21-30	ZR	Height (ft) of fire compartment.	0.0	
31-40	XCEIL	Thickness (ft) of compartment ceiling.	0.0	
41-50	XWALL	Thickness (ft) of compartment wall.	0.0	
51-60	XFLOOR	Thickness (ft) of compartment floor. If the compartment is on floor level with no other compartment below it, a large value for XFLOOR is suggested for heat transfer considerations.	0.0	
61-70	ZFIRE	Normalized height (ft) of the flame base from the floor level. Specifying this value requires the user's judgment. For example, when a glovebox is in a fire, ZFIRE is the height of the glovebox floor from the ground level. In all cases, ZFIRE must be given a positive, nonzero value.	0.0	

FIRE COMPARTMENT MATERIALS CARD

(FORMAT 3I10) MATERC, MATERW, MATERF

Col.(s)	Variable	Data Description	Default Value	Maximum Value
1-10	MATERC	Ceiling construction material. Use the numeric identifier MATERC = 1, 2,...15 (Table V*) for noncombustible solid materials. MATERC = 1 denotes concrete as the ceiling material.	0	
11-20	MATERW	Wall construction material. Use the numeric identifier as for MATERC.	0	
21-30	MATERF	Floor construction material. Use the numeric identifier as for MATERC.	0	

*Table V follows the completion of Table III on p. 110.

COMBUSTIBLES IDENTIFICATION CARD

This card type is required only when the ignition energy concept is applied, IGNITE = 1 (SCENARIO CONTROL SPECIFICATIONS, CARD 2).

(FORMAT 9I5) NBO(I), (I = 1, 9)

Col.(s)	Variable	Data Description	Default Value	Maximum Value
1-5 6-10 11-15 16-20 21-25 26-30 31-35 36-40 41-45	NBO	Numeric identifier for the nine combustibles at risk. Input NBO(I) = 0 for material that burns initially in the fire. NBO(I) = 1 for combustibles that are at risk and that can contribute to the fire through the ignition energy concept. NBO(I) = 2 for any of the nine combustible types that will not contribute to the fire at all. NBO(I) = 3 for material types that burn at the start of the fire and are also at risk because of ignition energy concept. Nine input values are required on this card. Enter NBO(I) = 2 for combustibles not involved in the fire.	0	3

EQUIPMENT/VESSEL IDENTIFIER CARD

This card is required only if equipment or vessels are at risk inside the fire compartment. For this to be true, MJE > 0 (SCENARIO CONTROL SPECIFICATIONS, CARD 2). Only one card is necessary.

(Format 4F10.2) NVES (IE), (IE = 1, 4)

Col.(s)	Variable	Data Description	Default Value	Maximum Value
1-10 11-20 21-30 31-40	NVES	Number of pieces of equipment or vessel of type 1E = 1, 2, 3, and 4 Type 1 - simple heat sink Type 2 - pressurized containers of powder Type 3 - pressurized containers of liquid Type 4 - open liquid containers Enter NVES(1E) = 0 if Type IE is not found in the fire compartment.	0	10

EQUIPMENT/VESSEL GEOMETRY CARDS

The following five card types decribe the pieces of equipment and vessels at risk inside the fire compartment. The number of sets of cards is governed by the number of pieces, MJE (SCENARIO CONTROL SPECIFICATION, CARD 2), one set for every piece of equipment or vessel. If MJE = 0, no cards are required.

EQUIPMENT/VESSEL GEOMETRY, CARD 1

(FORMAT 4F10.2) WD(IE, JE), (IE = 1, 4; JE = 1, MJE)

Col.(s)	Variable	Data Description	Default Value	Maximum Value
1-10 11-20 21-30 31-40	WD	Width (ft) of the equipment and/or vessels. The FIRIN module is limited to only four types of equipment or vessels (IE = 1, 4): simple heat sink, pressurized containers of powder, pressurized liquid containers, and open liquid containers. JE denotes number of each type of equipment or vessels, up to 10 for each type (MJE = 10).	0.0	

EQUIPMENT/VESSEL GEOMETRY, CARD 2

(FORMAT 4F10.2) HEQ(IE, JE), (IE = 1, 4; JE = 1, MJE)

Col.(s)	Variable	Data Description	Default Value	Maximum Value
1-10 11-20 21-30 31-40	HEQ	Length (ft) of the equipment (diameter of cylinders, length exposed to fire for boxes) and/or vessels present in the fire compartment. Same input requirement as WD(IE,JE) above.	0.0	

EQUIPMENT/VESSEL GEOMETRY, CARD 3

(FORMAT 4F10.2) HTF(IE, JE), (IE = 1, 4; JE = 1, MJE)

Col.(s)	Variable	Data Description	Default Value	Maximum Value
1-10 11-20 21-30 31-40	HTF	Height (ft) of the base of equipment and/or vessels from the floor level. Same input require ment as WD(IE, JE) above.	0.0	

EQUIPMENT/VESSEL GEOMETRY, CARD 4

(FORMAT 4I10) MATERE (IE, JE), (IE = 1; 4 JE = 1, MJE)

Col.(s)	Variable	Data Description	Default Value	Maximum Value
1-10 11-20 21-30 31-40	MATERE	Construction material of the four types of equipment or vessels mentioned above (IE = 1, 4). MATERE is a numeric identifier for types of noncombustible materials. IE denotes number of each type of equipment or vessels, with up to seven types of possible construction material. For example, MATERE (IE, JE) = 3 denotes the JEth piece of equipment or vessel Type IE constructed of stainless steel. See Table VI.*	0	

EQUIPMENT/VESSEL GEOMETRY, CARD 5

(FORMAT 4F10.2) WMASS (IE, JE), (IE = 1, 4; JE = 1, MJE)

Col.(s)	Variable	Data Description	Default Value	Maximum Value
1-10 11-20 21-30 31-40	WMASS	Weight (pounds) of equipment or vessels. Similar input requirements as for WD(IE,JE), HFT(IE,JE), and HEQ(IE,JE).	0.0	

EQUIPMENT/VESSEL CONTENTS CARDS

The following 15 card types describe the contents of the equipment and vessels at risk in the fire compartment. The number of entries on each card must equal the number of pieces of equipment and vessels, MJE (SCENARIO CONTROL SPECIFICATIONS CARD 2). If MJE = 0.0, no cards are required; otherwise, each card type must be entered.

EQUIPMENT/VESSEL CONTENTS, CARD 1

(FORMAT 10F8.2) VGAS2 (JE), (JE = 1, MJE)

Col.(s)	Variable	Data Description	Default Value	Maximum Value
1-8 every 8	VGAS2	Gas volume (ft^3) inside Vessel Type 2 (IE = 2, pressurized container). MJE values must be input on this card; for equipment or vessels not Type 2, enter 0.0 in the corresponding array spaces.	0.0	

EQUIPMENT/VESSEL CONTENTS, CARD 2

(FORMAT 10F8.2) VPWD(JE), (JE = 1, MJE)

Col.(s)	Variable	Data Description	Default Value	Maximum Value
1-8 every 8	VPWD	Volume of powder (ft^3) inside Vessel Type 2 (IE = 2, pressurized container). See EQUIPMENT/VESSEL CONTENTS, CARD 1.	0.0	

EQUIPMENT/VESSEL CONTENTS, CARD 3

(FORMAT 10F8.2) WH2O2 (JE), (JE = 1, MJE)

Col.(s)	Variable	Data Description	Default Value	Maximum Value
1-8 every 8	WH2O2	Moisture content (pounds) inside Vessel Type 2. See EQUIPMENT/VESSEL CONTENTS, CARD 1.	0.0	

EQUIPMENT/VESSEL CONTENTS, CARD 4

(FORMAT 10F8.2) VGAS3(JE), (JE = 1, MJE)

Col.(s)	Variable	Data Description	Default Value	Maximum Value
1-8 every 8	VGAS3	Volume of gas (ft^3) inside Vessel Type 3 (IE = 3, pressurized liquid containers). See EQUIPMENT/ VESSEL CONTENTS CARD 1.	0.0	

EQUIPMENT/VESSEL CONTENTS, CARD 5

(FORMAT 10F8.2) WH2O3(JE), (JE = 1, MJE)

Col.(s)	Variable	Data Description	Default Value	Maximum Value
1-8 every 8	WH2O3	Moisture content (pounds) inside Vessel Type 3. See EQUIPMENT/ VESSEL CONTENTS, CARD 1.	0.0	

EQUIPMENT/VESSEL CONTENTS, CARD 6

(FORMAT 10F8.2) FVOL(JE), (JE = 1, MJE)

Col.(s)	Variable	Data Description	Default Value	Maximum Value
1-8 every 8	FVOL	Liquid volume (ft^3) inside Vessel Type 4 (IE = 4, open liquid containers). See EQUIPMENT/VESSEL CONTENTS, CARD 1.	0.0	

EQUIPMENT/VESSEL CONTENTS, CARD 7

(FORMAT 10F8.2) TE1(JE), (JE = 1, MJE)

Col.(s)	Variable	Data Description	Default Value	Maximum Value
1-8 every 8	TE1	Initial surface temperature (°F) of equipment or Vessel Type 2 (IE = 2, pressurized containers). See EQUIPMENT/VESSEL CONTENTS, CARD 1.	0.0	

EQUIPMENT/VESSEL CONTENTS, CARD 8

(FORMAT 10F8.2) TE2(JE), (JE = 1, MJE)

Col.(s)	Variable	Data Description	Default Value	Maximum Value
1-8 every 8	TE2	Initial surface temperature (°F) of equipment or Vessel Type 2 (IE = 2, pressurized containers). See EQUIPMENT/VESSEL CONTENTS, CARD 1.	0.0	

EQUIPMENT/VESSEL CONTENTS, CARD 9

(FORMAT 10F8.2) TE3(JE), (JE = 1, MJE)

Col.(s)	Variable	Data Description	Default Value	Maximum Value
1-8 every 8	TE3	Initial surface temperature (°F) of equipment or Vessel Type 3 (IE = 3, pressurized liquid containers). See EQUIPMENT/VESSEL CONTENTS, CARD 1.	0.0	

EQUIPMENT/VESSEL CONTENTS, CARD 10

(FORMAT 10F8.2) TE4(JE), (JE = 1, MJE)

Col.(s)	Variable	Data Description	Default Value	Maximum Value
1-8 every 8	TE4	Initial surface temperature (°F) of equipment or Vessel Type 4 (IE = 4, open liquid containers). See EQUIPMENT/VESSEL CONTENTS, CARD 1.	0.0	

EQUIPMENT/VESSEL CONTENTS, CARD 11

(FORMAT 10F8.2) TI2(JE), (JE = 1, MJE)

Col.(s)	Variable	Data Description	Default Value	Maximum Value
1-8 every 8	TI2	Initial inside temperature (°F) of equipment or Vessel Type 2. See EQUIPMENT/VESSEL CONTENTS, CARD 1.	0.0	

EQUIPMENT/VESSEL CONTENTS, CARD 12

(FORMAT 10F8.2) TI3(JE), (JE = 1, MJE)

Col.(s)	Variable	Data Description	Default Value	Maximum Value
1-8 every 8	TI3	Initial inside temperature (°F) of equipment or Vessel Type 3. See EQUIPMENT/VESSEL CONTENTS, CARD 1.	0.0	

EQUIPMENT/VESSEL CONTENTS, CARD 13

(FORMAT 10F8.2) TL(JE), (JE = 1, MJE)

Col.(s)	Variable	Data Description	Default Value	Maximum Value
1-8 every 8	TL	Initial liquid temperature (°F) of Vessel Type 4. See EQUIPMENT/ VESSEL CONTENTS, CARD 1.	0.0	

EQUIPMENT/VESSEL CONTENTS, CARD 14

(FORMAT 10F8.2) PF2(JE), (JE = 1, MJE)

Col.(s)	Variable	Data Description	Default Value	Maximum Value
1-8 every 8	PF2	Failure (or rupture) pressure (psia) of equipment or Vessel Type 2. See EQUIPMENT/VESSEL CONTENTS, CARD 1.	0.0	

EQUIPMENT/VESSEL CONTENTS, CARD 15

(FORMAT 10F8.2) PF3(JE), (JE = 1, MJE)

Col.(s)	Variable	Data Description	Default Value	Maximum Value
1-8 every 8	PF3	Failure (or rupture) pressure (psia) of equipment or Vessel Type 3. See EQUIPMENT/VESSEL CONTENTS, CARD 1.	0.0	

ADDITIONAL FLOW PATH DATA CARDS

Description cards of the additional flow paths into the fire compartment. The number of cards required is equal to the number of flow paths, NFP (SCENARIO CONTROL SPECIFICATIONS, CARD 2). If NFP = 0, no cards are required.

(FORMAT 4F10.2) TFP(IFP), HFP(IFP), PFP(IFP), DFP(IFP), (IFP = 1, NFP)

Col.(s)	Variable	Data Description	Default Value	Maximum Value
1-10	TFP	Failure times (s) of the additional flow paths to the fire compartment during the course of the fire.	0.0	
11-20	HFP	Heights (ft) of the additional flow paths.	0.0	
21-30	PFP	Pressures (psia) at the outlets of the additional flow paths to the compartment.	0.0	
31-40	DFP	Diameters (ft) of the additional flow paths to the compartment.	0.0	

RADIOACTIVE SOURCE IDENTIFIER CARD

(FORMAT 7I10) NRAD(J), (J= 1, 7)

Col.(s)	Variable	Data Description	Default Value	Maximum Value
1-10 11-20 21-30 31-40 41-50 51-60 61-70	NRAD	Number of radioactive source terms that will be generated under the Jth type of release mechanism. J is the numeric identifier for the total of seven types of radioactive release mechanisms described in Table VI. Zeros are required to fill in the format of seven integers if the mechanism(s) is/are not involved. Thus, NRAD(1) = 2 denotes that there are two radioactive source terms resulting from burning two types of contaminated combustible solids. The values specified for NRAD(J) are the numbers of physical cards required for the next nine card types.	0	

CONTAMINATED COMBUSTIBLE SOLID IDENTIFIER CARD

Number of this card type is governed by NRAD(1) (RADIOACTIVE SOURCE IDENTIFIER CARD). If NRAD(1) = 0, no cards are required

(FORMAT 4I10) IFORM, I, JACT, IBO

Col.(s)	Variable	Data Description	Default Value	Maximum Value
1-10	IFORM	The physical form of radioactive contaminant found on the combustible solid. IFORM = 1 (powder) IFORM = 2 (liquid)	0	
11-20	I	The numeric identifier for types of combustible materials, where I = 1, 9. See Table IV for the combustible materials and their corresponding numeric identifiers.	0	
21-30	JACT	Any integer ranging from 1 to 20 assigned to a source term for identification among other possible source terms in a single fire scenario. Up to 20 radioactive source terms can be tracked.	0	20
31-40	IBO	The burning order of the contaminated combustible solids. See descriptions for FUEL SOURCE TERMS DATA CARDS.	0	

CONTAMINATED COMBUSTIBLE SOLID MASS CARD

Number of this card type is governed by NRAD(1) (RADIOACTIVE SOURCE IDENTIFIER CARD). If NRAD(1) = 0, no cards are required.

(FORMAT E10.4) QRAD1

Col.(s)	Variable	Data Description	Default Value	Maximum Value
1-10	QRAD1	Estimated total mass (pounds) of radioactive material	0.0	

CONTAMINATED COMBUSTIBLE LIQUID IDENTIFIER CARD

Number of this card type is governed by NRAD(2) (RADIOACTIVE SOURCE IDENTIFIER CARD). If NRAD(2) = 0, no cards are required.

(FORMAT 4I10) IFORM, I, JACT, IBO

Col.(s)	Variable	Data Description	Default Value	Maximum Value
1-10	IFORM	The physical form of radioactive contaminant found on the combustible solid. IFORM = 1 (powder) IFORM = 2 (liquid)	0	
11-20	I	The numeric identifier for types of combustible materials, where I = 1, 9. See Table IV for the combustible materials and their corresponding numeric identifiers.	0	
21-30	JACT	Any integer ranging from 1 to 20 assigned to a source term for identification among other possible source terms in a single fire scenario. Up to 20 radioactive source terms can be tracked.	0	20
31-40	IBO	The burning order of the contaminated combustible solids. See descriptions for FUEL SOURCE TERMS DATA CARDS.	0	

CONTAMINATED COMBUSTIBLE LIQUID MASS CARD

Number of this card type is governed by NRAD(2) (RADIOACTIVE SOURCE IDENTIFIER CARD). If NRAD(2) = 0, no cards are required.

(FORMAT E10.4) QRAD2

Col.(s)	Variable	Data Description	Default Value	Maximum Value
1-10	QRAD2	Estimated total mass (pounds) of radioactive material	0.0	

CONTAMINATED SURFACE CARD

Number of this card type is governed by NRAD(3) (RADIOACTIVE SOURCE IDENTIFIER CARD). If NRAD(3) = 0, no cards are required.

(FORMAT I10, E10.4) JACT, QRAD3

Col.(s)	Variable	Data Description	Default Value	Maximum Value
1-10	JACT	See JACT, CONTAMINATED COMBUSITBLE SOLID IDENTIFIER CARD.	0	20
11-20	QRAD3	Estimated mass (pounds) of radioactive material on the surface heated by the fire.	0.0	

UNPRESSURIZED RADIOACTIVE LIQUID CARD

Number of this card type is governed by NRAD(4) (RADIOACTIVE SOURCE IDENTIFIER CARD). If NRAD(4) = 0, no cards are required.

(Format 2I10, E10.4) IVES, JACT, QRAD4

Col.(s)	Variable	Data Description	Default Value	Maximum Value
1-10	IVES	A number from 1 to 10 identifying up to 10 vessels of radioactive liquid.	0	10
11-20	JACT	See JACT, CONTAMINATED COMBUSTIBLE SOLID IDENTIFIER CARD.	0	20
21-30	QRAD4	Estimated mass (pounds) of radioactive material in the liquid	0.0	

PRESSURIZED RADIOACTIVE POWDER CARD

Number of this card type is governed by NRAD(5) (RADIOACTIVE SOURCE IDENTIFIER CARD). If NRAD(5) = 0, no cards are required.

(FORMAT 2I10, E10.4) IVES, JACT, QRAD5

Col.(s)	Variable	Data Description	Default Value	Maximum Value
1-10	IVES	A number from 1 to 10 identifying up to 10 vessels of radioactive powder.	0	10
11-20	JACT	See JACT, CONTAMINATED COMBUSTIBLE SOLID IDENTIFIER CARD.	0	20
21-30	QRAD5	Estimated mass (pounds) of radioactive material in the liquid	0.0	

PRESSURIZED RADIOACTIVE LIQUID CARD

Number of this card type is governed by NRAD(6) (RADIOACTIVE SOURCE IDENTIFIER CARD). If NRAD(6) = 0, no cards are required.

(FORMAT 2I10, E10.4) IVES, JACT, QRAD6

Col.(s)	Variable	Data Description	Default Value	Maximum Value
1-10	IVES	See IVES, UNPRESSURIZED RADIOACTIVE LIQUID CARD.	0	10
11-20	JACT	See JACT, CONTAMINATED COMBUSTIBLE SOLID IDENTIFIER CARD.	0	20
21-30	QRAD6	Estimated mass (pounds) of radioactive material in the liquid	0.0	

RADIOACTIVE PYROPHONIC SOLID CARD

Number of this card type is governed by NRAD(7) (RADIOACTIVE SOURCE IDENTIFIER CARD). If NRAD(7) = 0, no cards are required.

(FORMAT 2I10, 2E10.4) JACT, IBO, QRAD7, SQ

Col.(s)	Variable	Data Description	Default Value	Maximum Value
1-10	JACT	See JACT, CONTAMINATED COMBUSTIBLE SOLID IDENTIFIER CARD.	0	20
11-10	IBO	See IBO, CONTAMINATED COMBUSTIBLE SOLID IDENTIFIER CARD.	0	MIBO
21-30	QRAD7	Estimated mass (pounds) of metal burned.	0.0	
31-40	SQ	Size (pounds) of radioactive metal.	0.0	

TIME STEP CARDS

The time span is separated into domains. Each domain may have different time-step sizes and edit intervals, and one card is required per domain. At least one card must be entered.

(FORMAT 10X, 4E10.0) DTMAX, TEND, EDINT

Col.(s)	Variable	Data Description	Default Value	Maximum Value
11-20	DTMAX	Time step size (s) for this time domain	0.0	
21-30	TEND	End of this time domain (s)	0.0	
31-40	EDINT	Print edit interval (s) for this domain	0.0	
41-50	FRFINT	Graphics interval	0.0	

TABLE IV

COMBUSTIBLE MATERIALS FOR THE FIRE COMPARTMENT

Material No.	Combustible Material
1	Polymethylmethacrylate
2	Polystyrene
3	Polyvinylchloride
4	Polychloroprene
5	Cellulose (Oak)[a]
6	Cellulosic Material
7	Kerosene
8	User's Option
9	User's Option

[a]Oak was selected to represent wood products based on the extensive information available.

TABLE V

NONCOMBUSTIBLE MATERIAL OPTIONS FOR THE FIRE COMPARTMENT

Material No.	Noncombustible Material
1	Concrete
2	Fire brick
3	Stainless Steel
4	Steel
5	Aluminum
6	Copper
7	Brass
8 to 15	User's Option

TABLE VI

SUBROUTINES FOR ESTIMATING RADIOACTIVE RELEASES

Subroutine Name	J	Release Mechanism[a]
RST1	1	Burning of contaminated combustible solids
RST2	2	Burning of contaminated combustible liquids
RST3	3	Heating of contaminated surface
RST4	4	Heating of unpressurized radioactive liquids
RST5[b]	5	Pressurized releases of radioactive powders
RST6[b]	6	Pressurized releases of radioactive liquids
RST7	7	Burning of radioactive pyrophonic metals

[a]Spilling of radioactive materials has yet to be incorporated into FIRIN1.
[b]A release factor is used to model pressurized releases at this time. A more realistic model is currently under development and will be incorporated when completed.

D. Input Processing

Before the system response to the selected transients can be calculated, the FIRAC input information must be examined by the input processor subroutine. The information supplied to the input processor (subroutine INPROC) is obtained from the user-prepared input deck FIN. As the input is retrieved from the input file, the user-selected input parameters are checked to ensure the problem set-up is consistent. If inconsistencies are found, diagnostic or error messages will appear in the output file FOUT and locally on the user's terminal. Typically, the error messages reveal the type of input error and its location when corrections are needed. Several input diagnostic messages and examples are shown in Sec. IV.

E. Output Processing

The improved FIRAC code produces seven primary output files: FOUT, PRINT1, PRINT2, PRINT3, RST, TAPE10, TAPE14 (shown in Fig. 13) and three secondary output files: TAPE11, TAPE13, and FCOMP. Tables VII and VIII present a description of the information stored on each primary and secondary output file, respectively. The first five primary output files listed are in a printed format

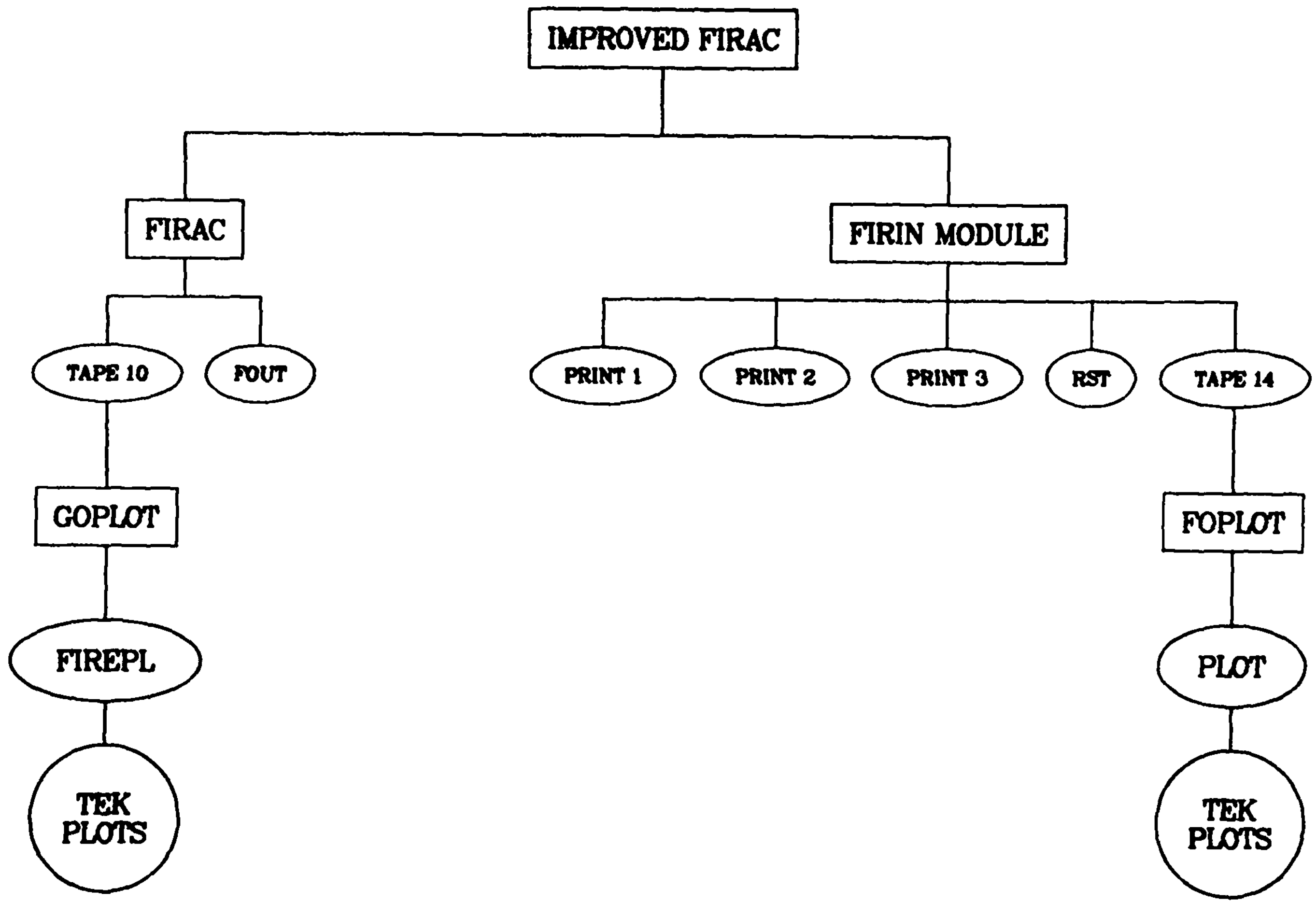

Fig. 13.
Improved FIRAC primary output files.

TABLE VII

PRIMARY OUTPUT DATA FILES

File Name	Subroutine(s) Generating Information	Type of Information Stored/File Purpose
FOUT	OUTPROC	System gas dynamic and material transport parameters
PRINT1	FIRIN	Fire compartment parameters
PRINT2	FIRIN	Fire source term parameters
PRINT3	FIRIN	Fire compartment particulate at flow boundaries
RST	FIRIN	Radioactive source term parameters
TAPE10	OUTPROC	File used for FOUT-line-printer processed graphics of gas dynamic and material transport parameters
TAPE14	TFNS and FIRIN	File used for post-processed graphics of fire compartment parameters

TABLE VIII

SECONDARY OUTPUT DATA FILES

File Name	Subroutine(s) Generating Information	Type of Information Stored/File Purpose
TAPE11	GCOMP	File used for post-processed graphics of gas dynamic and material transport parameters
TAPE13	OUTFLE and WPSPEC	File used for conversion of system gas dynamic and material transport parameters
FCOMP	FIRIN	Additional fire compartment parameters

and contain helpful information for analyzing and possibly debugging the calculation. FOUT presents the gas dynamic parameters plus material concentrations, mass fractions, material flow rates, and material accumulations. The pressures, temperatures, and densities are calculated at nodal points; volume flows, mass flows, pressure differentials, and heat transfer parameters are calculated for branches. The material concentrations and mass fractions are calculated at nodal points, but the material flow rates and the amount passing through branches or the accumulations on filters are calculated for branches. A complete table of pressures, temperatures, and flows always is given for the first and last calculation time step. These "archival data" also are broken down into component pressures and flows. Filter material accumulation data are given for all filters in the system in tabular form. Pressures, temperatures, and mass and volume flows are available on time plots if requested in the program control section of the input.

A summary of extreme values spanning the entire period of the problem is produced at the end of the problem. Pressures and flows are inspected at each time step during the calculation in compiling data for this list so that extreme values are not missed by poor selection of output frequency. Frequently, one might wish output lists for a specific point in time not covered in the selection of output frequency. A maximum of five special output times may be selected. These special output times do not appear in the printer plots because the points must be equidistant in time. The printed data are broken down into the following 14 categories.

- A-I An exact listing (echo) of the input file
- A-II A summary of the controlling information and any diagnostics for missing or inconsistent data
- A-III A summary of problem parameters
- A-IV A summary of model parameters
- A-V A summary of nodal information (type, initial pressure, and connecting branches)
- A-VI Dimensionless friction factors and critical mach numbers for choking
- A-VII Filter branch data
- A-VIII Blower branch data
- A-IX Summary of solution parameters

A-X Archival list of output parameters

A-XI Breakdown of archival data according to component type

A-XII Pressure differential between rooms

A-XIII Summary of extreme values for calculation time (step)

A-XIV Summary of extreme values for entire problem

The PRINT family of files (PRINT1, PRINT2, and PRINT3) contains the FIRIN-calculated results for the fire compartment. PRINT1 presents the volumetric flow rates at the boundaries, the average hot-layer temperature, the hot-layer thickness, the oxygen concentration near the burning material, and the compartment pressure. The fire source term information on PRINT2 contains the total smoke and soot generation rates, the total mass loss rate from burning combustible materials, the total heat rate to the gases, and the total heat loss rate to the surrounding heat sinks in the compartment. PRINT3 presents the smoke, soot, and radioactive mass at the flow boundaries. The FIRIN radioactive source term output file RST contains mass flow rates for each radioactive particle size distribution and the total mass flow rate of radioactive particles released by the fire. Table IX summarizes the FIRIN-generated output information for the four FIRIN output files. The output frequency for the FIRIN output is specified in the FIRIN data section of the input file.

A sample of the FIRAC and FIRIN output is found in Appendix E. The FOUT sample includes all output from the code in reaching a steady-state solution and the output from the last time step.

If plots are requested in the problem control data block, TAPE10 and TAPE11 will be generated and will contain information for the FOUT line printer plotting package and the post-processed graphics program GOPLOT. For the line printer plots, a maximum of 25 frames can be requested with a maximum of 4 curves per frame. Each curve is identified by an alphabetic character A through D. Overlapping curves are shown by the character X at the point of overlap. The program partially fills the plot frame page when the number of output times is sparse by spacing with blank lines between points. The extreme value summaries can serve as valuable guides in selecting the node or branch candidates for plotting. Further, the final extreme value summary can be checked for missing extrema on the plots. Printer plots are not precise; however, they can give the analyst a good picture of the system response.

TABLE IX

FIRIN OUTPUT INFORMATION

File	Variable	Description
PRINT1		
	PCOMP	Fire compartment pressure (atm)
	FMO2	Oxygen concentration near the burning objective
	ZHL	Thickness of the hot layer (m)
	VIF	Volumetric flow rate (m^3/s) at the inlet ventilator
	VOF	Volumetric flow rate (m^3/s) at the outlet ventilator
	THLUC	Average temperature in the hot layer (°F)
PRINT2		
	TIME	Fire transient real time (s)
	QLOSSN	Total heat loss rate (10^{-3} Btu/h) to equipment, vessels, walls, ceiling and floor from a fire (negative indicates heat loss)
	TQNET	Total heat rate (10^{-3} Btu/h) to the gases from a fire (negative indicates heat loss or heat transfer from the gases)
	TSMOKN	Total smoke generation rate (g/s) from burning of combustible materials
	TSOOTN	Total soot generation rate (g/s) from burning of combustible materials. TSOOTN is fraction of TSMOKN
	TMASSN	Total mass loss rate (10^{-3} lb/h) from burning combustible materials
PRINT3		
	WSMIF	Smoke (g) at the inlet
	WSOIF	Soot (g) at the inlet
	WRADIF	Radioactive materials (g) at the inlet
	WSMOF	Smoke (g) at the outlet
	WSOOF	Soot (g) at the outlet
	WRADOF	Radioactive materials (g) at the outlet

TABLE IX (CONT)

File	Variable	Description
RST		
	JACT	Source term identifier allowing isotopes with different levels of activity to be traced (for example, JACT = 2 could indicate radioactive particles form heating contaminated surfaces, whereas JACT = 1 could indicate particles given off from the burning gloves). Mass rate is given for the particle size bins indicated in the output file. In this way, the particle size distribution for the radioactive source terms is provided.
	TOTAL	Total mass rate (g/s) of radioactive particles given off in a fire. It is the sum of the mass rates of all size ranges.

TAPE10 contains FIRAC-generated output data formatted for using the GOPLOT graphics post-processor program. GOPLOT uses the DISSPLA library and other Los Alamos computing system libraries to produce the graphic results and is compiled with the FORTRAN-4 extended language compiler. This compiler is available under control of the CDC 7600 computer and produces a controller (or absolute binary file) that can be executed on the Livermore Time Sharing System (LTSS). GOPLOT produces a binary output file, FIREPL, that can be examined by the Los Alamos utility PSCAN on a graphics terminal. The plots requested in the problem control data for the line printer plots will produce the data for the more precise plots that can be created by GOPLOT automatically. The line printer plots and the GOPLOT-generated plots are identical in content and format.

The FIRIN-generated output written to TAPE14 can be post-processed by the FOPLOT graphics program. TAPE14 will be generated only if FIRIN is selected to simulate the fire transient. FOPLOT uses the DISSPLA library and other Los Alamos computing system libraries to produce the graphic results. FOPLOT also is compiled with the FORTRAN-4 extended language compiler. FOPLOT produces a binary output file PLOT that can be viewed on a high-resolution graphics terminal by the Los Alamos utility PSCAN. The information written to TAPE14 is rigidly formatted. That is, the user has no control over the number and types of plots that will be generated. The user can specify only the edit frequency by using the print edit frequency parameter in the FIRIN data block. Table X presents the order and descriptions of the plots that are generated automatically in the FIRIN module.

TABLE X

AVAILABLE PLOTS FROM FIRIN PLOTTING PACKAGE

Plot No.	Description
1	Hot layer height vs time
2	Fire compartment pressure vs time
3	Oxygen concentration vs time
4	Carbon dioxide concentration vs time
5	Carbon monoxide concentration vs time
6	Total smoke concentration vs time
7	Total radioactive particle concentration vs time
8	Radioactive particle concentrations (size distributions <0.1 to 0.8 μm) vs time
9	Radioactive particle concentrations (size distributions 0.8 to 4 μm) vs time
10	Radioactive particle concentrations (size distributions 8 to >20 μm) vs time
11	Fuel mass vs time
12	Fuel burning rate vs time

Because GOPLOT and FOPLOT use and require Los Alamos computing facility libraries and utilities, we recommend that these graphics post-processors not be used unless the user has access to LTSS.

F. Diagnostic Messages

Diagnostic (warning or error) messages are provided to help the user isolate possible input data or modeling errors. In most cases, the error is easily discerned from the message; however, out-of-order or missing cards tend to produce confusing messages. In these cases, a careful check of the input return list and a review of input specifications (Sec. IV.C.) usually can isolate the problem.

Diagnostic messages are produced during input processing or the system solver calculations; hence, there is no set pattern to their location in the output. ***DIAGNOSTIC MESSAGES always precedes these messages, and if the error is fatal, either ERROR WITH INPUT CAN'T CONTINUE or ****FATAL ERROR**** SEE PREVIOUS MESSAGES is printed following the message. See Fig. 14 for an example of the mixture of informative (nonfatal) messages and fatal error messages that can occur.

G. FIRAC Programming Details

This code was developed to be executed on the CDC 7600 computing system. The FORTRAN source code consists of 9149 lines of coding and is compiled with the FORTRAN-4 extended language compiler on LTSS. This compiler is available under control of the SCOPE 2 system for the CDC 7600 computer and produces a controllee (or absolute binary file) that requires 154 713 words of SCM and 275 040 words of LCM to execute on LTSS.

In addition to the above required storage capacity, 11 additional disk files [10 formatted (BCD) and 1 unformatted (binary)] are used. The names of these files, their types, and brief descriptions of their functions are shown in Table XI.

```
BRANCH  6 FLOW NEGATIVE, UP AND DOWN-STREAM NODES 6 5 REVERSED BY PROGRAM
----------------------PRESSURES READ IN (NOT CALC, FROM DP)
     INPUT RESISTANCE    1.00000E-04  USED FOR BRANCH          4
     INPUT RESISTANCE    6.94400E-07  USED FOR BRANCH          5
CAN'T CALC. RESISTANCE (SET TO MIN. VALUE) FOR BRANCH          6
     INPUT RESISTANCE    6.94400E-07  USED FOR BRANCH         13
     INPUT RESISTANCE    1.42800E-03  USED FOR BRANCH         14
     INPUT RESISTANCE    6.94400E-07  USED FOR BRANCH         23
     INPUT RESISTANCE    3.08600E-07  USED FOR BRANCH         24
BRANCH COUNT IMPOSSIBLE FOR NODE   1   COUNT =  1
BRANCH COUNT IMPOSSIBLE FOR NODE  25   COUNT =  1
******FATAL ERROR*****SEE PREVIOUS MESSAGES
```

Fig. 14.
Example of a multiple diagnostic list.

TABLE XI

NAME, TYPE, AND PURPOSE OF THE 11 FILES USED IN CODE EXECUTION

Name	Type	Purpose
FIN	BCD	User-prepared input file.
FOUT	BCD	Code-generated output file. Code results are contained in this file.
PRINT1	BCD	FIRIN output data from compartment effects (compartment history).
PRINT2	BCD	FIRIN output data from file source terms computation.
PRINT3	BCD	FIRIN output data from compartment effects (filter accumulations).
RST	BCD	FIRIN1 output data from radioactive source temporary file.
FCOMP	BCD	Additional FIRIN fire compartment output data.
TAPE10	BCD	Output for FIRAC graphics package.
TAPE13	Binary	Temporary file.
TAPE14	BCD	Output for FIRIN graphics package.
TAPE59	BCD	Code-generated output file. Brief error messages are contained in this file if abnormal termination of the run has occurred.

To allow a high degree of interchangeability of this code for other operating systems, US standard FORTRAN language has been used wherever practicable. We have identified five procedures used in the code that are not necessarily required to be supplied by the compiler in US Standard FORTRAN. In most cases, the majority of these programs will be included in a standard FORTRAN complier. To facilitate conversion of this code to other systems, information concerning these five programs is given in Table XII. These programs conveniently are divided into two catagories and are not required to be included in standard FORTRAN compilers but are included in the FORTRAN-4 extended language compiler.

TABLE XII

SUBROUTINES THAT ARE STANDARD IN FORTRAN-4 EXTENDED

Program Name and Arguments	Called from Subroutine	Purpose
EOF (LUN)	IEOF	Routine to test for end of file. LUN--Logical unit number EOF--1—End of file or end of information encountered on unit LUN —0--No end of file or end of information encountered on unit LUN
MOVLEV(SOURCE,SINK,NW)	SCCOPY	Routine to copy contiguous blocks of data. SOURCE—First word address of source data block. SINK--First word address of sink data block. NW--Number of words to be copied.
DATE (IDATE)	MAIN	Routine to return the current date IDATE--current date in the form 10H mm/dd/yy, where mm is the number of the month, dd is the number of the day within the month, and yy is the year.
TIME (ITIME)	MAIN	Routine to return the current reading of the system clock. ITIME—current time in the form 10H hh.mm.ss, where hh, mm, and ss are the number of hours, minutes, and seconds, respectively.
SECOND (CPTIME)		Routine to return the central processor time. CPTIME—the central processor time from start-of-job in seconds.

If any of these routines is not available, the brief description of their functions given in Table XII should allow the user to substitute an equivalent routine.

Dimensioned arrays used in the code limit the types of problems that may be run. The maximum size of key parameters has been selected as a compromise between absolute binary file size (63 400 words) and the ability to run realistic problems without modifying DIMENSION statements in the source code. Current input parameter limits defining restrictions on the code are listed in Table XIII. These restrictions can be modified easily by changing the DIMENSION statements within the source program.

Also, LTSS requires that several of the larger arrays be allocated to large core memory (LCM) with LEVEL 2 statements. The LEVEL 2 statement is applicable only to Control Data CYBER 170 Model 176, CYBER 70 Model 76, and CDC 7600 computers.

H. Compiling, Loading, and Executing Instructions

The compiling, loading, and executing procedures for the improved FIRAC source code on LTSS are outlined. The executing procedures for the graphics post-processor executable files GOPLOT and FOPLOT also are described. Even though the outlined procedures are specific to LTSS, a similar set of procedures exists for other computing systems. If the user plans to use LTSS to execute FIRAC, we recommend that the LTSS primer and LTSS user's guide be obtained from the Computing Division Documentation Group at Los Alamos.

1. Compiling and Loading the FIRAC Program. Before the improved code version can be compiled, loaded, or executed, the source file (program), which is supplied on magnetic tape, must be installed on the user's system. The user should contact the system's computing services information group to obtain the details of how a program written on a magnetic tape is placed on the system. When the program has been installed, the user should attempt to compile and load the program. A simple execute line called the ftn control statement is used to compile and load a FORTRAN program on LTSS. The control statement form recommended for LTSS is ftn (i = source, cname = exec).

TABLE XIII

MAXIMUM PROBLEM SIZE

System Parameter	Maximum No.
Branches	100
Nodes	100
Room	100
Blowers	40
Boundary nodes	10
Internal boundary nodes	3
Time functions of each type	5
Points per time function	50
Blower functions	15
Filter types	20
Points per blower function	20
Points per plot	100
Plots per frame	4
Frames	25
Number of particulate species information to be plotted	5

After the ftn statement is submitted, LTSS will respond with the following.

```
* * * running ftn compiler * * *
* ofile,source/pa.
* dfile,alistqz.
* cfile,alistqz/pr.
* dfile,atmpbin.
* cfile,atmpbin/ab.
* dfile,aqoqzzi.
* lfc(a,i=source,l=alistqz,lcm=i,z,b=atmpbin).
     14.164 cp seconds compilation time
* goto,1.
* 1,exit.
$ cpu time      14.350 sec
$ sys time       0.468 sec
$ i/o time      10.372 sec
$ total  =       0.419 minutes
* * * finished ftn compiler * * *
* * * lod summary * * *
code bloc       exec written
file size=   0162736   0030520
fld lgth=    0275536   0155411

 all done
```

The i parameter specifies the input file or program name. This file must be in packed-ASCII format. The cname parameter specifies the name of the absolute binary file (controllee) that will be loaded automatically. The name file is the file that will be used to execute the program. The sym parameter attaches the symbol table to the end of the controllee. The symbol table is necessary to debug the program if the program terminates as the result of an error (aborts).

The load summary indicated that the controller exec has been written. The first number in the file size line is the controller size; the second number is the symbol table size. The first number in the fld lgth line is the large-core field length; the second number is the small-core field length.

If FORTRAN errors are present, they can be located by examining the listftn file located in the user's local file space. If system-related errors (such as maximum file size exceeded) occur during the compilation or loading of the program, the user should contact the system's consultant office for assistance.

2. Executing the FIRAC Program. After the program has been loaded and compiled on the system without errors and the input deck has been created and placed in the user's local file space, the user can attempt to execute (run) the program. The program is executed simply by typing in the following statement.

```
exec
```

This executable file will run the program until the time limit specified for the execution has expired or until the simulation has been completed. A normal exit or termination for FIRAC is shown below.

```
 end of time step cards reached -- normal exit
 total iterations for problem ;  5887
    0 points written to the plot file
 stop ftn normal termination from main program
exec        ltss time   343.020 seconds
cpu=  286.301       i/o=    1.183       mem=   55.536

 all done
```

A summary of the compilation, loading, and execution procedures is shown in Table XIV. More information on computer time-limit requirements is presented in Sec. IV.J.

3. Executing the Graphics Post-Processors. The two graphic post-processor files, GOPLOT and FOPLOT, are absolute binary files (controllers) and therefore require no compilation and loading instructions. The programs are executed by typing in the file name. For example, to excute GOPLOT, the user would enter the following.

```
goplot
```

TABLE XIV

COMPILATION, LOADING, AND EXECUTION SUMMARY

```
 files
     27542r source
  all done


ftn (i=source,cname=exec,sym= )
* * * running ftn compiler * * *
* ofile,source/pa.
* dfile,alistqz.
* cfile,alistqz/pr.
* dfile,atmpbin.
* cfile,atmpbin/ab.
* dfile,aqoqzzi.
* lfc(a,i=source,l=alistqz,lcm=i,z,b=atmpbin).
      14.224 cp seconds compilation time
* goto,l.
* l,exit.
$ cpu time      14.410 sec
$ sys time       0.448 sec
$ i/o time      15.870 sec
$ total  =       0.512 minutes
* * * finished ftn compiler * * *
* * * lod summary * * *
code bloc       exec written

file size =  0162736   0030520
fld lgth  =  0275536   0155411

 all done

files
    162736r exec
    234571d lgo
```

```
    564566r listftn
      5513  map
    275424r source

all done

files
    162736r exec
      1251r fin
    234571d lgo
    564566r listftn
      5513  map
    275424r source

all done

exec
```

The excutable file goplot will run the program until the time limit specified for the execution has expired or until all the plot frames have been generated. A normal exit for GOPLOT is shown below.

```
firepl  done.  pages =    15.   words =     34852
graphics cl = u
 14 plot frames with   5 points for     representative facility
goplot     ltss time     13.358 seconds
cpu=   10.118     1/0=      1.562      mem= 1.679
```

In this example GOPLOT produced 14 plot frames consisting of 34 852 words. The 14 plot frames located in the file firepl can be examined with the LTSS utility PSCAN. Documentation on the PSCAN utility can be obtained from the computing facility documentation group at Los Alamos.

If the user elects to use the FIRIN graphics post-processor FOPLOT, the execution procedures outlined for GOPLOT should be followed. The results of FOPLOT are contained in a binary file named plot. This file can be examined by PSCAN also. A normal exit for FOPLOT is shown below.

```
PLOT      DONE.   PAGES =      14.   WORDS =      35316
GRAPHICS CL = U
   END FTN MAIN.
FOPLOT      LTSS TIME      15.373 SECONDS
CPU=   11.667      I/O=      2.053      MEM=      1.653

all done
```

Source files for GOPLOT and FOPLOT are not supplied to the user because the programs are constructed around Los Alamos computing facility libraries and utilities. These programs cannot be used unless the user has access to LTSS.

I. General User Hints and Suggestions

The suggestions and hints given in this section are divided primarily into the areas of input, output, and system modeling strategy.

The task of defining resistance coefficients (friction characteristics) for a system may be simplified and self-checked if the program is allowed to calculate these values from a "known" set of flows, pressures, and filter and blower characteristics for the system. The alternative approach is to prescribe a resistance coefficient for each branch separately. Such a set of data usually is referenced to a normal steady-state operating condition. In the case of a new system, information about the friction characteristics and flows must be estimated. This can be done using the method described in Appendix G. This approach usually allows the user to reach a steady-state solution the first time.

The amount of output obtained in the case of an abort caused by an input error depends on the time during the solution when this error is encountered. For example, an incorrect format specified in the input resulting from data being out of order will limit the output to Table A-I (echo of input). Modeling inconsistencies are diagnosed when the input echo is read in or when the input data are reworked before entering the solution. Appropriate messages are printed when this happens. An abort during the solution occurs when a particular time-step calculation fails to converge. A message to this effect is printed along with a partial dump of the mass flow rates, pressures, densities, and correction terms being used followed by a printout of Table A-VI through Table A-XII for time = 0.0 s and the last time step before the abort occurred.

The output is designed to help the user easily find discrepancies in the input that result in an incomplete or incorrect solution. For example, an echo of the input file is presented first to help uncover format errors. If the problem aborts at this point, some diagnostic messages follow that suggest possible reasons why this happened. When the input data are free of format errors and consistent, the program prepares for the solution. This preparation produces additional data that give the user an opportunity to check the accuracy of the input. This portion of the output also contains any default values. The steady-state and transient calculations are performed next. If a particular time-step calculation fails to converge, a dump of pertinent parameters and a list of possible reasons will be printed. The results of the previous time-step will be printed.

All the categories of data are printed automatically and cannot be suppressed or changed by the user. However, the user has control over the amount of output generated. Two options are available.

- If printed plots are requested, only the results from the first and last calculation times will be printed. This assumes that the plots will be sufficient for a cursory look at the results and that these very limited results are enough to bracket the solution.
- If prints of all the intermediate results are desired as well, the word "ALL" on the PRINT/PLOT CONTROL card will cause all the results to be output.

- Up to five special output times can be requested. This option serves two purposes: (1) it permits the user to specify outputs between the evenly spaced times computed by the program, and (2) it permits the printouts when the intermediate output times are suppressed.

If time, filter, and blower functions are not to be used in the described solution, they still may appear in the input if their existence is specified. This feature provides the flexibility that is especially useful in parametric studies.

J. Time and Cost Estimates

The CPU and problem times required for the two sample problems are compared below.

Sample Problem	CPU(s)	Problem Time(s)	Burn Time(s)	Number of Particulate Species	Branches	Nodes
1	1470	1000	~763	13	17	18
2	3575	1000	~810	13	37	22

The Sample Problem 1 CPU time was approximately one-half the CPU time required for Sample Problem 2 because of the differences in system model size. The Sample Problem 2 model required more than twice the number of branches than the system model for Sample Problem 1. If the user had elected to transport the total radioactive particulate species (instead of each individual particle size) for the Sample Problem 2 calculation, the CPU time would have been reduced ~10 .

V. SAMPLE PROBLEMS

A. Introduction

The Sample Problems are given to help the user prepare the input deck and implement several important user options. Sample Problem 1 illustrates the FIRIN module auto-ignition concept and the FIRAC duct heat transfer and material depletion options for a compartment fire in a simple facility as shown in

Fig. 15. The FIRIN sequential burning option for a compartment fire in a more complex facility (Fig. 16) is demonstrated in Sample Problem 2. Both ample problems predict releases from a compartment fire where radioactive materials are at risk. Sample Problem 1 predicts the release of material resulting from the heating of a contaminated surface and the burning of a contaminated combustible liquid. The radioactive release resulting from the burning of a contaminated combustible liquid is calculated in Sample Problem 2.

B. Sample Problem 1

1. Description and Computer Model of the Facility. This sample problem illustrates the application of the code to a simple ventilation system as shown in Fig. 15. This simple system is modeled after the Lawrence Livermore National Laboratory (LLNL) full-scale fire test facility. In this sample calculation, the fire compartment has a volume of approximately 5100 ft^3. The walls, ceiling, and floor of the compartment consist of an Al_2O_3 - S_1O_2 refractory material with the following properties.

	Walls	Ceiling/Floor
Density (lbm/ft^3)	89.90	119.90
(kg/m^3)	1440.00	1920.00
Thermal conductivity (Btu/ft h°F)	0.23	0.35
(W/m K)	0.41	0.63
Specific heat (Btu/lbm°F)	0.25	0.25
(J/kg K)	1046.00	1046.00

The fire compartment floor is assumed to be 3.3 ft (1.0 m) thick, and the ceiling and walls are assumed to be 0.5 ft (0.15 m) thick. The fire compartment has two flow boundaries. Fresh air drawn in by the blower enters the compartment near the floor, and air/combustion products are exhausted through a 26-$in.^2$ (0.017-m^2) duct located near the ceiling. A high-efficiency particulate air

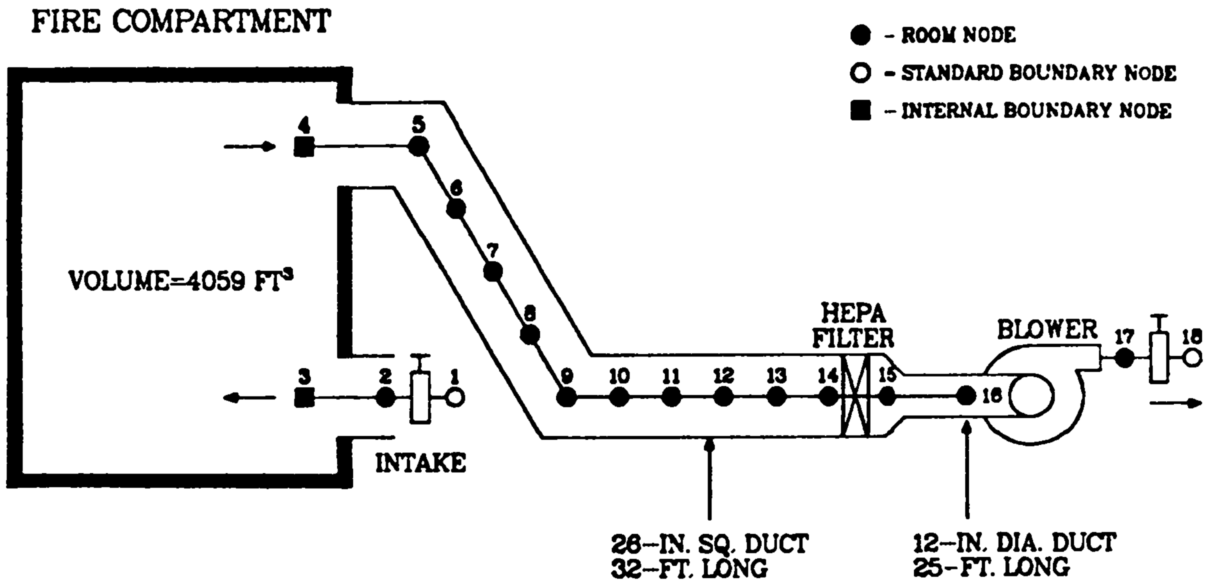

Fig. 15.
Schematic of the system used in sample problem 1.

REPRESENTATIVE FACILITY

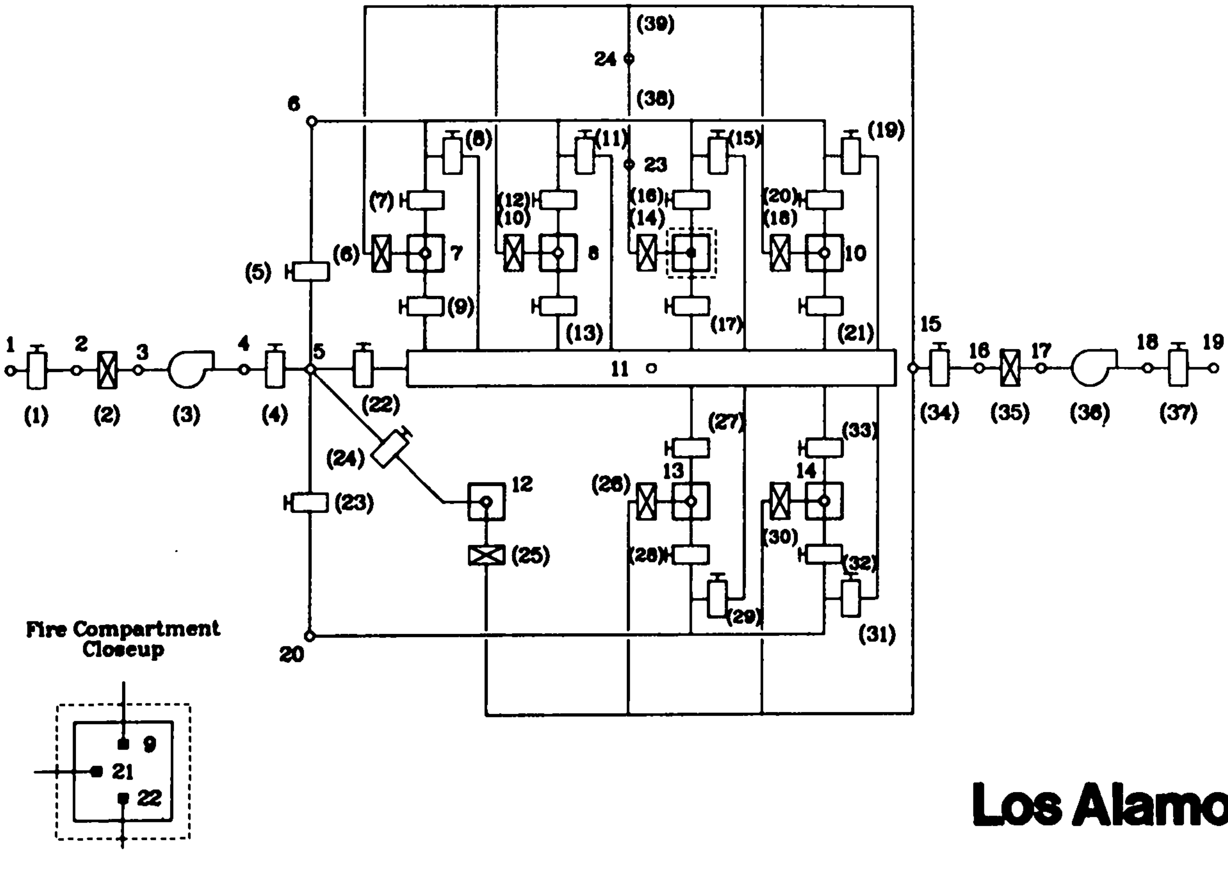

Los Alamos

Fig. 16.
Schematic of the system used in sample problem 2.

(HEPA) filter is located 32 ft (10 m) downstream of the fire compartment. A centrifugal blower with an exhaust damper is located approximately 25 ft (8 m) downstream of the HEPA filter. The filter and blower are connected by a 12-in. (0.30-m)-diam, 25-ft (8-m)-long duct. Air or combustion products passing through the damper are exhausted to the atmosphere. The 32-ft (9.75-m)-long duct is assumed to have 1/4-in. (6.3-mm)-thick steel walls; the 25-ft (8-m)-long duct is assumed to have 1/16-in. (0.16-mm)-thick steel walls.

Eighteen nodes and seventeen branches were used to model the facility. Nodes 1 and 18 are boundary nodes representing the assumed atmospheric conditions. Fourteen capacitance nodes were used to model the inlet to the fire compartment and the 32-ft (9.75-m)-long and the 25-ft (8-m)-long ducts. The fire compartment exhaust duct [32-ft (9.75-m)-long] is finely noded (11 nodes) to predict the temperature distribution between the fire compartment and the HEPA filter. The volume specified for each of the capacitance nodes is shown in Table XV. Note that the 26-in.^{2} (0.017-m^2) duct volume is distributed equally between 11 duct nodes, and the 12-in. (0.30-m)-diam round duct volume is distributed equally between nodes 16 and 17. The 17 branches used to connect adjacent nodes consist of 13 ducts, 2 dampers, 1 filter, and 1 blower. The branch types, along with their related flow and heat-transfer areas, are shown in Table XVI. The blower characteristic curve for this problem is shown in Table XVII.

Because the FIRIN module will be used to simulate the nonradioactive and radioactive source terms, two internal boundary nodes (nodes 3 and 4) were used to represent the fire compartment. The important fire compartment input parameters are outlined in Table XVIII.

In addition to the above information, a description of the system initial conditions as described in Sec. IV is required. The steady state of the system may be obtained by prescribing branch resistances, the nodal pressures, or a combination of branch resistances and nodal pressures. For this sample problem description, an assumed pressure distribution and user-prescribed branch resistances were used to obtain a steady-state solution. This information represents a data base sufficient for the code to establish a consistent steady state of all the calculated variables corresponding to any ambient temperature (56°F for this sample problem). A complete listing of the computer code input file (FIN) used to execute Sample Problem 1 is shown in Table XIX.

TABLE XV

INITIAL DATA FOR EACH NODE

Node	Volume (ft^3)	Initial Pressure (in. w.g.)
1	*	0.0
2	1.00	-0.06
3	*	0.0
4	*	0.0
5	13.64	-0.02
6	13.64	-0.04
7	13.64	-0.06
8	13.64	-0.08
9	13.64	-0.10
10	13.64	-0.12
11	13.64	-0.14
12	13.64	-0.16
13	13.64	-0.18
14	14.64	-0.20
15	13.64	-1.165
16	9.80	-1.365
17	9.80	0.035
18	*	0.0

*Boundary node - no volume specified.

TABLE XVI

BRANCH DATA

Branch No.	Branch Type	Flow Area (ft^2)	Heat-Transfer Area (ft^2)
1	Damper	4.6940	0.0
2	Duct	4.6940	0.0
3	Duct	4.6940	27.8
4	Duct	4.6940	27.8
5	Duct	4.6940	27.8
6	Duct	4.6940	27.8
7	Duct	4.6940	27.8
8	Duct	4.6940	27.8
9	Duct	4.6940	27.8
10	Duct	4.6940	27.8
11	Duct	4.6940	27.8
12	Duct	4.6940	27.8
13	Filter	0.7854	0.0
14	Duct	0.7854	78.5
15	Blower	0.7854	0.0
16	Damper	0.7854	0.0

TABLE XVII

DIGITIZED BLOWER CHARACTERISTIC CURVE
FOR SAMPLE PROBLEM

Volumetric flow (ft^3/min)	Head (in. w.g.)
-8000	8.0
0	1.8
1123	1.5278
6000	0.0

TABLE XVIII

FIRIN INPUT PARAMETERS FOR SAMPLE PROBLEM 1

Parameter(s)	Value(s)	Description(s)/Comment(s)
IPRINT	100	Edit frequency for FIRIN output
MIBO	2	Number of burning orders
IGNITE	1	Ignition energy concept option—this requires MIBO = 2
PFLOW, NFP EQUIP, MJE, IFLOW3	0	These options were not used for this calculation
TENIT	56.0	Initial fire compartment temperature (°F)
PINIT	-0.20	Initial fire compartment pressure (in. w.g.)
IBRCHI	2	Fire compartment inflow branch identities
IFCND1	3	Fire compartment internal boundary node connected to IBRCHI
ZIF	1.084	Elevation if the centerline plane of the inlet ventilation from the compartment floor (ft)
DIF	2.166	Diameter of the inlet ventilator (ft)
IBRCHO	3	Fire compartment outflow branch identifier
IFCND2	4	Fire compartment internal boundary node connected to IBRCHO
ZOF	11.76	Elevation of the centerline plans of the outflow ventilator from the compartment floor (ft)
DOF	2.166	Diameter of the outflow ventilator (ft)
FUEL(7,1)	5.75	Amount of kerosene fuel—burning order 1 (lbm)
FUEL(7,2)	2.16	Amount of kerosene fuel--burning order 2 (lbm)
AREC(7,1)	4.0	Burn area of fuel--burning order 1 (ft^2)
AREC(7,2)	2.0	Burn area of fuel--burning order 2 (ft^2)
RL	20.0	Fire compartment length (ft)

TABLE XVIII (CONT)

Parameter(s)	Value(s)	Description(s)/Comment(s)
WR	17.0	Fire compartment width (ft)
ZR	15.0	Fire compartment height (ft)
XCEIL	0.492	Ceiling thickness (ft)
XWALL	0.492	Wall thickness (ft)
XFLOOR	3.281	Floor thickness (ft)
ZFIRE	0.452	Height of the flame base from the floor (ft)
MATERW	8	Wall material identifiers
MATERF	9	Floor material identifier
NBO(1-6)	2	Combustibles at risk to auto-ignition concept identifier. NBO = 2 signifies the combustible is not at risk, NBO = 1 signifies the combustible is at risk to auto-ignition
NBO(7)	1	
NBO(8-9)	2	
NRAD(1,4-7)	0	Radioactive release mechanism identifiers: NRAD = 0 indicates that these release mechanisms will not be used, NRAD(2) = NRAD(3) = 1 indicates that the second and third release mechanisms will be used
NRAD(2)	1	
NRAD(3)	1	
IFORM	1	The following fire input values correspond to the NRAD(2) release mechanism. IFORM = 1 indicates that the contaminant found on the combustible is in powder form. I = 7 indicates that fuel type 7 (kerosene) is a contaminated combustible. JACT = 1 identifies the source term and IBO = 2 indicates the burning order of the contaminated combustible. QRAD 1 = 0.2205 specifies the total mass of radioactive material in/on the combustible.
I	7	
JACT	1	
IBU	2	

TABLE XVIII (CONT)

Parameter(s)	Value(s)	Description(s)/Comment(s)
QRAD1	0.2205	
JACT	2	The last two FIRIN input values describe the NRAD(3) release mechanism. JACT = 2 is the identifier associated with the source term and QRAD3 = 0.1653 specifies the total mass of radioactive material on the contaminated surface.
QRAD3	0.1653	

TABLE XIX

COPY OF INPUT DECK USED TO RUN
SAMPLE PROBLEM 1

```

 sample problem 1
#               run control card 1
   st          1.   999.0
#               print / plot control card
 all     2      1     1     2     5
    1    1      1
    2    1      1
    3    1      1
   10    1      1
   13    1      1
#               plot frame description card
    4    2      3     4     5
    4    4     14    15    17
    4    2      3    13    15
    4    2      3     8    15
    4    2      3     4     5
    4    9     14    16    17
    4    2      3    13    14
    4    2      3    13    14
    4    2      3    13    14
    4    2      3    13    14
    4    2      3    13    14
    4    2      3    13    14
    4    2      3    13    14
    4    2      3    13    14
    4    2      3    13    14
    4    2      3    13    14
#               run control card 2                     "1f1r1n"
                              t                          0          0    13
#               boundary control card
    0    4                   56.
#               geometry and component control card
   16   18          14     1     1
#               branch description data cards
    1    1      2      1200.    4.6944    .25    v         .06

    2    2      3      1200.    4.6944    .25    d         .14
9.5000e-08
    3    4      5      1200.    4.6944    3.2    d         .02
 1.389e-08                                               2.1666    6.9333        1
   2.167   27.77        1       .25       .3      .3   26.2    489.     .12      56.
    4    5      6      1200.    4.6944    3.2    d         .02
                                                         2.1666    6.9333        1
   2.167   27.77        1       .25       .3      .3   26.2    489.     .12      56.
    5    6      7      1200.    4.6944    3.2    d         .02
                                                         2.1666    6.9333        1
   2.167   27.77        1       .25       .3      .3   26.2    489.     .12      56.
    6    7      8      1200.    4.6944    3.2    d         .02
                                                         2.1666    6.9333        1
   2.167   27.77        1       .25       .3      .3   26.2    489.     .12      56.
    7    8      9      1200.    4.6944    3.2    d         .02
                                                         2.1666    6.9333        1
   2.167   27.77        1       .25       .3      .3   26.2    489.     .12      56.
    8    9     10      1200.    4.6944    3.2    d         .02
                                                         2.1666    6.9333        1
   2.167   27.77        1       .25       .3      .3   26.2    489.     .12      56.
    9   10     11      1200.    4.6944    3.2    d         .02
                                                         2.1666    6.9333        1
   2.167   27.77        1       .25       .3      .3   26.2    489.     .12      56.
   10   11     12      1200.    4.6944    3.2    d         .02
                                                         2.1666    6.9333        1
   2.167   27.77        1       .25       .3      .3   26.2    489.     .12      56.
   11   12     13      1200.    4.6944    3.2    d         .02
```

```
                                                               2.1666    6.9333       1
     2.167   27.77      1      .25      .3      .3    26.2    489.     .12     56.
     12   13   14     1200.    4.6944   3.2     d           .02
                                                               2.1666    6.9333       1
     2.167   27.77      1      .25      .3      .3    26.2    489.     .12     56.
     13   14   15     1200.     .7854           f          .965
                               1
     14   15   16     1200.     .7854   25.     d            .2
                                                                   2.       75.       1
        1.    78.5      1    .0625      .3      .3    26.2    489.     .12     56.
     15   16   17     1200.     .7854           b          -1.4              1

     16   17   18     1200.     .7854   0.5     v            .2
     1.0e-07
 #           particulate specie data cards
             1  smoke                     100.        1.
             2  total rad part             20.        1.
             3  rad part .1                 .1        1.
             4  rad part .2                 .2        1.
             5  rad part .4                 .4        1.
             6  rad part .6                 .6        1.
             7  rad part .8                 .8        1.
             8  rad part 1.                 1.        1.
             9  rad part 1.5               1.5        1.
            10  rad part 1.9               1.9        1.
            11  rad part 8.                 8.        1.
            12  rad part 15.               15.        1.
            13  rad part 20.               20.        1.
 #                 boundary node data
      1 0       0.              56.
      3 1       0.              56.
      4 1       0.              56.
     18 0       0.              56.
 #            room data
     2       1.0
     4.6944
     5     13.636
     4.6944
     6     13.636
     4.6944
     7     13.636
     4.6944
     8     13.636
     4.6944
     9     13.636
     4.6944
     10    13.636
     4.6944
     11    13.636
     4.6944
     12    13.636
     4.6944
     13    13.636
     4.6944
     14    13.636
     4.6944
     15    13.636
      .7854
     16         9.8
      .7854
     17         9.8
      .7854
 #                  blower curve cards
     1     4
```

TABLE XIX (CONT)

```
-8000.    8.         0.         1.8        1200       1.5278
6000.     0.
#          filter data
          1     .9995      1.
#              temperature data
             56.             56.             56.             56.             56.
             56.             56.             56.             56.             56.
             56.             56.             56.             56.             56.
             56.             56.             56.
#          fire scenario control specifications          "1flow3"
       1100.        100        2
          1       0.0        0        0.0        0         0
#         fire compartment initial conditions and noding
       56.0     -.20
          2          3     1.084      2.166
          3          4     11.76      2.166
#         fuel type, mass ,and burn area
      0.0      0.0      0.0      0.0      0.0      0.0    5.750      0.0      0.0
      0.0      0.0      0.0      0.0      0.0      0.0    2.150      0.0      0.0
      0.0      0.0      0.0      0.0      0.0      0.0      4.0      0.0      0.0
      0.0      0.0      0.0      0.0      0.0      0.0      2.0      0.0      0.0
#          fire compartment dimensions and materials
       20.0       17.0       15.0     0.492      0.492      3.281      0.492
          9          8          9
#         combustible identifier card (required if ignite > 0)
     2    2    2    2    2    2    1    2    2
#          radioactive source term input
          0          1          1          0          0          0          0
          1          7          1          2
     .22050
          2     0.1653
#          time step cards
               .001        3.0        1.0
                .01       10.0        1.0
                .05      999.0       50.0
```

2. Fire Accident Scenario. In Sample Problem 1, it is postulated that two open cans of flammable solvent (kerosene) are located within the fire compartment. One of the cans of kerosene is assumed to be contaminated with a mixed oxide powder; the other can is not contaminated. The uncontaminated can is assumed to have an exposed surface area of 4.0 ft^2 (0.37 m^2) and a mass of 5.75 lbm (2.61 kg). The smaller contaminated can has an exposed surface area of 2.0 ft^2 (0.18 m^2) and a mass of 2.16 lbm (0.98 kg). To initiate the accident sequence, it is postulated that the uncontaminated can becomes ignited. The second (contaminated) can of flammable solvent has been contaminated with 0.22 lbm (0.10 kg) of mixed oxide powder and is susceptible to ignition via the FIRIN auto-ignition model. The auto-ignition model assumes that the combustible at risk to ignition from other burning combustibles within the fire compartment will ignite if the heat flux levels are sufficient. In addition to the contaminated flammable solvent, 0.165 lbm (0.075 kg) of mixed oxide powder is assumed to be distributed evenly over the compartment floor. This material can become airborne as a result of the fire-induced heating of the contaminated surface (floor).

3. Calculated Results.

a. System Response. The fire (ignition of the uncontaminated kerosene) begins 2.0 s into the transient and initiates the accident sequence. The sequence of events for this sample calculation is presented in Table XX. The fire compartment (represented by nodes 3 and 4) rapidly pressurizes from its steady-state value of -20 in. w. g. (-50.0 cm w.g.) to a value approaching 0.10 in. w.g. (0.25 cm w.g.) as a result of the rapid volumetric expansion of the gases within the compartment. The heating of the air within the compartment of the fire causes the rapid expansion. Figures 17 and 18 show the pressure response of the system. The pressures near the filter and blower locations of the system are perturbed slightly. The system capacitance represented by the duct volume located between the fire compartment and filter and blower positions dampens the influence of the fire. Also, as a result of the rapid pressure increase in the fire compartment, a reversal of flow at the inlet and increase of exit flow to the fire compartment is calculated by FIRAC. The system volumetric and mass flow results are presented in Figs. 19 and 20. The system mass flow rates exhibit trends similar to those shown in the volumetric flow. Once the hot layer has descended to the centerline elevation of the exit branch (node 4, branch 3), the mass flow rates are reduced as the warmer gases are

TABLE XX

TRANSIENT EVENT SEQUENCE FOR SAMPLE PROBLEM 1

Event	Time (s)
Uncontaminated kerosene ignites	2
Maximum fire compartment pressure (0.05 in. w.g.) attained	~10
(hot layer descends to elevation of outflow boundary)	~12
Contaminated kerosene ignites via auto-ignition	~582
Transport of radioactive material initiated	~582
(hot layer descends to centerline elevation of inflow boundary)	~621
Maximum system temperature (~240°F) attained	~763
Fire terminated	~763
Release of radioactive material from continued heating of the residue	~763
End of calculation	1060

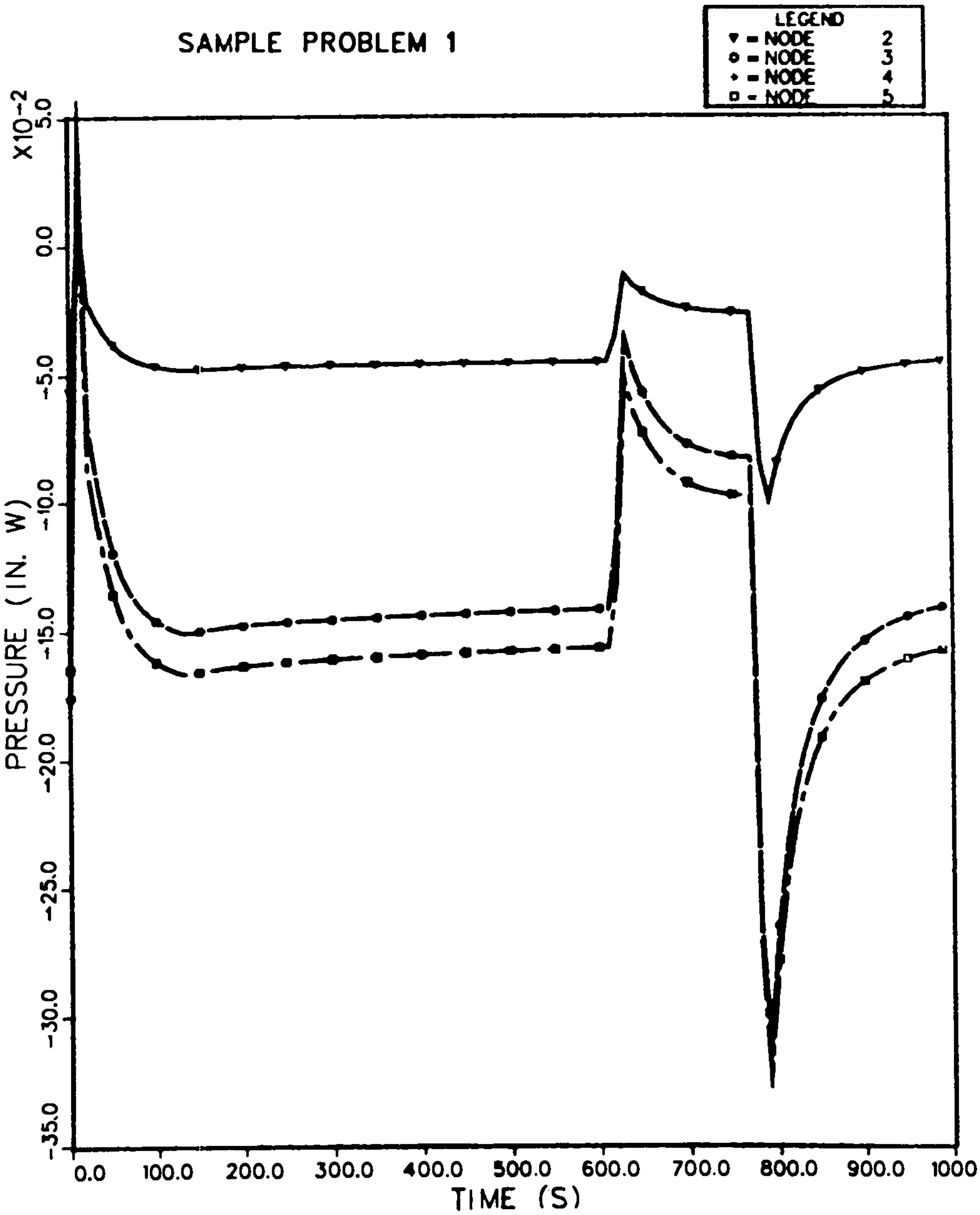

Fig. 17.
Pressure response for nodes 2, 3, 4, and 5.

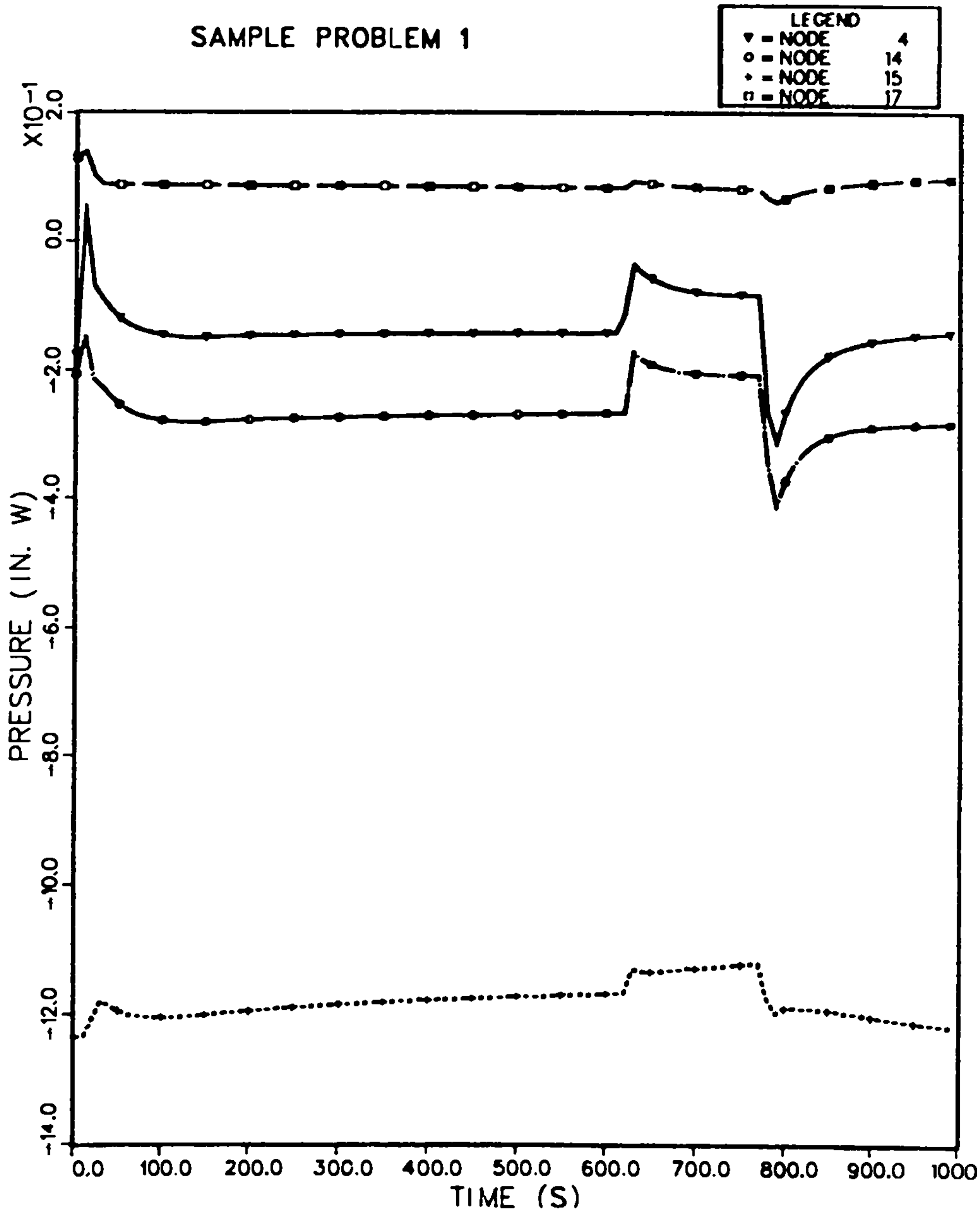

Fig. 18.
Pressure response for nodes 4, 14, 15, and 17.

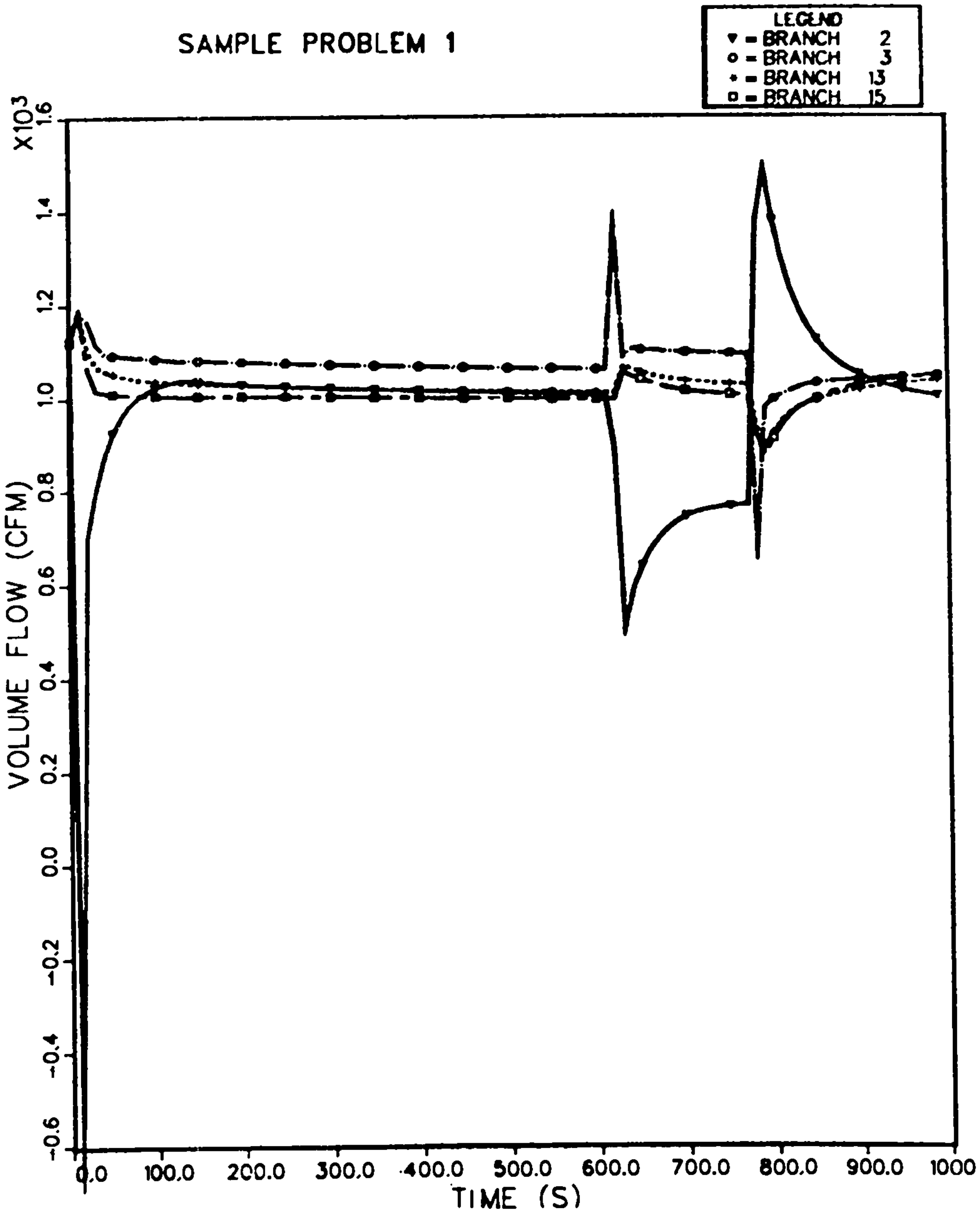

Fig. 19.
Volumetric flow rates for branches 2, 3, 13, and 15.

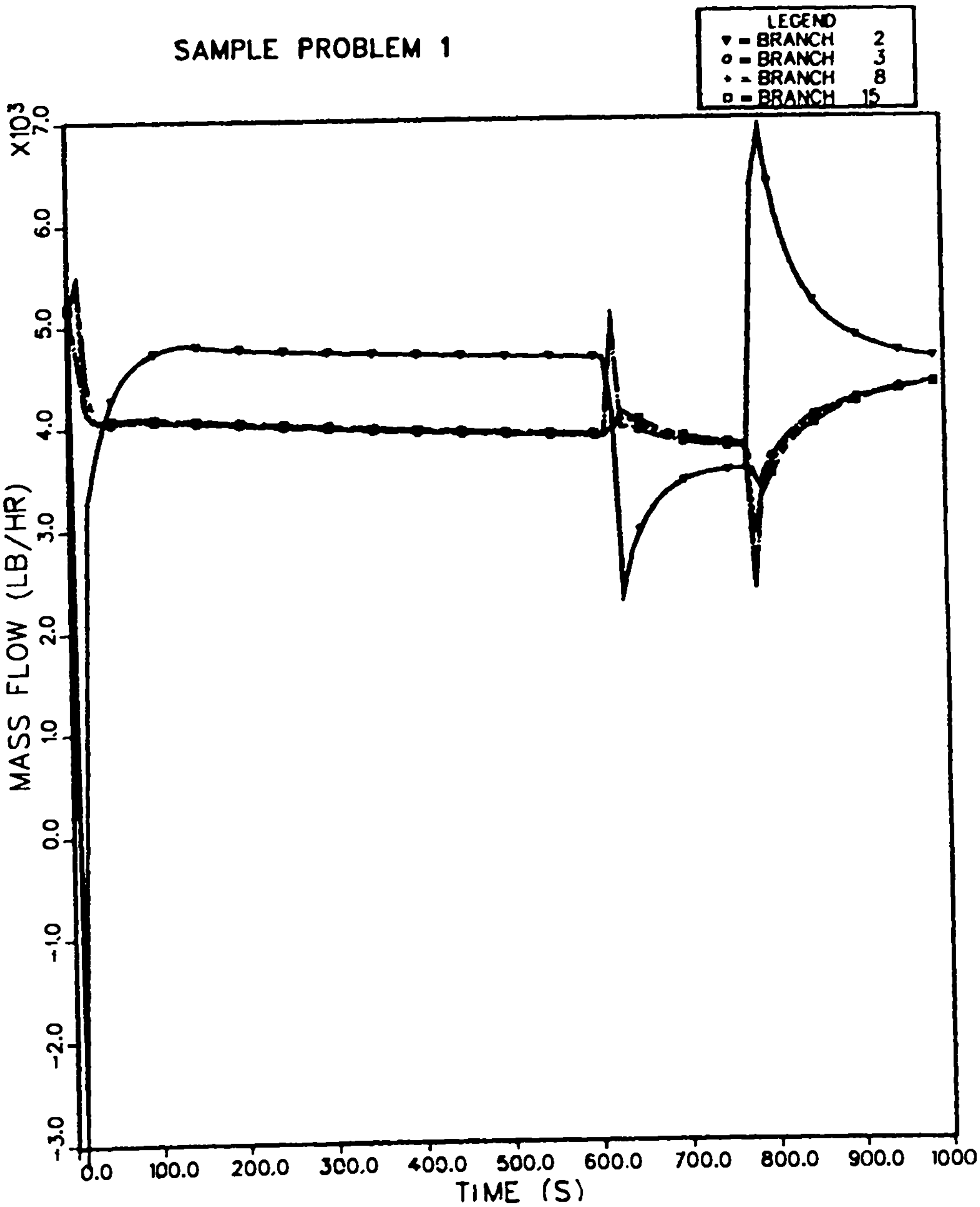

Fig. 20.
Mass flow rates for branches 2, 3, 8, and 15.

transported through the exhaust duct. The hot-layer position and temperature vs time are shown in Figs. 21 and 22, respectively. System temperature profiles in and around the fire compartment are shown in Fig. 23, and the temperature profiles midway between the fire compartment and the filter and at the filter inlet and blower exit are shown in Fig. 24. At any time during the transient, the decrease in gas temperature with increasing distance from the fire compartment is a result of the gas heat losses because of convection and radiation heat transfer occurring in the exhaust duct. After the hot layer has descended below the exhaust elevation of the fire compartment, the system response (pressures, flow rate, and temperatures) remains stable. At ~500 s, the hot layer has descended near the elevation of the inflow (node 3, branch 2). As the hot layer passes over the inflow boundary, node 3 is assigned an averaged hot-layer temperature value (Fig. 23). Until this time in the transient, the uncontaminated kerosene has been the only energy source for the fire. The other fuel source is the contaminated can of solvent susceptible to ignition via the FIRIN auto-ignition option. At ~582 s, FIRIN calculates that the fire compartment heat flux levels have reached the required level to ignite the second fuel source. The autoignition of the additional fuel is indicated in several of the graphic results. For example, the system pressures and flows are perturbed again as additional heat is added to the system. The pressures are calculated to increase throughout the system, whereas the inlet flow is reduced and the exhaust flow is slightly enhanced. Also, the additional heat source assists in the growth of the hot layer, an increase in hot-layer temperature, and an increased fuel burning rate. After the contaminated can of kerosene has ignited, the hot layer descends to the floor very quickly, and the inflow boundary node (node 3) achieves a value equivalent to the hot-layer temperature. Another assumption of the FIRIN auto-ignition concept is combining of fuels and fuel surface areas after auto-ignition has been achieved. The model assumes that the fuel (mass) remaining from the initial fuel source is lumped with the at-risk fuel mass and that the fuel surface burn areas are combined. For this calculation, the fuel burn area after ~582 s was 6.0 ft^2 (0.6 m^2). Combining the burn areas enhances the burning rate (consumption of fuel) as shown in Figs. 25 and 26. After the hot layer has descended to the floor, the inlet air becomes mixed with the hot

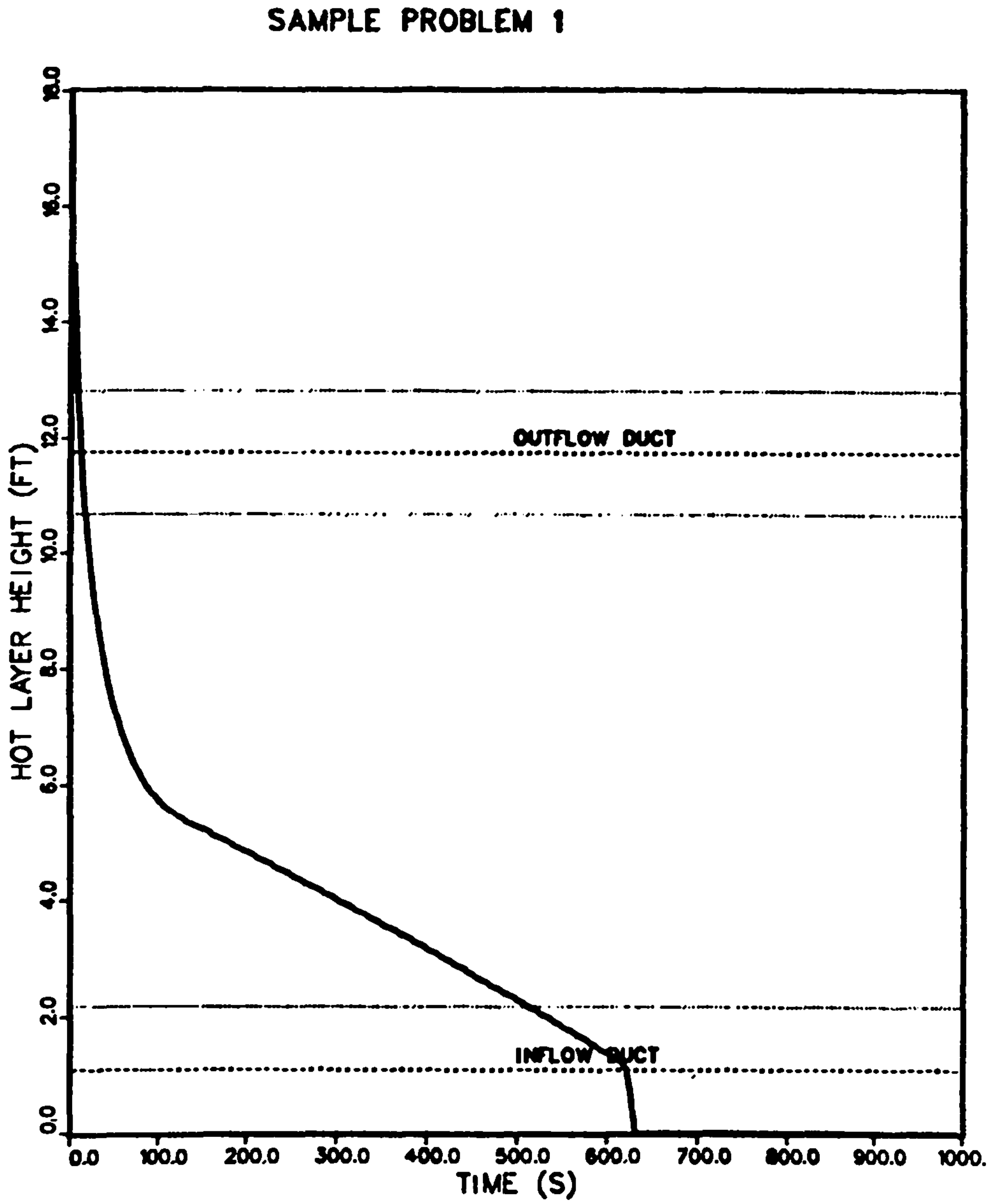

Fig. 21.
Hot-layer height vs time.

SAMPLE PROBLEM 1

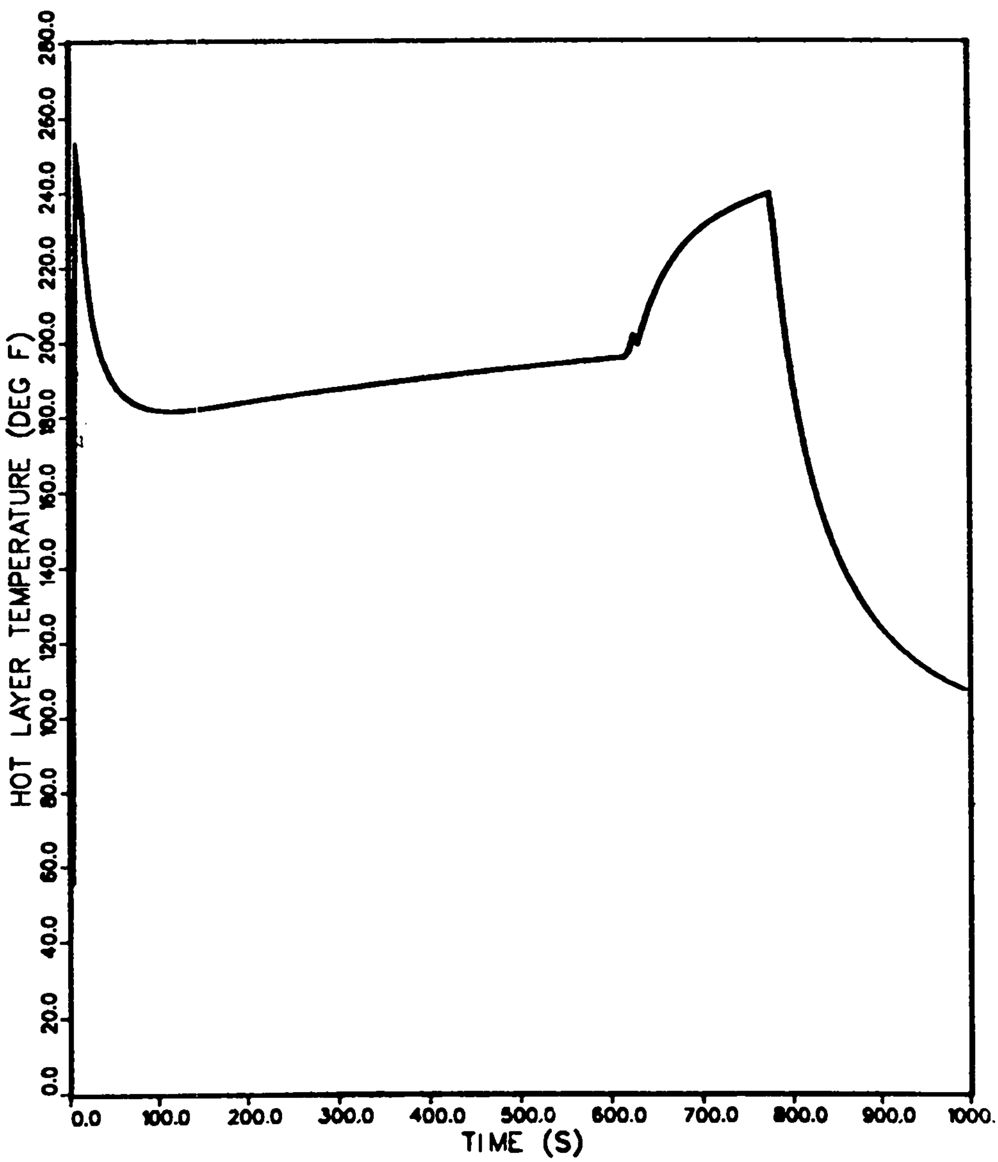

Fig. 22.
Hot-layer temperature vs time.

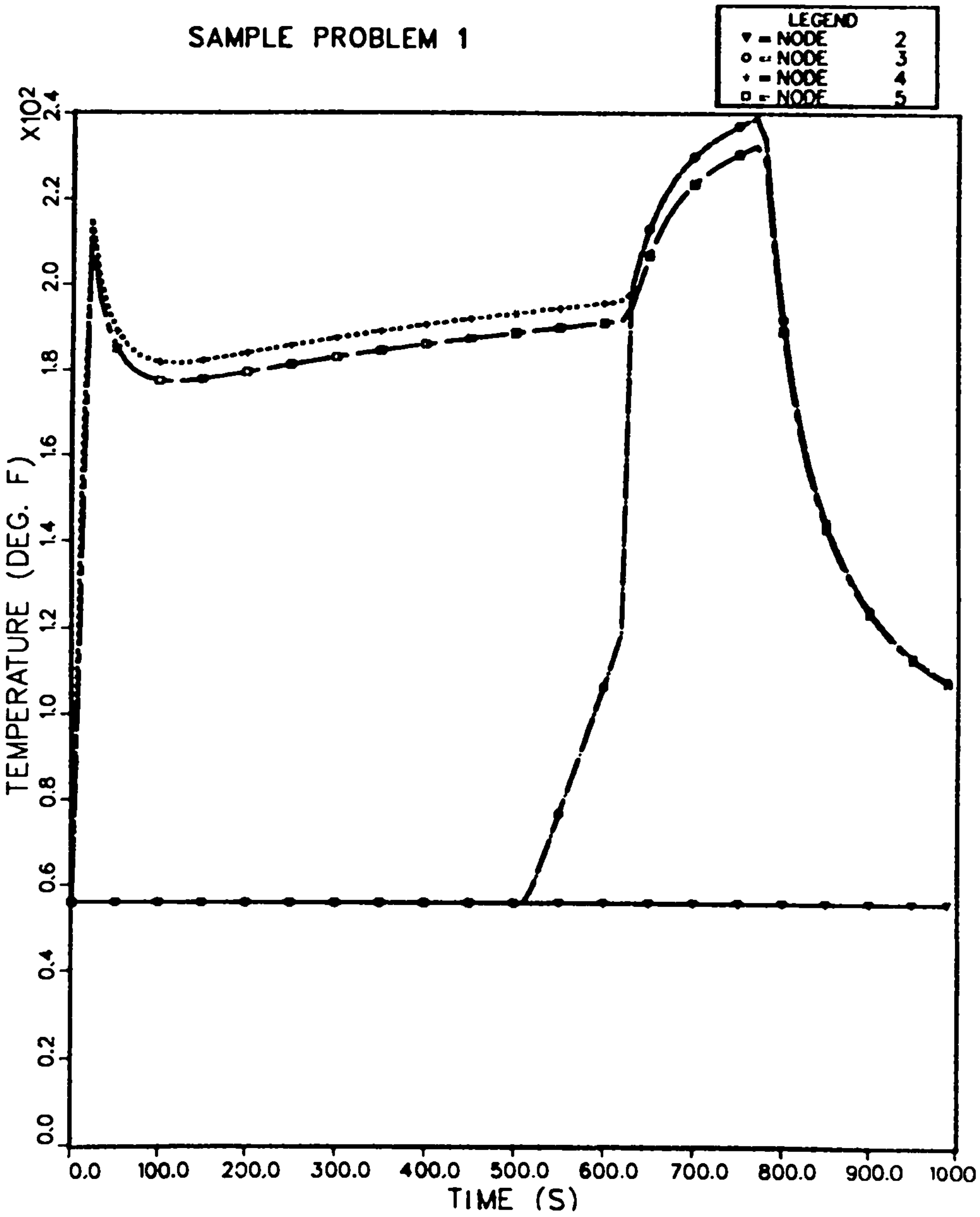

Fig. 23.
Temperature response for nodes 2, 3, 4, and 5.

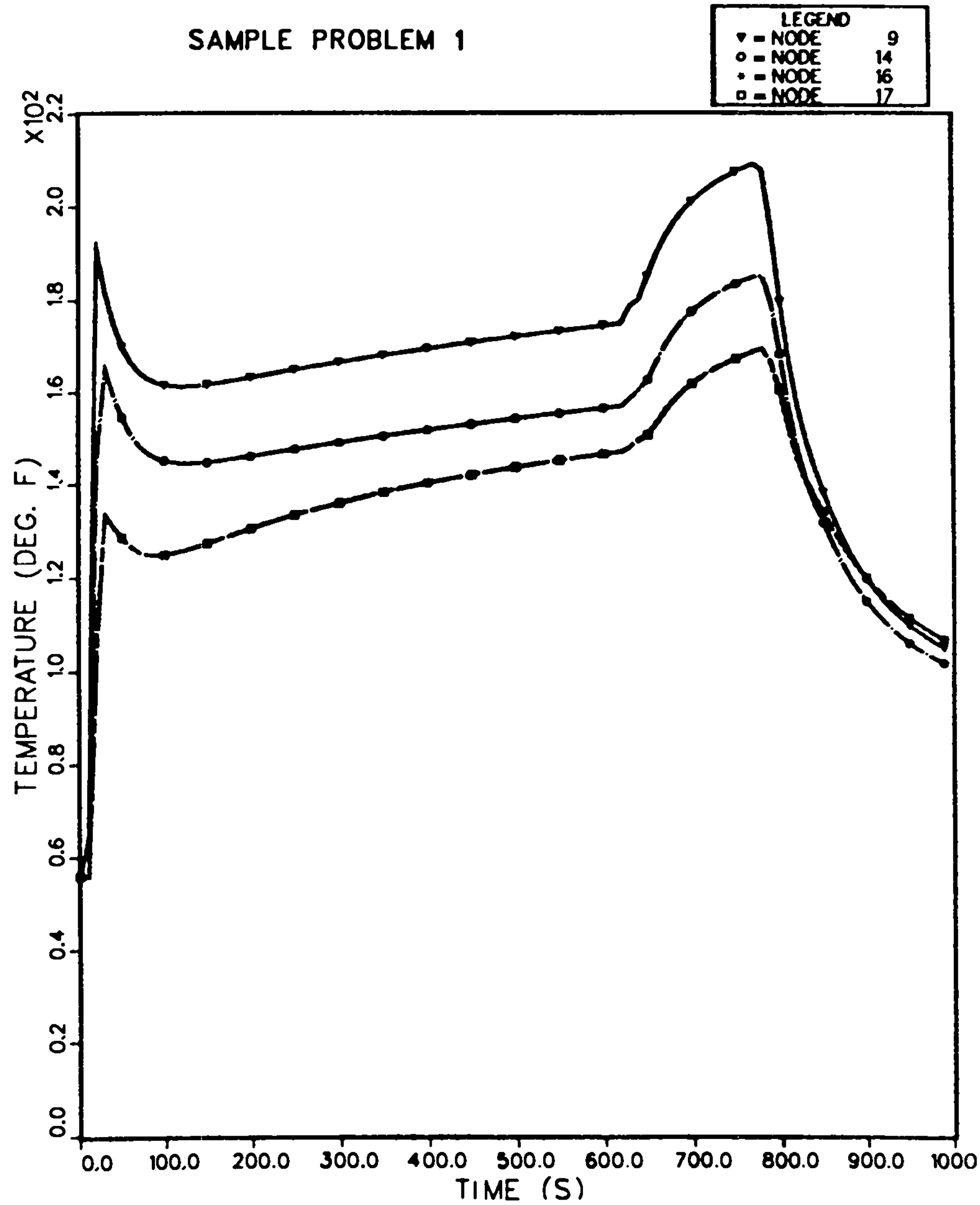

Fig. 24.
Temperature response for nodes 9, 14, 16, 17.

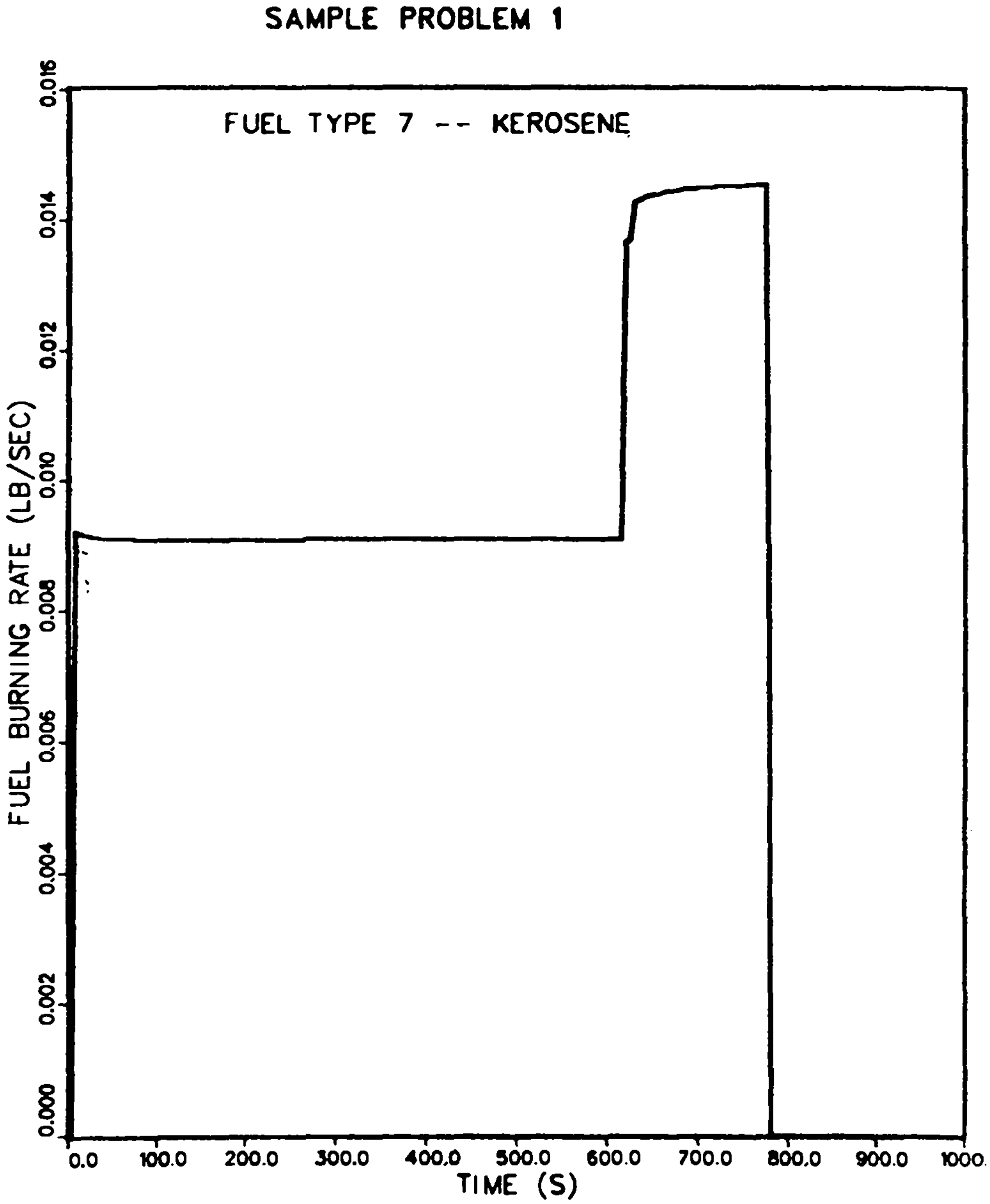

Fig. 25.
Fuel burning rate vs time.

SAMPLE PROBLEM 1

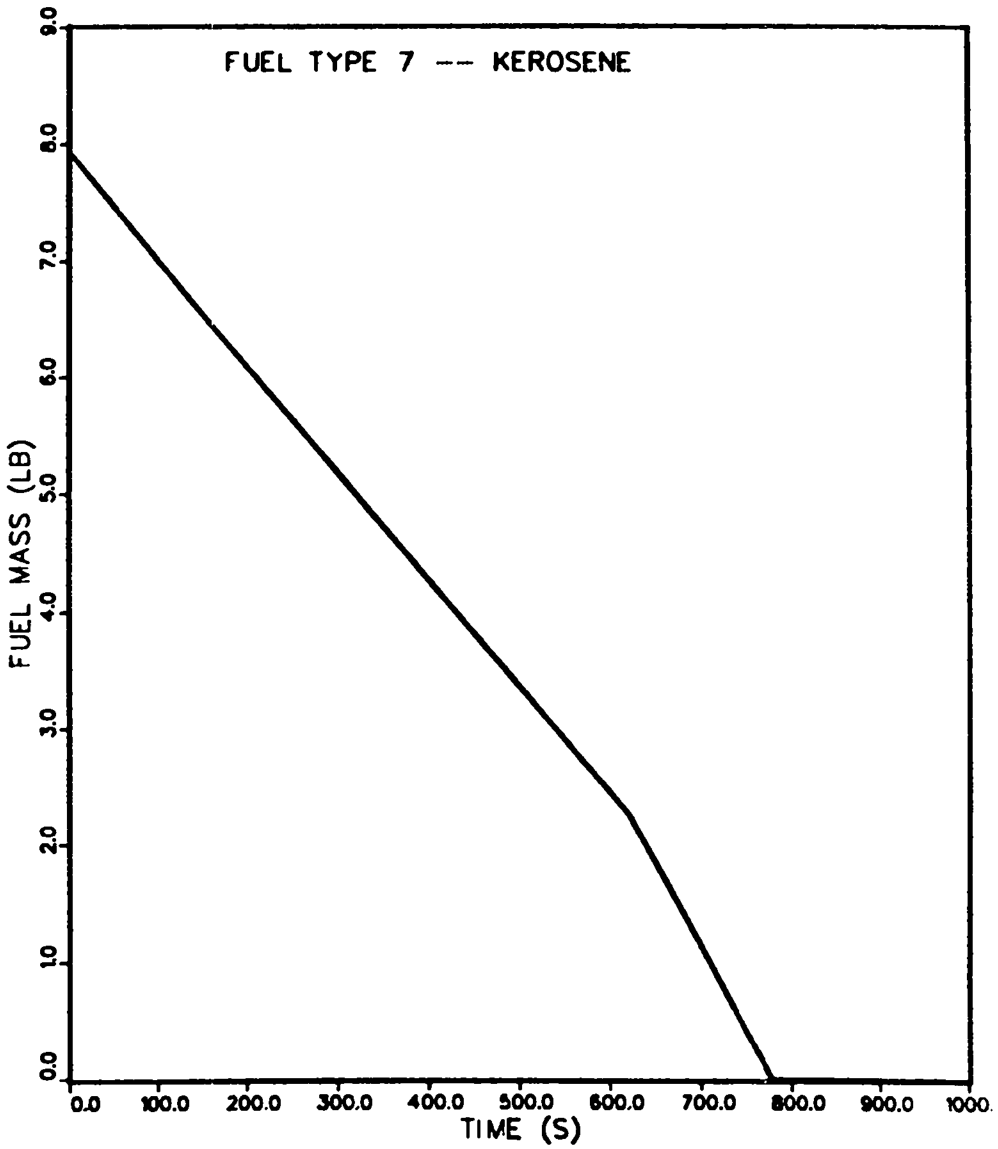

Fig. 26.
Fuel mass vs. time.

gases of the hot layer and is no longer supplying the fire with fresh air. The fire, which is assumed to be located approximately 0.6 ft (0.2 m) above the floor, begins to entrain a mixture of air and combustion products, which decreases the overall oxygen concentration of the compartment (Fig. 27). All the combustible materials were consumed by ~763 s. After the fire has terminated, the system begins to recover and reestablish the initial steady-state conditions.

b. Material Transport. The transport of smoke particulate and radioactive particulate was calculated for the sample problem. The quantity of smoke particulate generated by the burning of the kerosene and transported to the filter is shown in Fig. 28. This plot reveals that a significant portion of the smoke particulate was not transported to the filter because of deposition. As a result of the filter remaining unplugged, the blower performance was not affected by the smoke. The smoke particulate diameter was shown to be unrealistically large (~100 μm) so that the effects of particle size on the deposition rate could be seen in the results. Deposition is an important consideration and can affect the results of a calculation. For example, improper selection of particle diameter could lead to an unrealistic deposition rate that inhibits material from challenging the HEPA filter in a facility. This could lead to misleading results in terms of fire strength/duration and radioactive particle release rates.

During this fire transient, the radioactive release mechanisms were used to simulate the release of radioactive material. Heating of a contaminated surface and burning of a contaminated combustible liquid were the two mechanisms. The release resulting from the heating of the contaminated floor is not evident in the results. The release rate for this mechanism is several orders of magnitude less than the release rate for burning of a contaminated liquid. As a result, the particulate flow rate and accumulations for the 20-μm particles shown in Figs. 29 and 30 do not indicate a significant release before ~600 s. The 20-μm particulate size distribution is released by both mechanisms. After ~600 s, the burning of the contaminated combustible liquid produces the particle flow rate and accumulations shown in the figures. This mechanism has two stages for particulate release. Stage one is the burning phase, and stage two is the continued heating of the residue after the burning has stopped. Stage one occurs between ~600 s and ~763 s, and stage two occurs between ~763 s and 1000 s. The

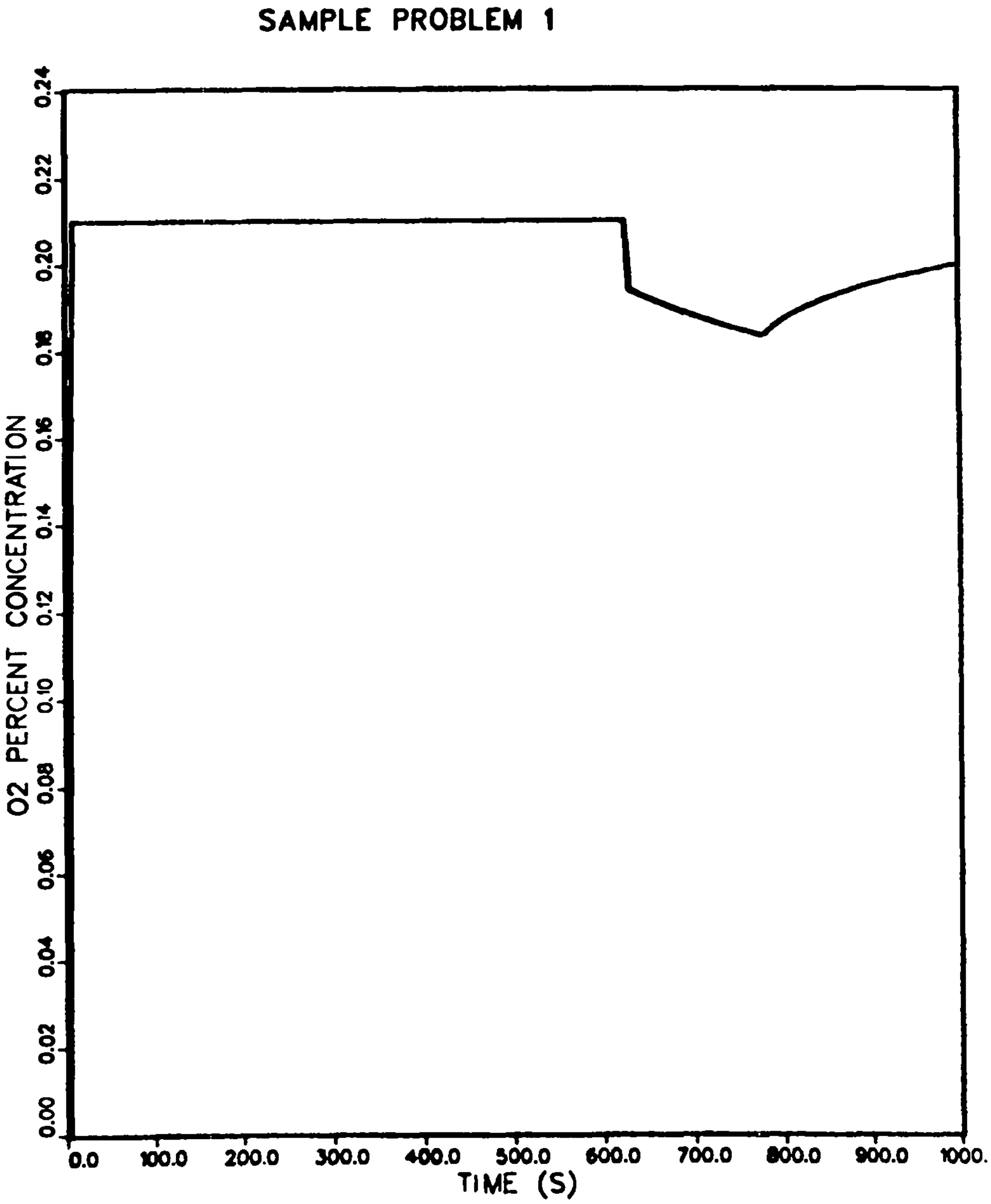

Fig. 27.
Fire compartment oxygen concentration vs time.

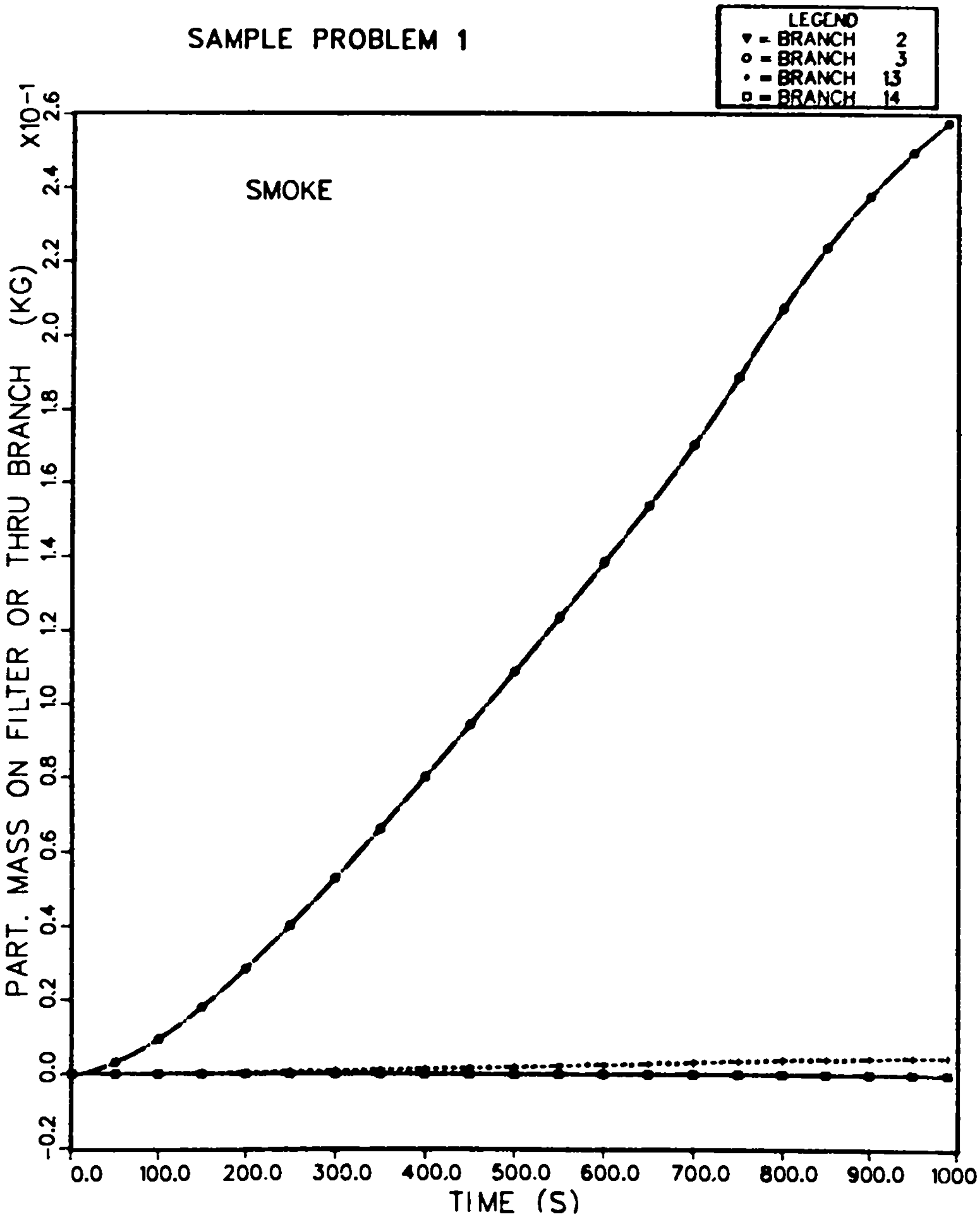

Fig. 28.
Accumulated smoke particulate mass for branches 2, 3, 13, and 14.

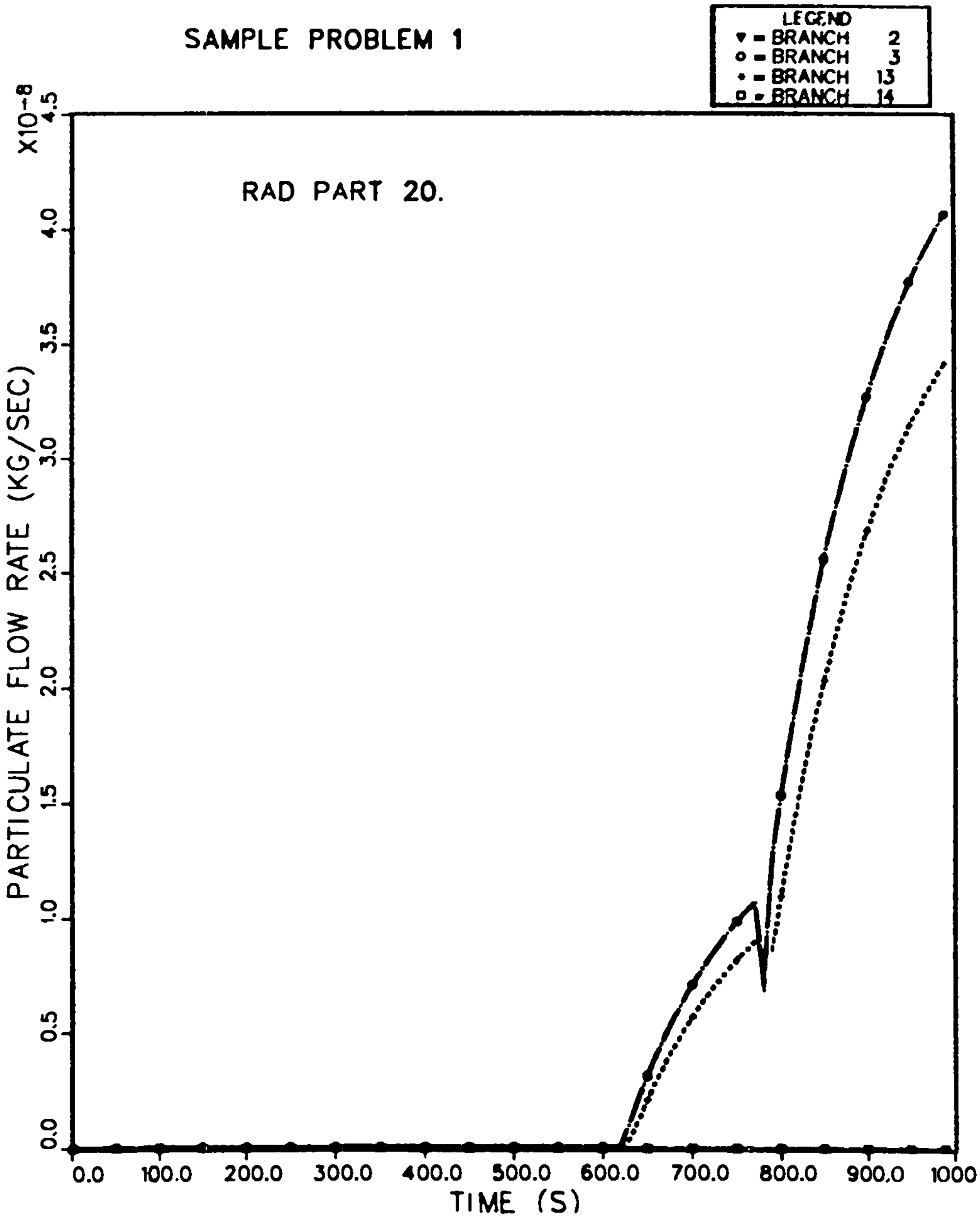

Fig. 29.
20-μm radioactive particulate mass flow rates for branches 2, 3, 13, and 14.

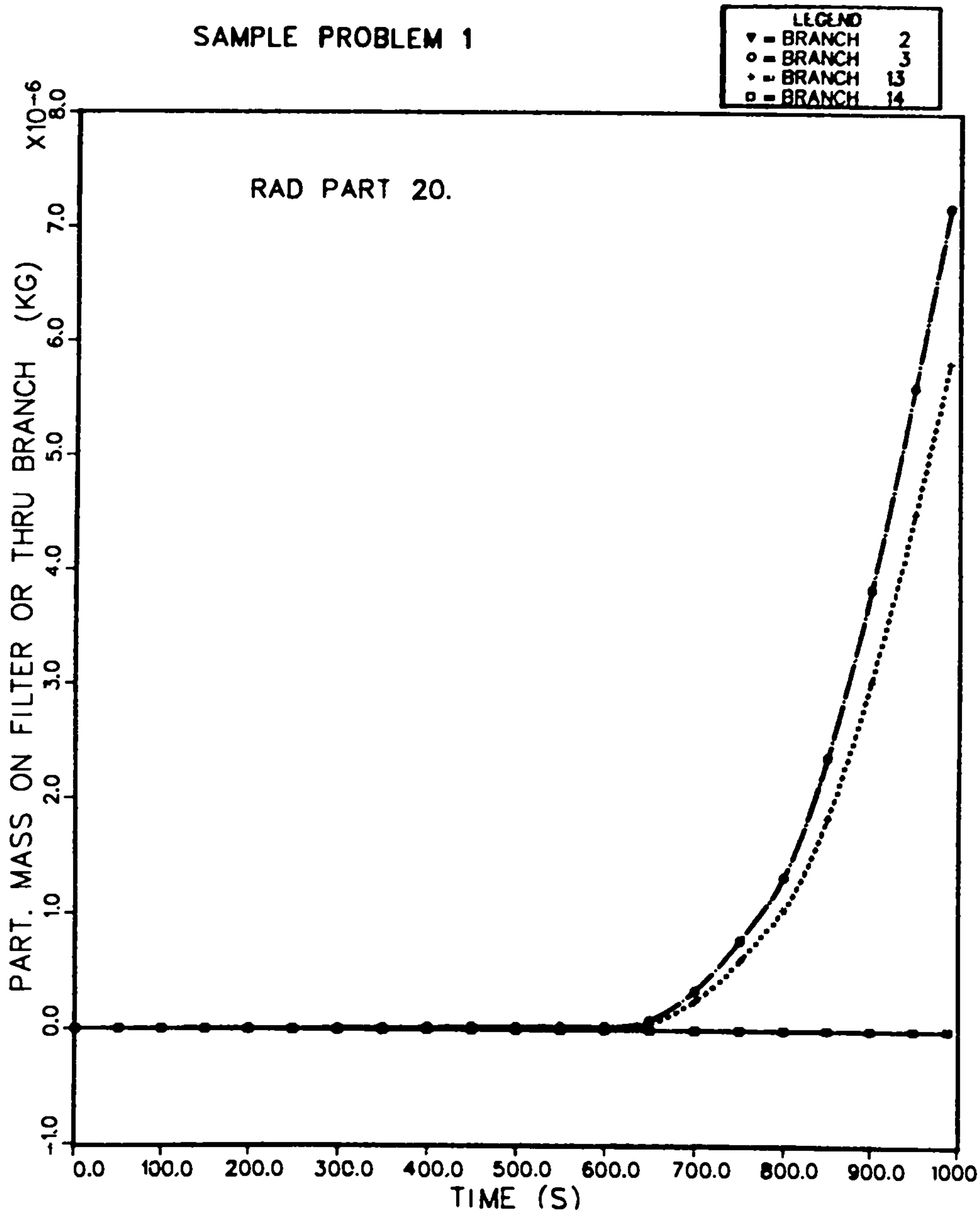

Fig. 30.
Accumulated 20-μm radioactive particulate mass for branches 2, 3, 13, and 14.

FIRIN rate of release mechanism assumes that the heating of the residue continues 10 min after the burning has stopped.

4. Summary. Sample Problem 1 demonstrated several user options of the improved FIRAC: auto-ignition of a contaminated combustible, release of radioactive material by the release mechanisms; heating of a contaminated surface and burning of a contaminated combustible liquid; 2 internal boundary nodes representing the fire compartment; transport of 11 radioactive particle size distributions and depletion of material; and duct heat transfer capability. This sample problem indicates how complicated the interpretation of the calculated results can become when several options have been enabled. The user should become familiar with all the options and how they will affect the calculation. Also, the interactions that can occur between the various options should be anticipated to assist in the analysis of the results.

C. Sample Problem 2.

1. Description and Computer Model of the Facility. To illustrate how the improved fire code can be applied to a more complex facility, consider the system schematic shown in Fig. 16. The facility presented in the schematic is representative of most nuclear fuel cycle ventilation systems in that it contains multiple fans, compartments, dampers, filter systems, and parallel/series flow configurations. For this scenario, the fire is assumed to occur in the compartment represented by internal boundary nodes 9, 21, and 22. Three internal boundary nodes were required because the compartment has three flow connections:* two inflow (branches 16 and 17) and one outflow (branch 14) connection. The inlet and outlet branches (ducts) to the fire compartment have been positioned so that the general ventilation flow direction in the room is downward. Most compartment ventilation ducts in fuel cycle facilities are configured in this manner to help settle contaminated airborne particulates, which reduces the risk of contamination throughout the facility. A closeup of the fire compartment noding is shown in Fig. 31.

The fire compartment is assumed to be 39 ft (12 m) long, 39 ft (12 m) wide and 20 ft (6 m) high. The centerline elevation (measured from the floor) of the

*A maximum of three internal boundary nodes can be used to represent the FIRIN fire compartment. For this sample calculation, two internal boundary nodes could have been used (Sec. III.C).

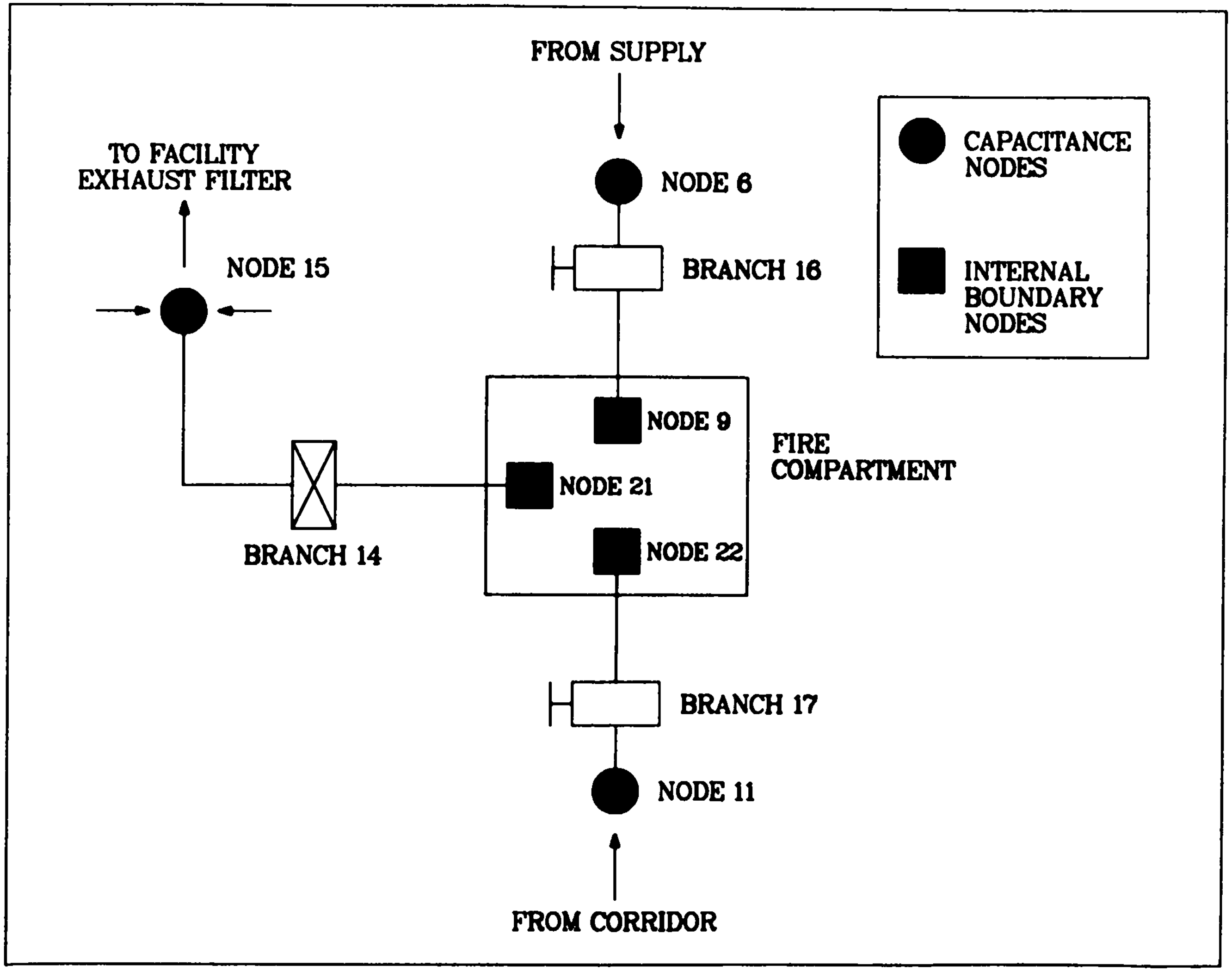

Fig. 31.
Close-up system schematic near the fire compartment for Sample Problem 2.

two inlet ventilations is 18.74 ft (5.71 m), and the centerline elevation of the outlet ventilation is 3.0 ft (0.9 m). Also, the fire compartment is assumed to have a concrete floor, ceiling, and walls. The ceiling and floor are assumed to be 1.0 ft (0.3 m) thick, and the walls are assumed to be 0.5 ft (0.2 m) thick.

When the system is operating under steady-state conditions, the fire compartment has a pressure of -0.30 in. w.g. (-0.76 cm w.g.) at a temperature of 70°F (21°C). The two inlet ventilators (branches 16 and 17) supply 3679 ft^3/min (1.736 m^3/s) and 290 ft^3/min (0.137 m^3/s) of air to the compartment. The outlet ventilator exhausts 3969 ft^3/min (1.873 m^3/s) under steady-state conditions. The fire compartment/overall system steady state was achieved by selecting an initial system pressure distribution and using resistance coefficients. The fire compartment exhaust filter (branch 17) is assumed to be 99.95 efficient and have a plugging factor of 20.1/kg. A large filter plugging factor was selected to illustrate the importance of the filter plugging model on the calculated results.

The facility model features 37 branches, 22 nodes [17 capacitance (room) nodes, 2 standard boundary, and 3 internal boundary], 2 blowers, and 9 filters. A complete listing of the input deck for sample problem 2 showing the assumed blower curves, initial system pressure distribution, fire compartment input specifications, and so on is presented in Table XXI.

2. Fire Accident Scenario. The purpose of sample problem 2 is to illustrate the use of the FIRIN sequential burning option. Two fuels (kerosene and polystyrene) will be burned sequentially in the calculation. The fire compartment is assumed to contain 3.0 lbm (1.4 kg) of uncontaminated kerosene. The container of kerosene has an exposed surface (burn) area of 5.0 ft^2 (0.5 m^2). In addition to the kerosene, the compartment contains 30.0 lbm (13.6 kg) of contaminated polystyrene. The polystyrene is assumed to have an exposed surface area of 7.0 ft^2 (0.7 m^2) and is contaminated with 0.22 lbm (0.10 kg) of mixed oxide powder.

Because the scenario assumed that the two combustibles at risk within the fire compartment will burn sequentially, the maximum number of burning orders (input parameter MIBO) is 2. The kerosene was selected to initiate the accident sequence and has a burning order (IBO) of 1. After all the kerosene has been consumed, the polystyrene (burning order IBO = 2) will ignite to continue the fire-induced transient. When using the sequential burning option, the combustibles input information must be entered according to the burning order. For

TABLE XXI

INPUT DECK LISTING FOR SAMPLE PROBLEM 2

```
       sample problem 2
#  run control 1
   st   0.   1.      999.
#              print / plot control card
  all    1     1     1     1    5
    1    1     1
    2    1     1
   11    1     1
   12    1     1
   13    1     1
#  frame description cards
    4    9    15    21    22
    3   14    16    17
    3   14    16    17
    4    9    15    21    22
    4   14    34    35    36
    4   14    34    35    36
    4   14    34    35    36
    4   14    34    35    36
    4   14    34    35    36
    4   14    34    35    36
    4   14    34    35    36
    4   14    34    35    36
    4   14    34    35    36
    4   14    34    35    36
#              run control card 2                          "ififin"
                                p    t                      0          0   13
#  boundary control          (p. t. e. m)
         5                  70.
#  geometry and component control
   37   22          17    2    3
#  branches
    1    1     2  17600.00     12.000     10.000v
 0.          0.                                                  3.464
    2    2     3  17600.00     12.000      0.000f
 0.          0.                 1                                3.464
    3    3     4  17600.00     12.000      0.000b
 0.          0.                                                  3.464
    4    4     5  17600.00     12.000     15.000v
 0.          0.                                                  3.464
    5    5     6   7710.00      5.000     10.000v
 0.          0.                                                  2.236
    6    7    15    578.00       .380      0.000f
 0.          0.                 1                                .6164
    7    6     7    413.00       .290     20.000v
 0.          0.                                                  .5385
    8    6    11     50.00       .290      1.000v
 0.          0.                                                  .5385
    9   11     7    143.00       .100      1.000v
 0.          0.                                                  .3162
   10    8    15    433.00       .290      0.000f
        0. 0.                   1                                .5385
   11    6    11     50.00       .290      1.000v
 0.          0.                                                  .5385
   12    6     8    290.00       .200     20.000v
        0. 0.                                                    .4472
   13   11     8    143.00       .100      1.000v
 0.          0.                                                  .3162
   14   21    15   3766.00      2.500      0.000f
 2.600e-04 0.                   2                                1.581
   15    6    11    100.00      0.100      1.000v
 0.          0.                                                  .3162
   16    6     9   3480.00      2.300     20.000v
```

```
2.875e-08 0.                                                         1.517
  17    11   22      286.00        .190      1.000v
0.           0.                                                      .4359
  18    10   15     2000.00       2.300      0.000f
0.           0.                   1                                  1.517
  19     6   11      100.00       0.100      1.000v
0.           0.                                                      .3162
  20     6   10     1714.00       2.100     20.000v
0.           0.                                                      1.449
  21    11   10      286.00        .190      1.000v
0.           0.                                                      .4359
  22     5   11      930.00        .620     10.000v
0.           0.                                                      .7874
  23     5   20     7260.00       4.800     20.000v
0.           0.                                                      2.191
  24     5   12     1700.00       1.100     20.000v
0.           0.                                                      1.049
  25    12   15     1700.00       1.100      0.000f
0.           0.                   1                                  1.049
  26    13   15     3746.00       2.400      0.000f
0.           0.                   1                                  1.549
  27    11   13      286.00        .190      1.000v
0.           0.                                                      .4359
  28    20   13     3460.00       2.300     20.000v
0.           0.                                                      1.517
  29    20   11      100.00        .070      1.000v
0.           0.                                                      .2646
  30    14   15     3886.00       2.500      0.000f
0.           0.                   1                                  1.581
  31    20   11      100.00        .070      1.000v
0.           0.                                                      .2646
  32    20   14     3600.00       2.400     20.000v
0.           0.                                                      1.549
  33    11   14      286.00        .190      1.000v
0.           0.                                                      .4359
  34    15   16    17600.00      12.000     10.000v
0.           0.                                                      3.464
  35    16   17    17600.00      12.000      0.000f
0.           0.                   3                                  3.464
  36    17   18    17600.00      12.000           b
0.           0.                                                      3.464
  37    18   19    17600.00      12.000     10.000v
                                                                     3.464
#          particulate specie data cards
           1  smoke                    1.          1.
           2  total rad part          20.          1.
           3  rad part .1               .1         1.
           4  rad part .2               .2         1.
           5  rad part .4               .4         1.
           6  rad part .6               .6         1.
           7  rad part .8               .8         1.
           8  rad part 1.              1.          1.
           9  rad part 1.5             1.5         1.
          10  rad part 1.9             1.9         1.
          11  rad part 8.              8.          1.
          12  rad part 15.            15.          1.
          13  rad part 20.            20.          1.
#    boundary data
     1 0                    70.
     9 1      -0.3          70.
    19 0                    70.
    21 1                    70.
    22 1                    70.
#    room data              (e. m, p. t)
```

TABLE XXI (CONT)

```
      2    500.00
     120.000
      3    500.00
     120.000
      4    500.00
     120.000
      5    500.00
     120.000
      6    500.00
     50.000
      7   3600.00
      180.00
      8   4440.00
      222.00
     10  87400.00
      4370.0
     11  10200.00
      510.00
     12 117300.00
      5865.0
     13  20000.00
      1000.0
     14  20000.00
      1000.0
     15    500.00
     120.000
     16    500.00
     120.000
     17    500.00
     120.000
     18    500.00
     120.000
     20    500.00
      50.00
#    blower curves
      1    6
   -5600.00      13.80        0.00       9.80  12000.00       9.70
   17600.00       8.15    25200.00       4.00  30800.00       0.00
      2    6
   -7700.00      18.10        0.00      12.10   8000.00      12.00
   17600.00      11.10    26700.00       6.00  34400.00       0.00
#    filter data
             1      .9995          0.
             2      .9995         20.
             3      .9995          0.
#    pressures
            0.0000        -5.1500         -7.1500         1.0000          .5000
            0.0000         -.3000          -.3000         -.3000         -.3000
            -.1500         -.1500          -.3000         -.3000        -1.3480
           -7.6000       -10.6000           .5000         0.0000         0.0000
            0.0000         0.0000
#      temperatures
               70.0           70.0           70.0           70.0           70.0
               70.0           70.0           70.0           70.0           70.0
               70.0           70.0           70.0           70.0           70.0
               70.0           70.0           70.0           70.0           70.0
               70.0           70.0
#             fire scenario control specifications          "iflow3"
         1100.          100          2
             0          0.0          0          0.0         0         1
#           fire compartment initial conditions and noding
          70.0   -0.30
             16           9      18.74      1.517
             14          21      3.000      1.581
```

TABLE XXI (CONT)

```
           17         22       18.74      .4359
#            fuel type, mass ,and burn area
        0.0       0.0       0.0       0.0       0.0       0.0      3.00       0.0       0.0
        0.0      30.0       0.0       0.0       0.0       0.0       0.0       0.0       0.0
        0.0       0.0       0.0       0.0       0.0       0.0       5.0       0.0       0.0
        0.0       7.0       0.0       0.0       0.0       0.0       0.0       0.0       0.0
#              fire compartment dimensions and materials
          39.0      39.0      20.0     1.000     0.500     1.000     1.500
           1         1         1
           radioactive source term input (polystyrene)
           1         0         0         0         0         0         0
           1         2         1         2
        .2205
#              time step cards
                   .001     3.001       0.5
                    .01     10.01       1.0
                    .05    999.05       50.
```

this problem, the amount (mass) of kerosene precedes the input value for the amount of polystyrene. The same format follows for the input of the respective fuel burn areas.

The radioactive source term input for the release rates resulting from the burning of the contaminated polystyrene requires that NRAD(1) = 1. This input value for NRAD(1) indicates the radioactive release of particulates will be estimated in the contaminated combustible solid release subroutine. The assumption that the contamination is in the form of a powder requires input parameter IFORM be assigned a value of 1. The combustibles material identifier (I) has been selected to be 2--polystyrene is fuel type (combustibles identifier) 2. The burning order (IBO) of the polystyrene is 2, and the total mass of powder contaminate (QRAD 1) is 0.22 lbm (0.10 kg).

3. Sample Problem 2 Results.

a. System Response. The sequence of events for the Sample Problem 2 calculation is given in Table XXII. The kerosene ignition initiates the accident

TABLE XXII

TRANSIENT EVENT SEQUENCE FOR SAMPLE PROBLEM 2

Event	Time (s)
Kerosene ignites	2
Hot layer descends to centerline elevation of inflow boudaries	~12
Hot layer descends to centerline elevation of outflow boundary	~190
Contaminated polystyrene ignites	~265
Transport of radioactive material initiated	~265
Fire compartment exhaust filter begins to plug	~325
Maximum system temperature (~190°F) attained	~806
Fire terminated	~806
End of calculation	1000

sequence 2 s into the simulation. The fire compartment (represented by nodes 9, 21, and 22 in the system model) rapidly pressurizes from its steady-state operating value of -0.30 in. w.g. (-0.76 cm w.g.) to approximately 0.5 in. w.g. (1.3 cm w.g.) because of the rapid volumetric expansion of the gases within the compartment caused by the fire. Figure 32 shows the fire compartment pressure response for the entire transient. As a result of the pressure increase in the compartment, a reduction in flow at the intakes (branches 16 and 17) and an increase in flow at the compartment exhaust (branch 14) is calculated by FIRAC. Volumetric and mass flow rate results for the fire compartment are presented in Figs. 33 and 34, respectively.

Between 2 and ~200 s, the hot layer gradually expands and descends toward the outflow ventilator (Fig. 35). As the outflow ventilator begins to exhaust the hot combustion products/gases composing the hot layer, the fire compartment begins to depressurize. The volumetric and mass flows at the intakes to the compartment are enhanced by the depressurization. The compartment exhaust flow rate decreases because of the depressurization and the presence of the hot (less dense) combustion gases at the outflow ventilator. The temperature history for the fire compartment is shown in Fig. 36.

The system is perturbed again as the kerosene fire terminates and the contaminated polystyrene ignites via the sequential burning option. This Fig. 32 transition occurs between ~250 and ~275 s as shown in Figs. 37 and 38. The ignition of the polystyrene repressurizes the fire compartment to approximately 1.0 in. w.g. (2.5 cm w.g.). The flow rates to the compartment are affected by the repressurization: enhanced exhaust flow (branch 14) and reduced flow at the intakes (branches 16 and 17). As the polystyrene burns, the compartment remains pressurized at approximately 0.9 in. w.g. (2.3 cm w.g.) and becomes more concentrated with smoke particulates. Burning polystyrene releases a significantly larger amount of smoke then does burning kerosene as shown in Fig. 39. The introduction of smoke at a faster rate within the compartment begins to deplete the amount of oxygen available to the fire (Fig. 40). The polystyrene continues to burn until ~806 s. At this time, all the combustible materials within the fire compartment have been consumed, and the system begins to recover to a new steady-state operating condition.

b. Material Transport. The combination of the smoke release rate of the burning polystyrene material and a fire compartment exhaust filter plugging factor of 20.1/kg significantly influences the system response to the fire.

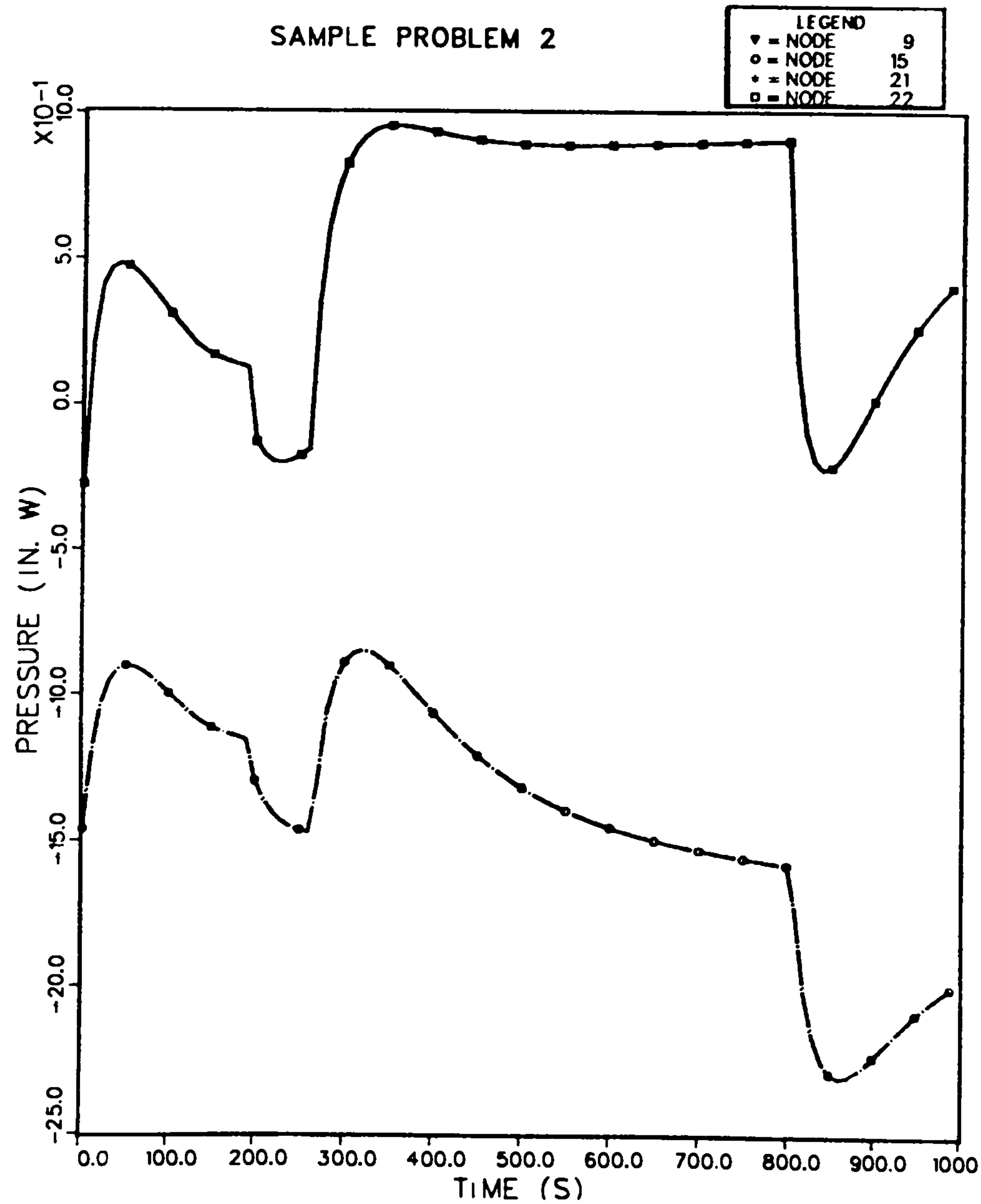

Fig. 32.
Pressure response for nodes 9, 15, 21, and 22.

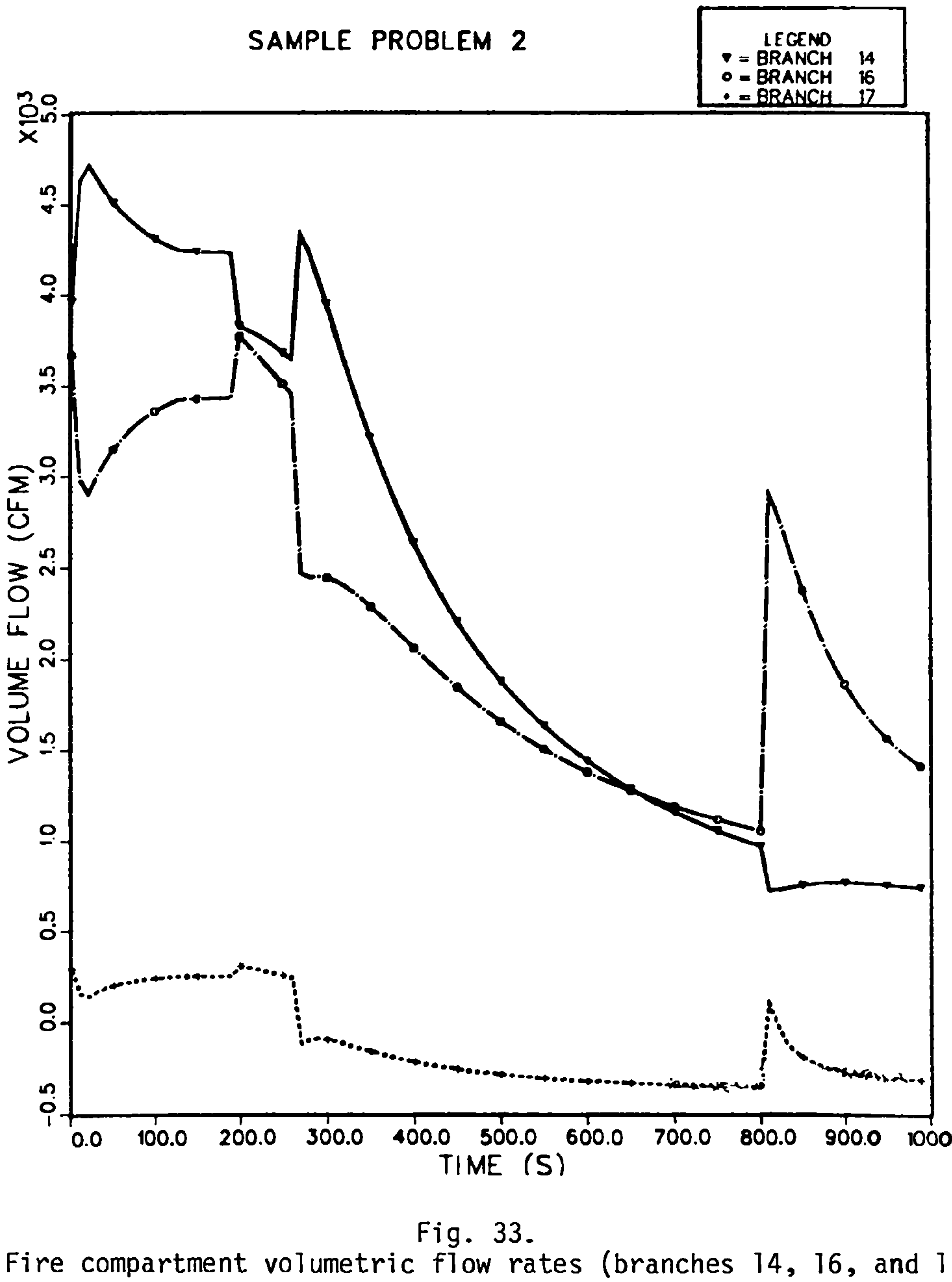

Fig. 33.
Fire compartment volumetric flow rates (branches 14, 16, and 17).

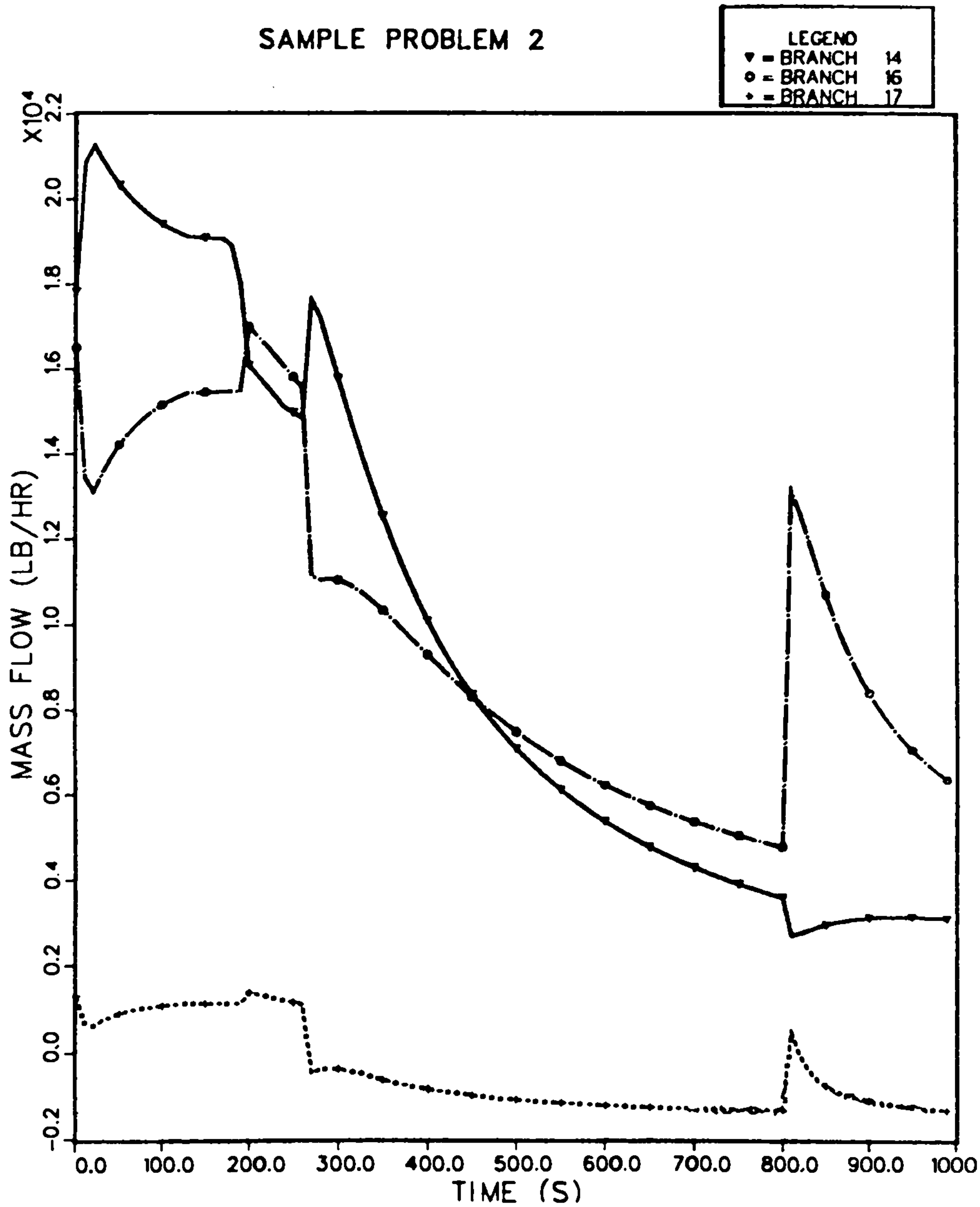

Fig. 34.
Fire compartment mass flow rates (branches 14, 16, and 17).

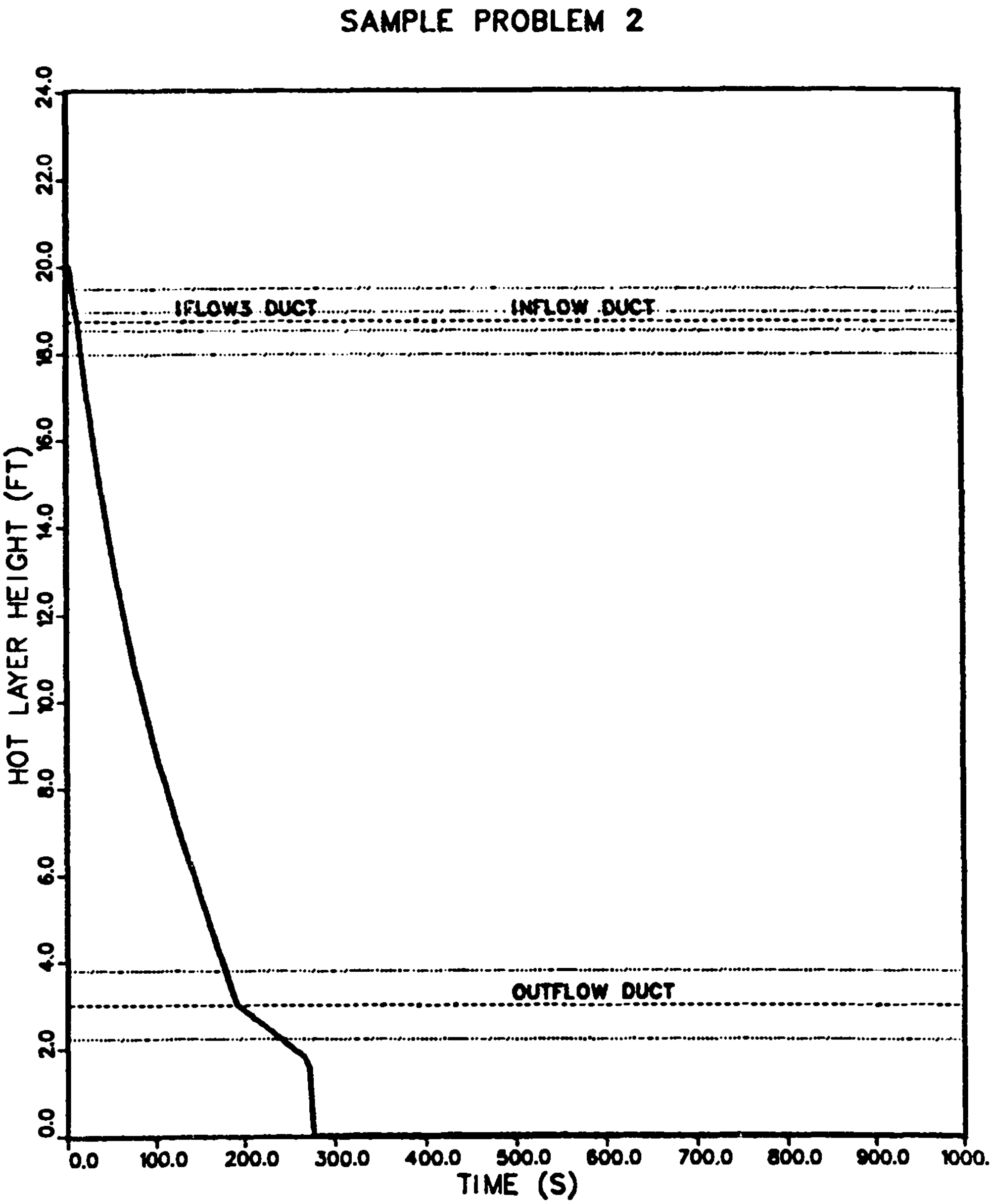

Fig. 35.
Hot-layer height vs time.

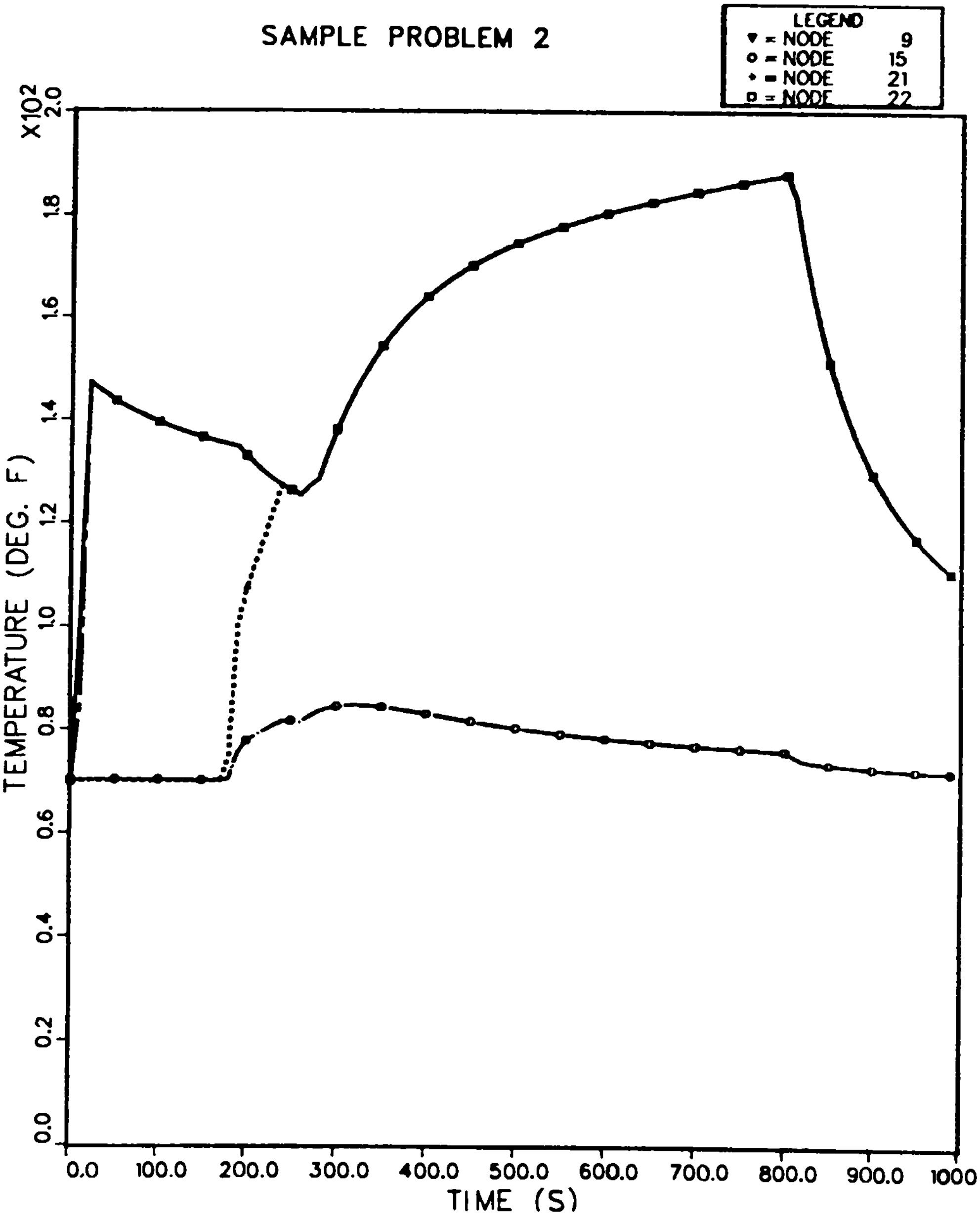

Fig. 36.
Temperature response for nodes 9, 15, 21, and 22.

SAMPLE PROBLEM 2

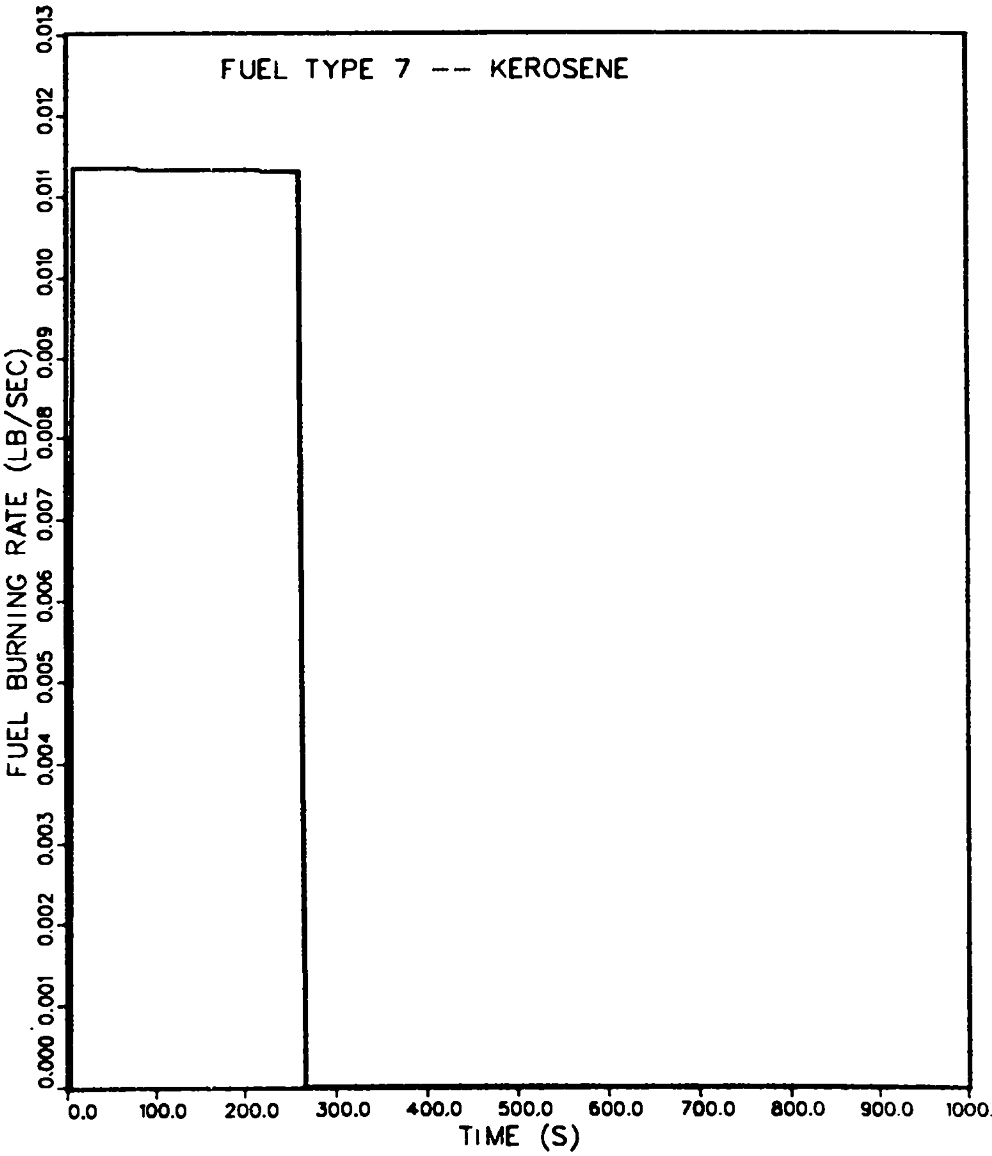

Fig. 37.
Kerosene burning rate vs time.

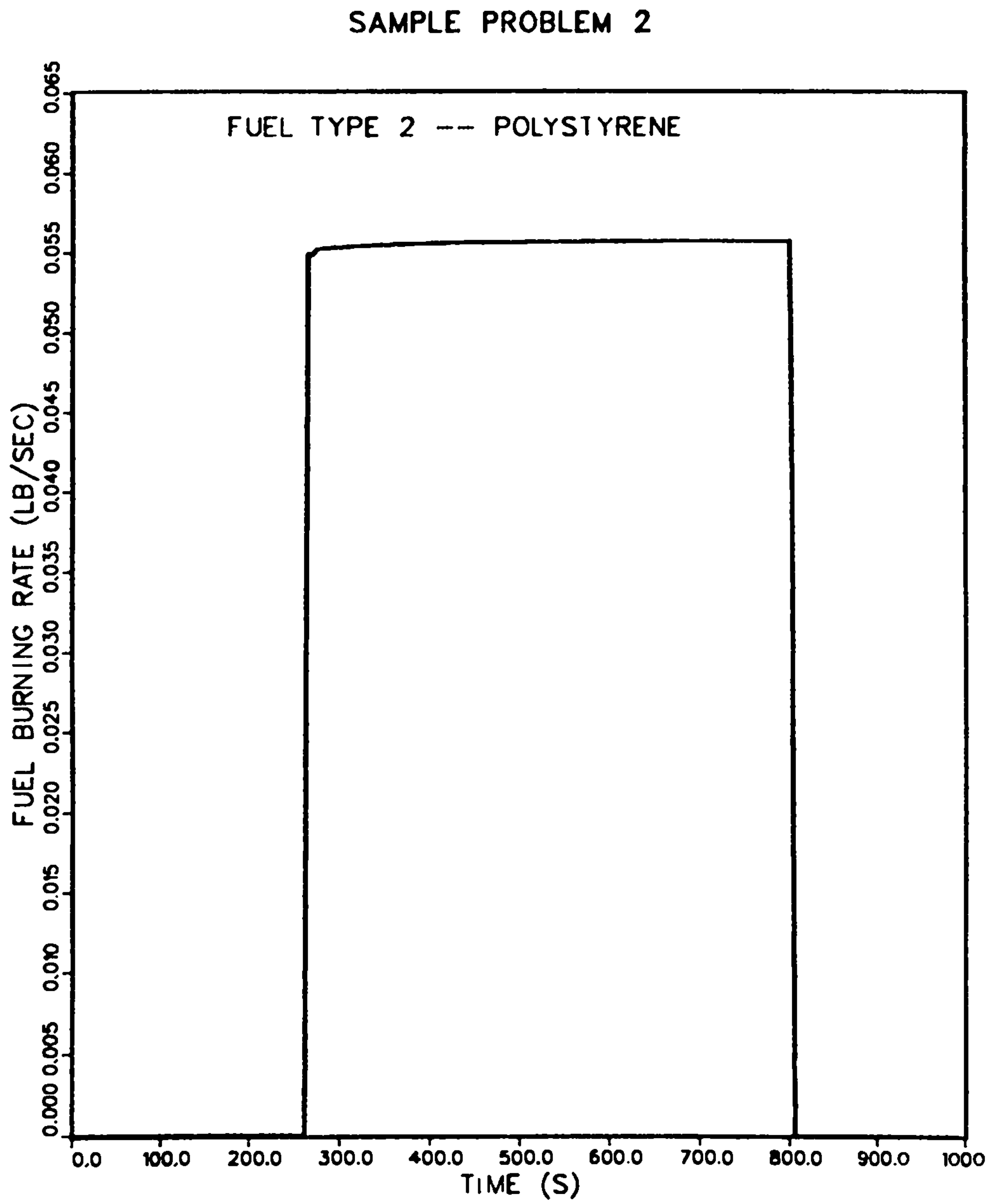

Fig. 38.
Polystyrene burning rate vs time.

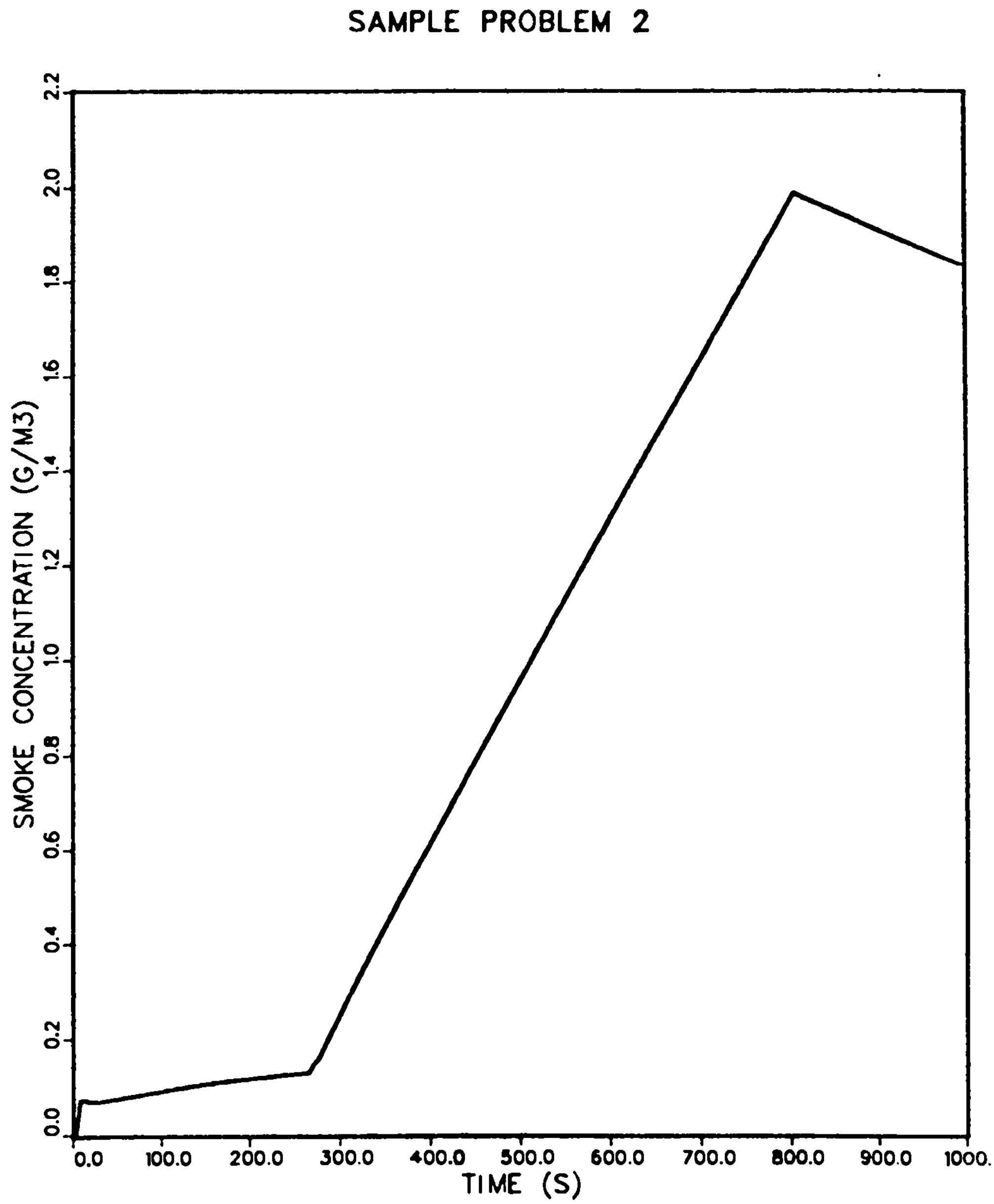

Fig. 39.
Fire compartment smoke concentration vs time.

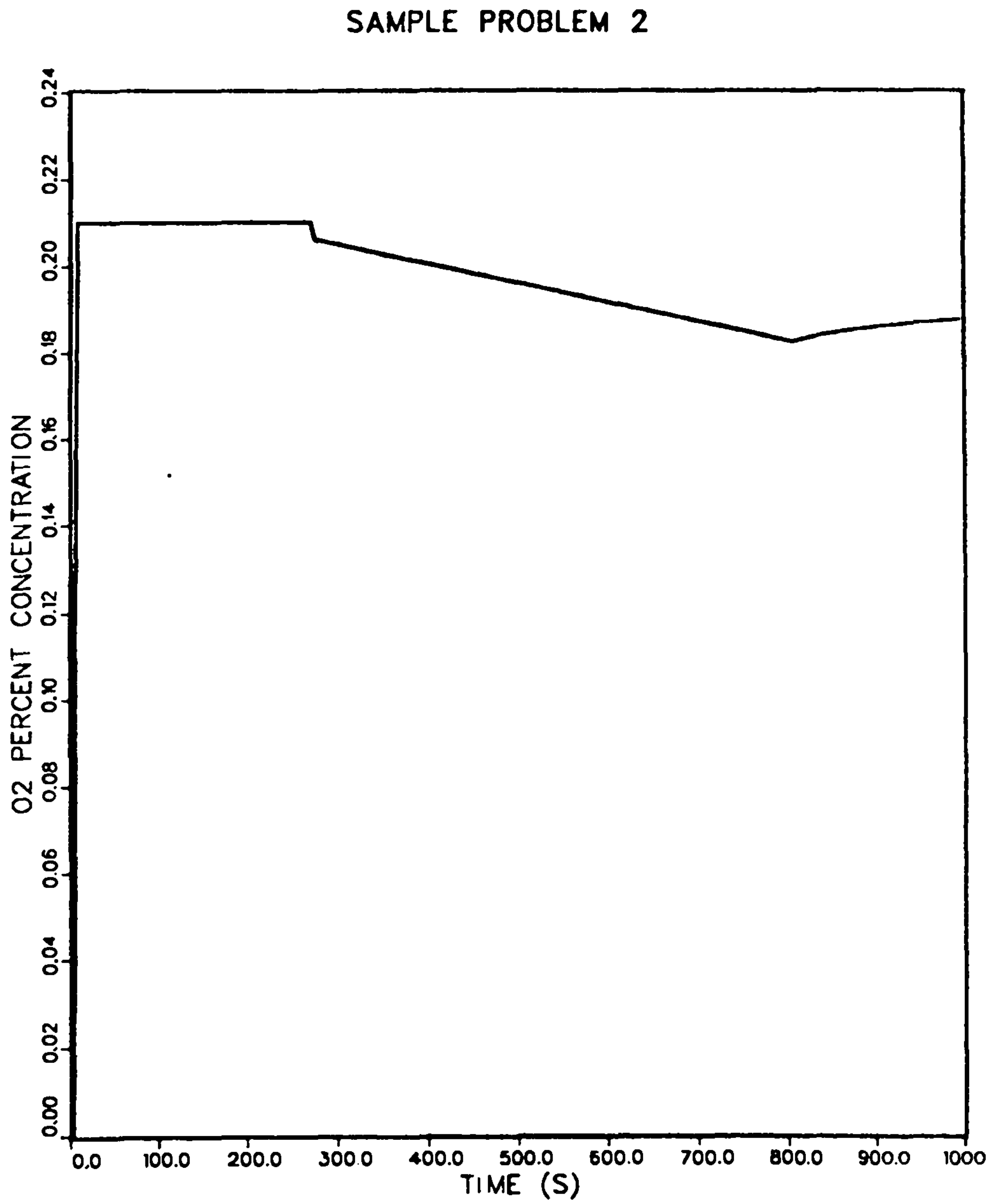

Fig. 40.
Fire compartment oxygen concentration vs time.

The system flow to and from the fire compartment is reduced gradually (after ~300 s) as the compartment exhaust filter (branch 14, filter no. 2) plugs with the smoke particulate. As the filter plugs, the polystyrene burns at a constant burning rate, thereby maintaining a constant fire compartment pressure. Even though the intake flows to the compartment are being reduced, a sufficient oxygen concentration level (>15%) is available to sustain a constant fuel burning rate (Fig. 40). Figures 41 and 42 present the smoke mass flow rate and mass accumulation on the compartment exhaust filter and at several locations near the exit to the facility. The smoke particulate release rates indicate an increasing accumulation rate in branch 14. After ~300 s, the flow rate in branch 14 decreases with time (Fig. 33); however, the smoke concentration in the hot layer (Fig. 39) steadily increases. The net result is the mass flow rate profile in Fig. 41.

The release mechanism for radioactive material is the burning of a contaminated combustible solid (polystyrene). Because the burning order (IBO) for the polystryrene is 2 and the kerosene was assumed to be uncontaminated, radioactive material is not transported through the system until the polystyrene has been ignited. The radioactive particulate mass flow rate and mass accumulations for the 20-μm particle size distribution are presented in Figs. 43 and 44. The radioactive particulate results are similar to the smoke particulate results and can be explained similarly.

Following the termination of the fire (~806 s), the smoke and radioactive particulate flow rate begins to decrease as the particulate concentrations in the hot layer decrease and as the compartment exhaust flow decreases. The system gradually will establish new steady-state operating conditions based on the consequences of the fire. By ~1000 s, more than 1.21 lbm (0.55 kg) of smoke particulate has been deposited on the fire compartment exhaust filter. To the system, the particulate mass on the filter represents an increase in resistance for branch 14. The system will readjust and establish new steady-state conditions based on the increase in flow path resistance for branch 14.

C. Summary

Sample Problem 2 illustrated how FIRAC can be applied to a more complex facility. Also implementation of the FIRIN sequential burning option, the influence of the filter plugging factor option, the release of radioactive material by burning a contaminated conbustible solid, three internal boundary

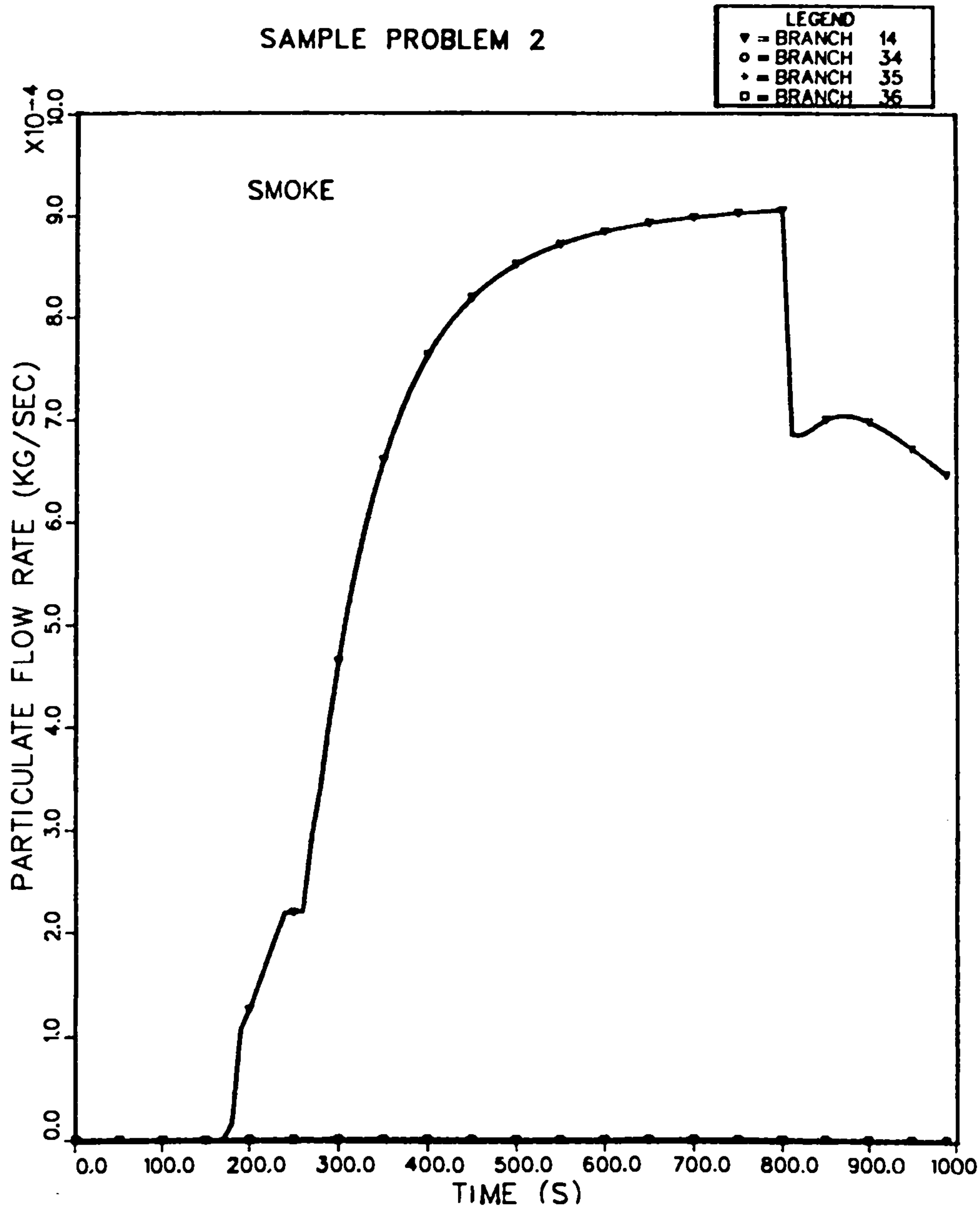

Fig. 41.
Smoke particulate mass flow rates for branches 14, 34, 35, and 36.

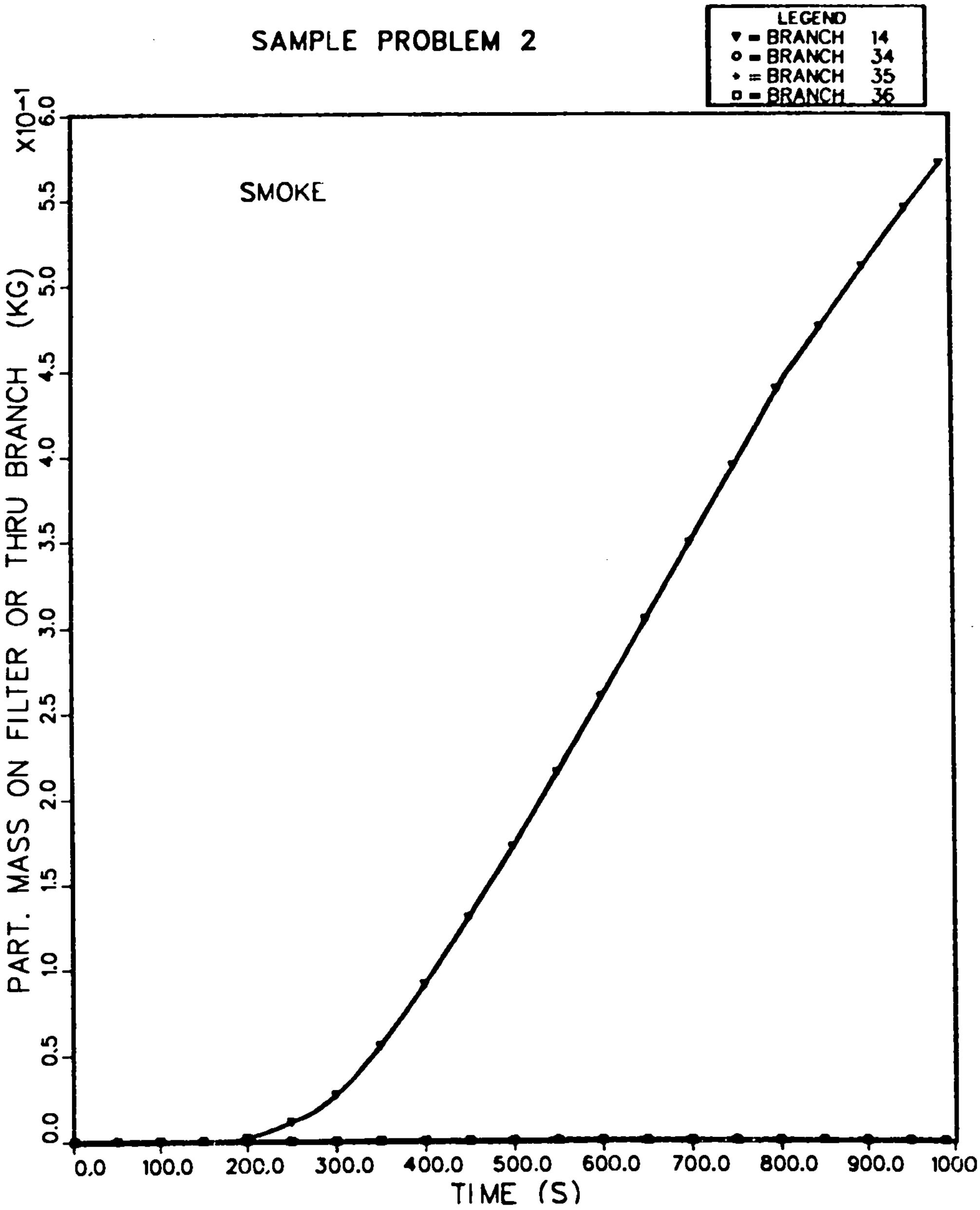

Fig. 42.
Accumulated smoke particulate mass for branches 14, 34, 35, and 36.

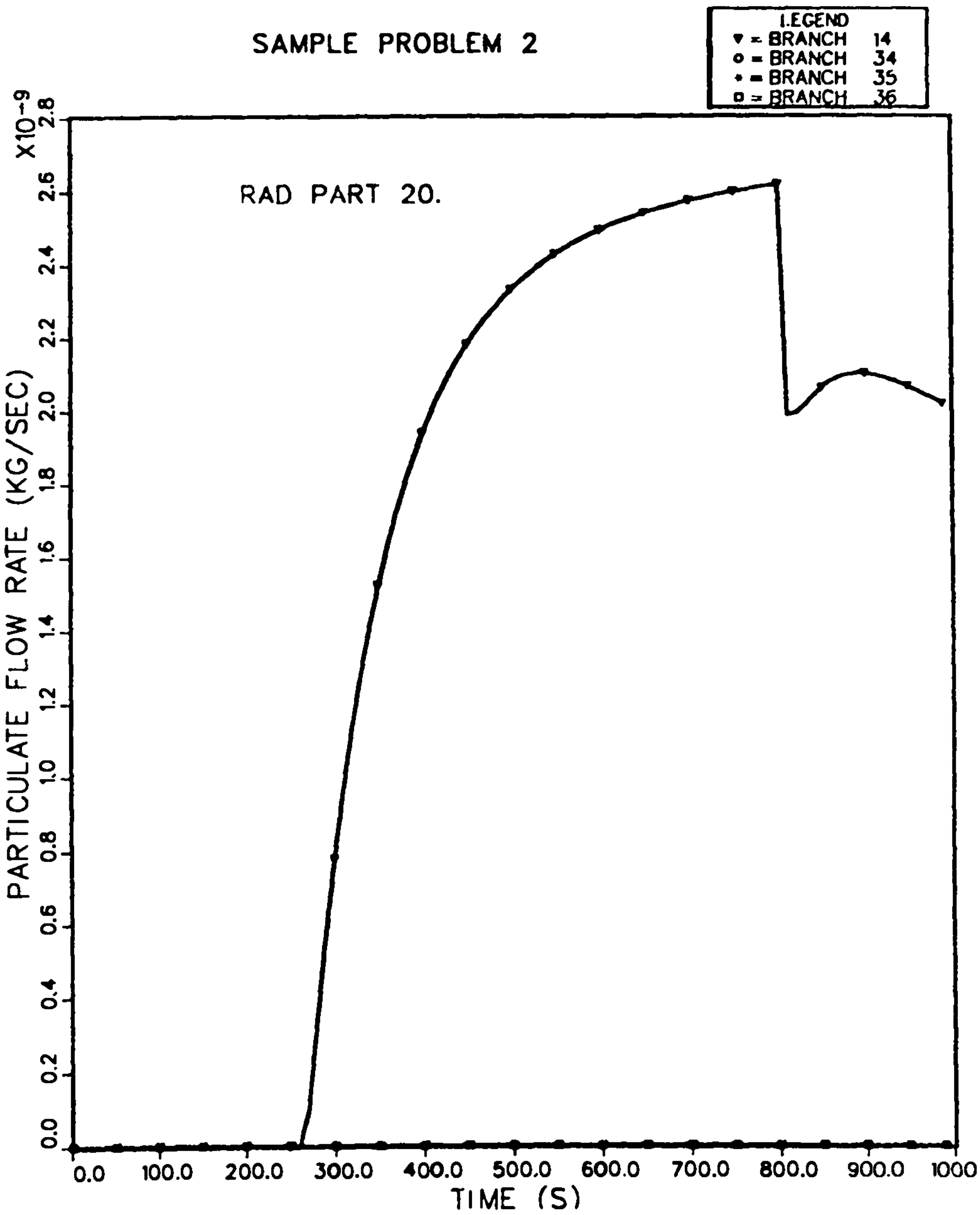

Fig. 43.
20-μm radioactive particulate mass flow rates for branches 14, 34, 35, and 36.

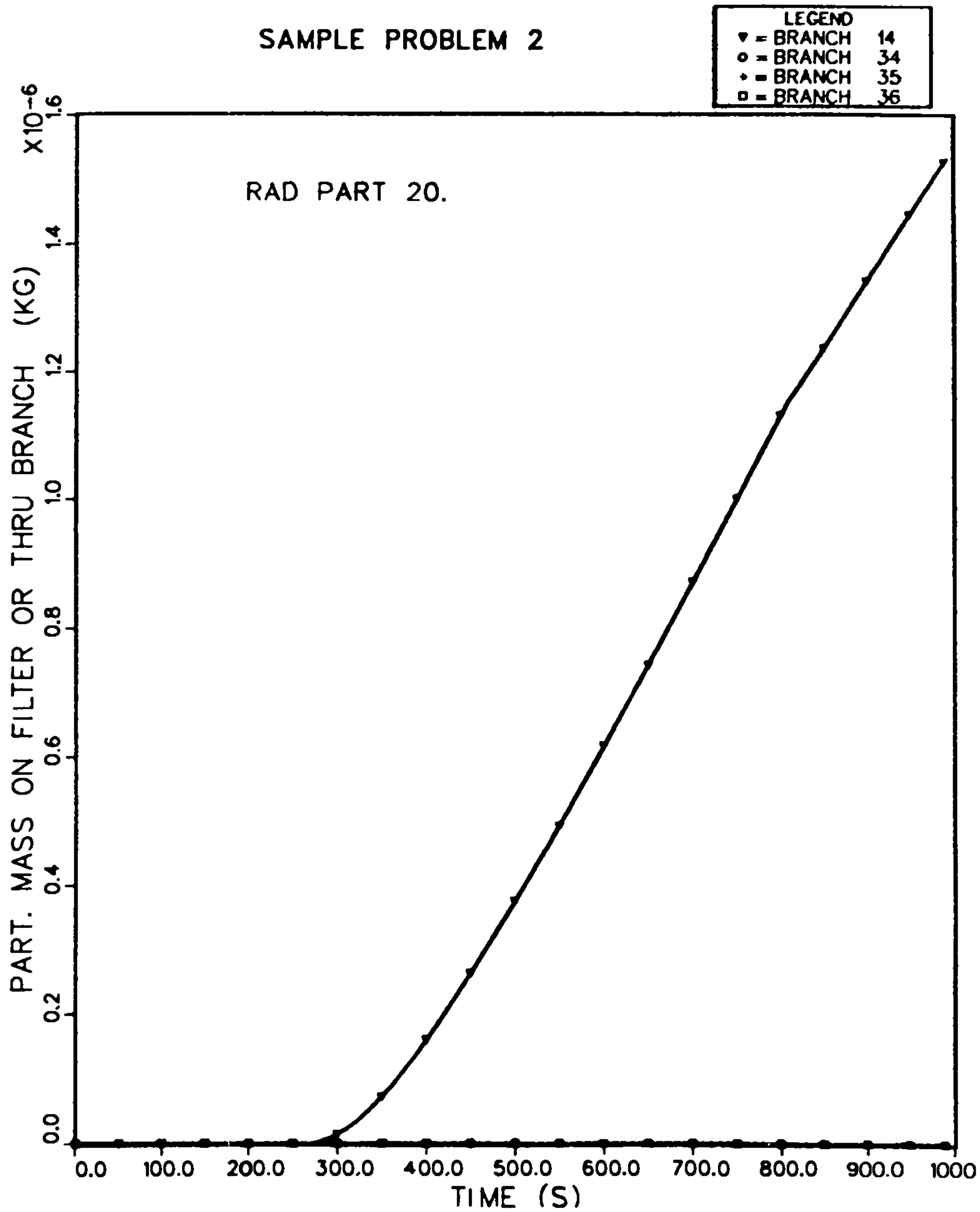

Fig. 44.
20-μm radioactive particulate mass for branches 14, 34, 35, and 36.

nodes representing the fire compartment, and the transport of 11 radioactive particle sizes and smoke particulate were demonstrated. Sample Problem 2 also indicates how complicated the interpretation of the calculated results can become when several user options are enabled. For this sample problem, the filter plugging factor proved to be an important input variable. The system's response to the fire would have been different if the filter plugging option had not been used. If the user plans to make a best-estimate calculation, input variables and code options that influence the results significantly should be recognized and used with consideration.

ACKNOWLEDGMENT

This manual represents the work of many individuals over a period of several years. The principal structure of the code was developed by J. W. Bolstad. The gas dynamics and material convection concepts were made by P. K. Tang. The material depletion mechanisms were implemented by R. A. Martin. M. W. Burkett was responsible for coupling the Pacific Northwest Laboratories' fire model with the FIRAC computer code and performing sensitivity studies with it. F. R. Krause contributed in the fire source simulation area. R. D. Foster's contribution was assisting in the development of heat transfer modules. R. W. Andrae assisted with programming and debugging the gas dynamics used in the code. D. V. Talbott converted the code to the CRAY, VAX, and PC computers; he also developed the damper model used in the code.

APPENDIX A

GAS DYNAMICS SUMMARY

I. INTRODUCTION

This discussion includes a very brief summary of the gas dynamics used in the code. The formulation of the equations is similar to those used in the EXPAC code,[3] and a more detailed discussion of the theoretical and numerical formulation of the working equations is described there.

The lumped-parameter method is the basic formulation that describes the system. No spatial distribution of parameters is considered in this approach, but an effect of spatial distribution can be approximated by noding. Network theory, using the lumped-parameter method, includes a number of system elements, called branches, joined at certain points, called nodes. Ventilation system components that exhibit flow resistance and inertia, such as dampers, ducts, valves, and filters, and that exhibit flow potential, such as blowers, are located within the branches of the system.

The connection points of branches are nodes for components that have finite volumes, such as rooms, gloveboxes, and plenums, and for boundaries where the volume is practically infinite. Therefore, all internal nodes possess some finite volume where fluid mass and energy storage are accounted for.

II. MASS EQUATION

The continuity equation (conservation of mass) is applied at each internal node. The mass equation for such nodal points is

$$V \frac{d\rho}{dt} = \sum_k \dot{m}_k + \dot{M}_s \quad , \tag{A-1}$$

where m_k is the mass flow rate in branch k, and ρ is the density of the node. M_s is the user-specified mass source per unit time for the volume, and V is the volume of the node. The convention used here is that positive mass flows represent flow into the node.

III. ENERGY EQUATION

The energy equation used in the code is

$$\frac{dp}{dt} = \frac{R}{C_v V} \left[\sum_k \left(\dot{m}_k \, C_p T_k + \frac{v_k^2}{2} \right) + \dot{M}_s C_p T_s + \dot{E}_s \right] \quad . \tag{A-2}$$

The nodal pressure is p, and R, C_v and C_p represent the gas constant, specific heat at constant volume, and specific heat at constant pressure, respectively. T_k and v_k are the branch gas temperature and velocity. The temperature associated with mass addition is T_s and the energy addition is E_s. A perfect gas law has been used to obtain this expression.

IV. MOMENTUM EQUATION

A momentum equation of incompressible form for a duct with constant area is used.

$$\frac{\ell}{A} \frac{d\dot{m}}{dt} = - \left(p_2 - p_1 \right) - \frac{f}{D} \frac{1}{A^2} \frac{\dot{m} \, |\dot{m}|}{2\rho} + \bar{\rho} g \, \Delta z \quad ,$$

where ℓ and A are the duct length and cross-section area, ρ is the average density in the branch, g is the acceleration of gravity, and Δz is the elevation change across the branch. The values f and D represent the Moody friction factor and hydraulic diameter. For a branch with sudden area change, the following momentum equation is obtained:

$$I \frac{d\dot{m}}{dt} = \left(p_i - p_j \right) - K_{eff} \frac{1}{A^2} \frac{\dot{m} \, |\dot{m}|}{2\bar{\rho}} + \bar{\rho} g \, \Delta z \quad ,$$

where

$$I = \frac{\ell_i}{2A_i} + \frac{\ell}{A} + \frac{\ell_j}{2A_j} \quad , \text{ and}$$

$$K_{eff} = \left(\frac{f\ell_i}{2D_i} + K_i\right)\left(\frac{A}{A_i}\right)^2 + \frac{f}{D} + K + \left(\frac{f\ell_j}{2D_j} + K_j\right)\left(\frac{A}{A_j}\right)^2 \quad .$$

I represents the inertia effect of the flow path between nodal points i and j. This includes the rooms as well as the duct. K_{eff} is the total effective resistance coefficient; the minor losses, such as turning, entrance, and exit are represented by the K's.

V. CHOKING OF COMPRESSIBLE FLOW WITH DISSIPATION

The steady-state flow rate in incompressible flow is determined by the pressure drop. In compressible flow, the flow rate will reach a maximum value regardless of how much the downstream pressure is decreased if the upstream pressure is constant. This phenomenon is called choking.

We treat the quasi-steady compressible flow inside a constant area duct, where the usual one-dimensional approximation is assumed. Heat transfer is not taken into account, but friction is. For a duct with friction loss, the Mach number at the duct entrance (location 1) can reach a maximum, and the value is less than 1. This upstream critical Mach number M_1 is uniquely related to the friction loss, so that

$$\dot{m} = \rho_1 v_1 A = AM_1 \quad \gamma p_1 \rho_1 \quad .$$

This is the maximum allowable mass flow rate that a particular branch can supply for a given condition at 1. This flow rate will be compared with that from the momentum equation. Choked flow is used if the former is smaller.

An implicit numerical scheme is used to solve for the pressure and density corrections at each node. The iterative process continues until both the pressure and density corrections, δp and δe, approach zero and the system is balanced. Additional detail can be found in Ref. 6.

The result of the gas dynamic transient provides the driving force for material convection and also interacts with the material source and sink. These effects are presented in Appendix C.

APPENDIX B

DUCT HEAT TRANSFER THEORY AND METHODS

I. INTRODUCTION

The purpose of this Appendix is to give the details of the heat transfer correlations and methods used in the duct heat transfer module. This module evaluates the gas temperature (T_{out}) leaving any section of the duct if the gas velocity and inlet temperature (T_{in}) are known. This temperature is the temperature (T_k) needed to evaluate the energy equation in the gas dynamics module [Eq. (A-2)]. In addition, this module describes how the combustion gas in the system heats up or cools down as it flows through the ducts in the ventilating system. These temperatures and the physical geometry are shown on Fig. B-1.

The user may divide the duct into one or more sections by breaking the duct into a number of branches. Each section of the duct (or branch) is characterized by an average gas temperature (T_g) for that branch. This average temperature is simply the mean of its inlet and outlet temperatures. The outlet temperature is a function of the inlet temperature and the amount of energy the gas loses as it passes through this section of the duct. This energy loss is a sum of two terms, Q_r and Q_c. Q_r is the net amount of energy loss because of radiation from the gas to the duct wall. Q_c is the energy loss resulting from forced convection heat transfer from the gas to the duct wall.

It will be shown that the gas temperature is a function of the energy loss, but furthermore, the energy loss is a function of the gas temperature and wall temperature (T_i), which itself is a function of the energy loss. Because the heat-transfer processes are nonlinear in temperature, solving the equations requires that a set of nonlinear coupled differential and algebraic equations be solved. This set of equations is solved using an iterative method.

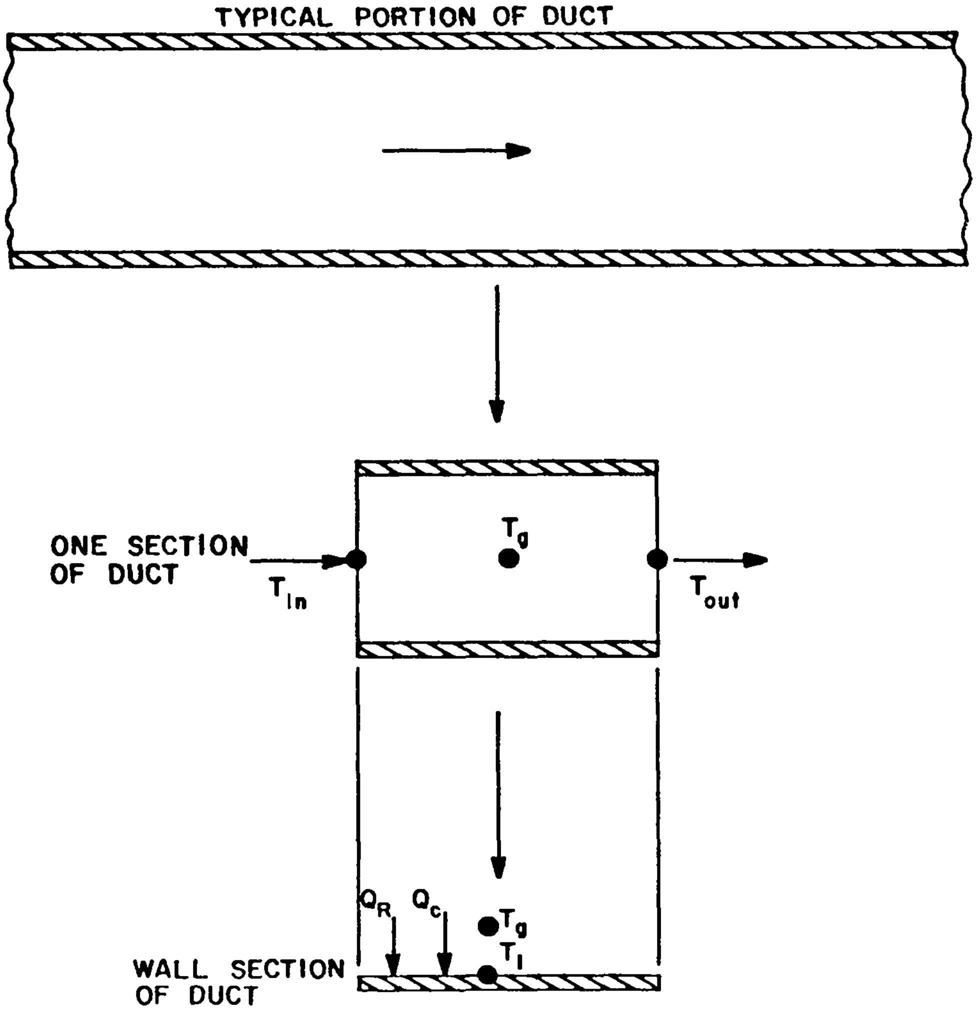

Fig. B-1.
Definition of temperatures and physical geometry used in the duct heat transfer module.

II. MODEL DESCRIPTION

A. Energy Equation for Duct

We consider a section of duct with a known inlet temperature and mass flow rate. We wish to determine the outlet temperature to solve the energy balance for the downstream room node. The energy balance across this section of duct gives

$$T_{out} = T_{in} - \frac{Q_i}{\dot{m}\, C_p} , \qquad \text{(B-1)}$$

where Q_i is the net amount of energy transferred from the gas to the duct wall, m is the mass flow rate through the duct, and C_p is the gas specific heat. The net amount of energy transferred is the sum of convection and radiation heat transfer processes from the flowing gas to the duct inside wall. The solution of Eq. (B-1) for the duct outlet temperature is the net result of the duct heat transfer model. The quantites mC_p and T_{in} are known, and thus the evaluation of the net energy transfer Q_i will allow the solution of the equation.

B. Heat Transfer from Combustion Gas to Inside Duct Walls

The net energy transfer between the combustion gas and duct walls may be broken into two components,

$$Q_i = Q_{ci} + Q_{ri} , \qquad \text{(B-2)}$$

where Q_{ci} is the net amount of energy transferred from the gas to the duct inside surface because of forced-convection heat transfer and Q_{ri} is the net amount of energy transferred from the gas to the duct wall because of radiation heat transfer. Each of these quantities may be determined independently. They are evaluated using standard correlations based on experimental data. These correlations are described in the following sections.

1. Forced-Convection Heat Transfer (Inside Duct). In general, the forced-convection heat transfer may be calculated from an equation of the form

$$Q_{ci} = h\, A\, (T_g - T_i) \quad , \tag{B-3}$$

where A is the wall (heat transfer) surface area, T_g is the bulk gas temperature, T_i is the inside duct wall temperature, and h is the heat transfer coefficient.[7] There are many available correlations for h. The best correlation for a particular application depends on many factors. Many correlations for forced convection are summarized in Ref. 8. A particularly suitable correlation for cooling of gases is

$$h = .023\, \frac{k}{D}\, (Re)^{.8} (Pr)^{.3} \quad , \tag{B-4}$$

where Re is the Reynolds number, Pr is the Prandtl number, k is the gas thermal conductivity, and D is the duct equivalent diameter.[9] This is the correlation used in the model, and it applies when the Prandtl number is between 0.7 and 120, the Reynolds number is in the range 10 000—120 000, and the length of the duct is at least 60 equivalent diameters.[40] For small temperature differences $[(T_g - T_i) < 100°F]$ the physical properties are evaluated at the gas (bulk) temperature. For larger temperature differences, the properties are evaluated at the average of the two temperatures. Thus, the heat transfer coefficient is a function of the duct geometry, fluid properties, gas mass flow rate, and the gas and duct wall temperatures. For a fixed geometry, Eq. (B-3) has the functional dependence

$$Q_{ci} = f(T_g, T_i) \quad . \tag{B-5}$$

The gas temperature is known, but the wall temperature must be described by an additional model to evaluate the forced-convection heat transfer.

2. Radiation Heat Transfer (Inside Duct). For the case of airflow in a duct, the emissivity and absorptivity go to zero, and radiation heat transfer is unimportant. Hottel[10] states that gases with symmetric molecules (for example, hydrogen, oxygen, and nitrogen) do not have emissivities of sufficient magnitude to cause radiation heat transfer to be an important effect.

On the other hand, if the gas contains any heterpolar constituents (for example CO_2, H_2O, SO_2, and hydrocarbons), radiation heat transfer from the gas to the structure may become significant. It becomes even more significant if the gas contains luminous flames, glowing char particles, soot, or black particles. In this case, the emissivity and absorptivity are complex functions of their temperature, partial pressure, superimposed radiation, and system geometry.

A complete treatment of radiation heat transfer that includes these complications is beyond the scope of this project. Furthermore, the basic code structure into which this model is intended to be integrated does not account for the various possible gas constituents. Therefore, we have chosen to include a simple gas radiation model that does not include many of the abovementioned complexities but still includes many of the salient features of the physical process as it is germane to this problem.

This model is intended to be applied in ducts away from the fire source. Therefore, we may assume that luminous flames do not exist in the region. This simplifies matters somewhat because the radiation from luminous flames depends on the concentration of particles, flame size and shape, and geometric factors. The second simplification results from the duct geometry. For this geometry, essentially all of the radiation emitted by the gas will be intercepted by the duct walls. Furthermore, we may assume that the duct length is much larger than its diameter, and for this case, the geometric considerations are greatly simplified.[11] Finally, we may assume that the gas pressure is near atmospheric pressure because variations from this pressure in a typical ventilation system are small. This fact greatly simplifies the use and interpretation of experimental data, which are generally available at 1 atm.

Taking into account the above assumptions, the net radiation energy transfer from a nonluminous gas to its surroundings (that is, the duct wall) may be found from

$$Q_{ri} = A\epsilon_i(I_g - I_s) \quad . \tag{B-6}$$

In this equation, ϵ_i is the emissivity of the surface, I_g is an intensity factor that is a function of the gas composition and temperature, and I_s is an intensity factor that is a function of the gas composition and wall temperature.

The intensity factors have been tabulated for a variety of individual gases and compositions of gases.[1,4] To evaluate the intensity factors appearing in Eq. (B-6), we have selected a typical gas consisting of 0.8 mole of water vapor per mole of carbon dioxide. A fit of these data for typical duct geometries gives the following equation for both the intensity factors (that is, I_g and I_s).

$$I(T) = 190\left(\frac{(T + 460)}{760}\right)^5 \quad , \tag{B-7}$$

where T is either the gas temperature or wall temperature and I(T) is in units of Btu/h-ft^2. Using Eq. (B-7) in Eq. (B-6), we have an expression for the net radiation energy transfer between the combustion gas and the duct wall. It takes the form

$$Q_{ri} = f(T_g{}^4, T_i{}^4) \quad . \tag{B-8}$$

Using Eqs. (B-5) and (B-8) in Eq. (B-2), we have an expression for the total net energy transfer between the combustion gas and duct walls. It is of the form

$$Q_i = f(T_g, T_i, T_g^4, T_i^4) \quad . \tag{B-9}$$

Therefore, we see that the total energy transfer is a function of the wall temperature as well as the gas temperature. Therefore, we cannot evaluate this term without a model for the duct wall temperature. This model is discussed below.

C. Heat Conduction Through the Duct Wall

The model for heat conduction through the duct wall is based on standard models such as Patankar[12] and will only be summarized here. The direction of heat flow is perpendicular to the direction of the gas flow, and axial conduction (along the wall) is neglected. The method may be understood by considering the quantities shown on Fig. B-2. This figure is an expanded view of the wall section of duct shown on Fig. B-1. On the inside of the wall there is an energy input, Q_i, given by Eq. (B-9); similarly, on the outside we have an energy loss, Q_o. Yet the origin of the coordinate system, be at the inside of the structure with positive direction out. We will calculate the temperature at specified points within the wall, x_j with $j = 1, N$. The number of nodal points could be only 1, in which case the temperature is the average duct wall temperature. For $N = 2$, the model will give the inside and outside wall temperatures. For $N > 2$, the model will give the wall temperatures as well as temperatures at interior nodes. (The nodes are assumed to be equally spaced.) An energy balance at each node gives the following set of coupled differential equations.

$$\begin{aligned}
\frac{d}{dt}(\rho C_{pw} T_1) &= b_1' T_1 + c_1' T_2 + Q_i \\
&\vdots \\
\frac{d}{dt}(\rho C_{pw} T_j) &= a_j' T_{j-1} + b_j' T_j + c_j' T_{j+1} \quad , \\
&\vdots \\
\frac{d}{dt}(\rho C_{pw} T_N) &= a_N' T_{N-1} + b_N' T_N + Q_o
\end{aligned} \tag{B-10}$$

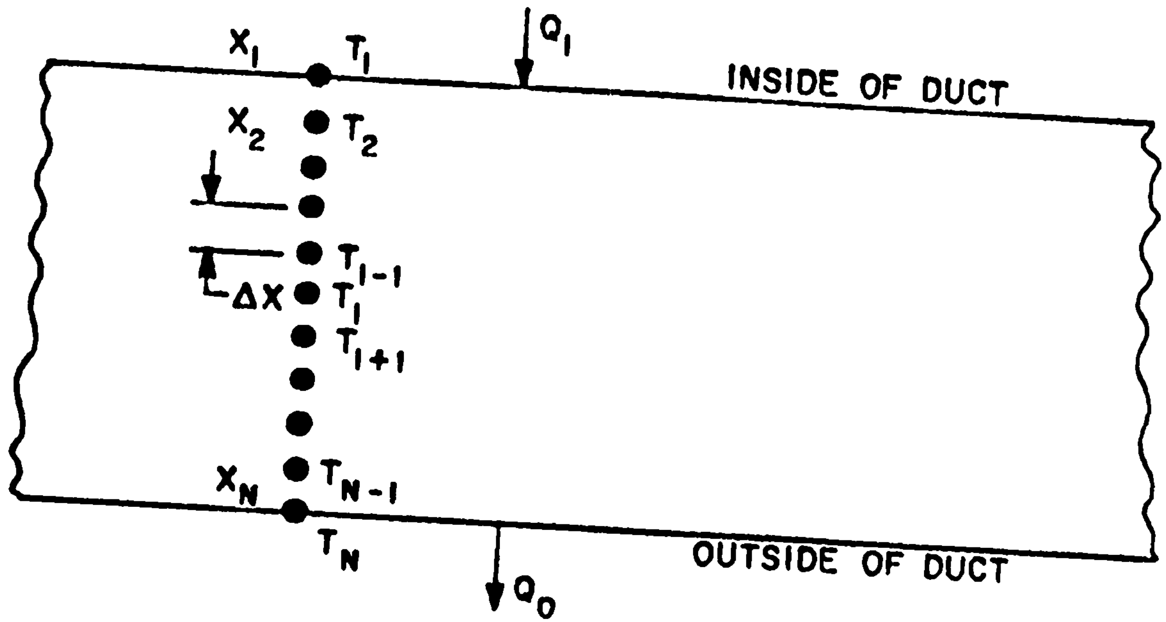

Fig. B-2.
Definition of geometry and noding for one-dimensional heat conduction through the duct wall.

where ρ is the density of the wall, C_{pw} is the constant pressure specific heat of the wall, and a_j', b_j', and c_j' are constants. To solve the set of equations, the derivative terms are put into a finite difference form:

$$\frac{dT_j}{dt} = \frac{T_j^{n+1} - T_j^{n}}{\Delta t} \quad .$$

Here T_j^n signifies the temperature at node j and time t^n. Using this expression in Eq. (B-10) reduces the set of differential equations to the following set of algebraic equations.

$$\begin{array}{ccccccc} d_1 & e_1 & & & & & \\ c_2 & d_2 & e_2 & & & & 0 \\ & & \ddots & & & & \\ & & & c_i & d_i & e_i & \\ 0 & & & & & \ddots & \\ & & & & & c_N & d_N \end{array} \begin{array}{c} T_1^{n+1} \\ T_2^{n+1} \\ \vdots \\ T_i^{n+1} \\ \vdots \\ T_N^{n+1} \end{array} = \begin{array}{c} b_1 \\ b_2 \\ \vdots \\ b_i \\ \vdots \\ b_N \end{array} + \begin{array}{c} Q_i \\ 0 \\ \\ 0 \\ \\ Q_o \end{array} \qquad \text{(B-11)}$$

The constants in the equations are functions of the wall properties ρ, C_{pw}, and k_w; the geometry Δx; the time-step size Δt; and the nodal temperatures at the previous (known) time. These constants are defined as

$$c_i = - \frac{k_w}{\Delta x} \quad ,$$

$$d_i = \frac{\rho C_{pw}\,\Delta x}{\Delta t} + 2\,\frac{k_w}{\Delta x} \quad ,$$

$$e_i = \frac{-\,k_w}{\Delta x} \quad , \text{ and}$$

$$b_i = \frac{\rho C_{pw}\,\Delta x}{\Delta t}\,T_i^{\,n} \quad .$$

The set of equations in Eq. (B-11) may be written in the compact matrix form

$$E\,\underline{T}^{n+1} = \underline{B} + \underline{Q} \quad .$$

The E matrix is tridiagonal as shown in Eq. (B-11). It is easily inverted by the tridiagonal-matrix algorithm detailed in Ref. 12 with the result

$$\underline{T}^{n+1} = E^{-1}\underline{B} + E^{-1}\underline{Q} \quad , \tag{B-12}$$

where E^{-1} is the inverse of matrix E. Thus, if the energy deposition on both sides of the duct wall is known (that is, Q_i and Q_o), all temperatures at an advanced time, t^{n+1}, can be obtained from those at a previous time t^n.

Eq. (B-9) gives an expression for Q_i; however, Eq. (B-12) shows that we still need to evaluate Q_o before we can solve for the temperatures. Furthermore, Eq. (B-9) shows that we must solve Eq. (B-12) for the temperatures before the energy source [Eq. (B-9)] can be evaluated.

D. Heat Transfer from Outside Duct Walls to the Atmosphere

The net energy transfer between the duct outside surface and the surroundings may be broken into two components:

$$Q_o = Q_{co} + Q_{ro} \quad , \tag{B-13}$$

where Q_{co} is the net amount of energy transferred from the duct wall because of natural convection heat transfer and Q_{ro} is the net amount of energy transferred from the outside duct wall to the atmosphere resulting from radiation heat transfer. Each of these quantities may be determined independently. The correlations used to evaluate these quantities are described in the following sections.

1. Natural Convection Heat Transfer (Outside Duct). Experimental data show[13] that natural convection heat transfer from horizontal ducts may be correlated well with the functional form

$$Q_{co} = h\,A\,(T_N - T_o) \quad , \tag{B-14}$$

where h is a heat-transfer coefficient based on experimental data, A is the duct outside heat-transfer area, T_N is the duct outside wall temperature, and T_o is the air temperature. The correlation used for h is divided into two distinct regimes.

$$\begin{aligned} h &= 0.53\,\frac{k}{D}\,(GrPr)^{.25} && GrPr < 10^9 \quad , \text{ and} \\ h &= 0.094249\,\frac{k}{D}\,(GrPr)^{1/3} && GrPr \geq 10^9 \quad . \end{aligned} \tag{B-15}$$

Here k is the air thermal conductivity, D is the duct equivalent diameter, Gr is the Grashof number, and Pr is the Prandtl number. All thermodynamic quantities are evaluated at the film temperature (average of wall and air temperatures).

2. Radiation Heat Transfer (Outside Duct). The net energy interchange between the outside duct walls and the environment may be approximated by the formula[14] for the energy transfer between a diffuse-gray surface and a black surface:

$$Q_{ro} = \sigma A\,(\epsilon T_N{}^4 - \alpha T_o{}^4) \quad . \tag{B-16}$$

Here σ is the Stephan-Boltzman constant, A is the duct outside heat-transfer area, ε is the emissivity of the outside duct wall evaluated at temperature T_N, and α is the absorptivity of the duct wall evaluated at temperature T_o.

Using Eqs. (B-14) through (B-16) in Eq. (B-13) gives the final expression for the total net energy transfer between the outside duct wall and the environment. It is of the form

$$Q_o = f\ (T_N^{\ 4}) \quad . \tag{B-17}$$

III. THE SOLUTION METHOD FOR THE EQUATIONS

The net result of the duct heat-transfer model is to predict the gas temperature (T_{out}) leaving any section of duct if the gas properties and inlet temperature (T_{in}) are known. The outlet temperature is given by the equation

$$T_{out} = T_{in} - \frac{Q_i}{\dot{m}\ C_p} \quad . \tag{B-18}$$

However, as shown above, the net energy transferred from the gas (Q_i) is dependent on the duct wall temperatures. In fact, the quantity Q_i is the partial solution of the following set of four equations in four unknowns.

$$Q_i = f\ (T_g,\ T_i,\ T_g^{\ 4},\ T_i^{\ 4}) \quad ,$$

$$Q_o = f\ (T_N^{\ 4}) \quad ,$$

$$T_i = f\ (Q_i,\ Q_o,\ T_N) \quad , \text{ and}$$

$$T_N = f\ (Q_i,\ Q_o,\ T_i) \quad .$$

The equations are nonlinear, and a direct solution is not possible. The heat-transfer module solves these four equations using an iterative method. To solve these equations, we define the tilde (temporary) quantities. These are the best (latest) estimates of the exact solution of the coupled equations. For the first iteration in a time step, these quantities are estimated to be the solution of the equations at the previous time step. The tilde quantities are calculated in the following order.

$$Q_o = f\ (T_g,\ T_n) \quad ,$$

$$Q_i = f\ (T_g,\ T_i) \quad ,$$

$$T_i = f\ (Q_o,\ Q_i) \quad , \text{ and}$$

$$T_n = f\ (Q_o,\ Q_i) \quad ,$$

where the functional form is defined by the above models. The duct outlet temperature then is evaluated:

$$T_{out} = T_{in} - \frac{Q_i}{\dot{m}\ C_p} \quad .$$

This duct outlet temperature is used as the room inlet temperature in the gas dynamics energy equation for a downstream room node. A solution of the room energy equations produces new duct gas temperatures (T_g and T_{in}), and the process is repeated until convergence is achieved in the gas dynamics iteration.

IV. SUMMARY

The duct heat transfer module evaluates the gas temperature leaving any duct for given duct inlet temperatures and gas properties. Four distinct heat-transfer regimes are modeled. These are forced convection and radiation heat transfer between the combustion products and the inside duct wall and natural convection and radiation heat transfer between the outside duct wall and the environment. The total amount of energy removed from the gas as it flows through the duct is shown to be the solution of a set of four coupled nonlinear algebraic equations. These equations are solved using an iterative procedure. The primary output from this module is the downstream (outlet) duct temperature. A secondary quantity calculated is the duct wall temperatures. The inputs necessary to execute the module include the following.

- Duct equivalent diameter
- Duct heat transfer area
- Duct outside wall emissivity
- Duct outside wall absorptivity
- Duct wall thermal conductivity
- Duct wall density
- Duct wall specific heat
- Number of heat transfer nodes in duct wall
- Duct wall thickness
- Duct wall temperatures at previous time step
- Environmental temperature outside duct
- Upstream (duct inlet) gas temperature
- Duct average gas temperature
- Duct average gas velocity
- Duct average gas density
- Time step size

APPENDIX C

MATERIAL TRANSPORT THEORY

I. INTRODUCTION

The purpose of the material transport algorithms in the code is to provide an estimate of the aerosol or gas transport within a nuclear fuel cycle facility. Ultimately, we would like to predict the quantity and physical and chemical characteristics of hazardous material that may be released from the facility as a result of an explosion. The transport can occur through rooms, cells, canyons, corridors, gloveboxes, and ductwork installed within the facility. The entire flow pathway forms, in many cases, a complex interconnected network system. Using the computer code, material concentrations and material mass flow rates can be calculated at any location in the network, including the supply and exhaust of the network system. Most importantly, the code will perform the transport calculations as a function of time for an arbitrary user-specified explosive transient. There is no need to assume steady flow as required in some material transport codes, but we can use the code to determine material transport under steady flow conditions if desired.

A generalized treatment of material transport under accident conditions could become very complex. Several different types of materials could be transported. More than one phase also could be involved including solids, liquids, and gases with phase transitions. Chemical reactions could occur during transport and lead to the formation of new species. Further, there will be a size distribution function for each type of material that varies with time and position, depending on the relative importance of effects such as homogeneous nucleation, coagulation (material interaction), diffusion (both by Brownian motion and by turbulence), and gravitational sedimentation. We know of no computer code that can handle transient-flow-induced material transport in a network system subject to the possibility of all of these complications. The transport portion of this code does not include this level of generality either. This initial material transport capability consists of the following.

- Gas dynamics decoupled from material transport
- Homogeneous mixture and dynamic equilibrium

- Material transport provided for an arbitrary number of particulate and gaseous species
- No material interaction during transport
- Material deposition based on gravitational settling using relationships from the literature
- Turbulent and Brownian diffusion, and thermophoretic effects are neglected
- Phase change, chemical reaction, and electrical migration not allowed
- Material entrainment can be specified arbitrarily using tabular inputs or calculated using semi-empirical relationships based on wind tunnel data

The code is organized into modules so that improved versions can be incorporated easily. This is discussed in the following section followed by information on material characteristics that may be useful to the analyst. The sections that follow are detailed descriptions of the material transport modules found within this version of the code.

II. MODULAR STRUCTURE

Movement or transport of material by a flowing fluid involves several basic mechanisms. The primary mechanism for movement is the flow of the fluid itself. This process will carry along material and is referred to as material convection. This mechanism is the primary material transport process. The other mechanisms involve physical models that could be upgraded as the state of the art improves. The basic mechanisms that we will consider in a fire-induced flow environment are

- transport initiation,
- convective transport,
- transport interaction, and
- transport depletion.

The material transport capability uses all of the basic mechanisms except transport interaction. In addition, the transport depletion module is restricted to gravitational settling and filtration.

III. MATERIAL CHARACTERISTICS

In applying the material transport capability, the user must identify the type (aerosol or gas), quantity, and location of material at risk. If the material is a solid or liquid aerosol, a characteristic size and density must be specified. For example, if the user is concerned primarily with the transport of aerosols in the size range of $D_p \leq 12$ μm and with densities of $0.5 \leq \rho_p \leq 12$ g/cm^3, he could run the code for some assumed cases of (D_p, ρ_p) to determine entrainment or deposition sensitivity.

The user may wish to characterize a nonideal aerosol contaminant with approximate or idealized values of (D_p, ρ_p). We advise caution in this because there are many different ways to characterize the diameter of aerosols of irregular shape and nonuniform density. For example, diameters representing a mean value relative to total count, surface area, volume, weight, or terminal settling velocity may be estimated based on frequency of occurrence data.

For the case of aerosol transport along fuel cycle facility pathways, we are interested in changes in aerosol concentration resulting from entrainment, dilution, deposition, and filtration. Entrainment, deposition, and filtration all depend on the quasi-steady aerodynamic drag characteristics of the aerosol. Unless the aerosol is very small (less than 0.5 μm), the probability that a spherical particle or droplet will deposit depends on the magnitude of its terminal settling velocity u_s.

$$u_s = \rho_p D_p^2 C g / 18\mu \quad , \tag{C-1}$$

where

ρ_p = actual density,

D_p = diameter,

C = Cunningham slip factor,

g = gravitational acceleration, and

μ = air dynamic viscosity.

Most aerosols (spherical or not) having the same settling velocity will be distributed throughout a ventilation system network in a similar manner. The recommended deposition parameter is the aerodynamic diameter or Stokes diameter.

(1) Aerodynamic diameter, D_a, is the diameter of a sphere of unit density having the same terminal speed as the contaminant.

(2) Stokes diameter, D_s, is the diameter of a sphere with the same bulk density and terminal speed as the contaminant.

These diameters are related by the equation

$$u_s = \rho_p D_s^2 C_s g/18\mu = \rho_o D_a^2 C_a g/18\mu \quad , \tag{C-2}$$

where C_s and C_a are the slip factors associated with D_s and D_a, respectively, and ρ_o is unit density. For the contaminant of interest, D_s or D_a may be measured directly using such aerodynamic classification devices as impactors, centrifuges, sedimentometers, or air elutriators. These devices are suitable for measuring the size of irregularly shaped particles. An aerodynamic diameter measurement should be based on activity if possible. Otherwise, we recommend using D_a based on mass measurements.

If count frequency data (for example, based on projected area diameter for irregular shaped particles) are available for the contaminant, it must be converted to aerodynamic diameter. Such data should be plotted on log-probability paper and fit with a straight line. If this straight-line fit to the data is acceptable, the size distribution is approximately log-normally distributed and may be described completely by two parameters, geometric count median diameter, D_{gc}, and geometric standard deviation, σ_g. Most fine particle systems formed by comminution of a bulk material or grown by accretion have log-normal size distributions; therefore, this assumption is recommended.

Thus, the user can obtain D_{gc} and σ_g from log-normally distributed count frequency data. Now the set of Hatch-Choate[15] transformation equations apply. These equations relate D_{gc} and σ_g to a number of other median and mean diameters that may be important depending on how the toxic substance or "activity" is related to the physical properties of the particle. For example, the activity may be proportional to the total number, total surface area, or total mass of the particles. We choose to work on a mass basis. The user may calculate the geometric mass median diameter D_{gm}, the volume mean diameter D_v, and the weight mean diameter D_w from

$$\begin{aligned} \log D_{gm} &= \log D_{gc} + 6.908 \log^2 \sigma_g \ , \\ \log D_v &= \log D_{gc} + 3.454 \log^2 \sigma_g \ , \text{ and} \\ \log D_w &= \log D_{gc} + 8.023 \log^2 \sigma_g \ , \end{aligned} \tag{C-3}$$

where the logarithms are calculated using base 10. The median diameters referenced above divide the count-based and mass-based size distributions in half. For example, half of the mass of the sample lies above D_{gm} and half below. A mean diameter is the diameter of a hypothetical particle that is intended to represent the total number of particles in the sample.

In the absence of specific information on the aerodynamic properties of the aerosol of interest, Stockham[15] recommends using D_w as an approximation to aerodynamic size. An alternative is to convert D_v to an aerodynamic diameter. (If we assume the material density to be uniform, independent of size, and known, the mass of the particle with size D_v is a mean mass.) To do this, use

$$D_a = \left(6/\pi \ \ \rho_p/\rho_o \ \ \alpha_3/K_r\right)^{1/2} D_v \ , \tag{C-4}$$

where

α_3 = volume shape factor, and

K_r = resistance shape factor.

Values of α_3, K_r are listed in Mercer, where this calculation is discussed.[16]

We also advise caution in estimating aerosol density. The aerosol produced by accident conditions may consist of flocculi and agglomerates with actual densities well below the theoretical density of the pure parent materials. The floc densities may be as much as an order of magnitude less than the normal density. Pertinent information concerning fuel grade powder size and density is given in Refs. 17 and 18, and useful information concerning drop sizes and densities is given in Ref. 17.

IV. TRANSPORT INITIATION

The code provides the analyst with two options for transport initiation: (1) user specification of mass injection rate vs time and (2) calculated aerodynamic entrainment. These options are quite different. They require different levels of effort and judgment from the analyst. In this section, we will provide background to help the user supply numbers for source term initiation using option (1). We will describe the procedure and equations used with option (2) in detail. The primary cause of initiation is assumed to be transient flow induced by an accident. Two examples illustrating the use of option (1) will be discussed first.

As a first example, consider a decomissioned fuel reprocessing facility with contaminated enclosures. The analyst can estimate the preaccident aerosol concentrations in these areas using the resuspension factor concept. The resuspension factor K was used extensively to quantify airborne contamination levels in operational fuel cycle facilities. By definition,

$$K = \frac{\text{aerosol concentration } (g/m^3)}{\text{surface loading } (g/m^2)} \text{ , } 1/m \text{ .}$$

Sutter[19] has tabulated ranges of K that were compiled from numerous references. The tables include values of K derived from measurements of airborne contamination resulting from numerous and varied cases of outdoor wind stresses and indoor mechanical stresses. Sutter's summary tables are useful for obtaining bracketing or bounding values of K. With assumed or measured values of K and surface loading, the user can calculate the airborne material concentration subject to transport. Based on the enclosure volume, a quantity or mass of contaminant subject to transport can be calculated from the concentration. This mass can be injected using the user-specified option at the system node representing the enclosure of interest. Mass injection rate must be specified by the analyst.

Healy[20] reviewed many measurements and applications of this simplistic resuspension factor concept. Several of its limitations are noteworthy. First, measured values of K range over 11 orders of magnitude. For benign conditions where K is most reliable, the uncertainty is at least 2 orders of magnitude. Further, K fails to account for particle, surface, or local flow characteristics except as they existed during a particular measurement. Thus, we recommend using the resuspension factor only for estimating preaccident airborne mass subject to transport as suggested by this example.

As a second example, consider a mixed-oxide fuel fabrication facility in which bulk MOX powder is being protected. The user may elect to model this facility and run the code for a transient without material transport. This preliminary run would supply an estimate of system flow rates and pressure drops during the accident. Some controlled areas may be subjected to abnormally high air velocities that could lead to entrainment because of aerodynamic stress. A knowledge of the air velocity time history will be useful to estimate the quantity of material made airborne.

We will summarize briefly three methods that can be used to estimate aerodynamic entrainment of aerosol material. Sutter[19] has reviewed and compiled data from numerous papers under the heading "aerodynamic entrainment." This paper is a good source of reference information. The analysts' objective here should be to estimate a quantity of material made airborne during the first part of or during the entire tornado transient. This quantity must be converted to a mass injection rate for input to the code as in the first example.

The first method for estimating the quantity of material made airborne by aerodynamic entrainment is to apply the "per cent airborne" and "resuspension flux" data measured by Mishima and Schwendiman.[18] For example, they measured entrainment of uranium dioxide powder and uranium nitrate solution at different air velocities. The application of these data will require engineering judgement.

A second method for estimating entrainment is to use the results developed by Singer et al.[21,22] to estimate coal dust entrainment. These results are discussed by Sutter as well.[19] Finally, the analyst may use the resuspension rate concept introduced by Sehmel and Lloyd.[23] Resuspension rate is defined as fraction of initial mass resuspended per second:

$$S = \frac{A}{G\Delta t} \quad ,$$

where S = resuspension rate, fraction/s;
A = mass suspended and flowing horizontally through a given cross-sectional area, g;
G = ground source mass, g; and
Δt = duration of sampling, s.

Measurements of S obtained during a number of atmospheric field tests are tabulated in Sutter's paper.

The procedure and equations used with option (2), calculated aerodynamic entrainment of dry powder from thick beds, will be discussed in detail. This technique is modeled in the code. It has the advantage of calculating entrainment automatically for the user. As with the three methods discussed in the second example above, our objective is to provide the material convection module with an estimate of the quantity of particulate material that can be entrained from a contaminated surface as a result of accident-induced transient flow conditions. However, the previous three methods are not suitable for use in the code because they are based on steady-state measurements for specific conditions. Except for Singer's work with coal dust,[21] they fail to couple unsteady flow (changing velocity) conditions to the amount of material entrained. In addition to local flow characteristics, the previous methods fail to account for material or surface characteristics in a systematic way. Thus, the resuspension factor, resuspension rate, and per cent airborne would have to be measured for innumerable cases to encompass accident conditions.

The analytical method used in the code for calculating aerodynamic entrainment was proposed and illustrated in a fuel cycle facility application in Ref. 5. To estimate the quantity of material entrained, this method considers the following questions. (1) When does the surface material begin to move? (2) What criterion determines when material will be suspended? (3) How much material becomes suspended? A valid answer to (1) implies that particle, surface, and flow characteristics have been taken into account. Some account also must be made for the forces acting, namely, aerodynamic, interparticle (cohesion), and surface to particle (adhesion) forces. This procedure is similar to the approach taken by Travis,[24] who developed a computer model to predict re-entrainment and redistribution of soil contaminants as a result of eolian effects.

The first question we must answer is: When does material begin to move Before particle motion can occur, a threshold air speed must be equalled or exceeded so that the aerodynamic forces will be sufficient to overcome restraining forces. To relate threshold air speed to surface effects, we introduce the friction speed

$$u_{*} = \tau / \rho \quad , \tag{C-5}$$

where τ = mean shear stress at the surface, and

ρ = fluid density.

Experimental measurements of threshold friction speed, u_{*t}, obtained at the onset of material movement are available for a wide range of material sizes and densities.

These measurements are fitted[25] to the following semi-empirical equations.

$$A = (0.108 + 0.0323/B - 0.00173/B^2) \tag{C-6a}$$

$$\times \; (1 + 0.055/\rho_p g D_p^2)^{1/2} \quad ,$$

where $A = u_{*t}/ \; (\rho_p - \rho) g D_p / \rho \; ^{1/2}$,

$B = u_{*t} D_p / \nu$,

D_p = average particle diameter,

ρ_p = particle density,

g = gravitational acceleration, and

$\nu = \mu/\rho$ = fluid kinematic viscosity.

Equation (C-6a) holds for $0.22 \leq B \leq 10$. The variable A is the threshold coefficient. The variable B is the particle friction Reynolds number. For the range $B \leq 0.22$ Eq. (C-6b) applies:

$$A = 0.266(1 + 0.055/\rho_p g D_p^2)^{1/2} \times (1 + 2.123B)^{-1/2} \quad . \tag{C-6b}$$

Equations (C-6) collapse the threshold friction speed data in the appropriate range of B onto a single curve with D_p and ρ_p as parameters. Given a particular aerosol size and density we can calculate u_{*t} from Eqs. (C-6). An iterative technique is used to solve for u_{*t} in Eqs. (C-6) because this variable appears implicitly on both sides of the equations. The value of ν was assumed to be constant at $\nu = 0.1454\ cm^2/s$, corresponding to standard atmospheric conditions.

In u_{*t} we have a measure of when particle motion will occur and, therefore, when entrainment is possible. Under given flow and surface conditions, a value of the friction velocity exceeding the threshold friction velocity can produce entrainment. That is, entrainment can occur only when $u_* > u_{*t}$. We may relate u_* to the corresponding velocity at the turbulent boundary layer edge using one of the following two equations. For a smooth surface with a laminar sublayer,[15]

$$u(y)/u_* = (1/0.41)\ \ln\ (yu_*/\nu) + 5.0 \quad . \tag{C-7}$$

For a rough surface with no laminar sublayer,[26]

$$u(y)/u_* = (1/k)\ \ln\ (y/y_0) \quad , \tag{C-8}$$

where y = distance from surface,

$k = 0.4$ = Von Karman constant,

$y_0 = R/30$ = roughness length, and

R = average surface roughness height,

and where the velocity $u(y)$ is calculated by the gas dynamics module of the code. For a duct with fully developed turbulent airflow conditions, the centerline velocity or velocity at the boundary layer edge may be 25 times higher than the average or bulk velocity. This version of the code uses Eq. (C-8) for a rough surface with an assumed boundary layer thickness of $y = 10$ cm and a roughness length of $y_0 = 0.0104$ cm (a moderately rough surface). Our use of Eq. (C-8) will lead to higher values of u_* for the same values of $u(y)$ and y than Eq. (C-7). Because entrainment is known to depend on the difference $(u_* - u_{*t})$, our choice of Eq. (C-8) will lead to conservative estimates of entrained material.

The next question is: What determines whether particles go into suspension That is, of all the particles, how do we divide those that could become airborne from those that remain close to the surface Iversen et al.[27] have shown that, for particles smaller than 52 µm, suspension occurs as soon as the threshold speed is reached. The criterion assumed here was that suspension will occur for those particles for which $u_s/u_* = 1$ and $u_* > u_{*t}$, where u_s is the particle fall or terminal speed. The friction speed u_* is of the same order of magnitude as the vertical component of turbulence in a boundary layer. Values of $D_p < 50$ µm for suspension are in agreement with measurements using soils.[24] We have assumed that all of the particles are subject to suspension.

How much material becomes suspended Travis[24] has suggested the following expression for q_v, the mass of particles per unit area per unit time that go into suspension:

$$q_v = q_h \; (c_v/u_{*t}^3 c_h) \;\; (u_*/u_{*t})^{P/3} - 1 \quad , \tag{C-9}$$

where P = mass percentage of suspendable particles, and

c_v, c_h = empirical constants (2 x 10^{-10} and 10^{-6}, respectively).

In Eq. (C-9), q_h is the mass of material moving horizontally through a vertical plane perpendicular to the surface per unit width per unit time and may be determined from[24]

$$q_h = 2.61(\rho/g)(u_* + u_{*t})^2(u_* - u_{*t}) \quad . \tag{C-10}$$

The calculated aerodynamic entrainment in the material transport module is a model that uses Eqs. (C-6) through (C-10). The steps can be summarized as follows. At a given time, the gas dynamics module of the code calculates the velocity u(y) for every volume with material subject to aerodynamic entrainment. This value of u(y) and the turbulent boundary layer velocity profile [Eq. (C-8)] are used to compute a surface friction velocity u_*. A characteristic value of threshold friction velocity u_{*t} for the input material characteristics is obtained from Eqs. (C-6). If $u_* \leq u_{*t}$, no entrainment occurs. [See Eq. (C-10).] If $u_* > u_{*t}$, then the semi-empirical entrainment Eqs. (C-9) and (C-10) are used to estimate the vertical flux of suspendable material q_v. Knowing q_v and the floor area over which the contaminant is uniformly distributed A, we can compute the source term

$$\dot{M}_p = q_v A \quad , \tag{C-11}$$

which has the units kilograms per second. As a source term, Eq. (C-11) represents a positive contribution to the M_p term on the right-hand side of Eq. C-29. The floor area A is assumed to be flat and free of obstacles or protuberances.

The question of how heavily a surface must be loaded before equations like Eqs. (C-6), (C-9), and (C-10) are applicable is debatable. For the realistic types of loadings such as we expect to find in many locations of a fuel cycle facility, the empirical constant in Eq. (C-10) may not be satisfactory because it was obtained for relatively thick powder beds. Furthermore, the empirical coefficients in Eq. (C-9) are suspect because they were obtained from experiments with soil particles.

We believe the recent experimental and theoretical work underlying Eqs. (C-6) and (C-10) is the best available.[25,27,28] Thus, the basis for predicting u_{*t} using Eq. (C-6) is sound; however, the data base to which Eq. (C-6) was fit is sparse for small, heavy particles. In principle, these uncertainties could be checked and reduced with appropriate experimentation.

V. CONVECTIVE TRANSPORT

A. Assumptions

The usual mathematical formulation for the motion of a multiphase, multicomponent material system is based on the concept of continuum mechanics with some pertinent qualifications.[29] We can obtain a set of partial differential equations for some macroscopic parameters with a few phenomenological descriptions of the stress, heat flux, and diffusion, plus other formulations for the physical and chemical interactions among phases and components and with the boundary. Some of the relationships are either incomplete or not yet known. Depending on the range of interest, an extensive simplification is necessary. The following assumptions are made to reduce the complexity of the problem but still allow us to meet our simple objective, namely, the capability of handling material transport without disturbing the main gas flow to any significant degree.

We define the material as any pneumatically transportable substance in a ventilation system. The material can be solid, liquid, or gas other than the main gas stream. The individual material is assumed to be quite small in size if it is in the condensed phase. A material cloud is an ensemble of material. Throughout the ventilation system, the main body of the gas and the material cloud form a mixture; the description of the flow system is based on the continuum point of view. We will neglect all chemical reactions and physical processes (deposition, entrainment, coalescence, material break-up, evaporation, and condensation). The material generation rate is a prescribed quantity; when the material cloud is formed and mixed with the main gas stream, our attention will be on the movement of the material.

Even for a dusty cloud, the volume occupied by the material is quite small compared with the gas volume, and we will assume this is the case and refer to it as the disperse condition. A consequence of this is that the material motion is dominated by the aerodynamic forces (mainly drag) but not by the inter-material forces. Furthermore, the material size we most often encounter in a ventilation system falls into the micron range, and the aerodynamic relaxation time is quite small compared with the typical residence time. This means the material can respond quickly to the variation of gas velocity, and most of the time the material velocity would be nearly identical to that of the gas at any location and time. Thus, we have obtained the dynamic equilibrium condition between the gas and the material cloud, and the only equation needed to find out the material flow rate is the material continuity equation. We can add one more equilibrium condition (that is, the material temperature is assumed to be the same as the gas), and we have a homogeneous equilibrium model for the gas and material cloud mixture. This mixture can be treated as a simple gas with proper thermodynamic and transport properties.

In principle, we could proceed to solve the set of gas dynamic equations for the mixture; however, the mixture transport properties are not easy to determine. On the other hand, we still can obtain governing equations for the main gas stream and for the material cloud separately. Some of these equations will contain terms that express the effect of interaction between the gas stream and the material. A closer examination of these terms reveals that if the material mass fraction is quite small compared with that of the gas, the effect of the interaction on the gas phase flow is negligible. This is the disperse condition for the material cloud relative to the gas mass, and we will assume this is the case. At this point, we have achieved the complete separation of the gas-phase flow dynamics from the material cloud. The gas dynamic aspect of the material transport problem can be solved first; then the continuity relation of the material will be used to determine the material flow. A more complete presentation of various multiphase, multicomponent flow problems is given in the literature.[29—31] All the above assumptions and steps leading to the final simplification of the material transport problem are based on those references.

B. Continuity Equation

In a volume V, a part of it is occupied by the material with mass M_p and volume V_p and the rest by the gas of mass M_g and volume V_g; obviously

$$V = V_p + V_g \quad . \tag{C-12}$$

We define a volume fraction of the material by

$$\alpha_p = \frac{V_p}{V} \quad , \tag{C-13}$$

and the densities of the material and gas based on the mixture volume,

$$\rho'_p = \frac{M_p}{V} \qquad \text{and} \qquad \rho'_g = \frac{M_g}{V} \quad , \tag{C-14}$$

which differ from the densities based on the volume of the individual phase,

$$\rho_p = \frac{M_p}{V_p} \qquad \text{and} \qquad \rho_g = \frac{M_g}{V_g} \quad . \tag{C-15}$$

Only ρ_g is related to the pressure and temperature through the equation of state. The mass fraction of the material is defined as

$$Y_p = \frac{M_p}{M_p + M_g} \quad . \tag{C-16}$$

We can express the mass fraction in terms of volume fraction through the following relation:

$$Y_p = \left[1 + \left(\frac{1-\alpha_p}{\alpha_p}\right)\left(\frac{\rho_g}{\rho_p}\right)\right]^{-1} . \tag{C-17}$$

Because the material-phase density of a liquid or solid is usually so much larger than the gas-phase density, the disperse condition (α_p<<1) does not imply the dilute condition (Y_p<<1) unless

$$\alpha_p << \frac{\rho_g}{\rho_p} , \tag{C-18}$$

which is a more stringent condition. We shall assume this is the case in the current material convection model.

The velocity of a mixture is defined as

$$u = \frac{\rho_p' \underline{u}_p + \rho_g' \underline{u}}{\rho} , \tag{C-19}$$

with

$$\rho = \rho_p' + \rho_g' . \tag{C-20}$$

ρ is the density of the mixture, and $\underline{u}$, $\underline{u}_p$, $\underline{u}_g$ represent the mixture velocity, material velocity, and gas velocity; they are vector quantities. Using the mass fraction Y_p, we have

$$\underline{u} = Y_p\underline{u}_p + (1-Y_p)\underline{u}_g , \tag{C-21}$$

If u_p and u_g are of the same order of magnitude and for the dilute condition ($Y_p << 1$),

$$\underset{\sim}{u} \quad \underset{\sim}{u}_g \quad . \tag{C-22}$$

The mixture velocity is dominated by the gas velocity. Also from Eq. (C-20), the mixture density is roughly the same as the gas density. We expect this should be the case for a light loading situation. From now on, we shall drop the subscript g for all quantities associated with the gas phase.

The continuity equation for any phase or component in a mixture is[31]

$$\frac{d}{dt} {}_V \rho'_p dV = - {}_S \rho'_p \underset{\sim}{u}_p \cdot d\underset{\sim}{S} + \dot{M}_p \quad . \tag{C-23}$$

The time derivative term on the left-hand side represents the change of the amount of material inside a control volume V. The first term on the right-hand side is the material flow through the boundary S of the volume V, and the last term is the material source. Assuming that ρ_p is uniform over the control volume and using the same representation we have for the gas continuity equation, Eq. (C-23) becomes

$$V \frac{d\rho'_p}{dt} = {}_i \rho'_{pi} u_{pi} A_i + \dot{M}_p \quad . \tag{C-24}$$

Here we drop the vector notion for the velocity but add subscript i to indicate the flow path connecting to that volume. A_i is the flow area and u_{pi} is the flow velocity normal to the area. The positiveness of the flux term is referred to as the flow into the volume. Again, we introduce Y_p into Eq. (C-24):

$$V \frac{d}{dt} [Y_p \rho] = {}_i Y_{pi} \rho_i u_{pi} A_i + \dot{M}_p \quad , \tag{C-25}$$

or

$$V \frac{dY_p}{dt} = \frac{1}{\rho} \quad {}_i \; Y_{pi} \;\; \rho_i \, u_{pi} \, A_i \;\; + \dot{M}_p - Y_p \, V \frac{d\rho}{dt} \quad . \tag{C-26}$$

The last term in Eq. (C-26) is the gas density change and is determined by the gas continuity equation.

Under the dynamic equilibrium condition, the material velocity is almost identical to the gas velocity everywhere and at any instance, namely,

$$u_{pi} = u_i \quad . \tag{C-27}$$

u_i represents the gas velocity in the pathway i. Substituting that into Eq. (C-26) and recalling that the gas mass flow in branch i is

$$\dot{m}_i = \rho_i \, u_i \, A_i \quad , \tag{C-28}$$

we obtain

$$V \frac{dY_p}{dt} = \frac{1}{\rho} \quad {}_i \; Y_p \, \dot{m}_i + \dot{M}_p - Y_p \, V \frac{d\rho}{dt} \quad . \tag{C-29}$$

Equation (C-29) is a differential equation for the unknown Y_p. Once the gas-dynamic quantities (ρ, m_i) are known, Eq. (C-29) can be integrated to obtain Y_p at a new time. The advantage of using Y_p instead of ρ_p' as unknown is that Y_p is not subject to the effect of compressibility as is ρ_p. Once Y_p is calculated, the material density can be obtained through

$$\rho_p' = Y_p \rho \quad . \tag{C-30}$$

The quantity mass fraction (or molar fraction) has been used extensively in fluid flow with chemical reaction.

Finally, we must emphasize again that the assumptions we have made about the dilute condition of material enable us to solve the gas dynamic problem independently. The validity of the assumptions depends on the individual case we are facing, but we do believe this simple model covers a broad range of problems related to actual nuclear fuel facilities.

VI. MATERIAL DEPLETION

As the flow Reynolds number based on the enclosure or duct hydraulic diameter and fluid bulk velocity will be greater than about 2100 for most cases of interest here, the flow will be assumed to be turbulent. We will assume that all flows are developed fully so that boundary layer or duct velocity profile shapes are constant with distance. This will be approximately true sufficiently far from inlets (20 to 50 hydraulic diameters) so that entrance effects are unimportant in our calculations.

Under these conditions, not all of the material that is made airborne at the location of material transport initiation will survive convective transport to the filtration systems or facility boundary. Depending on the aerosol aerodynamic characteristics and passage geometry, there may be a sizable reduction in aerosol concentration. As such, an enclosure or duct acts as an aerosol filter.

A number of processes that can cause aerosol depletion, and hence contribute to a material transport sink term, should be considered. Particles that come sufficiently close to surfaces can be intercepted mechanically and stick. Particles with enough inertia can deviate from the flow streamlines, impact, and stick to roughness elements, obstacles, or bends. Particles with sizes less than about 1 μm can be transported to surfaces by both turbulent (eddy) and molecular (Brownian) diffusion. Particles with sizes greater than about 1 μm and being transported parallel to surfaces can be deposited because of the fluctuating velocity components normal to the surface (turbulent inertial deposition). Also, particles moving through passages that are horizontal (or not exactly vertical) will deposit through gravitational sedimentation. Lower flow velocities enhance deposition caused by molecular diffusion and sedimentation.

Unless the surfaces are sticky, the net rate of deposition will depend on the relative rates of transport and reentrainment. Except for fibrous particles or very light particles, interception may be neglected because particles large enough to be intercepted will most likely deposit as a result of inertial effects or sedimentation.

Under certain conditions other effects may become important for the smallest particles. These effects include thermophoresis, diffusiophoresis, and electrical migration. The latter three effects are discussed in Ref. 26 and Ref. 32. They are believed to be relatively unimportant compared with other effects.

The current version of the code is restricted to gravitational sedimentation. The particle flux J resulting from gravitational sedimentation is[26]

$$J = u_s n \quad , \tag{C-31}$$

where the units of J are particles per unit area per unit time, u_s is the terminal settling velocity, and n is the uniform local aerosol number concentration in particles per unit volume. If we multiply both sides of Eq. (C-31) by the homogeneous particulate mass m_p, then

$$J' = u_s \, \rho_p \quad , \tag{C-32}$$

where the units of J' are mass per unit area per unit time and $\rho_p = nm_p$ is the aerosol mass concentration per unit volume. The terminal settling velocity is calculated from

$$u_s = \rho_p D_p^2 gC/18\mu \quad , \tag{C-33}$$

where

ρ_p = aerosol density,

D_p = aerosol diameter,

g = gravitational acceleration,

C = Cunningham slip correction factor, and

μ = fluid dynamic viscosity.

The code input variables for material depletion are ρ_p and D_p. These variables may be assumed or selected to be aerodynamic diameter with unit density or Stokes diameter with the material bulk density. This selection was discussed in Sec. A above. To calculate the slip correction factor, the code uses[26]

$$C = 1 + (2L/D_p)(A_1 + A_2 \exp(- A_3 D_p/L)) \quad , \tag{C-34}$$

where L is the molecular mean free path and the A's are dimensionless constants based on experimental measurements of small particle drag. The code uses

$L = 0.065\ \mu m$,

$A_1 = 1.257$,

$A_2 = 0.400$,

$A_3 = 0.550$,

$g = 981\ cm/s^2$, and

$\mu = 0.0001781\ g/cm\ s$,

where L, μ, and g are taken at standard sea level conditions.

We know ρ_p from the material transport mass balance calculation for the previous time step for each node (volume or duct). Then, knowing u_s and the projected floor area for sedimentation A, we can compute the sink term using Eq. (C-32):

$$M_p = - J'A = - u_s \rho_p A \quad . \tag{C-35}$$

Because aerosol depletion is a sink term, we have used a minus sign in Eq. (C-35). This equation represents a negative contribution to the M_p term on the right hand side of Eq. C-29 in Sec. V. above. Aerosol depletion by sedimentation may be selected for all volumes and ducts and is calculated in the same manner.

VII. FILTER MODEL

A. Introduction

Experimental evidence[33] indicates that the pressure drop across a filter commonly used for air cleaning in chemical and nuclear industries increases nonlinearly at high-speed flow, in contrast to the linear relation applicable to the low-speed flow region for normal or near normal application.[1] We can take an entirely experimental approach to determine all the influence coefficients on filter and flow properties, or we can model the filter flow based on the principle of flow through porous media and determine the relationship between the flow rate and the pressure drop with most if not all pertinent parameters explicitly included. Even so, some empirical constants still are needed; for practical purposes, we can combine some filter properties into these constants and determine them by experimental means. We will review some theoretical works and then present a model that is suitable for our needs.

The purpose of using an air filter in a ventilator system is to remove airborne material in the stream to prevent harmful elements from getting into the environment. Experience shows that the accumulation of material, usually in the condensed phase, will cause the pressure drop to increase for the same flow rate, thus causing degradation in system performance. In the case of fire, rapid flow resistance increases as the result of large amounts of material caught by the filter, which is known as filter plugging or clogging. Following the same analytical works in filter modeling, we will review the filter plugging phenomena briefly, but a semi-emperical formulation eventually is proposed to describe this condition.

B. Filter Model

The pioneer work of D'Arcy[34] established the foundation of the principles of fluid flow through porous media; his experimental results led to an understanding of the linear relationship between the flow rate and the pressure drop through an empirical constant, permeability. This parallels quite well the conclusion of fully-developed laminar flow through pipe made by Hagen-Poiseille.[35] It is not surprising to find that many theoretical models on flow through porous media are based on that concept with different qualifications, among them the most successful one is the Kozeny model.[36] According to his theory, the porous medium is represented by an assemblage of channels with various cross-sections and a definite length. The flow through the channels is determined by the Navier-Stokes equations, and the permeability is expressed in terms of viscosity and the porous medium properties. However, an empirical constant is needed to include the effect of the tortuous characteristic of the medium; a modification of the Kozeny model by Carman[37] defines the constant, known as tortuosity, in a more explicit way. This new model still requires an empirical coefficient to account for the uncertainty of determining various porous medium properties.

Another point of view on pressure drop with flow through a porous medium is based on the drag theory; the dragging obstacles can be particles or fibers. A model[38] using the fiber as porous medium leads to a permeability that is weakly dependent on flow rate. As a result of the actual complexity of the medium, some empirical adjustment is needed for this model.

So far we have discussed the D'Arcy law and its derivatives, which are adequate only when the flow velocity is low; the pressure drop is proportional to the viscous dissipation by the porous medium. For the channel flow, as the flow velocity increases, the dissipation mechanism changes from viscous effect to turbulence, and the pressure drop is proportional to the Kinetic energy of the stream.[35] Following the reasoning of Kozeny in modeling porous media as channels, a quadratic relation[39] is established between the pressure drop and flow rate at high velocity. Again, an empirical coefficient equivalent to the resistance factor in pipe flow under turbulence conditions is introduced. The summation of viscous effect and turbulent dissipation leads to an equation proposed by Ergun:[40]

$$\frac{\Delta p}{\ell} = 150 \frac{(1-\varepsilon)^2}{\varepsilon^3} \frac{\mu u_m}{d_p^2} + 1.75 \frac{(1-\varepsilon)}{\varepsilon^3} \frac{\rho u_m^2}{d_p} , \qquad \text{(C-36)}$$

with

Δp = pressure drop,
ℓ = bed length,
g = gravitational constant,
ε = void fraction,
μ = viscosity,
d_p = effective porous medium particle size,
ρ = fluid density, and
u_m = superficial velocity.

Superficial velocity is the flow velocity approaching the packed bed, not the average flow velocity in the interstitial region. Equation (C-36) also can be expressed in a different form:

$$\Delta p = K_L \mu \frac{Q}{A^{3/2}} + K_T \rho \frac{Q^2}{A^2} , \tag{C-37}$$

where Q and A represent volume flow rate and the frontal area of the packed column. It can be easily identified that

$$u_m = \frac{Q}{A} , \tag{C-38}$$

$$K_L = 150 \frac{(1-\varepsilon)^2}{\varepsilon^3} \frac{A^{1/2}}{d_p^2} , \tag{C-39}$$

and

$$K_T = 1.75 \frac{(1-\varepsilon)}{\varepsilon^3} \frac{\ell}{d_p} . \tag{C-40}$$

We can see that K_L and K_T are dimensionless and are dependent on the properties of the porous media. Equation (C-37) is identical to the expression of Reynolds[41] on pipe flow in laminar and turbulent regions.

As we discussed earlier, no matter what theoretical model we choose to use, some empirical coefficients must be included to account for the complexity and uncertainty of the porous medium. Obviously, it does not matter if we obtain K_L and K_T first from Eqs. (C-39) and (C-40) and add experimental correction later or if we go ahead to determine the effective K_L and K_T directly from experiment. The task is no more difficult than finding the correction factors alone because there are only two unknowns involved as presented in Eq. (C-37). From now on, we will use Eq. (C-37) as the foundation of our filter model regardless of what filtration media we use as long as we can determine the two coefficients through experiment or analytical means.

C. Filter Plugging

The physical phenomena involving the capture of suspended particulate in a stream by some filtration medium are quite complicated.[42] The porous material provides various sites for material retention: resting on the surface of the bed grain, wedged in a crevice, stopped at a constriction, and contained in a pore cavity. The normal pressure of the fluid, friction, interparticulate force and chemical bonding force give the required means of holding the particulate on the site. The mechanisms for the suspended material reaching the retention site include gravity, inertia, hydrodynamic force, interception, and Brownian motion. Attempting to relate the overall filter efficiency with the aforementioned sites, forces, and mechanisms without any experimental coefficient is almost impossible and impractical. A more useful approach is a phenomenological one; namely, we assume some form of dependence of filter efficiency on the total amount of retention; experiments indicate a small increase in the efficiency for increasing retention. For all practical purposes, we assume the filter efficiency remains constant in any flow condition.

The same conclusion cannot be made about the flow resistance of the filter for the increasing amount of material gathered. The increase in resistance can be quite substantial and should be dealt with properly. The plugging is related to material size, shape, and phase; the filter structure; and the quantity of captured material. Using the filter model of Carman-Kozeny,[37] the material retention reduces the specific surface, defined as the total surface of the bed grain per unit filter volume, and thus increases the effective resistance. We can express the general relation as

$$\frac{\Delta p}{(\Delta p)_o} = f(M_a) \quad , \tag{C-41}$$

where $(\Delta p)_o$ is the pressure drop for a clean filter, shown in Eq. (C-37), and f is a monotonically increasing function of material mass M_a on the filter. Clearly $f(M_a = o) = 1$. For light loading condition, f is a linear function of M_a:

$$f(M_a) = 1 + \alpha M_a \quad , \tag{C-42}$$

where α is a coefficient dependent on filter and material properties and has the unit of the reciprocal of mass. More recent work of Bergman[43] using the fiberous drag model of Davies[32] concludes that α depends on the fiber volume fraction, fiber size and particle size. However, the foundation of Davies' model is still empirical. For the time being, we shall postulate the phenomenological relation of Eq. (C-42) with α being determined by experiment. As future data warrant, we shall modify the equation with more explicit relations included.

APPENDIX D

BLOWER MODEL

Blowers or fans are approximated by a model that describes the interaction of the gas (or air) in the system with the blower. Specifically, the model calculates the volumetric flow rate through the blower as a function of the differential pressure across the blower and the gas density at the inlet to the blower.

The blower module depends on the measured constant speed performance curve of the fan. These data usually are reported by the manufacturer in the form of a curve.

$$\Delta p(Po) = f(Q) \quad , \tag{D-1}$$

where ΔP is the static pressure difference across the blower and Q is the volumetric flow rate through the blower. This curve applies at a given density (ρ = Po) and fan speed and may be obtained from the manufacturer's literature.

During a fire transient, the gas density at the fan may vary a great deal, and the curve Eq. (D-1) must be modified to take into account the density variation from standard conditions. Similarity analysis and experimental measurements show[44] that it is possible to correlate the blower performance at any density, ρ, if the performance at a given density (ρ = Po) is measured. Specifically, the result is of the form

$$\Delta p(\rho) = \frac{\rho}{Po} \Delta P(Po) \quad . \tag{D-2}$$

Because $\Delta p(Po)$ is known, Eq. (D-1), we have

$$\Delta p(\rho) = \frac{\rho}{Po} f(Q) \quad . \tag{D-3}$$

Therefore, the blower head-flow characteristic curve is known at all densities.

In the solution procedure for the gas dynamics it is necessary to have an expression for the flow rate as a function of the differential pressure; thus Eq. (D-3) must be inverted. The solution is of the form

$$Q = g(\frac{\rho_o}{\rho} \Delta p) \quad . \tag{D-4}$$

This inversion can be performed only if the function, f, is single valued. Therefore, as discussed in Sec. II.A.4, certain manufacturer's curves may not be modeled exactly but must be distorted slightly.

The actual user input to the code is a number of points on the blower characteristic curve. The curve then is approximated by a series of straight-line segments as shown in Fig. 1. If all of the segments have a negative slope, there will be no problem in obtaining the inverse function represented by Eq. (D-4).

APPENDIX E

CONTROL DAMPER MODEL

In many ventilation systems, control dampers are used to maintain a pressure in a room automatically. For this reason an option for modeling dampers that open or close based on the pressure in a given room. In the initial version there are three types of dampers with the ability to add more damper types as data become available.

The dampers initially modeled in FIRAC are 2-ft by 2-ft opposed-blade light-duty dampers, opposed-blade medium-duty dampers, and parallel-blade light-duty dampers. The dampers were manufactured by American Warming and Ventilation, Inc. Figure E-1 shows the configurations of these dampers.

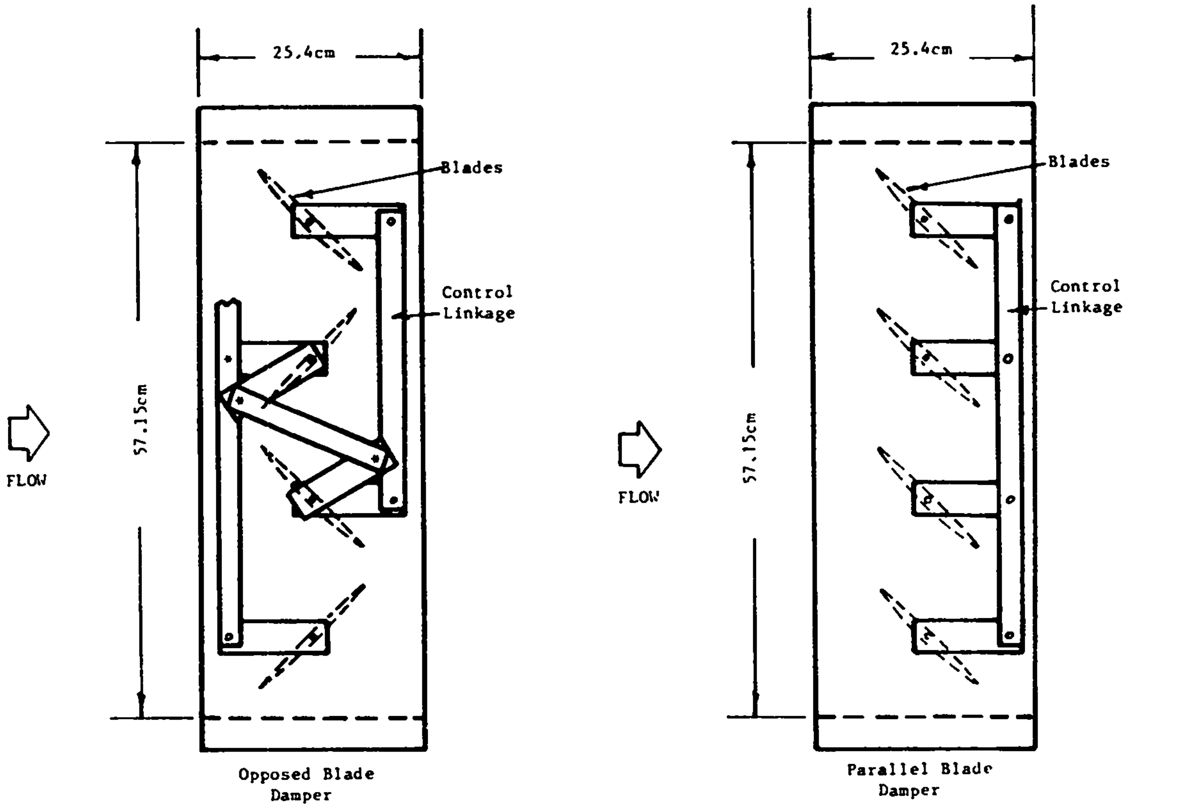

Fig. E-1.
Side views of the opposed-blade and the parallel-blade dampers.

The damper models are based on experimental data relating flow rate through a damper and the pressure drop across a damper. In FIRAC pressure drop and flow rate across a damper are related using the equation $P = R \times Q^2$, where R is a resistance coefficient. The resistance coefficients for these damper types were determined experimentally in reference to different damper angles. Using this information, a least-squares polynomial fit was made to the data. The resulting equations are quartics of the following general form.

$$R = a + b(\text{theta}) + c(\text{theta})^2 + d(\text{theta})^3 + e(\text{theta})^4 \quad .$$

The coefficients of these equations should be calculated with the units of R being $kPa/[(m^3/s)^2]$ and theta being in degrees.

Adding more damper types can be done by simple modifications to the subroutine damper. The first step in adding a damer type is to increase the array size of the coefficients in subroutine damper to the total number of damper types available, including the one being added. The second step is to add the coefficients for the new damper type to the end of the data statements that define the coefficients. After these two changes have been made, the damper can be modeled by specifying a damper type on the control damper card that corresponds to the array location of the coefficients in subroutine damper.

A control damper is modeled in FIRAC by changing the resistance coefficient of a damper to correspond with the opening and closing of the damper. A damper can be made to open or close based on the pressure in any room in the system. This is done by specifying a minimum and a maximum pressure in the room, the damper type, the amount the damper opens or closes at one response time, and the time between responses. If the damper closes at pressures above pmax then dthata (the amount the damper opens at pressures above pmax) should be a negative number.

APPENDIX F

MODELING DUCTS AND VALVES

Ducts and valves are modeled in FIRAC based on resistance coeffecients relating the pressure drop across a duct to the volumetric flow rate through the duct. The equation showing this relationship is

$$dP = RC * Q^2 \quad . \tag{F-1}$$

Reasonable values for these resistance coefficients can be calculated based on ambient conditions, flow rate though the duct or valve, and the configuration of the duct or valve. The pressures throughout the system can be approximated based on these resistance coefficients.

To calculate the resistance coefficient (RC) for a component using this method, a dimensionless coefficient or k value for the component first must be computed. Some of the more common values for this coefficeint are given in Fig. F-1. A more complete list of values can be found in Ref. 45. Using this dimensionless k value, the resistnace coefficient can be calculated using the equation

$$RC = \frac{k \times P_{ambient}}{2 \times A^2 \times R_{air} \times T} \quad ,$$

where k is the crane k value, $P_{ambient}$ is the ambient pressure, A is the flow area of the duct, R_{air} is the gas constant for air, and T is the ambient temperature. A value for R that will allow you to input temperature in ^{o}R, area in ft^2, and ambient pressure in psia is

$$R_{air} = 222.64 \times 10^3 \; \frac{ft^2 \quad psia}{min^2 \; in.\; wg. \; ^{o}R} \quad .$$

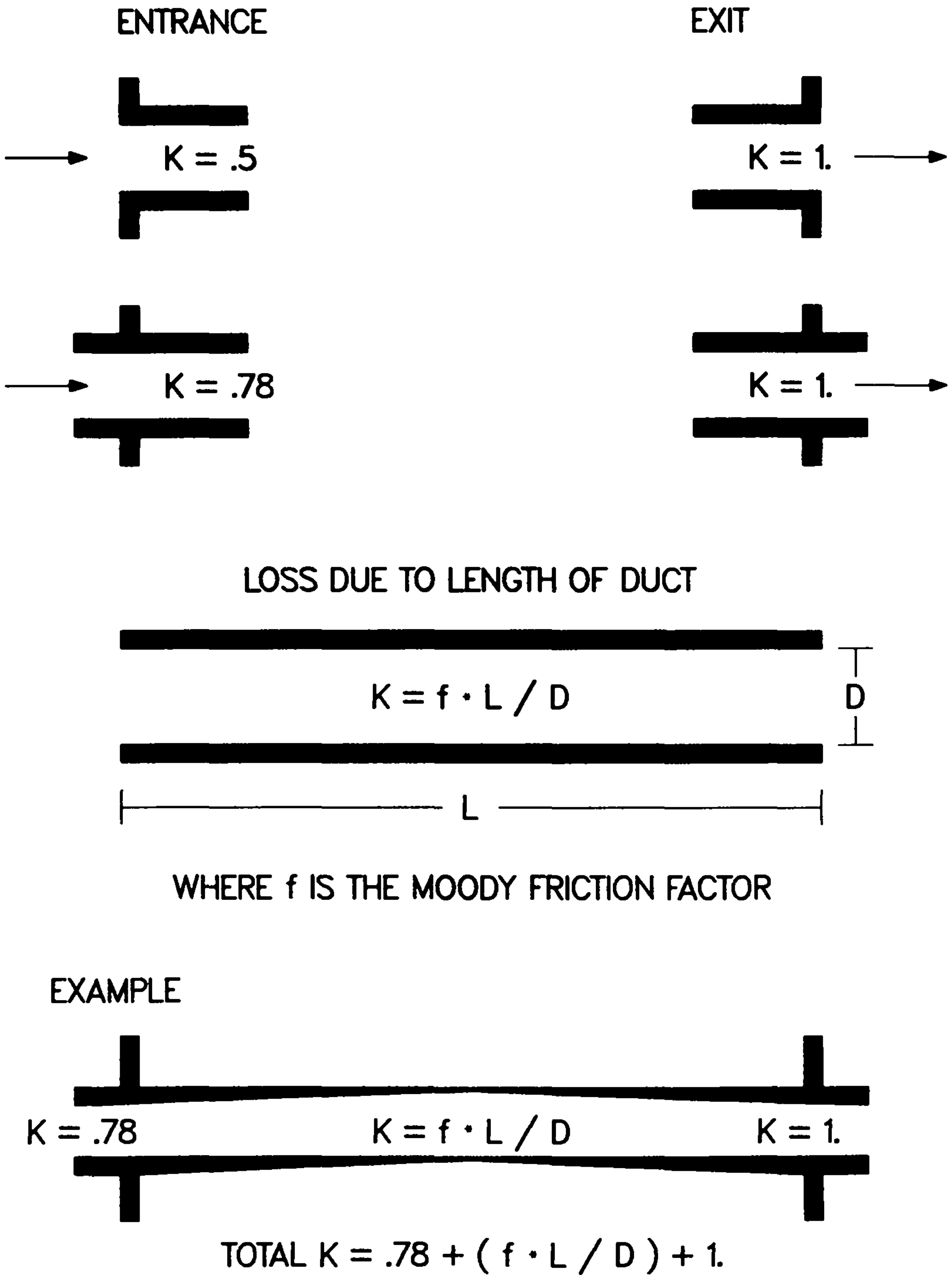

Fig. F-1.
Typical K values.

Using this value for R_{air} produces resistance coefficients with the units of inches water gauge per cubic foot per minute squared, which are the units needed for FIRAC input. The pressure drop across a duct can then be calculated using Eq. (E-1).

APPENDIX G

SAMPLE OUTPUT

(1) Sample Problem 1 system response (FOUT) output file.

(2) Sample Problem 1 fire compartment effects (PRINT 1) output file.

(3) Sample Problem 1 radioactive source term (RST) output file.

(1) Sample Problem 1 system response (FOUT) output file.

```
executed on ;  84/06/11        time :21:56:02
                                      table no. 1

                                 list of input data

               10        20        30        40        50        60        70        80
      12345678901234567890123456789012345678901234567890123456789012345678901234567890
   1$
   2$  sample problem 1
   3$#            run control card 1
   4$   st        1.   999.0
   5$#            print / plot control card
   6$  all    2   1    1    2    5
   7$    1    1   1
   8$    2    1   1
   9$    3    1   1
  10$   10    1   1
  11$   13    1   1
  12$#            plot frame description card
  13$    4    2   3    4    5
  14$    4    4  14   15   17
  15$    4    2   3   13   15
  16$    4    2   3    8   15
  17$    4    2   3    4    5
  18$    4    9  14   16   17
  19$    4    2   3   13   14
  20$    4    2   3   13   14
  21$    4    2   3   13   14
  22$    4    2   3   13   14
  23$    4    2   3   13   14
  24$    4    2   3   13   14
  25$    4    2   3   13   14
  26$    4    2   3   13   14
  27$    4    2   3   13   14
  28$    4    2   3   13   14
  29$#            run control card 2                "ifirin"
  30$                                t                 0         0    13
  31$#            boundary control card
  32$    0    4                56.
  33$#            geometry and component control card
  34$   16   18      14    1    1
  35$#            branch description data cards
  36$    1    1   2     1200.     4.6944    .25     v          .06
  37$
  38$    2    2   3     1200.     4.6944    .25     d          .14
  39$9.5000e-08
  40$    3    4   5     1200.     4.6944    3.2     d          .02
  41$ 1.389e-08                                             2.1666    6.9333        1
  42$   2.167    27.77        1       .25      .3       .3   26.2    489.     .12      56.
  43$    4    5   6     1200.     4.6944    3.2     d          .02
  44$                                                        2.1666    6.9333        1
  45$   2.167    27.77        1       .25      .3       .3   26.2    489.     .12      56.
  46$    5    6   7     1200.     4.6944    3.2     d          .02
  47$                                                        2.1666    6.9333        1
  48$   2.167    27.77        1       .25      .3       .3   26.2    489.     .12      56.
  49$    6    7   8     1200.     4.6944    3.2     d          .02
  50$                                                        2.1666    6.9333        1
  51$   2.167    27.77        1       .25      .3       .3   26.2    489.     .12      56.
  52$    7    8   9     1200.     4.6944    3.2     d          .02
```

```
executed on :  84/06/11       time :21:56:02
                              table no. 1 (page  2)

                         l i s t  o f  i n p u t  d a t a

            10        20        30        40        50        60        70        80
    12345678901234567890123456789012345678901234567890123456789012345678901234567890
 53$                                                      2.1666    6.9333         1
 54$   2.167   27.77       1     .25      .3      .3    26.2    489.     .12     56.
 55$    8    9   10     1200.   4.6944    3.2    d           .02
 56$                                                      2.1666    6.9333         1
 57$   2.167   27.77       1     .25      .3      .3    26.2    489.     .12     56.
 58$    9   10   11     1200.   4.6944    3.2    d           .02
 59$                                                      2.1666    6.9333         1
 60$   2.167   27.77       1     .25      .3      .3    26.2    489.     .12     56.
 61$   10   11   12     1200.   4.6944    3.2    d           .02
 62$                                                      2.1666    6.9333         1
 63$   2.167   27.77       1     .25      .3      .3    26.2    489.     .12     56.
 64$   11   12   13     1200.   4.6944    3.2    d           .02
 65$                                                      2.1666    6.9333         1
 66$   2.167   27.77       1     .25      .3      .3    26.2    489.     .12     56.
 67$   12   13   14     1200.   4.6944    3.2    d           .02
 68$                                                      2.1666    6.9333         1
 69$   2.167   27.77       1     .25      .3      .3    26.2    489.     .12     56.
 70$   13   14   15     1200.     .7854              f          .965
 71$                             1
 72$   14   15   16     1200.     .7854   25.      d            .2
 73$                                                          2.       75.         1
 74$      1.    78.5       1   .0625      .3      .3    26.2    489.     .12     56.
 75$   15   16   17     1200.     .7854              b          -1.4           1
 76$
 77$   16   17   18     1200.     .7854   0.5      v            .2
 78$   1.0e-07
 79$#        particulate specie data cards
 80$         1  smoke                   100.        1.
 81$         2  total rad part           20.        1.
 82$         3  rad part .1               .1        1.
 83$         4  rad part .2               .2        1.
 84$         5  rad part .4               .4        1.
 85$         6  rad part .6               .6        1.
 86$         7  rad part .8               .8        1.
 87$         8  rad part 1.               1.        1.
 88$         9  rad part 1.5             1.5        1.
 89$        10  rad part 1.9             1.9        1.
 90$        11  rad part 8.               8.        1.
 91$        12  rad part 15.             15.        1.
 92$        13  rad part 20.             20.        1.
 93$#             boundary node data
 94$    1 0      0.              56.
 95$    3 1      0.              56.
 96$    4 1      0.              56.
 97$   18 0      0.              56.
 98$#         room data
 99$    2       1.0
100$    4.6944
101$    5    13.636
102$    4.6944
103$    6    13.636
104$    4.6944
```

```
executed on :  84/06/11       time :21:56:02
                              table no. 1 (page  3)

                         l i s t  o f  i n p u t  d a t a

             10        20        30        40        50        60        70        80
    12345678901234567890123456789012345678901234567890123456789012345678901234567890
105$    7    13.636
106$    4.6944
107$    8    13.636
108$    4.6944
109$    9    13.636
110$    4.6944
111$   10    13.636
112$    4.6944
113$   11    13.636
114$    4.6944
115$   12    13.636
116$    4.6944
117$   13    13.636
118$    4.6944
119$   14    13.636
120$    4.6944
121$   15    13.636
122$     .7854
123$   16        9.8
124$     .7854
125$   17        9.8
126$     .7854
127$#            blower curve cards
128$    1    4
129$-8000.   8.        0.        1.8       1200.     1.5278
130$6000.    0.
131$#        filter data
132$         1    .9995        1.
133$#            temperature data
134$           56.            56.            56.            56.            56.
135$           56.            56.            56.            56.            56.
136$           56.            56.            56.            56.            56.
137$           56.            56.            56.
138$#        fire scenario control specifications         "iflow3"
139$    1100.       100         2
140$        1       0.0         0       0.0         0         0
141$#       fire compartment initial conditions and noding
142$     56.0    -.20
143$        2         3     1.084     2.166
144$        3         4     11.76     2.166
145$#       fuel type, mass ,and burn area
146$    0.0     0.0     0.0     0.0     0.0     0.0   5.750     0.0     0.0
147$    0.0     0.0     0.0     0.0     0.0     0.0   2.150     0.0     0.0
148$    0.0     0.0     0.0     0.0     0.0     0.0     4.0     0.0     0.0
149$    0.0     0.0     0.0     0.0     0.0     0.0     2.0     0.0     0.0
150$#        fire compartment dimensions and materials
151$     20.0      17.0      15.0     0.492     0.492     3.281     0.492
152$        9         8         9
153$#       combustible identifier card (required if ignite > 0)
154$    2   2    2    2    2    2    1    2    2
155$#        radioactive source term input
156$        0         1         1         0         0         0         0
```

```
executed on :  84/06/11        time ;21:56:02
                               table no. 1 (page  4)

                          l i s t  o f  i n p u t  d a t a

          10        20        30        40        50        60        70        80
    12345678901234567890123456789012345678901234567890123456789012345678901234567890
157$         1         7         1         2
158$    .22050
159$         2    0.1653
160$#        time step cards
161$              .001       3.0       1.0
162$               .01      10.0       1.0
163$               .05     999.0      50.0
```

table no. 11

summary of control information and diagnostics

********** -- warning -- the number of particulate species must be between 0 and 5 -- nspeces = 13

```
boundary nodes =    4
pressure functions =    0
energy functions =    0
temperature functions =    0
mass addition functions =    0
particulate addition functions =    0
gas addition functions =    0
branches = 16
nodes    = 18
rooms    = 14
number of blower curves =  1
number of filter types =  1
buoyancy effects will not be considered
```

table no. 111

summary of problem control parameters

problem type ss/trans

maximum iterations per time step 1000
convergence criteria 1.00e-04

times for line printer plots

0.0000	10.0000	20.0000	30.0000	40.0000	50.0000	60.0000	70.0000
80.0000	90.0000	100.0000	110.0000	120.0000	130.0000	140.0000	150.0000
160.0000	170.0000	180.0000	190.0000	200.0000	210.0000	220.0000	230.0000
240.0000	250.0000	260.0000	270.0000	280.0000	290.0000	300.0000	310.0000
320.0000	330.0000	340.0000	350.0000	360.0000	370.0000	380.0000	390.0000
400.0000	410.0000	420.0000	430.0000	440.0000	450.0000	460.0000	470.0000
480.0000	490.0000	500.0000	510.0000	520.0000	530.0000	540.0000	550.0000
560.0000	570.0000	580.0000	590.0000	600.0000	610.0000	620.0000	630.0000
640.0000	650.0000	660.0000	670.0000	680.0000	690.0000	700.0000	710.0000
720.0000	730.0000	740.0000	750.0000	760.0000	770.0000	780.0000	790.0000
800.0000	810.0000	820.0000	830.0000	840.0000	850.0000	860.0000	870.0000
880.0000	890.0000	900.0000	910.0000	920.0000	930.0000	940.0000	950.0000
960.0000	970.0000	980.0000	990.0000				

boundary data

p-ambient= 14.7000 psia t-ambient= 56.000 f number of boundary nodes= 4

node no.	initial pressure	p fn no.	initial temp.	t fn no.	node no.	initial pressure	p fn no.	initial temp.	t fn no.	node no.	initial pressure	p fn no.	initial temp.	t fn no.
1	0.00	0	56.00	0	3	0.00	0	56.00	0	4	0.00	0	56.00	0
18	0.00	0	56.00	0										

g e o m e t r y a n d c o m p o n e n t d a t a

number of branches= 16 number of nodes (boundary+ ordinary)= 18
number of blowers = 1 number of blower curves= 1
number of rooms = 14

table no. iv

summary of model control parameters

branch data

no.	in node	out node	initial flow	flow area	comp type	curve	exp q	resist	intercept	initial delta-p	inertia	rev resist
1	1	2	1.200e+03	4.694e+00	valv		2.0	4.167e-08		6.000e-02	5.325e-02	4.167e-08
2	2	3	1.200e+03	4.694e+00	duct		2.0	9.500e-08		6.000e-02	5.325e-02	9.500e-08
3	4	5	1.200e+03	4.694e+00	duct		2.0	1.389e-08		2.000e-02	6.817e-01	1.389e-08
4	5	6	1.200e+03	4.694e+00	duct		2.0	1.389e-08		2.000e-02	6.817e-01	1.389e-08
5	6	7	1.200e+03	4.694e+00	duct		2.0	1.389e-08		2.000e-02	6.817e-01	1.389e-08
6	7	8	1.200e+03	4.694e+00	duct		2.0	1.389e-08		2.000e-02	6.817e-01	1.389e-08
7	8	9	1.200e+03	4.694e+00	duct		2.0	1.389e-08		2.000e-02	6.817e-01	1.389e-08
8	9	10	1.200e+03	4.694e+00	duct		2.0	1.389e-08		2.000e-02	6.817e-01	1.389e-08
9	10	11	1.200e+03	4.694e+00	duct		2.0	1.389e-08		2.000e-02	6.817e-01	1.389e-08
10	11	12	1.200e+03	4.694e+00	duct		2.0	1.389e-08		2.000e-02	6.817e-01	1.389e-08
11	12	13	1.200e+03	4.694e+00	duct		2.0	1.389e-08		2.000e-02	6.817e-01	1.389e-08
12	13	14	1.200e+03	4.694e+00	duct		2.0	1.389e-08		2.000e-02	6.817e-01	1.389e-08
13	14	15	1.200e+03	7.854e-01	filt		1.0	8.042e-04		9.650e-01	0.	8.042e-04
14	15	16	1.200e+03	7.854e-01	duct		2.0	1.389e-07		2.000e-01	3.183e+01	1.389e-07
15	16	17	1.200e+03	7.854e-01	blwr	1	1.0	-4.409e+03	7.94e+03	1.400e+00	0.	0.
16	17	18	1.200e+03	7.854e-01	valv		2.0	1.000e-07		3.500e-02	6.366e-01	1.000e-07

heat transfer data

branch	nodes	htarea	diameter	delta-x	emmisivity	absorbtivity	k	rho	cp	initial temperature
3	1	2.78e+01	2.17e+00	2.50e-01	.300	.300	2.62e+01	4.89e+02	1.20e-01	56.00
4	1	2.78e+01	2.17e+00	2.50e-01	.300	.300	2.62e+01	4.89e+02	1.20e-01	56.00
5	1	2.78e+01	2.17e+00	2.50e-01	.300	.300	2.62e+01	4.89e+02	1.20e-01	56.00
6	1	2.78e+01	2.17e+00	2.50e-01	.300	.300	2.62e+01	4.89e+02	1.20e-01	56.00
7	1	2.78e+01	2.17e+00	2.50e-01	.300	.300	2.62e+01	4.89e+02	1.20e-01	56.00
8	1	2.78e+01	2.17e+00	2.50e-01	.300	.300	2.62e+01	4.89e+02	1.20e-01	56.00
9	1	2.78e+01	2.17e+00	2.50e-01	.300	.300	2.62e+01	4.89e+02	1.20e-01	56.00
10	1	2.78e+01	2.17e+00	2.50e-01	.300	.300	2.62e+01	4.89e+02	1.20e-01	56.00
11	1	2.78e+01	2.17e+00	2.50e-01	.300	.300	2.62e+01	4.89e+02	1.20e-01	56.00
12	1	2.78e+01	2.17e+00	2.50e-01	.300	.300	2.62e+01	4.89e+02	1.20e-01	56.00
14	1	7.85e+01	1.00e+00	6.25e-02	.300	.300	2.62e+01	4.89e+02	1.20e-01	56.00

room data

room	node	vol.	area	room	node	vol.	area	room	node	vol.	area	room	node	vol.	area
1	2	1.000e+00	4.694e+00	2	5	1.364e+01	4.694e+00	3	6	1.364e+01	4.694e+00	4	7	1.364e+01	4.694e+00
5	8	1.364e+01	4.694e+00	6	9	1.364e+01	4.694e+00	7	10	1.364e+01	4.694e+00	8	11	1.364e+01	4.694e+00
9	12	1.364e+01	4.694e+00	10	13	1.364e+01	4.694e+00	11	14	1.364e+01	4.694e+00	12	15	1.364e+01	7.854e-01
13	16	9.800e+00	7.854e-01	14	17	9.800e+00	7.854e-01								

blower curve data coefficients

curve no.	segment	left bound(flow)	right bound(flow)	a	b
1					
	1	-8.000e+03	0.	2.3226e+03	-1.2903e+03
	2	0.	1.200e+03	7.9353e+03	-4.4085e+03
	3	1.200e+03	6.000e+03	6.0000e+03	-3.1418e+03

filter data

the total number of filters is 1

the total number of special filter types is 1

filter no.	branch no.	filter type	filter efficiency	plugging factor	akt	akl
1	13	1	9.9950e-01	1.00	0.	0.

table no. v

summary of node type. initial pressure and branch connections

node no.	node(-,for boundary type(+,room no+1000)	pressure	associated branches	
1	-1	0.		
2	1001	-6,0000e-02	1	2
3	-1	0.		
4	-1	0.		
5	1002	-2.0000e-02	3	4
6	1003	-4,0000e-02	4	5
7	1004	-6.0000e-02	5	6
8	1005	-8.0000e-02	6	7
9	1006	-1,0000e-01	7	8
10	1007	-1,2000e-01	8	9
11	1008	-1.4000e-01	9	10
12	1009	-1.6000e-01	10	11
13	1010	-1.8000e-01	11	12
14	1011	-2,0000e-01	12	13
15	1012	-1,1650e+00	13	14
16	1013	-1,3650e+00	14	15
17	1014	3,5000e-02	15	16
18	-1	0,		

table no. vi

dimensionless resistance factors and critical mach numbers

branch no.	up. node	dn. node	fwd rf	rev rf	fwd mach	rev mach
1	1	2	1.435e+01	1.335e+01	.20108	.20735
2	2	3	3.172e+01	3.272e+01	.14159	.13959
3	4	5	4.784e+00	3.784e+00	.31158	.33899
4	5	6	4.783e+00	4.783e+00	.31159	.31159
5	6	7	4.783e+00	4.783e+00	.31159	.31159
6	7	8	4.783e+00	4.783e+00	.31159	.31159
7	8	9	4.783e+00	4.783e+00	.31159	.31159
8	9	10	4.783e+00	4.783e+00	.31159	.31159
9	10	11	4.783e+00	4.783e+00	.31159	.31159
10	11	12	4.783e+00	4.783e+00	.31159	.31159
11	12	13	4.783e+00	4.783e+00	.31159	.31159
12	13	14	4.783e+00	4.783e+00	.31159	.31159
13	14	15	0.	-6.934e-01	1.00000	1.00000
14	15	16	1.339e+00	1.339e+00	.47051	.47051
15	16	17	0.	0.	1.00000	1.00000
16	17	18	-3.596e-02	9.640e-01	1.00000	.51353

```
*****************************************************************************************************************************
time = 0.           delt = 0.          nstep =    0   ktotr =    0   igtot =    0    iptot =       0   cpu time = 8.10e-01
*****************************************************************************************************************************
```

branch data

branch	vol. flow (m**3/s)	mass flow (kg/s)	velocity (m/s)
1	5.663e-01	6.988e-01	1.299e+00
2	5.663e-01	6.987e-01	1.299e+00
3	5.663e-01	6.988e-01	1.299e+00
4	5.663e-01	6.988e-01	1.299e+00
5	5.663e-01	6.988e-01	1.299e+00
6	5.663e-01	6.987e-01	1.299e+00
7	5.663e-01	6.987e-01	1.299e+00
8	5.663e-01	6.987e-01	1.299e+00
9	5.663e-01	6.986e-01	1.299e+00
10	5.663e-01	6.986e-01	1.299e+00
11	5.663e-01	6.986e-01	1.299e+00
12	5.663e-01	6.985e-01	1.299e+00
13	5.663e-01	6.983e-01	7.762e+00
14	5.663e-01	6.969e-01	7.762e+00
15	5.663e-01	6.965e-01	7.762e+00
16	5.663e-01	6.989e-01	7.762e+00

node data

node	p (pa)	t (k)	rho (kg/m**3)
1	1.0135e+05	2.865e+02	1.234e+00
2	1.0134e+05	2.865e+02	1.234e+00
3	1.0135e+05	2.865e+02	1.234e+00
4	1.0135e+05	2.865e+02	1.234e+00
5	1.0135e+05	2.865e+02	1.234e+00
6	1.0134e+05	2.865e+02	1.234e+00
7	1.0134e+05	2.865e+02	1.234e+00
8	1.0133e+05	2.865e+02	1.234e+00
9	1.0133e+05	2.865e+02	1.234e+00
10	1.0132e+05	2.865e+02	1.234e+00
11	1.0132e+05	2.865e+02	1.234e+00
12	1.0131e+05	2.865e+02	1.233e+00
13	1.0131e+05	2.865e+02	1.233e+00
14	1.0130e+05	2.865e+02	1.233e+00
15	1.0106e+05	2.865e+02	1.230e+00
16	1.0101e+05	2.865e+02	1.230e+00
17	1.0136e+05	2.865e+02	1.234e+00
18	1.0135e+05	2.865e+02	1.234e+00

heat transfer information

branch	tavg	qqq	hco	qco	qro	hci	qci	qri	rvn
3	2.865e+02	0.	0.	0.	0.	0.	0.	0.	0.

wall temperatures (k) 2.865e+02

branch	tavg	qqq	hco	qco	qro	hcl	qcl	qrl	ryn
4	2.865e+02	0.	0.	0.	0.	0.	0.	0.	0.

wall temperatures (k) 2.865e+02

branch	tavg	qqq	hco	qco	qro	hcl	qcl	qrl	ryn
5	2.865e+02	0.	0.	0.	0.	0.	0.	0.	0.

wall temperatures (k) 2.865e+02

branch	tavg	qqq	hco	qco	qro	hcl	qcl	qrl	ryn
6	2.865e+02	0.	0.	0.	0.	0.	0.	0.	0.

wall temperatures (k) 2.865e+02

branch	tavg	qqq	hco	qco	qro	hcl	qcl	qrl	ryn
7	2.865e+02	0.	0.	0.	0.	0.	0.	0.	0.

wall temperatures (k) 2.865e+02

branch	tavg	qqq	hco	qco	qro	hcl	qcl	qrl	ryn
8	2.865e+02	0.	0.	0.	0.	0.	0.	0.	0.

wall temperatures (k) 2.865e+02

branch	tavg	qqq	hco	qco	qro	hcl	qcl	qrl	ryn
9	2.865e+02	0.	0.	0.	0.	0.	0.	0.	0.

wall temperatures (k) 2.865e+02

branch	tavg	qqq	hco	qco	qro	hcl	qcl	qrl	ryn
10	2.865e+02	0.	0.	0.	0.	0.	0.	0.	0.

wall temperatures (k) 2.865e+02

branch	tavg	qqq	hco	qco	qro	hcl	qcl	qrl	ryn
11	2.865e+02	0.	0.	0.	0.	0.	0.	0.	0.

wall temperatures (k) 2.865e+02

branch	tavg	qqq	hco	qco	qro	hcl	qcl	qrl	ryn
12	2.865e+02	0.	0.	0.	0.	0.	0.	0.	0.

wall temperatures (k) 2.865e+02

branch	tavg	qqq	hco	qco	qro	hcl	qcl	qrl	ryn
14	2.865e+02	0.	0.	0.	0.	0.	0.	0.	0.

wall temperatures (k) 2.865e+02

```
**************************************** particulate specie data ***************************************************
                                          species no.  1      smoke
specie nodal mass fraction
frac.           0.        0.        0.        0.        0.        0.        0.        0.
                0.        0.        0.        0.        0.        0.        0.        0.
                0.        0.
specie nodal concentration (kg/m**3)
conc.           0.        0.        0.        0.        0.        0.        0.        0.
                0.        0.        0.        0.        0.        0.        0.        0.
                0.        0.
specie branch flux (kg/sec)
dflux           0.        0.        0.        0.        0.        0.        0.        0.
                0.        0.        0.        0.        0.        0.        0.        0.
specie integrated branch flux (kg)
int.mass        0.        0.        0.        0.        0.        0.        0.        0.
                0.        0.        0.        0.        0.        0.        0.        0.
front filter mass (kg)
fil.mass        0.
back filter mass (kg)
fil.mass        0.
total specie mass on filters : 0.
airborn mass (kg)
air mass        0.        0.        0.        0.        0.        0.        0.        0.
                0.        0.        0.        0.        0.        0.        0.        0.
                0.        0.
total specie airborn mass ; 0.
specie mass on duct wall (kg)
mass            0.        0.        0.        0.        0.        0.        0.        0.
                0.        0.        0.        0.        0.        0.        0.        0.
deposition rate at each branch (kg/s)
rate            0.        0.        0.        0.        0.        0.        0.        0.
                0.        0.        0.        0.        0.        0.        0.        0.
entrainment rate at each branch (kg/s)
rate            0.        0.        0.        0.        0.        0.        0.        0.
                0.        0.        0.        0.        0.        0.        0.        0.

                                      species no.  2      total rad part
```

specie nodal mass fraction

frac.	0.	0.	0.	0.	0.	0.	0.	0.
	0.	0.	0.	0.	0.	0.	0.	0.
	0.	0.						

specie nodal concentration (kg/m**3)

conc.	0.	0.	0.	0.	0.	0.	0.	0.
	0.	0.	0.	0.	0.	0.	0.	0.
	0.	0.						

specie branch flux (kg/sec)

dflux	0.	0.	0.	0.	0.	0.	0.	0.
	0.	0.	0.	0.	0.	0.	0.	0.

specie integrated branch flux (kg)

int.mass	0.	0.	0.	0.	0.	0.	0.	0.
	0.	0.	0.	0.	0.	0.	0.	0.

front filter mass (kg)

fil.mass 0.

back filter mass (kg)

fil.mass 0.

total specie mass on filters : 0.

airborn mass (kg)

air mass	0.	0.	0.	0.	0.	0.	0.	0.
	0.	0.	0.	0.	0.	0.	0.	0.
	0.	0.						

total specie airborn mass ; 0.

specie mass on duct wall (kg)

mass	0.	0.	0.	0.	0.	0.	0.	0.
	0.	0.	0.	0.	0.	0.	0.	0.

deposition rate at each branch (kg/s)

rate	0.	0.	0.	0.	0.	0.	0.	0.
	0.	0.	0.	0.	0.	0.	0.	0.

entrainment rate at each branch (kg/s)

rate	0.	0.	0.	0.	0.	0.	0.	0.
	0.	0.	0.	0.	0.	0.	0.	0.

species no. 3 rad part .1

specie nodal mass fraction

frac.	0.	0.	0.	0.	0.	0.	0.	0.
	0.	0.	0.	0.	0.	0.	0.	0.
	0.	0.						

```
specie nodal concentration (kg/m**3)

conc.         0.       0.       0.       0.       0.       0.       0.       0.
              0.       0.       0.       0.       0.       0.       0.       0.
              0.       0.

specie branch flux (kg/sec)

dflux         0.       0.       0.       0.       0.       0.       0.       0.
              0.       0.       0.       0.       0.       0.       0.       0.

specie integrated branch flux (kg)

int.mass      0.       0.       0.       0.       0.       0.       0.       0.
              0.       0.       0.       0.       0.       0.       0.       0.

front filter mass (kg]

fil.mass      0.

back filter mass (kg)

fil.mass      0.

total specie mass on filters ; 0.

airborn mass (kg)

air mass      0.       0.       0.       0.       0.       0.       0.       0.
              0.       0.       0.       0.       0.       0.       0.       0.
              0.       0.

total specie airborn mass : 0.

specie mass on duct wall (kg)

mass          0.       0.       0.       0.       0.       0.       0.       0.
              0.       0.       0.       0.       0.       0.       0.       0.

deposition rate at each branch (kg/s)

rate          0.       0.       0.       0.       0.       0.       0.       0.
              0.       0.       0.       0.       0.       0.       0.       0.

entrainment rate at each branch (kg/s)

rate          0.       0.       0.       0.       0.       0.       0.       0.
              0.       0.       0.       0.       0.       0.       0.       0.


                              species no.  4     rad part .2

specie nodal mass fraction

frac.         0.       0.       0.       0.       0.       0.       0.       0.
              0.       0.       0.       0.       0.       0.       0.       0.
              0.       0.

specie nodal concentration (kg/m**3)

conc.         0.       0.       0.       0.       0.       0.       0.       0.
              0.       0.       0.       0.       0.       0.       0.       0.
```

	0.	0.						

specie branch flux (kg/sec)

dflux	0.	0.	0.	0.	0.	0.	0.	0.
	0.	0.	0.	0.	0.	0.	0.	0.

specie integrated branch flux (kg)

int.mass	0.	0.	0.	0.	0.	0.	0.	0.
	0.	0.	0.	0.	0.	0.	0.	0.

front filter mass (kg)

fil.mass 0.

back filter mass (kg)

fil.mass 0.

total specie mass on filters ; 0.

airborn mass (kg)

air mass	0.	0.	0.	0.	0.	0.	0.	0.
	0.	0.	0.	0.	0.	0.	0.	0.
	0.	0.						

total specie airborn mass ; 0.

specie mass on duct wall (kg)

mass	0.	0.	0.	0.	0.	0.	0.	0.
	0.	0.	0.	0.	0.	0.	0.	0.

deposition rate at each branch (kg/s)

rate	0.	0.	0.	0.	0.	0.	0.	0.
	0.	0.	0.	0.	0.	0.	0.	0.

entrainment rate at each branch (kg/s)

rate	0.	0.	0.	0.	0.	0.	0.	0.
	0.	0.	0.	0.	0.	0.	0.	0.

species no. 5 rad part .4

specie nodal mass fraction

frac.	0.	0.	0.	0.	0.	0.	0.	0.
	0.	0.	0.	0.	0.	0.	0.	0.
	0.	0.						

specie nodal concentration (kg/m**3)

conc.	0.	0.	0.	0.	0.	0.	0.	0.
	0.	0.	0.	0.	0.	0.	0.	0.
	0.	0.						

specie branch flux (kg/sec)

dflux	0.	0.	0.	0.	0.	0.	0.	0.

	0,	0.	0,	0.	0,	0,	0.	0.

specie integrated branch flux (kg)

int.mass	0,	0.	0.	0,	0,	0.	0.	0,
	0,	0,	0.	0.	0,	0.	0,	0,

front filter mass (kg)

fil.mass 0.

back filter mass (kg)

fil.mass 0.

total specie mass on filters ; 0,

airborn mass (kg)

air mass	0.	0.	0.	0.	0.	0,	0.	0,
	0,	0.	0,	0.	0.	0.	0,	0,
	0.	0,						

total specie airborn mass ; 0.

specie mass on duct wall (kg)

mass	0.	0.	0,	0.	0.	0.	0.	0.
	0.	0,	0.	0.	0,	0.	0.	0,

deposition rate at each branch (kg/s)

rate	0,	0,	0,	0.	0,	0.	0,	0,
	0,	0.	0,	0,	0,	0.	0,	0,

entrainment rate at each branch (kg/s)

rate	0.	0,	0,	0,	0,	0,	0.	0,
	0.	0.	0,	0,	0.	0.	0,	0.

species no. 6 rad part .6

specie nodal mass fraction

frac.	0.	0.	0.	0.	0.	0.	0.	0.
	0.	0.	0,	0.	0,	0,	0,	0,
	0.	0.						

specie nodal concentration (kg/m**3)

conc.	0.	0.	0,	0.	0,	0,	0.	0.
	0.	0.	0,	0,	0.	0.	0.	0.
	0,	0,						

specie branch flux (kg/sec)

dflux	0.	0.	0,	0.	0,	0.	0.	0.
	0.	0.	0.	0,	0.	0.	0,	0.

specie integrated branch flux (kg)

int.mass	0,	0.	0,	0.	0,	0.	0.	0.

```
                0.        0.        0.        0.        0.        0.        0.        0.

front filter mass (kg)

fil.mass        0.

back filter mass (kg)

fil.mass        0.

total specie mass on filters : 0.

airborn mass (kg)

air mass        0.        0.        0.        0.        0.        0.        0.        0.
                0.        0.        0.        0.        0.        0.        0.        0.
                0.        0.

total specie airborn mass : 0.

specie mass on duct wall (kg)

mass            0.        0.        0.        0.        0.        0.        0.        0.
                0.        0.        0.        0.        0.        0.        0.        0.

deposition rate at each branch (kg/s)

rate            0.        0.        0.        0.        0.        0.        0.        0.
                0.        0.        0.        0.        0.        0.        0.        0.

entrainment rate at each branch (kg/s)

rate            0.        0.        0.        0.        0.        0.        0.        0.
                0.        0.        0.        0.        0.        0.        0.        0.


                              species no. 7     rad part .8

specie nodal mass fraction

frac.           0.        0.        0.        0.        0.        0.        0.        0.
                0.        0.        0.        0.        0.        0.        0.        0.
                0.        0.

specie nodal concentration (kg/m**3)

conc.           0.        0.        0.        0.        0.        0.        0.        0.
                0.        0.        0.        0.        0.        0.        0.        0.
                0.        0.

specie branch flux (kg/sec)

dflux           0.        0.        0.        0.        0.        0.        0.        0.
                0.        0.        0.        0.        0.        0.        0.        0.

specie integrated branch flux (kg)

int.mass        0.        0.        0.        0.        0.        0.        0.        0.
                0.        0.        0.        0.        0.        0.        0.        0.

front filter mass (kg)

fil.mass        0.
```

```
back filter mass (kg)

fil.mass        0.

total specie mass on filters : 0.

airborn mass (kg)

air mass        0.        0.        0.        0.        0.        0.        0.        0.
                0.        0.        0.        0.        0.        0.        0.        0.
                0.        0.

total specie airborn mass : 0.

specie mass on duct wall (kg)

mass            0.        0.        0.        0.        0.        0.        0.        0.
                0.        0.        0.        0.        0.        0.        0.        0.

deposition rate at each branch (kg/s)

rate            0.        0.        0.        0.        0.        0.        0.        0.
                0.        0.        0.        0.        0.        0.        0.        0.

entrainment rate at each branch (kg/s)

rate            0.        0.        0.        0.        0.        0.        0.        0.
                0.        0.        0.        0.        0.        0.        0.        0.


                              species no.  8     rad part 1.

specie nodal mass fraction

frac.           0.        0.        0.        0.        0.        0.        0.        0.
                0.        0.        0.        0.        0.        0.        0.        0.
                0.        0.

specie nodal concentration (kg/m**3)

conc.           0.        0.        0.        0.        0.        0.        0.        0.
                0.        0.        0.        0.        0.        0.        0.        0.
                0.        0.

specie branch flux (kg/sec)

dflux           0.        0.        0.        0.        0.        0.        0.        0.
                0.        0.        0.        0.        0.        0.        0.        0.

specie integrated branch flux (kg)

int.mass        0.        0.        0.        0.        0.        0.        0.        0.
                0.        0.        0.        0.        0.        0.        0.        0.

front filter mass (kg)

fil.mass        0.

back filter mass (kg)

fil.mass        0.
```

total specie mass on filters : 0.

airborn mass (kg)

air mass	0.	0.	0.	0.	0.	0.	0.	0.
	0.	0.	0.	0.	0.	0.	0.	0.
	0.	0.						

total specie airborn mass : 0.

specie mass on duct wall (kg)

mass	0.	0.	0.	0.	0.	0.	0.	0.
	0.	0.	0.	0.	0.	0.	0.	0.

deposition rate at each branch (kg/s)

rate	0.	0.	0.	0.	0.	0.	0.	0.
	0.	0.	0.	0.	0.	0.	0.	0.

entrainment rate at each branch (kg/s)

rate	0.	0.	0.	0.	0.	0.	0.	0.
	0.	0.	0.	0.	0.	0.	0.	0.

species no. 9 rad part 1.5

specie nodal mass fraction

frac.	0.	0.	0.	0.	0.	0.	0.	0.
	0.	0.	0.	0.	0.	0.	0.	0.
	0.	0.						

specie nodal concentration (kg/m**3)

conc.	0.	0.	0.	0.	0.	0.	0.	0.
	0.	0.	0.	0.	0.	0.	0.	0.
	0.	0.						

specie branch flux (kg/sec)

dflux	0.	0.	0.	0.	0.	0.	0.	0.
	0.	0.	0.	0.	0.	0.	0.	0.

specie integrated branch flux (kg)

int.mass	0.	0.	0.	0.	0.	0.	0.	0.
	0.	0.	0.	0.	0.	0.	0.	0.

front filter mass (kg)

fil.mass 0.

back filter mass (kg)

fil.mass 0.

total specie mass on filters : 0.

airborn mass (kg)

air mass	0.	0.	0.	0.	0.	0.	0.	0.

	0.	0.	0.	0.	0.	0.	0.	0.
	0.	0.						

total specie airborn mass : 0.

specie mass on duct wall (kg)

mass	0.	0.	0.	0.	0.	0.	0.	0.
	0.	0.	0.	0.	0.	0.	0.	0.

deposition rate at each branch (kg/s)

rate	0.	0.	0.	0.	0.	0.	0.	0.
	0.	0.	0.	0.	0.	0.	0.	0.

entrainment rate at each branch (kg/s)

rate	0.	0.	0.	0.	0.	0.	0.	0.
	0.	0.	0.	0.	0.	0.	0.	0.

species no. 10 rad part 1.9

specie nodal mass fraction

frac.	0.	0.	0.	0.	0.	0.	0.	0.
	0.	0.	0.	0.	0.	0.	0.	0.
	0.	0.						

specie nodal concentration (kg/m**3)

conc.	0.	0.	0.	0.	0.	0.	0.	0.
	0.	0.	0.	0.	0.	0.	0.	0.
	0.	0.						

specie branch flux (kg/sec)

dflux	0.	0.	0.	0.	0.	0.	0.	0.
	0.	0.	0.	0.	0.	0.	0.	0.

specie integrated branch flux (kg)

int.mass	0.	0.	0.	0.	0.	0.	0.	0.
	0.	0.	0.	0.	0.	0.	0.	0.

front filter mass (kg)

fil.mass 0.

back filter mass (kg)

fil.mass 0.

total specie mass on filters : 0.

airborn mass (kg)

air mass	0.	0.	0.	0.	0.	0.	0.	0.
	0.	0.	0.	0.	0.	0.	0.	0.
	0.	0.						

total specie airborn mass : 0.

specie mass on duct wall (kg)

mass	0.	0.	0.	0.	0.	0.	0.	0.
	0.	0.	0.	0.	0.	0.	0.	0.

deposition rate at each branch (kg/s)

rate	0.	0.	0.	0.	0.	0.	0.	0.
	0.	0.	0.	0.	0.	0.	0.	0.

entrainment rate at each branch (kg/s)

rate	0.	0.	0.	0.	0.	0.	0.	0.
	0.	0.	0.	0.	0.	0.	0.	0.

species no. 11 rad part 8.

specie nodal mass fraction

frac.	0.	0.	0.	0.	0.	0.	0.	0.
	0.	0.	0.	0.	0.	0.	0.	0.
	0.	0.						

specie nodal concentration (kg/m**3)

conc.	0.	0.	0.	0.	0.	0.	0.	0.
	0.	0.	0.	0.	0.	0.	0.	0.
	0.	0.						

specie branch flux (kg/sec)

dflux	0.	0.	0.	0.	0.	0.	0.	0.
	0.	0.	0.	0.	0.	0.	0.	0.

specie integrated branch flux (kg)

int.mass	0.	0.	0.	0.	0.	0.	0.	0.
	0.	0.	0.	0.	0.	0.	0.	0.

front filter mass (kg)

fil.mass 0.

back filter mass (kg)

fil.mass 0.

total specie mass on filters : 0.

airborn mass (kg)

air mass	0.	0.	0.	0.	0.	0.	0.	0.
	0.	0.	0.	0.	0.	0.	0.	0.
	0.	0.						

total specie airborn mass : 0.

specie mass on duct wall (kg)

mass	0.	0.	0.	0.	0.	0.	0.	0.
	0.	0.	0.	0.	0.	0.	0.	0.

deposition rate at each branch (kg/s)

rate	0.	0.	0.	0.	0.	0.	0.	0.
	0.	0.	0.	0.	0.	0.	0.	0.

entrainment rate at each branch (kg/s)

rate	0.	0.	0.	0.	0.	0.	0.	0.
	0.	0.	0.	0.	0.	0.	0.	0.

species no. 12 rad part 15.

specie nodal mass fraction

frac.	0.	0.	0.	0.	0.	0.	0.	0.
	0.	0.	0.	0.	0.	0.	0.	0.
	0.	0.						

specie nodal concentration (kg/m**3)

conc.	0.	0.	0.	0.	0.	0.	0.	0.
	0.	0.	0.	0.	0.	0.	0.	0.
	0.	0.						

specie branch flux (kg/sec)

dflux	0.	0.	0.	0.	0.	0.	0.	0.
	0.	0.	0.	0.	0.	0.	0.	0.

specie integrated branch flux (kg)

int.mass	0.	0.	0.	0.	0.	0.	0.	0.
	0.	0.	0.	0.	0.	0.	0.	0.

front filter mass (kg)

fil.mass 0.

back filter mass (kg)

fil.mass 0.

total specie mass on filters ; 0.

airborn mass (kg)

air mass	0.	0.	0.	0.	0.	0.	0.	0.
	0.	0.	0.	0.	0.	0.	0.	0.
	0.	0.						

total specie airborn mass : 0.

specie mass on duct wall (kg)

mass	0.	0.	0.	0.	0.	0.	0.	0.
	0.	0.	0.	0.	0.	0.	0.	0.

deposition rate at each branch (kg/s)

rate	0.	0.	0.	0.	0.	0.	0.	0.
	0.	0.	0.	0.	0.	0.	0.	0.

entrainment rate at each branch (kg/s)

rate	0.	0.	0.	0.	0.	0.	0.	0.
	0.	0.	0.	0.	0.	0.	0.	0.

species no. 13 rad part 20.

specie nodal mass fraction

frac.	0.	0.	0.	0.	0.	0.	0.	0.
	0.	0.	0.	0.	0.	0.	0.	0.
	0.	0.						

specie nodal concentration (kg/m**3)

conc.	0.	0.	0.	0.	0.	0.	0.	0.
	0.	0.	0.	0.	0.	0.	0.	0.
	0.	0.						

specie branch flux (kg/sec)

dflux	0.	0.	0.	0.	0.	0.	0.	0.
	0.	0.	0.	0.	0.	0.	0.	0.

specie integrated branch flux (kg)

int.mass	0.	0.	0.	0.	0.	0.	0.	0.
	0.	0.	0.	0.	0.	0.	0.	0.

front filter mass (kg)

fil.mass 0.

back filter mass (kg)

fil.mass 0.

total specie mass on filters ; 0.

airborn mass (kg)

air mass	0.	0.	0.	0.	0.	0.	0.	0.
	0.	0.	0.	0.	0.	0.	0.	0.
	0.	0.						

total specie airborn mass ; 0.

specie mass on duct wall (kg)

mass	0.	0.	0.	0.	0.	0.	0.	0.
	0.	0.	0.	0.	0.	0.	0.	0.

deposition rate at each branch (kg/s)

rate	0.	0.	0.	0.	0.	0.	0.	0.
	0.	0.	0.	0.	0.	0.	0.	0.

entrainment rate at each branch (kg/s)

rate	0.	0.	0.	0.	0.	0.	0.	0.
	0.	0.	0.	0.	0.	0.	0.	0.

new time domain reached

delt = 1.00e-03   tend = 3.00e+00   edint = 1.00e+00   grfint = 0.

steady state results

****

time = 0.   delt = 1.00e-03   nstep = 1   ktotr = 144   igtot = 0   iptot = 0   cpu time = 1.96e+00

****

branch data

branch	vol. flow (m**3/s)	mass flow (kg/s)	velocity (m/s)
1	5.296e-01	6.535e-01	1.214e+00
2	5.296e-01	6.535e-01	1.214e+00
3	5.296e-01	6.532e-01	1.214e+00
4	5.286e-01	6.521e-01	1.212e+00
5	5.286e-01	6.520e-01	1.212e+00
6	5.287e-01	6.522e-01	1.212e+00
7	5.290e-01	6.526e-01	1.213e+00
8	5.294e-01	6.530e-01	1.214e+00
9	5.298e-01	6.535e-01	1.215e+00
10	5.301e-01	6.538e-01	1.215e+00
11	5.302e-01	6.539e-01	1.216e+00
12	5.299e-01	6.536e-01	1.215e+00
13	5.298e-01	6.533e-01	7.260e+00
14	5.299e-01	6.516e-01	7.262e+00
15	5.292e-01	6.508e-01	7.253e+00
16	5.268e-01	6.502e-01	7.220e+00

node data

node	p (pa)	t (k)	rho (kg/m**3)
1	1.0135e+05	2.865e+02	1.234e+00
2	1.0134e+05	2.865e+02	1.234e+00
3	1.0131e+05	2.865e+02	1.233e+00
4	1.0131e+05	2.865e+02	1.233e+00
5	1.0131e+05	2.865e+02	1.234e+00
6	1.0131e+05	2.865e+02	1.234e+00
7	1.0131e+05	2.865e+02	1.234e+00
8	1.0131e+05	2.865e+02	1.234e+00
9	1.0131e+05	2.865e+02	1.234e+00
10	1.0131e+05	2.865e+02	1.233e+00
11	1.0131e+05	2.865e+02	1.233e+00
12	1.0130e+05	2.865e+02	1.233e+00
13	1.0130e+05	2.865e+02	1.233e+00
14	1.0130e+05	2.865e+02	1.233e+00
15	1.0105e+05	2.865e+02	1.230e+00
16	1.0099e+05	2.865e+02	1.230e+00
17	1.0139e+05	2.865e+02	1.234e+00
18	1.0135e+05	2.865e+02	1.234e+00

heat transfer information

branch	tavg	qqq	hco	qco	qro	hci	qci	qri	ryn
3	2.865e+02	1.393e-02	-5.943e-03	0.	0.	5.592e+00	1.057e-02	3.363e-03	5.499e+04

wall temperatures (k) 2.865e+02

branch	tavg	qqq	hco	qco	qro	hci	qci	qri	ryn
4	2.865e+02	2.571e-01	-1.226e-02	0.	0.	5.578e+00	1.949e-01	6.217e-02	5.481e+04

wall temperatures (k) 2.865e+02

branch	tavg	qqq	hco	qco	qro	hci	qci	qri	ryn
5	2.865e+02	3.963e-01	-1.366e-02	0.	0.	5.577e+00	3.004e-01	9.584e-02	5.481e+04

wall temperatures (k) 2.865e+02

branch	tavg	qqq	hco	qco	qro	hci	qci	qri	ryn
6	2.865e+02	3.906e-01	-1.360e-02	0.	0.	5.578e+00	2.962e-01	9.446e-02	5.482e+04

wall temperatures (k) 2.865e+02

branch	tavg	qqq	hco	qco	qro	hci	qci	qri	ryn
7	2.865e+02	3.393e-01	-1.311e-02	0.	0.	5.581e+00	2.572e-01	8.202e-02	5.485e+04

wall temperatures (k) 2.865e+02

branch	tavg	qqq	hco	qco	qro	hci	qci	qri	ryn
8	2.865e+02	2.815e-01	-1.249e-02	0.	0.	5.584e+00	2.135e-01	6.803e-02	5.489e+04

wall temperatures (k) 2.865e+02

branch	tavg	qqq	hco	qco	qro	hci	qci	qri	ryn
9	2.865e+02	2.257e-01	-1.181e-02	0.	0.	5.586e+00	1.712e-01	5.452e-02	5.492e+04

wall temperatures (k) 2.865e+02

branch	tavg	qqq	hco	qco	qro	hci	qci	qri	ryn
10	2.865e+02	1.724e-01	-1.103e-02	0.	0.	5.588e+00	1.308e-01	4.163e-02	5.495e+04

wall temperatures (k) 2.865e+02

branch	tavg	qqq	hco	qco	qro	hci	qci	qri	ryn
11	2.865e+02	1.212e-01	-1.010e-02	0.	0.	5.588e+00	9.196e-02	2.928e-02	5.495e+04

wall temperatures (k) 2.865e+02

branch	tavg	qqq	hco	qco	qro	hci	qci	qri	ryn
12	2.865e+02	7.235e-02	-8.908e-03	0.	0.	5.586e+00	5.487e-02	1.748e-02	5.492e+04

wall temperatures (k)   2.865e+02

branch	tavg	qqq	hco	qco	qro	hcl	qcl	qrl	ryn
14	2.865e+02	2.848e+00	-2.974e-02	0.	0.	2.717e+01	2.673e+00	1.751e-01	1.509e+05

wall temperatures (k)   2.865e+02

** particulate specie data **

species no. 1   smoke

specie nodal mass fraction

frac.	0.	0.	0.	0.	0.	0.	0.	0.
	0.	0.	0.	0.	0.	0.	0.	0.
	0.	0.						

specie nodal concentration (kg/m**3)

conc.	0.	0.	0.	0.	0.	0.	0.	0.
	0.	0.	0.	0.	0.	0.	0.	0.
	0.	0.						

specie branch flux (kg/sec)

dflux	0.	0.	0.	0.	0.	0.	0.	0.
	0.	0.	0.	0.	0.	0.	0.	0.

specie integrated branch flux (kg)

int.mass	0.	0.	0.	0.	0.	0.	0.	0.
	0.	0.	0.	0.	0.	0.	0.	0.

front filter mass (kg)

fil.mass   0.

back filter mass (kg)

fil.mass   0.

total specie mass on filters : 0.

airborn mass (kg)

air mass	0.	0.	0.	0.	0.	0.	0.	0.
	0.	0.	0.	0.	0.	0.	0.	0.
	0.	0.						

total specie airborn mass : 0.

specie mass on duct wall (kg)

mass	0.	0.	0.	0.	0.	0.	0.	0.
	0.	0.	0.	0.	0.	0.	0.	0.

deposition rate at each branch (kg/s)

rate	0.	0.	0.	0.	0.	0.	0.	0.
	0.	0.	0.	0.	0.	0.	0.	0.

```
entrainment rate at each branch (kg/s)

rate            0.        0.        0.        0.        0.        0.        0.        0.
                0.        0.        0.        0.        0.        0.        0.        0.


                                          species no.  2     total rad part

specie nodal mass fraction

frac.           0.        0.        0.        0.        0.        0.        0.        0.
                0.        0.        0.        0.        0.        0.        0.        0.
                0.        0.

specie nodal concentration (kg/m**3)

conc.           0.        0.        0.        0.        0.        0.        0.        0.
                0.        0.        0.        0.        0.        0.        0.        0.
                0.        0.

specie branch flux (kg/sec)

dflux           0.        0.        0.        0.        0.        0.        0.        0.
                0.        0.        0.        0.        0.        0.        0.        0.

specie integrated branch flux (kg)

int.mass        0.        0.        0.        0.        0.        0.        0.        0.
                0.        0.        0.        0.        0.        0.        0.        0.

front filter mass (kg)

fil.mass        0.

back filter mass (kg)

fil.mass        0.

total specie mass on filters : 0.

airborn mass (kg)

air mass        0.        0.        0.        0.        0.        0.        0.        0.
                0.        0.        0.        0.        0.        0.        0.        0.
                0.        0.

total specie airborn mass : 0.

specie mass on duct wall (kg)

mass            0.        0.        0.        0.        0.        0.        0.        0.
                0.        0.        0.        0.        0.        0.        0.        0.

deposition rate at each branch (kg/s)

rate            0.        0.        0.        0.        0.        0.        0.        0.
                0.        0.        0.        0.        0.        0.        0.        0.

entrainment rate at each branch (kg/s)

rate            0.        0.        0.        0.        0.        0.        0.        0.
                0.        0.        0.        0.        0.        0.        0.        0.
```

species no. 3   rad part .1

specie nodal mass fraction

frac.	0.	0.	0.	0.	0.	0.	0.	0.
	0.	0.	0.	0.	0.	0.	0.	0.
	0.	0.						

specie nodal concentration (kg/m**3)

conc.	0.	0.	0.	0.	0.	0.	0.	0.
	0.	0.	0.	0.	0.	0.	0.	0.
	0.	0.						

specie branch flux (kg/sec)

dflux	0.	0.	0.	0.	0.	0.	0.	0.
	0.	0.	0.	0.	0.	0.	0.	0.

specie integrated branch flux (kg)

int.mass	0.	0.	0.	0.	0.	0.	0.	0.
	0.	0.	0.	0.	0.	0.	0.	0.

front filter mass (kg)

fil.mass   0.

back filter mass (kg)

fil.mass   0.

total specie mass on filters : 0.

airborn mass (kg)

air mass	0.	0.	0.	0.	0.	0.	0.	0.
	0.	0.	0.	0.	0.	0.	0.	0.
	0.	0.						

total specie airborn mass : 0.

specie mass on duct wall (kg)

mass	0.	0.	0.	0.	0.	0.	0.	0.
	0.	0.	0.	0.	0.	0.	0.	0.

deposition rate at each branch (kg/s)

rate	0.	0.	0.	0.	0.	0.	0.	0.
	0.	0.	0.	0.	0.	0.	0.	0.

entrainment rate at each branch (kg/s)

rate	0.	0.	0.	0.	0.	0.	0.	0.
	0.	0.	0.	0.	0.	0.	0.	0.

species no. 4   rad part .2

specie nodal mass fraction

frac.	0.	0.	0.	0.	0.	0.	0.	0.
	0.	0.	0.	0.	0.	0.	0.	0.
	0.	0.						

specie nodal concentration (kg/m**3)

conc.	0.	0.	0.	0.	0.	0.	0.	0.
	0.	0.	0.	0.	0.	0.	0.	0.
	0.	0.						

specie branch flux (kg/sec)

dflux	0.	0.	0.	0.	0.	0.	0.	0.
	0.	0.	0.	0.	0.	0.	0.	0.

specie integrated branch flux (kg)

int.mass	0.	0.	0.	0.	0.	0.	0.	0.
	0.	0.	0.	0.	0.	0.	0.	0.

front filter mass (kg)

fil.mass 0.

back filter mass (kg)

fil.mass 0.

total specie mass on filters : 0.

airborn mass (kg)

air mass	0.	0.	0.	0.	0.	0.	0.	0.
	0.	0.	0.	0.	0.	0.	0.	0.
	0.	0.						

total specie airborn mass : 0.

specie mass on duct wall (kg)

mass	0.	0.	0.	0.	0.	0.	0.	0.
	0.	0.	0.	0.	0.	0.	0.	0.

deposition rate at each branch (kg/s)

rate	0.	0.	0.	0.	0.	0.	0.	0.
	0.	0.	0.	0.	0.	0.	0.	0.

entrainment rate at each branch (kg/s)

rate	0.	0.	0.	0.	0.	0.	0.	0.
	0.	0.	0.	0.	0.	0.	0.	0.

species no. 5 rad part .4

specie nodal mass fraction

frac.	0.	0.	0.	0.	0.	0.	0.	0.
	0.	0.	0.	0.	0.	0.	0.	0.
	0.	0.						

specie nodal concentration (kg/m**3)

conc.	0.	0.	0.	0.	0.	0.	0.	0.
	0.	0.	0.	0.	0.	0.	0.	0.
	0.	0.						

specie branch flux (kg/sec)

dflux	0.	0.	0.	0.	0.	0.	0.	0.
	0.	0.	0.	0.	0.	0.	0.	0.

specie integrated branch flux (kg)

int.mass	0.	0.	0.	0.	0.	0.	0.	0.
	0.	0.	0.	0.	0.	0.	0.	0.

front filter mass (kg)

fil.mass 0.

back filter mass (kg)

fil.mass 0.

total specie mass on filters : 0.

airborn mass (kg)

air mass	0.	0.	0.	0.	0.	0.	0.	0.
	0.	0.	0.	0.	0.	0.	0.	0.
	0.	0.						

total specie airborn mass : 0.

specie mass on duct wall (kg)

mass	0.	0.	0.	0.	0.	0.	0.	0.
	0.	0.	0.	0.	0.	0.	0.	0.

deposition rate at each branch (kg/s)

rate	0.	0.	0.	0.	0.	0.	0.	0.
	0.	0.	0.	0.	0.	0.	0.	0.

entrainment rate at each branch (kg/s)

rate	0.	0.	0.	0.	0.	0.	0.	0.
	0.	0.	0.	0.	0.	0.	0.	0.

species no. 6 rad part .6

specie nodal mass fraction

frac.	0.	0.	0.	0.	0.	0.	0.	0.
	0.	0.	0.	0.	0.	0.	0.	0.
	0.	0.						

specie nodal concentration (kg/m**3)

conc.	0.	0.	0.	0.	0.	0.	0.	0.
	0.	0.	0.	0.	0.	0.	0.	0.

```
               0.          0.

specie branch flux (kg/sec)

dflux          0.          0.          0.          0.          0.          0.          0.          0.
               0.          0.          0.          0.          0.          0.          0.          0.

specie integrated branch flux (kg)

int.mass       0.          0.          0.          0.          0.          0.          0.          0.
               0.          0.          0.          0.          0.          0.          0.          0.

front filter mass (kg)

fil.mass       0.

back filter mass (kg)

fil.mass       0.

total specie mass on filters ; 0.

airborn mass (kg)

air mass       0.          0.          0.          0.          0.          0.          0.          0.
               0.          0.          0.          0.          0.          0.          0.          0.
               0.          0.

total specie airborn mass ; 0.

specie mass on duct wall (kg)

mass           0.          0.          0.          0.          0.          0.          0.          0.
               0.          0.          0.          0.          0.          0.          0.          0.

deposition rate at each branch (kg/s)

rate           0.          0.          0.          0.          0.          0.          0.          0.
               0.          0.          0.          0.          0.          0.          0.          0.

entrainment rate at each branch (kg/s)

rate           0.          0.          0.          0.          0.          0.          0.          0.
               0.          0.          0.          0.          0.          0.          0.          0.


                                        species no.  7     rad part ,8

specie nodal mass fraction

frac.          0.          0.          0.          0.          0.          0.          0.          0.
               0.          0.          0.          0.          0.          0.          0.          0.
               0.          0.

specie nodal concentration (kg/m**3)

conc.          0.          0.          0.          0.          0.          0.          0.          0.
               0.          0.          0.          0.          0.          0.          0.          0.
               0.          0.

specie branch flux (kg/sec)

dflux          0.          0.          0.          0.          0.          0.          0.          0.
```

	0.	0.	0.	0.	0.	0.	0.	0.

specie integrated branch flux (kg)

int.mass	0.	0.	0.	0.	0.	0.	0.	0.
	0.	0.	0.	0.	0.	0.	0.	0.

front filter mass (kg)

fil.mass 0.

back filter mass (kg)

fil.mass 0.

total specie mass on filters : 0.

airborn mass (kg)

air mass	0.	0.	0.	0.	0.	0.	0.	0.
	0.	0.	0.	0.	0.	0.	0.	0.
	0.	0.						

total specie airborn mass : 0.

specie mass on duct wall (kg)

mass	0.	0.	0.	0.	0.	0.	0.	0.
	0.	0.	0.	0.	0.	0.	0.	0.

deposition rate at each branch (kg/s)

rate	0.	0.	0.	0.	0.	0.	0.	0.
	0.	0.	0.	0.	0.	0.	0.	0.

entrainment rate at each branch (kg/s)

rate	0.	0.	0.	0.	0.	0.	0.	0.
	0.	0.	0.	0.	0.	0.	0.	0.

species no. 8 rad part 1.

specie nodal mass fraction

frac.	0.	0.	0.	0.	0.	0.	0.	0.
	0.	0.	0.	0.	0.	0.	0.	0.
	0.	0.						

specie nodal concentration (kg/m**3)

conc.	0.	0.	0.	0.	0.	0.	0.	0.
	0.	0.	0.	0.	0.	0.	0.	0.
	0.	0.						

specie branch flux (kg/sec)

dflux	0.	0.	0.	0.	0.	0.	0.	0.
	0.	0.	0.	0.	0.	0.	0.	0.

specie integrated branch flux (kg)

int.mass	0.	0.	0.	0.	0.	0.	0.	0.

```
                  0.         0.         0.         0.         0.         0.         0.         0.
front filter mass (kg)
fil.mass          0.
back filter mass (kg)
fil.mass          0.
total specie mass on filters : 0.
airborn mass (kg)
air mass          0.         0.         0.         0.         0.         0.         0.         0.
                  0.         0.         0.         0.         0.         0.         0.         0.
                  0.         0.
total specie airborn mass : 0.
specie mass on duct wall (kg)
mass              0.         0.         0.         0.         0.         0.         0.         0.
                  0.         0.         0.         0.         0.         0.         0.         0.
deposition rate at each branch (kg/s)
rate              0.         0.         0.         0.         0.         0.         0.         0.
                  0.         0.         0.         0.         0.         0.         0.         0.
entrainment rate at each branch (kg/s)
rate              0.         0.         0.         0.         0.         0.         0.         0.
                  0.         0.         0.         0.         0.         0.         0.         0.

                              species no.  9     rad part 1.5
specie nodal mass fraction
frac.             0.         0.         0.         0.         0.         0.         0.         0.
                  0.         0.         0.         0.         0.         0.         0.         0.
                  0.         0.
specie nodal concentration (kg/m**3)
conc.             0.         0.         0.         0.         0.         0.         0.         0.
                  0.         0.         0.         0.         0.         0.         0.         0.
                  0.         0.
specie branch flux (kg/sec)
dflux             0.         0.         0.         0.         0.         0.         0.         0.
                  0.         0.         0.         0.         0.         0.         0.         0.
specie integrated branch flux (kg)
int.mass          0.         0.         0.         0.         0.         0.         0.         0.
                  0.         0.         0.         0.         0.         0.         0.         0.
front filter mass (kg)
fil.mass          0.
```

back filter mass (kg)

fil.mass 0.

total specie mass on filters : 0.

airborn mass (kg)

air mass	0.	0.	0.	0.	0.	0.	0.	0.
	0.	0.	0.	0.	0.	0.	0.	0.
	0.	0.						

total specie airborn mass : 0.

specie mass on duct wall (kg)

mass	0.	0.	0.	0.	0.	0.	0.	0.
	0.	0.	0.	0.	0.	0.	0.	0.

deposition rate at each branch (kg/s)

rate	0.	0.	0.	0.	0.	0.	0.	0.
	0.	0.	0.	0.	0.	0.	0.	0.

entrainment rate at each branch (kg/s)

rate	0.	0.	0.	0.	0.	0.	0.	0.
	0.	0.	0.	0.	0.	0.	0.	0.

species no. 10 rad part 1.9

specie nodal mass fraction

frac.	0.	0.	0.	0.	0.	0.	0.	0.
	0.	0.	0.	0.	0.	0.	0.	0.
	0.	0.						

specie nodal concentration (kg/m**3)

conc.	0.	0.	0.	0.	0.	0.	0.	0.
	0.	0.	0.	0.	0.	0.	0.	0.
	0.	0.						

specie branch flux (kg/sec)

dflux	0.	0.	0.	0.	0.	0.	0.	0.
	0.	0.	0.	0.	0.	0.	0.	0.

specie integrated branch flux (kg)

int.mass	0.	0.	0.	0.	0.	0.	0.	0.
	0.	0.	0.	0.	0.	0.	0.	0.

front filter mass (kg)

fil.mass 0.

back filter mass (kg)

fil.mass 0.

total specie mass on filters : 0.

airborn mass (kg)

air mass	0.	0.	0.	0.	0.	0.	0.	0.
	0.	0.	0.	0.	0.	0.	0.	0.
	0.	0.						

total specie airborn mass : 0.

specie mass on duct wall (kg)

mass	0.	0.	0.	0.	0.	0.	0.	0.
	0.	0.	0.	0.	0.	0.	0.	0.

deposition rate at each branch (kg/s)

rate	0.	0.	0.	0.	0.	0.	0.	0.
	0.	0.	0.	0.	0.	0.	0.	0.

entrainment rate at each branch (kg/s)

rate	0.	0.	0.	0.	0.	0.	0.	0.
	0.	0.	0.	0.	0.	0.	0.	0.

species no. 11 rad part 8.

specie nodal mass fraction

frac.	0.	0.	0.	0.	0.	0.	0.	0.
	0.	0.	0.	0.	0.	0.	0.	0.
	0.	0.						

specie nodal concentration (kg/m**3)

conc.	0.	0.	0.	0.	0.	0.	0.	0.
	0.	0.	0.	0.	0.	0.	0.	0.
	0.	0.						

specie branch flux (kg/sec)

dflux	0.	0.	0.	0.	0.	0.	0.	0.
	0.	0.	0.	0.	0.	0.	0.	0.

specie integrated branch flux (kg)

int.mass	0.	0.	0.	0.	0.	0.	0.	0.
	0.	0.	0.	0.	0.	0.	0.	0.

front filter mass (kg)

fil.mass 0.

back filter mass (kg)

fil.mass 0.

total specie mass on filters : 0.

airborn mass (kg)

air mass	0.	0.	0.	0.	0.	0.	0.	0.

```
              0.        0.        0.        0.        0.        0.        0.        0.
              0.        0.

total specie airborn mass : 0.

specie mass on duct wall (kg)

mass          0.        0.        0.        0.        0.        0.        0.        0.
              0.        0.        0.        0.        0.        0.        0.        0.

deposition rate at each branch (kg/s)

rate          0.        0.        0.        0.        0.        0.        0.        0.
              0.        0.        0.        0.        0.        0.        0.        0.

entrainment rate at each branch (kg/s)

rate          0.        0.        0.        0.        0.        0.        0.        0.
              0.        0.        0.        0.        0.        0.        0.        0.


                              species no. 12     rad part 15.

specie nodal mass fraction

frac.         0.        0.        0.        0.        0.        0.        0.        0.
              0.        0.        0.        0.        0.        0.        0.        0.
              0.        0.

specie nodal concentration (kg/m**3)

conc.         0.        0.        0.        0.        0.        0.        0.        0.
              0.        0.        0.        0.        0.        0.        0.        0.
              0.        0.

specie branch flux (kg/sec)

dflux         0.        0.        0.        0.        0.        0.        0.        0.
              0.        0.        0.        0.        0.        0.        0.        0.

specie integrated branch flux (kg)

int.mass      0.        0.        0.        0.        0.        0.        0.        0.
              0.        0.        0.        0.        0.        0.        0.        0.

front filter mass (kg)

fil.mass      0.

back filter mass (kg)

fil.mass      0.

total specie mass on filters : 0.

airborn mass (kg)

air mass      0.        0.        0.        0.        0.        0.        0.        0.
              0.        0.        0.        0.        0.        0.        0.        0.
              0.        0.

total specie airborn mass : 0.
```

specie mass on duct wall (kg)

mass	0.	0.	0.	0.	0.	0.	0.	0.
	0.	0.	0.	0.	0.	0.	0.	0.

deposition rate at each branch (kg/s)

rate	0.	0.	0.	0.	0.	0.	0.	0.
	0.	0.	0.	0.	0.	0.	0.	0.

entrainment rate at each branch (kg/s)

rate	0.	0.	0.	0.	0.	0.	0.	0.
	0.	0.	0.	0.	0.	0.	0.	0.

species no. 13 rad part 20.

specie nodal mass fraction

frac.	0.	0.	0.	0.	0.	0.	0.	0.
	0.	0.	0.	0.	0.	0.	0.	0.
	0.	0.						

specie nodal concentration (kg/m**3)

conc.	0.	0.	0.	0.	0.	0.	0.	0.
	0.	0.	0.	0.	0.	0.	0.	0.
	0.	0.						

specie branch flux (kg/sec)

dflux	0.	0.	0.	0.	0.	0.	0.	0.
	0.	0.	0.	0.	0.	0.	0.	0.

specie integrated branch flux (kg)

int.mass	0.	0.	0.	0.	0.	0.	0.	0.
	0.	0.	0.	0.	0.	0.	0.	0.

front filter mass (kg)

fil.mass 0.

back filter mass (kg)

fil.mass 0.

total specie mass on filters ; 0.

airborn mass (kg)

air mass	0.	0.	0.	0.	0.	0.	0.	0.
	0.	0.	0.	0.	0.	0.	0.	0.
	0.	0.						

total specie airborn mass ; 0.

specie mass on duct wall (kg)

mass	0.	0.	0.	0.	0.	0.	0.	0.
	0.	0.	0.	0.	0.	0.	0.	0.

deposition rate at each branch (kg/s)

rate	0.	0.	0.	0.	0.	0.	0.	0.
	0.	0.	0.	0.	0.	0.	0.	0.

entrainment rate at each branch (kg/s)

rate	0.	0.	0.	0.	0.	0.	0.	0.
	0.	0.	0.	0.	0.	0.	0.	0.

```
******************************************************************************************************************
```

end of time step cards reached -- normal exit

```
******************************************************************************************************************
```

time = 9.9905e+02 delt = 5.00e-02 nstep =23481 ktotr =27086 igtot = 0 iptot = 298699 cpu time = 1.47e+03

```
******************************************************************************************************************
```

branch data

branch	vol. flow (m**3/s)	mass flow (kg/s)	velocity (m/s)
1	4.732e-01	5.839e-01	1.085e+00
2	4.732e-01	5.839e-01	1.085e+00
3	4.951e-01	5.559e-01	1.135e+00
4	4.947e-01	5.558e-01	1.134e+00
5	4.941e-01	5.557e-01	1.133e+00
6	4.935e-01	5.556e-01	1.132e+00
7	4.929e-01	5.555e-01	1.130e+00
8	4.923e-01	5.554e-01	1.129e+00
9	4.916e-01	5.554e-01	1.127e+00
10	4.910e-01	5.553e-01	1.126e+00
11	4.904e-01	5.552e-01	1.124e+00
12	4.898e-01	5.552e-01	1.123e+00
13	4.897e-01	5.551e-01	6.711e+00
14	4.935e-01	5.549e-01	6.763e+00
15	4.949e-01	5.547e-01	6.782e+00
16	4.931e-01	5.546e-01	6.758e+00

node data

node	p (pa)	t (k)	rho (kg/m**3)
1	1.0135e+05	2.865e+02	1.234e+00
2	1.0134e+05	2.865e+02	1.234e+00
3	1.0132e+05	3.151e+02	1.121e+00
4	1.0132e+05	3.151e+02	1.121e+00
5	1.0131e+05	3.148e+02	1.123e+00
6	1.0131e+05	3.145e+02	1.124e+00
7	1.0131e+05	3.141e+02	1.125e+00
8	1.0130e+05	3.138e+02	1.126e+00
9	1.0130e+05	3.134e+02	1.127e+00
10	1.0130e+05	3.131e+02	1.129e+00
11	1.0129e+05	3.127e+02	1.130e+00
12	1.0129e+05	3.123e+02	1.131e+00
13	1.0129e+05	3.120e+02	1.132e+00

14	1.0128e+05	3.116e+02	1.134e+00
15	1.0105e+05	3.116e+02	1.131e+00
16	1.0101e+05	3.143e+02	1.121e+00
17	1.0138e+05	3.144e+02	1.125e+00
18	1.0135e+05	2.865e+02	1.234e+00

heat transfer information

branch	tavg	qqq	hco	qco	qro	hci	qci	qri	ryn
3	3.149e+02	-2.315e+02	3.055e+00	-1.266e+02	-7.205e+01	5.017e+00	-1.603e+02	-7.118e+01	4.366e+04

wall temperatures (k) 3.025e+02

branch	tavg	qqq	hco	qco	qro	hci	qci	qri	ryn
4	3.146e+02	-2.352e+02	3.030e+00	-1.213e+02	-6.941e+01	5.018e+00	-1.631e+02	-7.210e+01	4.371e+04

wall temperatures (k) 3.020e+02

branch	tavg	qqq	hco	qco	qro	hci	qci	qri	ryn
5	3.143e+02	-2.387e+02	3.004e+00	-1.160e+02	-6.677e+01	5.016e+00	-1.657e+02	-7.299e+01	4.374e+04

wall temperatures (k) 3.015e+02

branch	tavg	qqq	hco	qco	qro	hci	qci	qri	ryn
6	3.139e+02	-2.417e+02	2.978e+00	-1.110e+02	-6.426e+01	5.014e+00	-1.680e+02	-7.368e+01	4.377e+04

wall temperatures (k) 3.009e+02

branch	tavg	qqq	hco	qco	qro	hci	qci	qri	ryn
7	3.136e+02	-2.440e+02	2.953e+00	-1.062e+02	-6.187e+01	5.012e+00	-1.698e+02	-7.422e+01	4.379e+04

wall temperatures (k) 3.004e+02

branch	tavg	qqq	hco	qco	qro	hci	qci	qri	ryn
8	3.132e+02	-2.444e+02	2.933e+00	-1.025e+02	-5.999e+01	5.010e+00	-1.703e+02	-7.416e+01	4.382e+04

wall temperatures (k) 3.000e+02

branch	tavg	qqq	hco	qco	qro	hci	qci	qri	ryn
9	3.128e+02	-2.459e+02	2.909e+00	-9.821e+01	-5.781e+01	5.008e+00	-1.715e+02	-7.442e+01	4.385e+04

wall temperatures (k) 2.996e+02

branch	tavg	qqq	hco	qco	qro	hci	qci	qri	ryn
10	3.125e+02	-2.470e+02	2.885e+00	-9.408e+01	-5.572e+01	5.006e+00	-1.725e+02	-7.458e+01	4.388e+04

wall temperatures (k) 2.991e+02

branch	tavg	qqq	hco	qco	qro	hci	qci	qri	ryn
11	3.121e+02	-2.478e+02	2.861e+00	-9.014e+01	-5.371e+01	5.005e+00	-1.732e+02	-7.463e+01	4.392e+04

wall temperatures (k) 2.987e+02

branch	tavg	qqq	hco	qco	qro	hc1	qc1	qr1	ryn
12	3.117e+02	-2.482e+02	2.837e+00	-8.640e+01	-5.179e+01	5.003e+00	-1.736e+02	-7.456e+01	4.395e+04

wall temperatures (k) 2.983e+02

branch	tavg	qqq	hco	qco	qro	hc1	qc1	qr1	ryn
14	3.129e+02	1.454e+03	4.414e+00	-1.091e+03	-4.713e+02	2.439e+01	1.323e+03	1.304e+02	1.206e+05

wall temperatures (k) 3.204e+02

*** particulate specie data ***

species no. 1 smoke

specie nodal mass fraction

frac.	0.	0.	3.32871e-04	3.32871e-C4	2.24168e-04	1.50882e-04	1.01504e-04	6.82509e-05
	4.58681e-05	3.08097e-05	2.06841e-05	1.38789e-05	9.30777e-06	6.23883e-06	3.12745e-09	3.13339e-09
	3.13915e-09	0.						

specie nodal concentration (kg/m**3)

conc.	0.	0.	3.73287e-04	3.73287e-04	2.51637e-04	1.69545e-04	1.14180e-04	7.68578e-05
	5.17094e-05	3.47719e-05	2.33705e-05	1.56994e-05	1.05408e-05	7.07348e-06	3.53708e-09	3.51248e-09
	3.53087e-09	0.						

specie branch flux (kg/sec)

dflux	0.	0.	1.85049e-04	1.24590e-04	8.38438e-05	5.63958e-05	3.79147e-05	2.54771e-05
	1.71108e-05	1.14860e-05	7.70627e-06	5.16764e-06	3.46312e-06	1.73537e-09	1.73815e-09	1.74095e-09

specie integrated branch flux (kg)

int.mass	-3.60396e-06	-3.17228e-06	2.59534e-01	1.75789e-01	1.18815e-01	8.01375e-02	5.39381e-02	3.62299e-02
	2.42867e-02	1.62485e-02	1.08497e-02	7.23117e-03	4.80895e-03	2.40382e-06	2.40320e-06	2.40225e-06

front filter mass (kg)

fil.mass 4.80655e-03

back filter mass (kg)

fil.mass 0.

total specie mass on filters ; 4.807e-03

airborn mass (kg)

air mass	0.	0.	3.73287e-04	3.73287e-04	9.71643e-05	6.54662e-05	4.40883e-05	2.96770e-05
	1.99665e-05	1.34264e-05	9.02401e-06	6.06198e-06	4.07009e-06	2.73127e-06	1.36577e-09	9.74731e-10
	9.79835e-10	0.						

total specie airborn mass : 1.038e-03

specie mass on duct wall (kg)

mass	0.	0.	8.37179e-02	5.69816e-02	3.86803e-02	2.62003e-02	1.77084e-02	1.19431e-02
	8.03806e-03	5.39854e-03	3.61835e-03	2.42034e-03	0.	3.77453e-11	0.	0.

deposition rate at each branch (kg/s)

rate	0.	0.	6.07779e-05	4.09648e-05	2.75945e-05	1.85793e-05	1.25033e-05	8.41019e-06
	5.65410e-06	3.79927e-06	2.55161e-06	1.71278e-06	0.	7.54906e-10	0.	0.

entrainment rate at each branch (kg/s)

rate	0.	0.	0.	0.	0.	0.	0.	0.
	0.	0.	0.	0.	0.	7.55023e-10	0.	0.

species no. 2 total rad part

specie nodal mass fraction

frac.	0.	0.	0.	0.	0.	0.	0.	0.
	0.	0.	0.	0.	0.	0.	0.	0.
	0.	0.						

specie nodal concentration (kg/m**3)

conc.	0.	0.	0.	0.	0.	0.	0.	0.
	0.	0.	0.	0.	0.	0.	0.	0.
	0.	0.						

specie branch flux (kg/sec)

dflux	0.	0.	0.	0.	0.	0.	0.	0.
	0.	0.	0.	0.	0.	0.	0.	0.

specie integrated branch flux (kg)

int.mass	0.	0.	0.	0.	0.	0.	0.	0.
	0.	0.	0.	0.	0.	0.	0.	0.

front filter mass (kg)

fil.mass 0.

back filter mass (kg)

fil.mass 0.

total specie mass on filters : 0.

airborn mass (kg)

air mass	0.	0.	0.	0.	0.	0.	0.	0.
	0.	0.	0.	0.	0.	0.	0.	0.
	0.	0.						

total specie airborn mass : 0.

specie mass on duct wall (kg)

mass	0.	0.	0.	0.	0.	0.	0.	0.
	0.	0.	0.	0.	0.	0.	0.	0.

deposition rate at each branch (kg/s)

rate	0.	0.	0.	0.	0.	0.	0.	0.
	0.	0.	0.	0.	0.	0.	0.	0.

```
entrainment rate at each branch (kg/s)

rate            0.           0.           0.           0.           0.           0.           0.           0.
                0.           0.           0.           0.           0.           0.           0.           0.


                                        species no.  3     rad part .1

specie nodal mass fraction

frac.           0.           0.           9.83100e-08  9.83100e-08  9.81983e-08  9.80857e-08  9.79724e-08  9.78583e-08
                9.77434e-08  9.76277e-08  9.75112e-08  9.73938e-08  9.72756e-08  9.71565e-08  4.85186e-11  4.84758e-11
                4.84327e-11  0.

specie nodal concentration (kg/m**3)

conc.           0.           0.           1.10246e-07  1.10246e-07  1.10231e-07  1.10219e-07  1.10208e-07  1.10199e-07
                1.10191e-07  1.10183e-07  1.10176e-07  1.10169e-07  1.10162e-07  1.10154e-07  5.48735e-11  5.43406e-11
                5.44765e-11  0.

specie branch flux (kg/sec)

dflux           0.           0.           5.46522e-08  5.45775e-08  5.45055e-08  5.44338e-08  5.43623e-08  5.42909e-08
                5.42197e-08  5.41487e-08  5.40778e-08  5.40071e-08  5.39306e-08  2.69221e-11  2.68905e-11  2.68605e-11

specie integrated branch flux (kg)

int.mass       -8.91080e-12 -7.84346e-12  8.82546e-06  8.77966e-06  8.73508e-06  8.69060e-06  8.64624e-06  8.60202e-06
                8.55795e-06  8.51403e-06  8.47026e-06  8.42662e-06  8.38181e-06  4.16849e-09  4.15237e-09  4.13626e-09

front filter mass (kg)

fil.mass        8.37762e-06

back filter mass (kg)

fil.mass        0.

total specie mass on filters : 8.378e-06

airborn mass (kg)

air mass        0.           0.           1.10246e-07  1.10246e-07  4.25634e-08  4.25586e-08  4.25545e-08  4.25510e-08
                4.25479e-08  4.25448e-08  4.25420e-08  4.25392e-08  4.25365e-08  4.25337e-08  2.11882e-11  1.50798e-11
                1.51175e-11  0.

total specie airborn mass : 6.460e-07

specie mass on duct wall (kg)

mass            0.           0.           1.00902e-11  1.00683e-11  1.00460e-11  1.00233e-11  1.00002e-11  9.97655e-12
                9.95230e-12  9.92752e-12  9.90221e-12  9.87635e-12  0.                        6.92048e-15  0.           0.

deposition rate at each branch (kg/s)

rate            0.           0.           6.20898e-14  6.20812e-14  6.20742e-14  6.20682e-14  6.20631e-14  6.20587e-14
                6.20542e-14  6.20500e-14  6.20460e-14  6.20421e-14  0.                        4.37591e-17  0.           0.

entrainment rate at each branch (kg/s)

rate            0.           0.           0.           0.           0.           0.           0.           0.
                0.           0.           0.           0.           0.           0.           0.           0.
```

```
                                   species no.  4     rad part .2

specie nodal mass fraction

frac.          0.           0.           9.02179e-08  9.02179e-08  9.01050e-08  8.99913e-08  8.98768e-08  8.97615e-08
               8.96453e-08  8.95284e-08  8.94106e-08  8.92920e-08  8.91725e-08  8.90522e-08  4.44659e-11  4.44226e-11
               4.43791e-11  0.

specie nodal concentration (kg/m**3)

conc.          0.           0.           1.01172e-07  1.01172e-07  1.01146e-07  1.01123e-07  1.01101e-07  1.01081e-07
               1.01062e-07  1.01042e-07  1.01023e-07  1.01004e-07  1.00985e-07  1.00966e-07  5.02899e-11  4.97970e-11
               4.99170e-11  0.

specie branch flux (kg/sec)

dflux          0.           0.           5.01537e-08  5.00794e-08  5.00075e-08  4.99358e-08  4.98643e-08  4.97929e-08
               4.97216e-08  4.96504e-08  4.95793e-08  4.95083e-08  4.94320e-08  2.46734e-11  2.46421e-11  2.46124e-11

specie integrated branch flux (kg)

int.mass      -4.00986e-12 -3.52956e-12  7.44874e-06  7.40615e-06  7.36455e-06  7.32308e-06  7.28175e-06  7.24057e-06
               7.19954e-06  7.15867e-06  7.11795e-06  7.07738e-06  7.03609e-06  3.49745e-09  3.48265e-09  3.46790e-09

front filter mass (kg)

fil.mass       7.03258e-06

back filter mass (kg)

fil.mass       0.

total specie mass on filters : 7.033e-06

airborn mass (kg)

air mass       0.           0.           1.01172e-07  1.01172e-07  3.90554e-08  3.90464e-08  3.90381e-08  3.90303e-08
               3.90228e-08  3.90153e-08  3.90079e-08  3.90006e-08  3.89932e-08  3.89858e-08  1.94184e-11  1.38189e-11
               1.38522e-11  0.

total specie airborn mass : 5.926e-07

specie mass on duct wall (kg)

mass           0.           0.           2.22586e-11  2.21924e-11  2.21258e-11  2.20586e-11  2.19906e-11  2.19217e-11
               2.18516e-11  2.17806e-11  2.17085e-11  2.16355e-11  0.           1.51409e-14  0.           0.

deposition rate at each branch (kg/s)

rate           0.           0.           1.48762e-13  1.48724e-13  1.48690e-13  1.48658e-13  1.48628e-13  1.48600e-13
               1.48571e-13  1.48543e-13  1.48515e-13  1.48487e-13  0.           1.04704e-16  0.           0.

entrainment rate at each branch (kg/s)

rate           0.           0.           0.           0.           0.           0.           0.           0.
               0.           0.           0.           0.           0.           0.           0.           0.


                                   species no.  5     rad part .4
```

specie nodal mass fraction

frac.	0.	0.	5.15304e-08	5.15304e-08	5.14654e-08	5.14000e-08	5.13341e-08	5.12678e-08
	5.12010e-08	5.11337e-08	5.10660e-08	5.09978e-08	5.09291e-08	5.08599e-08	2.53954e-11	2.53704e-11
	2.53456e-11	0.						

specie nodal concentration (kg/m**3)

conc.	0.	0.	5.77869e-08	5.77869e-08	5.77718e-08	5.77580e-08	5.77451e-08	5.77330e-08
	5.77215e-08	5.77098e-08	5.76983e-08	5.76870e-08	5,76756e-08	5.76640e-08	2.87217e-11	2.84399e-11
	2.85083e-11	0.						

specie branch flux (kg/sec)

dflux	0.	0.	2.86466e-08	2.86039e-08	2.85626e-08	2.85214e-08	2.84803e-08	2.84392e-08
	2.83983e-08	2.83573e-08	2.83165e-08	2.82756e-08	2.82318e-08	1.40915e-11	1.40735e-11	1.40565e-11

specie integrated branch flux (kg)

int.mass	-2.22770e-12	-1.96087e-12	4.24477e-06	4.22041e-06	4.19662e-06	4.17289e-06	4.14925e-06	4.12570e-06
	4.10223e-06	4.07885e-06	4.05556e-06	4.03236e-06	4.00875e-06	1.99261e-09	1.98414e-09	1.97572e-09

front filter mass (kg)

fil.mass 4.00675e-06

back filter mass (kg)

fil.mass 0.

total specie mass on filters ; 4.007e-06

airborn mass (kg)

air mass	0.	0.	5.77869e-08	5.77869e-08	2.23073e-08	2.23020e-08	2.22971e-08	2.22924e-08
	2.22879e-08	2.22834e-08	2.22790e-08	2.22746e-08	2.22702e-08	2,22657e-08	1.10903e-11	7.89221e-12
	7.91121e-12	0.						

total specie airborn mass : 3.385e-07

specie mass on duct wall (kg)

mass	0.	0.	3.84417e-11	3.83263e-11	3.82103e-11	3.80931e-11	3.79746e-11	3.78545e-11
	3.77325e-11	3.76088e-11	3.74833e-11	3.73561e-11	0.	2.61413e-14	0,	0.

deposition rate at each branch (kg/s)

rate	0.	0.	2.57503e-13	2.57436e-13	2.57374e-13	2.57317e-13	2.57263e-13	2.57211e-13
	2.57159e-13	2.57108e-13	2.57058e-13	2,57007e-13	0.	1.81222e-16	0.	0.

entrainment rate at each branch (kg/s)

rate	0.	0.	0.	0.	0.	0.	0.	0.
	0.	0.	0,	0.	0.	0.	0.	0.

species no. 6 rad part .6

specie nodal mass fraction

frac.	0.	0.	3,23457e-08	3.23457e-08	3.23056e-08	3.22652e-08	3.22245e-08	3.21835e 08
	3.21422e-08	3.21007e-08	3.20589e-08	3.20167e-08	3,19743e-08	3,19316e-08	1.59446e-11	1.59291e-11
	1,59139e-11	0.						

specie nodal concentration (kg/m**3)

conc.	0.	0.	3.62730e-08	3.62730e-08	3.62642e-08	3.62563e-08	3.62489e-08	3.62421e-08
	3.62356e-08	3.62290e-08	3.62226e-08	3.62163e-08	3.62099e-08	3.62035e-08	1.80331e-11	1.78563e-11
	1.78997e-11	0.						

specie branch flux (kg/sec)

dflux	0.	0.	1.79815e-08	1.79551e-08	1.79295e-08	1.79040e-08	1.78786e-08	1.78532e-08
	1.78278e-08	1.78025e-08	1.77773e-08	1.77520e-08	1.77249e-08	8.84742e-12	8.83620e-12	8.82574e-12

specie integrated branch flux (kg)

int.mass	-1.78216e-12	-1.56869e-12	2.72434e-06	2.70908e-06	2.69418e-06	2.67932e-06	2.66451e-06	2.64976e-06
	2.63505e-06	2.62041e-06	2.60581e-06	2.59127e-06	2.57644e-06	1.28084e-09	1.27551e-09	1.27022e-09

front filter mass (kg)

fil.mass 2.57515e-06

back filter mass (kg)

fil.mass 0.

total specie mass on filters : 2.575e-06

airborn mass (kg)

air mass	0.	0.	3.62730e-08	3.62730e-08	1.40026e-08	1.39996e-08	1.39967e-08	1.39941e-08
	1.39916e-08	1.39891e-08	1.39866e-08	1.39841e-08	1.39817e-08	1.39792e-08	6.96308e-12	4.95521e-12
	4.96726e-12	0.						

total specie airborn mass : 2.125e-07

specie mass on duct wall (kg)

mass	0.	0.	4.99955e-11	4.98558e-11	4.97152e-11	4.95729e-11	4.94287e-11	4.92824e-11
	4.91334e-11	4.89821e-11	4.88284e-11	4.86724e-11	0.	3.40719e-14	0.	0.

deposition rate at each branch (kg/s)

rate	0.	0.	3.27632e-13	3.27553e-13	3.27481e-13	3.27415e-13	3.27353e-13	3.27294e-13
	3.27235e-13	3.27177e-13	3.27120e-13	3.27063e-13	0.	2.30633e-16	0.	0.

entrainment rate at each branch (kg/s)

rate	0.	0.	0.	0.	0.	0.	0.	0.
	0.	0.	0.	0.	0.	0.	0.	0.

species no. 7 rad part .8

specie nodal mass fraction

frac.	0.	0.	3.20275e-08	3.20275e-08	3.19852e-08	3.19426e-08	3.18998e-08	3.18566e-08
	3.18132e-08	3.17694e-08	3.17254e-08	3.16810e-08	3.16363e-08	3.15914e-08	1.57736e-11	1.57571e-11
	1.57412e-11	0.						

specie nodal concentration (kg/m**3)

conc.	0.	0.	3.59161e-08	3.59161e-08	3.59046e-08	3.58938e-08	3.58837e-08	3.58740e-08
	3.58646e-08	3.58551e-08	3.58458e-08	3.58365e-08	3.58272e-08	3.58177e-08	1.78396e-11	1.76635e-11

	1.77055e-11	0.

specie branch flux (kg/sec)

dflux	0.	0.	1.78046e-08	1.77770e-08	1.77503e-08	1.77236e-08	1.76970e-08	1.76704e-08
	1.76439e-08	1.76173e-08	1.75909e-08	1.75644e-08	1.75361e-08	8.75251e-12	8.74079e-12	8.72998e-12

specie integrated branch flux (kg)

int.mass	-8.91080e-13	-7.84346e-13	2.56123e-06	2.54597e-06	2.53105e-06	2.51618e-06	2.50136e-06	2.48660e-06
	2.47189e-06	2.45724e-06	2.44265e-06	2.42812e-06	2.41338e-06	1.19938e-09	1.19408e-09	1.18885e-09

front filter mass (kg)

fil.mass 2.41217e-06

back filter mass (kg)

fil.mass 0.

total specie mass on filters : 2.412e-06

airborn mass (kg)

air mass	0.	0.	3.59161e-08	3.59161e-08	1.38638e-08	1.38596e-08	1.38557e-08	1.38520e-08
	1.38483e-08	1.38447e-08	1.38411e-08	1.38375e-08	1.38339e-08	1.38302e-08	6.88838e-12	4.90171e-12
	4.91336e-12	0.						

total specie airborn mass : 2.103e-07

specie mass on duct wall (kg)

mass	0.	0.	7.91149e-11	7.88521e-11	7.85884e-11	7.83227e-11	7.80545e-11	7.77835e-11
	7.75086e-11	7.72305e-11	7.69492e-11	7.66644e-11	0.	5.36213e-14	0.	0.

deposition rate at each branch (kg/s)

rate	0.	0.	5.45663e-13	5.45488e-13	5.45325e-13	5.45170e-13	5.45023e-13	5.44880e-13
	5.44736e-13	5.44595e-13	5.44453e-13	5.44312e-13	0.	3.83767e-16	0.	0.

entrainment rate at each branch (kg/s)

rate	0.	0.	0.	0.	0.	0.	0.	0.
	0.	0.	0.	0.	0.	0.	0.	0.

species no. 8 rad part 1.

specie nodal mass fraction

frac.	0.	0.	1.93438e-08	1.93438e-08	1.93188e-08	1.92937e-08	1.92684e-08	1.92429e-08
	1.92172e-08	1.91914e-08	1.91654e-08	1.91392e-08	1.91129e-08	1.90863e-08	9.53029e-12	9.52045e-12
	9.51117e-12	0.						

specie nodal concentration (kg/m**3)

conc.	0.	0.	2.16924e-08	2.16924e-08	2.16861e-08	2.16802e-08	2.16747e-08	2.16695e-08
	2.16645e-08	2.16595e-08	2.16546e-08	2.16496e-08	2.16447e-08	2.16397e-08	1.07786e-11	1.06723e-11
	1.06980e-11	0.						

specie branch flux (kg/sec)

dflux	0.	0.	1.07535e-08	1.07372e-08	1.07214e-08	1.07056e-08	1.06898e-08	1.06741e-08

```
                 1.06584e-08  1.06427e-08  1.06270e-08  1.06114e-08  1.05946e-08  5.28820e-12  5.28118e-12  5.27484e-12

specie integrated branch flux (kg)

int.mass        -8.91080e-13 -7.84346e-13  1.60198e-06  1.59279e-06  1.58380e-06  1.57485e-06  1.56592e-06  1.55703e-06
                 1.54817e-06  1.53935e-06  1.53055e-06  1.52179e-06  1.51288e-06  7.52027e-10  7.48807e-10  7.45646e-10

front filter mass (kg)

fil.mass         1.51212e-06

back filter mass (kg)

fil.mass        0.

total specie mass on filters : 1.512e-06

airborn mass (kg)

air mass        0.           0.           2.16924e-08  2.16924e-08  8.37361e-09  8.37136e-09  8.36924e-09  8.36723e-09
                8.36530e-09  8.36335e-09  8.36144e-09  8.35954e-09  8.35764e-09  8.35571e-09  4.16191e-12  2.96161e-12
                2.96876e-12  0.

total specie airborn mass : 1.270e-07

specie mass on duct wall (kg)

mass            0.           0.           7.46557e-11  7.44327e-11  7.42085e-11  7.39820e-11  7.37528e-11  7.35206e-11
                7.32845e-11  7.30452e-11  7.28024e-11  7.25562e-11  0.           5.07759e-14  0.           0.

deposition rate at each branch (kg/s)

rate            0.           0.           4.97449e-13  4.97303e-13  4.97170e-13  4.97044e-13  4.96925e-13  4.96810e-13
                4.96694e-13  4.96581e-13  4.96468e-13  4.96355e-13  0.           3.49983e-16  0.           0.

entrainment rate at each branch (kg/s)

rate            0.           0.           0.           0.           0.           0.           0.           0.
                0.           0.           0.           0.           0.           0.           0.           0.


                                   species no. 9     rad part 1.5

specie nodal mass fraction

frac.           0.           0.           6.45323e-08  6.45323e-08  6.44459e-08  6.43590e-08  6.42715e-08  6.41835e-08
                6.40949e-08  6.40057e-08  6.39160e-08  6.38256e-08  6.37347e-08  6.36432e-08  3.17789e-11  3.17438e-11
                3.17130e-11  0.

specie nodal concentration (kg/m**3)

conc.           0.           0.           7.23675e-08  7.23675e-08  7.23429e-08  7.23200e-08  7.22983e-08  7.22775e-08
                7.22574e-08  7.22372e-08  7.22172e-08  7.21974e-08  7.21775e-08  7.21575e-08  3.59412e-11  3.55843e-11
                3.56703e-11  0.

specie branch flux (kg/sec)

dflux           0.           0.           3.58746e-08  3.58183e-08  3.57638e-08  3.57095e-08  3.56552e-08  3.56011e-08
                3.55470e-08  3.54930e-08  3.54391e-08  3.53853e-08  3.53277e-08  1.76336e-11  1.76089e-11  1.75878e-11

specie integrated branch flux (kg)

int.mass        3.11878e-12 -2.74521e-12  5.36713e-06  5.33618e-06  5.30595e-06  5.27582e-06  5.24579e-06  5.21587e-06
```

	5.18606e-06	5.15637e-06	5.12679e-06	5.09731e-06	5.06732e-06	2.51894e-09	2.50801e-09	2.49747e-09

front filter mass (kg)

fil.mass 5.06478e-06

back filter mass (kg)

fil.mass 0.

total specie mass on filters : 5.065e-06

airborn mass (kg)

air mass	0.	0.	7.23675e-08	7.23675e-08	2.79337e-08	2.79248e-08	2.79164e-08	2.79084e-08
	2.79007e-08	2.78928e-08	2.78851e-08	2.78775e-08	2.78698e-08	2.78621e-08	1.38779e-11	9.87483e-12
	9.89870e-12	0.						

total specie airborn mass : 4.237e-07

specie mass on duct wall (kg)

mass	0.	0.	5.36370e-10	5.34761e-10	5.33144e-10	5.31510e-10	5.29857e-10	5.28181e-10
	5.26478e-10	5.24751e-10	5.23000e-10	5.21224e-10	0.	3.64760e-13	0.	0.

deposition rate at each branch (kg/s)

rate	0.	0.	3.55899e-12	3.55778e-12	3.55665e-12	3.55558e-12	3.55456e-12	3.55357e-12
	3.55258e-12	3.55160e-12	3.55062e-12	3.54964e-12	0.	2.50274e-15	0.	0.

entrainment rate at each branch (kg/s)

rate	0.	0.	0.	0.	0.	0.	0.	0.
	0.	0.	0.	0.	0.	0.	0.	0.

species no. 10 rad part 1.9

specie nodal mass fraction

frac.	0.	0.	1.09721e-07	1.09721e-07	1.09568e-07	1.09414e-07	1.09259e-07	1.09103e-07
	1.08947e-07	1.08789e-07	1.08630e-07	1.08471e-07	1.08310e-07	1.08148e-07	5.40017e-11	5.39378e-11
	5.38855e-11	0.						

specie nodal concentration (kg/m**3)

conc.	0.	0.	1.23043e-07	1.23043e-07	1.22994e-07	1.22948e-07	1.22904e-07	1.22862e-07
	1.22821e-07	1.22780e-07	1.22739e-07	1.22698e-07	1.22658e-07	1.22617e-07	6.10748e-11	6.04634e-11
	6.06096e-11	0.						

specie branch flux (kg/sec)

dflux	0.	0.	6.09957e-08	6.08966e-08	6.08006e-08	6.07048e-08	6.06092e-08	6.05137e-08
	6.04184e-08	6.03233e-08	6.02283e-08	6.01334e-08	6.00322e-08	2.99646e-11	2.99204e-11	2.98846e-11

specie integrated branch flux (kg)

int.mass	-5.34648e-12	-4.70608e-12	9.13227e-06	9.07914e-06	9.02724e-06	8.97550e-06	8.92395e-06	8.87258e-06
	8.82141e-06	8.77043e-06	8.71965e-06	8.66907e-06	8.61759e-06	4.28379e-09	4.26486e-09	4.24695e-09

front filter mass (kg)

fil.mass 8.61328e-06

back filter mass (kg)

fil.mass	0.

total specie mass on filters : 8.613e-06

airborn mass (kg)

air mass	0.	0.	1.23043e-07	1.23043e-07	4.74915e-08	4.74738e-08	4.74569e-08	4.74406e-08
	4.74248e-08	4.74088e-08	4.73931e-08	4.73774e-08	4.73617e-08	4.73459e-08	2.35827e-11	1.67789e-11
	1.68195e-11	0.						

total specie airborn mass : 7.203e-07

specie mass on duct wall (kg)

mass	0.	0.	1.43395e-09	1.42957e-09	1.42518e-09	1.42074e-09	1.41625e-09	1.41170e-09
	1.40708e-09	1.40239e-09	1.39764e-09	1.39282e-09	0.	9.74659e-13	0.	0.

deposition rate at each branch (kg/s)

rate	0.	0.	9.50768e-12	9.50392e-12	9.50038e-12	9.49700e-12	9.49374e-12	9.49056e-12
	9.48737e-12	9.48422e-12	9.48108e-12	9.47794e-12	0.	6.68215e-15	0.	0.

entrainment rate at each branch (kg/s)

rate	0.	0.	0.	0.	0.	0.	0.	0.
	0.	0.	0.	0.	0.	0.	0.	0.

species no. 11 rad part 8.

specie nodal mass fraction

frac.	0.	0.	3.88467e-08	3.88467e-08	3.86988e-08	3.85509e-08	3.84031e-08	3.82554e-08
	3.81076e-08	3.79600e-08	3.78123e-08	3.76647e-08	3.75171e-08	3.73696e-08	1.86601e-11	1.85734e-11
	1.85556e-11	0.						

specie nodal concentration (kg/m**3)

conc.	0.	0.	4.35633e-08	4.35633e-08	4.34408e-08	4.33196e-08	4.31992e-08	4.30796e-08
	4.29607e-08	4.28418e-08	4.27233e-08	4.26051e-08	4.24870e-08	4.23690e-08	2.11042e-11	2.08205e-11
	2.08711e-11	0.						

specie branch flux (kg/sec)

dflux	0.	0.	2.15956e-08	2.15084e-08	2.14225e-08	2.13369e-08	2.12516e-08	2.11666e-08
	2.10819e-08	2.09975e-08	2.09133e-08	2.08294e-08	2.07435e-08	1.03542e-11	1.03030e-11	1.02909e-11

specie integrated branch flux (kg)

int.mass	-2.22790e-12	-1.96104e-12	3.28554e-06	3.25874e-06	3.23248e-06	3.20636e-06	3.18038e-06	3.15456e-06
	3.12890e-06	3.10339e-06	3.07803e-06	3.05283e-06	3.02738e-06	1.50505e-09	1.49318e-09	1.48701e-09

front filter mass (kg)

fil.mass	3.02586e-06

back filter mass (kg)

fil.mass	0.

total specie mass on filters : 3.026e-06

airborn mass (kg)

air mass	0.	0.	4.35633e-08	4.35633e-08	1.67737e-08	1.67269e-08	1.66805e-08	1.66343e-08
	1.65883e-08	1.65424e-08	1.64967e-08	1.64510e-08	1.64054e-08	1.63599e-08	8.14894e-12	5.77778e-12
	5.79184e-12	0.						

total specie airborn mass : 2.528e-07

specie mass on duct wall (kg)

mass	0.	0.	8.58131e-09	8.53545e-09	8.48954e-09	8.44346e-09	8.39717e-09	8.35065e-09
	8.30380e-09	8.25668e-09	8.20930e-09	8.16166e-09	0	5.69542e-12	0.	0.

deposition rate at each branch (kg/s)

rate	0.	0.	5.60056e-11	5.58481e-11	5.56921e-11	5.55373e-11	5.53835e-11	5.52305e-11
	5.50776e-11	5.49251e-11	5.47730e-11	5.46212e-11	0.	3.83966e-14	0.	0.

entrainment rate at each branch (kg/s)

rate	0.	0.	0.	0.	0.	0.	0.	0.
	0.	0.	0.	0.	0.	0.	0.	0.

species no. 12 rad part 15.

specie nodal mass fraction

frac.	0.	0.	3.91916e-08	3.91916e-08	3.87937e-08	3.83990e-08	3.80076e-08	3.76193e-08
	3.72341e-08	3.68522e-08	3.64733e-08	3.60975e-08	3.57248e-08	3.53551e-08	1.76552e-11	1.76392e-11
	1.76232e-11	0.						

specie nodal concentration (kg/m**3)

conc.	0.	0.	4.39501e-08	4.39501e-08	4.35474e-08	4.31489e-08	4.27543e-08	4.23633e-08
	4.19759e-08	4.15915e-08	4.12103e-08	4.08323e-08	4.04572e-08	4.00850e-08	1.99677e-11	1.97733e-11
	1.98223e-11	0.						

specie branch flux (kg/sec)

dflux	0.	0.	2.17873e-08	2.15611e-08	2.13381e-08	2.11171e-08	2.08983e-08	2.06815e-08
	2.04667e-08	2.02539e-08	2.00431e-08	1.98343e-08	1.96253e-08	9.79659e-12	9.78485e-12	9.77371e-12

specie integrated branch flux (kg)

int.mass	-3.25661e-12	-2.86653e-12	3.46152e-06	3.41201e-06	3.36349e-06	3.31552e-06	3.26812e-06	3.22127e-06
	3.17499e-06	3.12926e-06	3.08409e-06	3.03946e-06	2.99492e-06	1.48930e-09	1.48343e 09	1.47757e-09

front filter mass (kg)

fil.mass 2.99342e-06

back filter mass (kg)

fil.mass 0.

total specie mass on filters : 2.993e-06

airborn mass (kg)

air mass	0.	0.	4.39501e-08	4.39501e-08	1.68149e-08	1.66610e-08	1.65086e-08	1.63577e-08

```
               1.62081e-08  1.60597e-08  1.59125e-08  1.57665e-08  1.56217e-08  1.54780e-08  7.71010e-12  5.48720e-12
               5.50079e-12  0.

total specie airborn mass : 2.493e-07

specie mass on duct wall (kg)

mass           0.           0.           3.13663e-08  3.10093e-08  3.06544e-08  3.03015e-08  2.99504e-08  2.96009e-08
               2.92529e-08  2.89065e-08  2.85617e-08  2.82187e-08  0.           6.29737e-15  0.           0.

deposition rate at each branch (kg/s)

rate           0.           0.           1.96154e-10  1.94356e-10  1.92576e-10  1.90814e-10  1.89068e-10  1.87338e-10
               1.85621e-10  1.83919e-10  1.82231e-10  1.80556e-10  0.           1.25947e-13  0.           0.

entrainment rate at each branch (kg/s)

rate           0.           0.           0.           0.           0.           0.           0.           0.
               0.           0.           0.           0.           0.           1.25936e-13  0.           0.


                                      species no. 13    rad part 20.

specie nodal mass fraction

frac.          0.           0.           7.42179e-08  7.42179e-08  7.29677e-08  7.17366e-08  7.05242e-08  6.93304e-08
               6.81548e-08  6.69972e-08  6.58574e-08  6.47350e-08  6.36298e-08  6.25417e-08  3.12383e-11  3.12150e-11
               3.11915e-11  0.

specie nodal concentration (kg/m**3)

conc.          0.           0.           8.32290e-08  8.32290e-08  8.19089e-08  8.06101e-08  7.93319e-08  7.80735e-08
               7.68344e-08  7.56134e-08  7.44108e-08  7.32261e-08  7.20588e-08  7.09086e-08  3.53299e-11  3.49915e-11
               3.50838e-11  0.

specie branch flux (kg/sec)

dflux          0.           0.           4.12590e-08  4.05546e-08  3.98635e-08  3.91835e-08  3.85144e-08  3.78561e-08
               3.72084e-08  3.65711e-08  3.59440e-08  3.53271e-08  3.47163e-08  1.73336e-11  1.73156e-11  1.72987e-11

specie integrated branch flux (kg)

int.mass      -1.28616e-11 -1.13211e-11  7.55564e-06  7.40159e-06  7.25118e-06  7.10335e-06  6.95810e-06  6.81540e-06
               6.67525e-06  6.53761e-06  6.40244e-06  6.26971e-06  6.13814e-06  3.05471e-09  3.04435e-09  3.03395e-09

front filter mass (kg)

fil.mass       6.13507e-06

back filter mass (kg)

fil.mass       0.

total specie mass on filters : 6.135e-06

airborn mass (kg)

air mass       0.           0.           8.32290e-08  8.32290e-08  3.16274e-08  3.11259e-08  3.06323e-08  3.01464e-08
               2.96680e-08  2.91965e-08  2.87321e-08  2.82747e-08  2.78240e-08  2.73798e-08  1.36419e-11  9.71033e-12
               9.73594e-12  0.

total specie airborn mass : 4.611e-07
```

specie mass on duct wall (kg)

mass	0.	0.	1.20748e-07	1.18683e-07	1.16641e-07	1.14622e-07	1.12626e-07	1.10651e-07
	1.08698e-07	1.06766e-07	1.04857e-07	1.02969e-07	0.	1.96574e-14	0.	0.

deposition rate at each branch (kg/s)

rate	0.	0.	6.56298e-10	6.45884e-10	6.35636e-10	6.25551e-10	6.15622e-10	6.05845e-10
	5.96212e-10	5.86723e-10	5.77376e-10	5.68166e-10	0.	3.93148e-13	0.	0.

entrainment rate at each branch (kg/s)

rate	0.	0.	0.	0.	0.	0.	0.	0.
	0.	0.	0.	0.	0.	3.93119e-13	0.	0.

table no. vii

summary of solution parameters

sample problem 1

executed on : 84/06/11 time :21:56:02

run type = st

convergence criterion = 1.00e-04

total problem run time = 9.99e+02

total gas dynamics iterations for problem = 27086

total gas species iterations for problem = 0

total number of particulate species iterations for problem = 298699

total number of time steps = 23481

table no. viii

archival list of output parameters

(2) Sample Problem 1 fire compartment effects (PRINT 1) output file.

output for compartment effects -- compartment history

tstep (sec)	pcomp (atm)	fmo2 (fraction)	zhl (m)	vif (m**3/s)	vof (m**3/s)	thluc (f)
2.00	.9998	.2100	0.0000	.5296	-.5091	55.6700
2.10	1.0004	.2100	.0143	-.1621	-.5766	223.2095
2.20	1.0006	.2100	.0290	-.4743	-.5175	231.4592
2.30	1.0008	.2100	.0437	-.5592	-.5841	235.5993
2.40	1.0008	.2100	.0584	-.5948	-.5662	238.2493
2.50	1.0009	.2100	.0731	-.6268	-.5839	240.1369
2.60	1.0009	.2100	.0877	-.6362	-.5975	241.5759
2.70	1.0009	.2100	.1022	-.6479	-.5834	242.7129
2.80	1.0009	.2100	.1166	-.6495	-.6090	243.6421
2.90	1.0009	.2100	.1310	-.6512	-.5865	244.4142
3.00	1.0009	.2100	.1454	-.6504	-.6087	245.0676
3.99	1.0008	.2100	.2833	-.6107	-.5852	248.3836
4.99	1.0007	.2100	.4151	-.5522	-.5766	249.3557
5.99	1.0006	.2100	.5398	-.4908	-.5696	249.4960
6.99	1.0006	.2100	.6578	-.4313	-.5638	249.2310
7.99	1.0005	.2100	.7697	-.3698	-.5643	248.7405
8.99	1.0004	.2100	.8757	-.3153	-.5622	248.1126
9.99	1.0004	.2100	.9764	-.2629	-.5620	247.3998
14.95	1.0002	.2100	1.2807	.2706	-.5574	227.7814
19.95	1.0001	.2100	1.5210	.3309	-.5502	215.2139
24.95	1.0001	.2100	1.7209	.3561	-.5354	206.9032
29.95	1.0001	.2100	1.8898	.3778	-.5267	201.0574
34.95	1.0000	.2100	2.0332	.3970	-.5219	196.7217
39.95	1.0000	.2100	2.1557	.4120	-.5183	193.4104
44.95	1.0000	.2100	2.2610	.4254	-.5167	190.8245
49.95	1.0000	.2100	2.3518	.4367	-.5159	188.7718
54.95	1.0000	.2100	2.4304	.4460	-.5153	187.1274
59.95	1.0000	.2100	2.4988	.4537	-.5149	185.8039
64.95	1.0000	.2100	2.5586	.4599	-.5145	184.7370
69.95	.9999	.2100	2.6110	.4651	-.5141	183.8798
74.95	.9999	.2100	2.6570	.4694	-.5137	183.1929
79.95	.9999	.2100	2.6976	.4730	-.5133	182.6491
84.95	.9999	.2100	2.7335	.4761	-.5129	182.2217
89.95	.9999	.2100	2.7652	.4786	-.5126	181.8953
94.95	.9999	.2100	2.7934	.4809	-.5122	181.6516
99.95	.9999	.2100	2.8185	.4828	-.5118	181.4768
104.95	.9999	.2100	2.8408	.4845	-.5115	181.3623
109.95	.9999	.2100	2.8607	.4859	-.5111	181.3009
114.95	.9999	.2100	2.8784	.4872	-.5108	181.2809
119.95	.9999	.2100	2.8942	.4884	-.5105	181.2962
124.95	.9999	.2100	2.9083	.4894	-.5102	181.3416
129.95	.9999	.2100	2.9210	.4903	-.5099	181.4131
134.95	.9999	.2100	2.9325	.4906	-.5102	181.5097
139.95	.9999	.2100	2.9441	.4903	-.5102	181.6232
144.95	.9999	.2100	2.9557	.4898	-.5102	181.7493
149.95	.9999	.2100	2.9673	.4893	-.5100	181.8865
154.95	.9999	.2100	2.9791	.4888	-.5099	182.0331
159.95	.9999	.2100	2.9909	.4884	-.5097	182.1877
164.95	.9999	.2100	3.0028	.4880	-.5096	182.3486
169.95	.9999	.2100	3.0148	.4876	-.5094	182.5147
174.95	.9999	.2100	3.0268	.4871	-.5093	182.6927
179.95	.9999	.2100	3.0389	.4867	-.5091	182.8745
184.95	.9999	.2100	3.0511	.4864	-.5089	183.0571
189.95	.9999	.2100	3.0633	.4862	-.5088	183.2400
194.95	.9999	.2100	3.0755	.4859	-.5086	183.4229
199.95	.9999	.2100	3.0878	.4857	-.5084	183.6055
204.95	.9999	.2100	3.1001	.4855	-.5083	183.7877

209.95	.9999	.2100	3.1124	.4851	-.5083	183.9729
214.95	.9999	.2100	3.1249	.4848	-.5081	184.1646
219.95	.9999	.2100	3.1373	.4846	-.5079	184.3536
224.95	.9999	.2100	3.1498	.4845	-.5077	184.5398
229.95	.9999	.2100	3.1623	.4843	-.5076	184.7234
234.95	.9999	.2100	3.1748	.4842	-.5074	184.9047
239.95	.9999	.2100	3.1874	.4840	-.5073	185.0837
244.95	.9999	.2100	3.2000	.4839	-.5071	185.2607
249.95	.9999	.2100	3.2126	.4835	-.5071	185.4480
254.95	.9999	.2100	3.2253	.4833	-.5069	185.6318
259.95	.9999	.2100	3.2380	.4832	-.5067	185.8119
264.95	.9999	.2100	3.2507	.4831	-.5066	185.9885
269.95	.9999	.2100	3.2635	.4829	-.5065	186.1620
274.95	.9999	.2100	3.2763	.4828	-.5064	186.3327
279.95	.9999	.2100	3.2890	.4827	-.5062	186.5009
284.95	.9999	.2100	3.3019	.4824	-.5062	186.6777
289.95	.9999	.2100	3.3147	.4822	-.5060	186.8533
294.95	.9999	.2100	3.3276	.4821	-.5059	187.0249
299.95	.9999	.2100	3.3405	.4820	-.5058	187.1928
304.95	.9999	.2100	3.3534	.4819	-.5056	187.3573
309.95	.9999	.2100	3.3664	.4818	-.5055	187.5189
314.95	.9999	.2100	3.3793	.4817	-.5054	187.6777
319.95	.9999	.2100	3.3923	.4814	-.5055	187.8445
324.95	.9999	.2100	3.4054	.4812	-.5053	188.0118
329.95	.9999	.2100	3.4184	.4811	-.5051	188.1748
334.95	.9999	.2100	3.4315	.4810	-.5050	188.3341
339.95	.9999	.2100	3.4446	.4810	-.5049	188.4900
344.95	.9999	.2100	3.4577	.4809	-.5048	188.6428
349.95	.9999	.2100	3.4708	.4808	-.5047	188.7930
354.95	.9999	.2100	3.4839	.4804	-.5048	188.9516
359.95	.9999	.2100	3.4971	.4803	-.5046	189.1108
364.95	.9999	.2100	3.5103	.4802	-.5044	189.2659
369.95	.9999	.2100	3.5235	.4802	-.5043	189.4172
374.95	.9999	.2100	3.5367	.4801	-.5042	189.5651
379.95	.9999	.2100	3.5500	.4800	-.5041	189.7100
384.95	.9999	.2100	3.5632	.4800	-.5040	189.8523
389.95	.9999	.2100	3.5765	.4796	-.5041	190.0047
394.95	.9999	.2100	3.5899	.4795	-.5039	190.1565
399.95	.9999	.2100	3.6032	.4794	-.5038	190.3042
404.95	.9999	.2100	3.6166	.4793	-.5037	190.4482
409.95	.9999	.2100	3.6299	.4793	-.5036	190.5889
414.95	.9999	.2100	3.6433	.4793	-.5035	190.7267
419.95	.9999	.2100	3.6567	.4792	-.5034	190.8619
424.95	.9999	.2100	3.6701	.4788	-.5035	191.0100
429.95	.9999	.2100	3.6835	.4787	-.5033	191.1550
434.95	.9999	.2100	3.6970	.4786	-.5032	191.2959
439.95	.9999	.2100	3.7105	.4786	-.5031	191.4332
444.95	.9999	.2100	3.7240	.4786	-.5030	191.5673
449.95	.9999	.2100	3.7375	.4785	-.5029	191.6986
454.95	.9999	.2100	3.7510	.4783	-.5032	191.8301
459.95	.9999	.2100	3.7645	.4781	-.5029	191.9728
464.95	.9999	.2100	3.7781	.4780	-.5028	192.1114
469.95	.9999	.2100	3.7917	.4779	-.5027	192.2461
474.95	.9999	.2100	3.8053	.4779	-.5026	192.3773
479.95	.9999	.2100	3.8189	.4779	-.5025	192.5054
484.95	.9999	.2100	3.8325	.4779	-.5024	192.6308
489.95	.9999	.2100	3.8461	.4776	-.5026	192.7611
494.95	.9999	.2100	3.8598	.4774	-.5024	192.8978
499.95	.9999	.2100	3.8735	.4773	-.5023	193.0306
504.95	.9999	.2100	3.8872	.4773	-.5022	193.1595
509.95	.9999	.2100	3.9009	.4773	-.5021	193.2850
514.95	.9999	.2100	3.9146	.4773	-.5020	193.4076
519.95	.9999	.2100	3.9284	.4772	-.5020	193.5276
524.95	.9999	.2100	3.9421	.4768	-.5021	193.6582

529.95	.9999	.2100	3.9559	.4767	-.5019	193.7894
534.95	9999	.2100	3.9697	.4767	-.5018	193.9155
539.95	.9999	.2100	3.9835	.4767	-.5017	194.0400
544.95	.9999	.2100	3.9973	.4767	-.5016	194.1603
549.95	.9999	.2100	4.0111	.4767	-.5016	194.2777
554.95	.9999	.2100	4.0249	.4765	-.5019	194.3950
559.95	.9999	.2100	4.0388	.4762	-.5016	194.5247
564.95	.9999	.2100	4.0527	.4761	-.5015	194.6505
569.95	.9999	.2100	4.0666	.4761	-.5014	194.7724
574.95	.9999	.2100	4.0805	.4761	-.5013	194.8908
579.95	.9999	.2100	4 0944	.4761	-.5012	195.0062
584.95	.9999	.2100	4.1083	.4761	-.5012	195.1190
589.95	.9999	.2100	4.1223	.4758	-.5014	195.2391
594.95	.9999	.2100	4.1362	.4756	-.5012	195.3637
599.95	.9999	.2100	4.1502	.4756	-.5010	195.4843
604.95	.9999	.2100	4.1642	.4756	-.5010	195.6013
609.95	.9999	.2100	4.1782	.4756	-.5009	195.7150
614.95	.9999	.2100	4.1922	.4756	-.5008	195.8259

combustible type 7 has ignited at time: 619.8000 sec

619.95	1.0000	.2100	4.2078	.3952	-.6725	196.0940
624.95	1.0002	.2100	4.3131	.2550	-.5735	200.1731
629.95	1.0002	.1941	4.5720	.2365	-.5116	198.3183
634.95	1.0002	.1936	4.5720	.2648	-.5216	202.5975
639.95	1.0002	.1931	4.5720	.2793	-.5215	206.3777
644.95	1.0001	.1927	4.5720	.2910	-.5207	209.7353
649.95	1.0001	.1922	4.5720	.3016	-.5205	212.7189
654.95	1.0001	.1918	4.5720	.3108	-.5203	215.3725
659.95	1.0001	.1914	4.5720	.3186	-.5201	217.7370
664.95	1.0001	.1910	4.5720	.3252	-.5198	219.8490
669.95	1.0001	.1906	4.5720	.3308	-.5195	221.7403
674.95	1.0001	.1902	4.5720	.3357	-.5192	223.4390
679.95	1.0001	.1898	4.5720	.3398	-.5189	224.9693
684.95	1.0001	.1894	4.5720	.3434	-.5187	226.3525
689.95	1.0001	.1890	4.5720	.3465	-.5184	227.6073
694.95	1.0001	.1887	4.5720	.3491	-.5182	228.7497
699.95	1.0001	.1883	4.5720	.3514	-.5181	229.7939
704.95	1.0001	.1880	4.5720	.3533	-.5179	230.7522
709.95	1.0001	.1876	4.5720	.3550	-.5177	231.6353
714.95	1.0001	.1873	4.5720	.3564	-.5176	232.4524
719.95	1.0001	.1870	4.5720	.3576	-.5174	233.2116
724.95	1.0001	.1866	4.5720	.3586	-.5173	233.9199
729.95	1.0001	.1863	4.5720	.3595	-.5172	234.5834
734.95	1.0001	.1860	4.5720	.3602	-.5171	235.2073
739.95	1.0001	.1857	4.5720	.3609	-.5169	235.7963
744.95	1.0001	.1854	4.5720	.3614	-.5168	236.3544
749.95	1.0001	.1851	4.5720	.3618	-.5167	236.8850
754.95	1.0001	.1848	4.5720	.3622	-.5166	237.3913
759.95	1.0001	.1845	4.5720	.3625	-.5165	237.8758
764.95	1.0001	.1842	4.5720	.3628	-.5164	238.3409
769.95	1.0001	.1840	4.5720	.3630	-.5163	238.7886
774.95	1.0001	.1837	4.5720	.3631	-.5162	239.2206

all combustible materials were consumed by: 777.9000 sec

780.00	.9996	.1838	4.5720	.6459	-.3209	233.9694
785.00	.9995	.1847	4.5720	.7280	-.4459	221.0477
790.00	.9995	.1855	4.5720	.7046	-.4625	209.7719
795.00	.9996	.1862	4.5720	.6763	-.4680	200.0444
800.00	.9996	.1869	4.5720	.6507	-.4709	191.5945
805.00	.9997	.1875	4.5720	.6290	-.4734	184.1942
810.00	.9997	.1881	4.5720	.6106	-.4756	177.6634
815.00	.9997	.1887	4.5720	.5948	-.4775	171.8608
820.00	.9998	.1892	4.5720	.5811	-.4792	166.6738
825.00	.9998	.1897	4.5720	.5696	-.4809	162.0115

830.00	.9998	.1902	4.5720	.5597	-.4826	157.7987
835.00	.9998	.1906	4.5720	.5510	-.4840	153.9748
840.00	.9998	.1911	4.5720	.5434	-.4853	150.4892
845.00	.9998	.1915	4.5720	.5366	-.4864	147.2996
850.00	.9998	.1919	4.5720	.5303	-.4870	144.3704
855.00	.9999	.1923	4.5720	.5247	-.4874	141.6716
860.00	.9999	.1926	4.5720	.5196	-.4878	139.1764
865.00	.9999	.1930	4.5720	.5152	-.4881	136.8613
870.00	.9999	.1933	4.5720	.5113	-.4884	134.7061
875.00	.9999	.1937	4.5720	.5079	-.4888	132.6935
880.00	.9999	.1940	4.5720	.5049	-.4891	130.8086
885.00	.9999	.1943	4.5720	.5022	-.4894	129.0377
890.00	.9999	.1946	4.5720	.4998	-.4897	127.3718
895.00	.9999	.1949	4.5720	.4975	-.4901	125.8033
900.00	.9999	.1952	4.5720	.4954	-.4905	124.3269
905.00	.9999	.1955	4.5720	.4933	-.4908	122.9377
910.00	.9999	.1958	4.5720	.4914	-.4911	121.6302
915.00	.9999	.1960	4.5720	.4896	-.4914	120.3985
920.00	.9999	.1963	4.5720	.4879	-.4917	119.2370
925.00	.9999	.1966	4.5720	.4864	-.4920	118.1402
930.00	.9999	.1968	4.5720	.4849	-.4922	117.1038
935.00	.9999	.1971	4.5720	.4836	-.4925	116.1238
940.00	.9999	.1973	4.5720	.4824	-.4927	115.1964
945.00	.9999	.1975	4.5720	.4813	-.4930	114.3180
950.00	.9999	.1978	4.5720	.4802	-.4932	113.4858
955.00	.9999	.1980	4.5720	.4792	-.4934	112.6969
960.00	.9999	.1982	4.5720	.4783	-.4937	111.9487
965.00	.9999	.1984	4.5720	.4774	-.4939	111.2384
970.00	.9999	.1986	4.5720	.4767	-.4941	110.5636
975.00	.9999	.1988	4.5720	.4759	-.4943	109.9219
980.00	.9999	.1990	4.5720	.4753	-.4944	109.3111
985.00	.9999	.1992	4.5720	.4747	-.4946	108.7292
990.00	.9999	.1994	4.5720	.4741	-.4948	108.1742
995.00	.9999	.1996	4.5720	.4736	-.4950	107.6445

(3) Sample Problem 1 radioactive source term (RST) output file.

209.95	2	0.	0.	0.	0.	0.	0.	0.	0.	.192e-10	.135e-07	.817e-07	.962e-07
214.95	2	0.	0.	0.	0.	0.	0.	0.	0.	.193e-10	.136e-07	.819e-07	.963e-07
219.95	2	0.	0.	0.	0.	0.	0.	0.	0.	.193e-10	.136e-07	.820e-07	.965e-07
224.95	2	0.	0.	0.	0.	0.	0.	0.	0.	.193e-10	.136e-07	.822e-07	.967e-07
229.95	2	0.	0.	0.	0.	0.	0.	0.	0.	.194e-10	.136e-07	.823e-07	.968e-07
234.95	2	0.	0.	0.	0.	0.	0.	0.	0.	.194e-10	.137e-07	.824e-07	.970e-07
239.95	2	0.	0.	0.	0.	0.	0.	0.	0.	.194e-10	.137e-07	.826e-07	.971e-07
244.95	2	0.	0.	0.	0.	0.	0.	0.	0.	.195e-10	.137e-07	.827e-07	.973e-07
249.95	2	0.	0.	0.	0.	0.	0.	0.	0.	.195e-10	.137e-07	.828e-07	.974e-07
254.95	2	0.	0.	0.	0.	0.	0.	0.	0.	.195e-10	.137e-07	.830e-07	.976e-07
259.95	2	0.	0.	0.	0.	0.	0.	0.	0.	.196e-10	.138e-07	.831e-07	.978e-07
264.95	2	0.	0.	0.	0.	0.	0.	0.	0.	.196e-10	.138e-07	.832e-07	.979e-07
269.95	2	0.	0.	0.	0.	0.	0.	0.	0.	.196e-10	.138e-07	.834e-07	.981e-07
274.95	2	0.	0.	0.	0.	0.	0.	0.	0.	.196e-10	.138e-07	.835e-07	.982e-07
279.95	2	0.	0.	0.	0.	0.	0.	0.	0.	.197e-10	.139e-07	.836e-07	.984e-07
284.95	2	0.	0.	0.	0.	0.	0.	0.	0.	.197e-10	.139e-07	.838e-07	.985e-07
289.95	2	0.	0.	0.	0.	0.	0.	0.	0.	.197e-10	.139e-07	.839e-07	.987e-07
294.95	2	0	0.	0.	0.	0.	0.	0.	0.	.198e-10	.139e-07	.840e-07	.988e-07
299.95	2	0.	0.	0.	0.	0.	0.	0.	0.	.198e-10	.139e-07	.842e-07	.990e-07
304.95	2	0.	0.	0.	0.	0.	0.	0.	0.	.198e-10	.140e-07	.843e-07	.992e-07
309.95	2	0.	0.	0.	0.	0.	0.	0.	0.	.199e-10	.140e-07	.844e-07	.993e-07
314.95	2	0.	0.	0.	0.	0.	0.	0.	0.	.199e-10	.140e-07	.845e-07	.994e-07
319.95	2	0.	0.	0.	0.	0.	0.	0.	0.	.199e-10	.140e-07	.847e-07	.996e-07
324.95	2	0.	0.	0.	0.	0.	0.	0.	0.	.200e-10	.140e-07	.848e-07	.998e-07
329.95	2	0.	0.	0.	0.	0.	0.	0.	0.	.200e-10	.141e-07	.849e-07	.999e-07
334.95	2	0.	0.	0.	0.	0.	0.	0.	0.	.200e-10	.141e-07	.850e-07	.100e-06
339.95	2	0.	0.	0.	0.	0.	0.	0.	0.	.200e-10	.141e-07	.852e-07	.100e-06
344.95	2	0.	0.	0.	0.	0.	0.	0.	0.	.201e-10	.141e-07	.853e-07	.100e-06
349.95	2	0.	0.	0.	0.	0.	0.	0.	0.	.201e-10	.141e-07	.854e-07	.100e-06
354.95	2	0.	0.	0.	0.	0.	0.	0.	0.	.201e-10	.142e-07	.855e-07	.101e-06
359.95	2	0.	0.	0.	0.	0.	0.	0.	0.	.202e-10	.142e-07	.857e-07	.101e-06
364.95	2	0.	0.	0.	0.	0.	0.	0.	0.	.202e-10	.142e-07	.858e-07	.101e-06
369.95	2	0.	0.	0.	0.	0.	0.	0.	0.	.202e-10	.142e-07	.859e-07	.101e-06
374.95	2	0.	0.	0.	0.	0.	0.	0.	0.	.202e-10	.143e-07	.860e-07	.101e-06
379.95	2	0.	0.	0.	0.	0.	0.	0.	0.	.203e-10	.143e-07	.862e-07	.101e-06
384.95	2	0.	0.	0.	0.	0.	0.	0.	0.	.203e-10	.143e-07	.863e-07	.101e-06
389.95	2	0.	0.	0.	0.	0.	0.	0.	0.	.203e-10	.143e-07	.864e-07	.102e-06
394.95	2	0.	0.	0.	0.	0.	0.	0.	0.	.204e-10	.143e-07	.865e-07	.102e-06
399.95	2	0.	0.	0.	0.	0.	0.	0.	0.	.204e-10	.144e-07	.866e-07	.102e-06
404.95	2	0.	0.	0.	0.	0.	0.	0.	0.	.204e-10	.144e-07	.868e-07	.102e-06
409.95	2	0.	0.	0.	0.	0.	0.	0.	0.	.204e-10	.144e-07	.869e-07	.102e-06
414.95	2	0.	0.	0.	0.	0.	0.	0.	0.	.205e-10	.144e-07	.870e-07	.102e-06
419.95	2	0.	0.	0.	0.	0.	0.	0.	0.	.205e-10	.144e-07	.871e-07	.102e-06
424.95	2	0.	0.	0.	0.	0.	0.	0.	0.	.205e-10	.144e-07	.872e-07	.103e-06
429.95	2	0.	0.	0.	0.	0.	0.	0.	0.	.206e-10	.145e-07	.873e-07	.103e-06
434.95	2	0.	0.	0.	0.	0.	0.	0.	0.	.206e-10	.145e-07	.875e-07	.103e-06
439.95	2	0.	0.	0.	0.	0.	0.	0.	0.	.206e-10	.145e-07	.876e-07	.103e-06
444.95	2	0.	0.	0.	0.	0.	0.	0.	0.	.206e-10	.145e-07	.877e-07	.103e-06
449.95	2	0.	0.	0.	0.	0.	0.	0.	0.	.207e-10	.145e-07	.878e-07	.103e-06
454.95	2	0.	0.	0.	0.	0.	0.	0.	0.	.207e-10	.146e-07	.879e-07	.103e-06
459.95	2	0.	0.	0.	0.	0.	0.	0.	0.	.207e-10	.146e-07	.880e-07	.104e-06
464.95	2	0.	0.	0.	0.	0.	0.	0.	0.	.207e-10	.146e-07	.882e-07	.104e-06
469.95	2	0.	0.	0.	0.	0.	0.	0.	0.	.208e-10	.146e-07	.883e-07	.104e-06
474.95	2	0.	0.	0.	0.	0.	0.	0.	0.	.208e-10	.146e-07	.884e-07	.104e-06
479.95	2	0.	0.	0.	0.	0.	0.	0.	0.	.208e-10	.147e-07	.885e-07	.104e-06
484.95	2	0.	0.	0.	0.	0.	0.	0.	0.	.209e-10	.147e-07	.886e-07	.104e-06
489.95	2	0.	0.	0.	0.	0.	0.	0.	0.	.209e-10	.147e-07	.887e-07	.104e-06
494.95	2	0.	0.	0.	0.	0.	0.	0.	0.	.209e-10	.147e-07	.888e-07	.105e-06
499.95	2	0.	0.	0.	0.	0.	0.	0.	0.	.209e-10	.147e-07	.890e-07	.105e-06
504.95	2	0.	0.	0.	0.	0.	0.	0.	0.	.210e-10	.148e-07	.891e-07	.105e-06
509.95	2	0.	0.	0.	0.	0.	0.	0.	0.	.210e-10	.148e-07	.892e-07	.105e-06
514.95	2	0.	0.	0.	0.	0.	0.	0.	0.	.210e-10	.148e-07	.893e-07	.105e-06
519.95	2	0.	0.	0.	0.	0.	0.	0.	0.	.210e-10	.148e-07	.894e-07	.105e-06
524.95	2	0.	0.	0.	0.	0.	0.	0.	0.	.211e-10	.148e-07	.895e-07	.105e-06

output for radioactive source terms

time (sec)	jact	mass rate (g/sec) accordingto size distribution (microns) (< .1)	(.1-.3)	(.3-.5)	(.5-.7)	(.7-.9)	(.9-1.1)	(1.1-2)	(2-6)	(6-10)	(10-20)	(>20)	total
2.00	0	0.	0.	0.	0.	0.	0.	0.	0.	0.	0.	0.	0.
2.10	2	0.	0.	0.	0.	0.	0.	0.	0.	.236e-10	.166e-07	.100e-06	.118e-06
2.20	2	0.	0.	0.	0.	0.	0.	0.	0.	.248e-10	.174e-07	.105e-06	.124e-06
2.30	2	0.	0.	0.	0.	0.	0.	0.	0.	.254e-10	.179e-07	.108e-06	.127e-06
2.40	2	0.	0.	0.	0.	0.	0.	0.	0.	.258e-10	.182e-07	.110e-06	.129e-06
2.50	2	0.	0.	0.	0.	0.	0.	0.	0.	.261e-10	.184e-07	.111e-06	.131e-06
2.60	2	0.	0.	0.	0.	0.	0.	0.	0.	.264e-10	.186e-07	.112e-06	.132e-06
2.70	2	0.	0.	0.	0.	0.	0.	0.	0.	.266e-10	.187e-07	.113e-06	.133e-06
2.80	2	0.	0.	0.	0.	0.	0.	0.	0.	.267e-10	.188e-07	.113e-06	.134e-06
2.90	2	0.	0.	0.	0.	0.	0.	0.	0.	.268e-10	.189e-07	.114e-06	.134e-06
3.00	2	0.	0.	0.	0.	0.	0.	0.	0.	.269e-10	.190e-07	.114e-06	.135e-06
3.99	2	0.	0.	0.	0.	0.	0.	0.	0.	.275e-10	.194e-07	.117e-06	.138e-06
4.99	2	0.	0.	0.	0.	0.	0.	0.	0.	.277e-10	.195e-07	.118e-06	.138e-06
5.99	2	0.	0.	0.	0.	0.	0.	0.	0.	.277e-10	.195e-07	.118e-06	.139e-06
6.99	2	0.	0.	0.	0.	0.	0.	0.	0.	.277e-10	.195e-07	.118e-06	.138e-06
7.99	2	0.	0.	0.	0.	0.	0.	0.	0.	.276e-10	.194e-07	.117e-06	.138e-06
8.99	2	0.	0.	0.	0.	0.	0.	0.	0.	.275e-10	.194e-07	.117e-06	.137e-06
9.99	2	0.	0.	0.	0.	0.	0.	0.	0.	.274e-10	.193e-07	.116e-06	.137e-06
14.95	2	0.	0.	0.	0.	0.	0.	0.	0.	.243e-10	.171e-07	.103e-06	.122e-06
19.95	2	0.	0.	0.	0.	0.	0.	0.	0.	.226e-10	.159e-07	.959e-07	.113e-06
24.95	2	0.	0.	0.	0.	0.	0.	0.	0.	.215e-10	.151e-07	.914e-07	.107e-06
29.95	2	0.	0.	0.	0.	0.	0.	0.	0.	.208e-10	.146e-07	.883e-07	.104e-06
34.95	2	0.	0.	0.	0.	0.	0.	0.	0.	.203e-10	.143e-07	.861e-07	.101e-06
39.95	2	0.	0.	0.	0.	0.	0.	0.	0.	.199e-10	.140e-07	.845e-07	.995e-07
44.95	2	0.	0.	0.	0.	0.	0.	0.	0.	.196e-10	.138e-07	.833e-07	.980e-07
49.95	2	0.	0.	0.	0.	0.	0.	0.	0.	.194e-10	.136e-07	.824e-07	.969e-07
54.95	2	0.	0.	0.	0.	0.	0.	0.	0.	.192e-10	.135e-07	.817e-07	.961e-07
59.95	2	0.	0.	0.	0.	0.	0.	0.	0.	.191e-10	.134e-07	.811e-07	.954e-07
64.95	2	0.	0.	0.	0.	0.	0.	0.	0.	.190e-10	.134e-07	.807e-07	.949e-07
69.95	2	0.	0.	0.	0.	0.	0.	0.	0.	.189e-10	.133e-07	.803e-07	.945e-07
74.95	2	0.	0.	0.	0.	0.	0.	0.	0.	.188e-10	.133e-07	.800e-07	.942e-07
79.95	2	0.	0.	0.	0.	0.	0.	0.	0.	.188e-10	.132e-07	.798e-07	.939e-07
84.95	2	0.	0.	0.	0.	0.	0.	0.	0.	.188e-10	.132e-07	.797e-07	.938e-07
89.95	2	0.	0.	0.	0.	0.	0.	0.	0.	.187e-10	.132e-07	.796e-07	.936e-07
94.95	2	0.	0.	0.	0.	0.	0.	0.	0.	.187e-10	.132e-07	.795e-07	.936e-07
99.95	2	0.	0.	0.	0.	0.	0.	0.	0.	.187e-10	.132e-07	.795e-07	.935e-07
104.95	2	0.	0.	0.	0.	0.	0.	0.	0.	.187e-10	.132e-07	.795e-07	.935e-07
109.95	2	0.	0.	0.	0.	0.	0.	0.	0.	.187e-10	.132e-07	.795e-07	.936e-07
114.95	2	0.	0.	0.	0.	0.	0.	0.	0.	.187e-10	.132e-07	.796e-07	.936e-07
119.95	2	0.	0.	0.	0.	0.	0.	0.	0.	.187e-10	.132e-07	.796e-07	.937e-07
124.95	2	0.	0.	0.	0.	0.	0.	0.	0.	.188e-10	.132e-07	.797e-07	.938e-07
129.95	2	0.	0.	0.	0.	0.	0.	0.	0.	.188e-10	.132e-07	.798e-07	.939e-07
134.95	2	0.	0.	0.	0.	0.	0.	0.	0.	.188e-10	.132e-07	.799e-07	.940e-07
139.95	2	0.	0.	0.	0.	0.	0.	0.	0.	.188e-10	.132e-07	.800e-07	.941e-07
144.95	2	0.	0.	0.	0.	0.	0.	0.	0.	.188e-10	.133e-07	.801e-07	.942e-07
149.95	2	0.	0.	0.	0.	0.	0.	0.	0.	.189e-10	.133e-07	.802e-07	.943e-07
154.95	2	0.	0.	0.	0.	0.	0.	0.	0.	.189e-10	.133e-07	.803e-07	.945e-07
159.95	2	0.	0.	0.	0.	0.	0.	0.	0.	.189e-10	.133e-07	.804e-07	.946e-07
164.95	2	0.	0.	0.	0.	0.	0.	0.	0.	.190e-10	.133e-07	.805e-07	.948e-07
169.95	2	0.	0.	0.	0.	0.	0.	0.	0.	.190e-10	.134e-07	.807e-07	.949e-07
174.95	2	0.	0.	0.	0.	0.	0.	0.	0.	.190e-10	.134e-07	.808e-07	.951e-07
179.95	2	0.	0.	0.	0.	0.	0.	0.	0.	.190e-10	.134e-07	.809e-07	.952e-07
184.95	2	0.	0.	0.	0.	0.	0.	0.	0.	.191e-10	.134e-07	.811e-07	.954e-07
189.95	2	0.	0.	0.	0.	0.	0.	0.	0.	.191e-10	.135e-07	.812e-07	.955e-07
194.95	2	0.	0.	0.	0.	0.	0.	0.	0.	.191e-10	.135e-07	.813e-07	.957e-07
199.95	2	0.	0.	0.	0.	0.	0.	0.	0.	.192e-10	.135e-07	.815e-07	.959e-07
204.95	2	0.	0.	0.	0.	0.	0.	0.	0.	.192e-10	.135e-07	.816e-07	.960e-07

529.95	2	0.	0	0	0	0	0.	0.	0.	.211e-10	.148e-07	.896e-07	.105e-06
534.95	2	0.	0.	0.	0.	0.	0.	0.	0.	.211e-10	.149e-07	.897e-07	.106e-06
539.95	2	0.	0.	0.	0.	0.	0.	0.	0.	.211e-10	.149e-07	.898e-07	.106e-06
544.95	2	0.	0.	0.	0.	0.	0.	0.	0.	.212e-10	.149e-07	.900e-07	.106e-06
549.95	2	0.	0.	0.	0.	0.	0.	0.	0.	.212e-10	.149e-07	.901e-07	.106e-06
554.95	2	0.	0.	0.	0.	0.	0.	0.	0.	.212e-10	.149e-07	.902e-07	.106e-06
559.95	2	0.	0.	0.	0.	0.	0.	0.	0.	.212e-10	.150e-07	.903e-07	.106e-06
564.95	2	0.	0.	0.	0.	0.	0.	0.	0.	.213e-10	.150e-07	.904e-07	.106e-06
569.95	2	0.	0.	0.	0.	0.	0.	0.	0.	.213e-10	.150e-07	.905e-07	.106e-06
574.95	2	0.	0.	0.	0.	0.	0.	0.	0.	.213e-10	.150e-07	.906e-07	.107e-06
579.95	2	0.	0.	0.	0.	0.	0.	0.	0.	.213e-10	.150e-07	.907e-07	.107e-06
584.95	2	0.	0.	0.	0.	0.	0.	0.	0.	.214e-10	.150e-07	.908e-07	.107e-06
589.95	2	0.	0.	0.	0.	0.	0.	0.	0.	.214e-10	.151e-07	.909e-07	.107e-06
594.95	2	0.	0.	0.	0.	0.	0.	0.	0.	.214e-10	.151e-07	.910e-07	.107e-06
599.95	2	0.	0.	0.	0.	0.	0.	0.	0.	.214e-10	.151e-07	.912e-07	.107e-06
604.95	2	0.	0.	0.	0.	0.	0.	0.	0.	.215e-10	.151e-07	.913e-07	.107e-06
609.95	2	0.	0.	0.	0.	0.	0.	0.	0.	.215e-10	.151e-07	.914e-07	.107e-06
614.95	2	0.	0.	0.	0.	0.	0.	0.	0.	.215e-10	.152e-07	.915e-07	.108e-06

combustible type 7 has ignited at time: 619.8000 sec

619.95	1	.222e-04	.997e-05	.554e-05	.443e-05	.222e-05	.222e-05	.776e-05	.133e-04	.554e-05	.776e-05	.299e-04	.111e-03
619.95	2	0.	0.	0.	0.	0.	0.	0.	0.	.216e-10	.152e-07	.916e-07	.108e-06
624.95	1	.222e-04	.998e-05	.555e-05	.444e-05	.222e-05	.222e-05	.776e-05	.133e-04	.555e-05	.776e-05	.299e-04	.111e-03
624.95	2	0.	0.	0.	0.	0.	0.	0.	0.	.221e-10	.155e-07	.938e-07	.110e-06
629.95	1	.234e-04	.105e-04	.584e-05	.467e-05	.234e-05	.234e-05	.818e-05	.140e-04	.584e-05	.818e-05	.315e-04	.117e-03
629.95	2	0.	0.	0.	0.	0.	0.	0.	0.	.643e-10	.452e-07	.273e-06	.321e-06
634.95	1	.234e-04	.105e-04	.586e-05	.468e-05	.234e-05	.234e-05	.820e-05	.141e-04	.586e-05	.820e-05	.316e-04	.117e-03
634.95	2	0.	0.	0.	0.	0.	0.	0.	0.	.673e-10	.474e-07	.286e-06	.336e-06
639.95	1	.235e-04	.106e-04	.587e-05	.470e-05	.235e-05	.235e-05	.822e-05	.141e-04	.587e-05	.822e-05	.317e-04	.117e-03
639.95	2	0.	0.	0.	0.	0.	0.	0.	0.	.700e-10	.493e-07	.298e-06	.350e-06
644.95	1	.235e-04	.106e-04	.588e-05	.470e-05	.235e-05	.235e-05	.823e-05	.141e-04	.588e-05	.823e-05	.318e-04	.118e-03
644.95	2	0.	0.	0.	0.	0.	0.	0.	0.	.726e-10	.511e-07	.308e-06	.363e-06
649.95	1	.236e-04	.106e-04	.589e-05	.471e-05	.236e-05	.236e-05	.825e-05	.141e-04	.589e-05	.825e-05	.318e-04	.118e-03
649.95	2	0.	0.	0.	0.	0.	0.	0.	0.	.749e-10	.527e-07	.318e-06	.375e-06
654.95	1	.236e-04	.106e-04	.590e-05	.472e-05	.236e-05	.236e-05	.826e-05	.142e-04	.590e-05	.826e-05	.319e-04	.118e-03
654.95	2	0.	0.	0.	0.	0.	0.	0.	0.	.770e-10	.542e-07	.327e-06	.385e-06
659.95	1	.236e-04	.106e-04	.591e-05	.473e-05	.236e-05	.236e-05	.827e-05	.142e-04	.591e-05	.827e-05	.319e-04	.118e-03
659.95	2	0.	0.	0.	0.	0.	0.	0.	0.	.790e-10	.556e-07	.336e-06	.395e-06
664.95	1	.237e-04	.106e-04	.592e-05	.473e-05	.237e-05	.237e-05	.828e-05	.142e-04	.592e-05	.828e-05	.319e-04	.118e-03
664.95	2	0.	0.	0.	0.	0.	0.	0.	0.	.808e-10	.569e-07	.343e-06	.404e-06
669.95	1	.237e-04	.107e-04	.592e-05	.474e-05	.237e-05	.237e-05	.829e-05	.142e-04	.592e-05	.829e-05	.320e-04	.118e-03
669.95	2	0.	0.	0.	0.	0.	0.	0.	0.	.824e-10	.580e-07	.350e-06	.412e-06
674.95	1	.237e-04	.107e-04	.593e-05	.474e-05	.237e-05	.237e-05	.830e-05	.142e-04	.593e-05	.830e-05	.320e-04	.119e-03
674.95	2	0.	0.	0.	0.	0.	0.	0.	0.	.839e-10	.591e-07	.357e-06	.420e-06
679.95	1	.237e-04	.107e-04	.593e-05	.475e-05	.237e-05	.237e-05	.831e-05	.142e-04	.593e-05	.831e-05	.320e-04	.119e-03
679.95	2	0.	0.	0.	0.	0.	0.	0.	0.	.853e-10	.601e-07	.363e-06	.427e-06
684.95	1	.238e-04	.107e-04	.594e-05	.475e-05	.238e-05	.238e-05	.831e-05	.143e-04	.594e-05	.831e-05	.321e-04	.119e-03
684.95	2	0.	0.	0.	0.	0.	0.	0.	0.	.866e-10	.610e-07	.368e-06	.433e-06
689.95	1	.238e-04	.107e-04	.594e-05	.475e-05	.238e-05	.238e-05	.832e-05	.143e-04	.594e-05	.832e-05	.321e-04	.119e-03
689.95	2	0.	0.	0.	0.	0.	0.	0.	0.	.878e-10	.618e-07	.373e-06	.439e-06
694.95	1	.238e-04	.107e-04	.595e-05	.476e-05	.238e-05	.238e-05	.832e-05	.143e-04	.595e-05	.832e-05	.321e-04	.119e-03
694.95	2	0.	0.	0.	0.	0.	0.	0.	0.	.889e-10	.626e-07	.378e-06	.445e-06
699.95	1	.238e-04	.107e-04	.595e-05	.476e-05	.238e-05	.238e-05	.833e-05	.143e-04	.595e-05	.833e-05	.321e-04	.119e-03
699.95	2	0.	0.	0.	0.	0.	0.	0.	0.	.899e-10	.633e-07	.382e-06	.450e-06
704.95	1	.238e-04	.107e-04	.595e-05	.476e-05	.238e-05	.238e-05	.833e-05	.143e-04	.595e-05	.833e-05	.321e-04	.119e-03
704.95	2	0.	0.	0.	0.	0.	0.	0.	0.	.909e-10	.640e-07	.386e-06	.455e-06
709.95	1	.238e-04	.107e-04	.595e-05	.476e-05	.238e-05	.238e-05	.834e-05	.143e-04	.595e-05	.834e-05	.322e-04	.119e-03
709.95	2	0.	0.	0.	0.	0.	0.	0.	0.	.918e-10	.647e-07	.390e-06	.459e-06
714.95	1	.238e-04	.107e-04	.596e-05	.477e-05	.238e-05	.238e-05	.834e-05	.143e-04	.596e-05	.834e-05	.322e-04	.119e-03
714.95	2	0.	0.	0.	0.	0.	0.	0.	0.	.927e-10	.653e-07	.394e-06	.464e-06
719.95	1	.238e-04	.107e-04	.596e-05	.477e-05	.238e-05	.238e-05	.834e-05	.143e-04	.596e-05	.834e-05	.322e-04	.119e-03
719.95	2	0.	0.	0.	0.	0.	0.	0.	0.	.936e-10	.659e-07	.398e-06	.468e-06
724.95	1	.238e-04	.107e-04	.596e-05	.477e-05	.238e-05	.238e-05	.834e-05	.143e-04	.596e-05	.834e-05	.322e-04	.119e-03
724.95	2	0.	0.	0.	0.	0.	0.	0.	0.	.943e-10	.664e-07	.401e-06	.472e-06

729.95	1	.238e-04	.107e-04	.596e-05	.477e-05	.238e-05	.238e-05	.835e-05	.143e-04	.596e-05	.835e-05	.322e-04	.119e-03
729.95	2	O.	O.	O.	O.	O.	O.	O.	O.	.951e-10	.669e-07	.404e-06	.475e-06
734.95	1	.239e-04	.107e-04	.596e-05	.477e-05	.239e-05	.239e-05	.835e-05	.143e-04	.596e-05	.835e-05	.322e-04	.119e-03
734.95	2	O.	O.	O.	O.	O.	O.	O.	O.	.958e-10	.675e-07	.407e-06	.479e-06
739.95	1	.239e-04	.107e-04	.597e-05	.477e-05	.239e-05	.239e-05	.835e-05	.143e-04	.597e-05	.835e-05	.322e-04	.119e-03
739.95	2	O.	O.	O.	O.	O.	O.	O.	O.	.965e-10	.679e-07	.410e-06	.483e-06
744.95	1	.239e-04	.107e-04	.597e-05	.477e-05	.239e-05	.239e-05	.835e-05	.143e-04	.597e-05	.835e-05	.322e-04	.119e-03
744.95	2	O.	O.	O.	O.	O.	O.	O.	O.	.972e-10	.684e-07	.413e-06	.486e-06
749.95	1	.239e-04	.107e-04	.597e-05	.477e-05	.239e-05	.239e-05	.835e-05	.143e-04	.597e-05	.835e-05	.322e-04	.119e-03
749.95	2	O.	O.	O.	O.	O.	O.	O.	O.	.978e-10	.689e-07	.416e-06	.489e-06
754.95	1	.239e-04	.107e-04	.597e-05	.478e-05	.239e-05	.239e-05	.836e-05	.143e-04	.597e-05	.836e-05	.322e-04	.119e-03
754.95	2	O.	O.	O.	O.	O.	O.	O.	O.	.985e-10	.693e-07	.419e-06	.492e-06
759.95	1	.239e-04	.107e-04	.597e-05	.478e-05	.239e-05	.239e-05	.836e-05	.143e-04	.597e-05	.836e-05	.322e-04	.119e-03
759.95	2	O.	O.	O.	O.	O.	O.	O.	O.	.991e-10	.698e-07	.421e-06	.495e-06
764.95	1	.239e-04	.107e-04	.597e-05	.478e-05	.239e-05	.239e-05	.836e-05	.143e-04	.597e-05	.836e-05	.322e-04	.119e-03
764.95	2	O.	O.	O.	O.	O.	O.	O.	O.	.997e-10	.702e-07	.424e-06	.498e-06
769.95	1	.239e-04	.107e-04	.597e-05	.478e-05	.239e-05	.239e-05	.836e-05	.143e-04	.597e-05	.836e-05	.322e-04	.119e-03
769.95	2	O.	O.	O.	O.	O.	O.	O.	O.	.100e-09	.706e-07	.426e-06	.501e-06
774.95	1	.239e-04	.108e-04	.597e-05	.478e-05	.239e-05	.239e-05	.836e-05	.143e-04	.597e-05	.836e-05	.323e-04	.119e-03
774.95	2	O.	O.	O.	O.	O.	O.	O.	O.	.101e-09	.710e-07	.429e-06	.504e-06

all combustible materials were consumed by: 777.9000 sec

780.00	1	.135e-03	.126e-03	.720e-04	.450e-04	.450e-04	.270e-04	.900e-04	.153e-03	.540e-04	.540e-04	.990e-04	.900e-03
780.00	2	O.	O.	O.	O.	O.	O.	O.	O.	.966e-10	.680e-07	.410e-06	.483e-06
785.00	1	.135e-03	.126e-03	.720e-04	.450e-04	.450e-04	.270e-04	.900e-04	.153e-03	.540e-04	.540e-04	.990e-04	.900e-03
785.00	2	O.	O.	O.	O.	O.	O.	O.	O.	.860e-10	.606e-07	.366e-06	.430e-06
790.00	1	.135e-03	.126e-03	.720e-04	.450e-04	.450e-04	.270e-04	.900e-04	.153e-03	.540e-04	.540e-04	.990e-04	.900e-03
790.00	2	O.	O.	O.	O.	O.	O.	O.	O.	.775e-10	.546e-07	.329e-06	.388e-06
795.00	1	.135e-03	.126e-03	.720e-04	.450e-04	.450e-04	.270e-04	.900e-04	.153e-03	.540e-04	.540e-04	.990e-04	.900e-03
795.00	2	O.	O.	O.	O.	O.	O.	O.	O.	.707e-10	.498e-07	.300e-06	.353e-06
800.00	1	.135e-03	.126e-03	.720e-04	.450e-04	.450e-04	.270e-04	.900e-04	.153e-03	.540e-04	.540e-04	.990e-04	.900e-03
800.00	2	O.	O.	O.	O.	O.	O.	O.	O.	.651e-10	.458e-07	.277e-06	.325e-06
805.00	1	.135e-03	.126e-03	.720e-04	.450e-04	.450e-04	.270e-04	.900e-04	.153e-03	.540e-04	.540e-04	.990e-04	.900e-03
805.00	2	O.	O.	O.	O.	O.	O.	O.	O.	.604e-10	.426e-07	.257e-06	.302e-06
810.00	1	.135e-03	.126e-03	.720e-04	.450e-04	.450e-04	.270e-04	.900e-04	.153e-03	.540e-04	.540e-04	.990e-04	.900e-03
810.00	2	O.	O.	O.	O.	O.	O.	O.	O.	.566e-10	.398e-07	.240e-06	.283e-06
815.00	1	.135e-03	.126e-03	.720e-04	.450e-04	.450e-04	.270e-04	.900e-04	.153e-03	.540e-04	.540e-04	.990e-04	.900e-03
815.00	2	O.	O.	O.	O.	O.	O.	O.	O.	.533e-10	.375e-07	.226e-06	.266e-06
820.00	1	.135e-03	.126e-03	.720e-04	.450e-04	.450e-04	.270e-04	.900e-04	.153e-03	.540e-04	.540e-04	.990e-04	.900e-03
820.00	2	O.	O.	O.	O.	O.	O.	O.	O.	.504e-10	.355e-07	.214e-06	.252e-06
825.00	1	.135e-03	.126e-03	.720e-04	.450e-04	.450e-04	.270e-04	.900e-04	.153e-03	.540e-04	.540e-04	.990e-04	.900e-03
825.00	2	O.	O.	O.	O.	O.	O.	O.	O.	.480e-10	.338e-07	.204e-06	.240e-06
830.00	1	.135e-03	.126e-03	.720e-04	.450e-04	.450e-04	.270e-04	.900e-04	.153e-03	.540e-04	.540e-04	.990e-04	.900e-03
830.00	2	O.	O.	O.	O.	O.	O.	O.	O.	.459e-10	.323e-07	.195e-06	.229e-06
835.00	1	.135e-03	.126e-03	.720e-04	.450e-04	.450e-04	.270e-04	.900e-04	.153e-03	.540e-04	.540e-04	.990e-04	.900e-03
835.00	2	O.	O.	O.	O.	O.	O.	O.	O.	.440e-10	.310e-07	.187e-06	.220e-06
840.00	1	.135e-03	.126e-03	.720e-04	.450e-04	.450e-04	.270e-04	.900e-04	.153e-03	.540e-04	.540e-04	.990e-04	.900e-03
840.00	2	O.	O.	O.	O.	O.	O.	O.	O.	.423e-10	.298e-07	.180e-06	.212e-06
845.00	1	.135e-03	.126e-03	.720e-04	.450e-04	.450e-04	.270e-04	.900e-04	.153e-03	.540e-04	.540e-04	.990e-04	.900e-03
845.00	2	O.	O.	O.	O.	O.	O.	O.	O.	.409e-10	.288e-07	.174e-06	.204e-06
850.00	1	.135e-03	.126e-03	.720e-04	.450e-04	.450e-04	.270e-04	.900e-04	.153e-03	.540e-04	.540e-04	.990e-04	.900e-03
850.00	2	O.	O.	O.	O.	O.	O.	O.	O.	.396e-10	.279e-07	.168e-06	.198e-06
855.00	1	.135e-03	.126e-03	.720e-04	.450e-04	.450e-04	.270e-04	.900e-04	.153e-03	.540e-04	.540e-04	.990e-04	.900e-03
855.00	2	O.	O.	O.	O.	O.	O.	O.	O.	.384e-10	.270e-07	.163e-06	.192e-06
860.00	1	.135e-03	.126e-03	.720e-04	.450e-04	.450e-04	.270e-04	.900e-04	.153e-03	.540e-04	.540e-04	.990e-04	.900e-03
860.00	2	O.	O.	O.	O.	O.	O.	O.	O.	.373e-10	.263e-07	.159e-06	.187e-06
865.00	1	.135e-03	.126e-03	.720e-04	.450e-04	.450e-04	.270e-04	.900e-04	.153e-03	.540e-04	.540e-04	.990e-04	.900e-03
865.00	2	O.	O.	O.	O.	O.	O.	O.	O.	.363e-10	.256e-07	.154e-06	.182e-06
870.00	1	.135e-03	.126e-03	.720e-04	.450e-04	.450e-04	.270e-04	.900e-04	.153e-03	.540e-04	.540e-04	.990e-04	.900e-03
870.00	2	O.	O.	O.	O.	O.	O.	O.	O.	.355e-10	.250e-07	.151e-06	.177e-06
875.00	1	.135e-03	.126e-03	.720e-04	.450e-04	.450e-04	.270e-04	.900e-04	.153e-03	.540e-04	.540e-04	.990e-04	.900e-03
875.00	2	O.	O.	O.	O.	O.	O.	O.	O.	.346e-10	.244e-07	.147e-06	.173e-06
880.00	1	.135e-03	.126e-03	.720e-04	.450e-04	.450e-04	.270e-04	.900e-04	.153e-03	.540e-04	.540e-04	.990e-04	.900e-03
880.00	2	O.	O.	O.	O.	O.	O.	O.	O.	.339e-10	.239e-07	.144e-06	.170e-06

885.00	1	.135e-03	.126e-03	.720e-04	.450e-04	.450e-04	.270e-04	.900e-04	.153e-03	.540e-04	.540e-04	.990e-04	.900e-03
885.00	2	0.	0.	0.	0.	0.	0.	0.	0.	.332e-10	.234e-07	.141e-06	.166e-06
890.00	1	.135e-03	.126e-03	.720e-04	.450e-04	.450e-04	.270e-04	.900e-04	.153e-03	.540e-04	.540e-04	.990e-04	.900e-03
890.00	2	0.	0.	0.	0.	0.	0.	0.	0.	.326e-10	.229e-07	.138e-06	.163e-06
895.00	1	.135e-03	.126e-03	.720e-04	.450e-04	.450e-04	.270e-04	.900e-04	.153e-03	.540e-04	.540e-04	.990e-04	.900e-03
895.00	2	0.	0.	0.	0.	0.	0.	0.	0.	.320e-10	.225e-07	.136e-06	.160e-06
900.00	1	.135e-03	.126e-03	.720e-04	.450e-04	.450e-04	.270e-04	.900e-04	.153e-03	.540e-04	.540e-04	.990e-04	.900e-03
900.00	2	0.	0.	0.	0.	0.	0.	0.	0.	.314e-10	.221e-07	.134e-06	.157e-06
905.00	1	.135e-03	.126e-03	.720e-04	.450e-04	.450e-04	.270e-04	.900e-04	.153e-03	.540e-04	.540e-04	.990e-04	.900e-03
905.00	2	0.	0.	0.	0.	0.	0.	0.	0.	.309e-10	.218e-07	.131e-06	.155e-06
910.00	1	.135e-03	.126e-03	.720e-04	.450e-04	.450e-04	.270e-04	.900e-04	.153e-03	.540e-04	.540e-04	.990e-04	.900e-03
910.00	2	0.	0.	0.	0.	0.	0.	0.	0.	.305e-10	.214e-07	.129e-06	.152e-06
915.00	1	.135e-03	.126e-03	.720e-04	.450e-04	.450e-04	.270e-04	.900e-04	.153e-03	.540e-04	.540e-04	.990e-04	.900e-03
915.00	2	0.	0.	0.	0.	0.	0.	0.	0.	.300e-10	.211e-07	.128e-06	.150e-06
920.00	1	.135e-03	.126e-03	.720e-04	.450e-04	.450e-04	.270e-04	.900e-04	.153e-03	.540e-04	.540e-04	.990e-04	.900e-03
920.00	2	0.	0.	0.	0.	0.	0.	0.	0.	.296e-10	.208e-07	.126e-06	.148e-06
925.00	1	.135e-03	.126e-03	.720e-04	.450e-04	.450e-04	.270e-04	.900e-04	.153e-03	.540e-04	.540e-04	.990e-04	.900e-03
925.00	2	0.	0.	0.	0.	0.	0.	0.	0.	.292e-10	.206e-07	.124e-06	.146e-06
930.00	1	.135e-03	.126e-03	.720e-04	.450e-04	.450e-04	.270e-04	.900e-04	.153e-03	.540e-04	.540e-04	.990e-04	.900e-03
930.00	2	0.	0.	0.	0.	0.	0.	0.	0.	.289e-10	.203e-07	.123e-06	.144e-06
935.00	1	.135e-03	.126e-03	.720e-04	.450e-04	.450e-04	.270e-04	.900e-04	.153e-03	.540e-04	.540e-04	.990e-04	.900e-03
935.00	2	0.	0.	0.	0.	0.	0.	0.	0.	.285e-10	.201e-07	.121e-06	.143e-06
940.00	1	.135e-03	.126e-03	.720e-04	.450e-04	.450e-04	.270e-04	.900e-04	.153e-03	.540e-04	.540e-04	.990e-04	.900e-03
940.00	2	0.	0.	0.	0.	0.	0.	0.	0.	.282e-10	.199e-07	.120e-06	.141e-06
945.00	1	.135e-03	.126e-03	.720e-04	.450e-04	.450e-04	.270e-04	.900e-04	.153e-03	.540e-04	.540e-04	.990e-04	.900e-03
945.00	2	0.	0.	0.	0.	0.	0.	0.	0.	.279e-10	.197e-07	.119e-06	.140e-06
950.00	1	.135e-03	.126e-03	.720e-04	.450e-04	.450e-04	.270e-04	.900e-04	.153e-03	.540e-04	.540e-04	.990e-04	.900e-03
950.00	2	0.	0.	0.	0.	0.	0.	0.	0.	.276e-10	.195e-07	.117e-06	.138e-06
955.00	1	.135e-03	.126e-03	.720e-04	.450e-04	.450e-04	.270e-04	.900e-04	.153e-03	.540e-04	.540e-04	.990e-04	.900e-03
955.00	2	0.	0.	0.	0.	0.	0.	0.	0.	.274e-10	.193e-07	.116e-06	.137e-06
960.00	1	.135e-03	.126e-03	.720e-04	.450e-04	.450e-04	.270e-04	.900e-04	.153e-03	.540e-04	.540e-04	.990e-04	.900e-03
960.00	2	0.	0.	0.	0.	0.	0.	0.	0.	.271e-10	.191e-07	.115e-06	.136e-06
965.00	1	.135e-03	.126e-03	.720e-04	.450e-04	.450e-04	.270e-04	.900e-04	.153e-03	.540e-04	.540e-04	.990e-04	.900e-03
965.00	2	0.	0.	0.	0.	0.	0.	0.	0.	.269e-10	.189e-07	.114e-06	.135e-06
970.00	1	.135e-03	.126e-03	.720e-04	.450e-04	.450e-04	.270e-04	.900e-04	.153e-03	.540e-04	.540e-04	.990e-04	.900e-03
970.00	2	0.	0.	0.	0.	0.	0.	0.	0.	.267e-10	.188e-07	.113e-06	.133e-06
975.00	1	.135e-03	.126e-03	.720e-04	.450e-04	.450e-04	.270e-04	.900e-04	.153e-03	.540e-04	.540e-04	.990e-04	.900e-03
975.00	2	0.	0.	0.	0.	0.	0.	0.	0.	.265e-10	.186e-07	.113e-06	.132e-06
980.00	1	.135e-03	.126e-03	.720e-04	.450e-04	.450e-04	.270e-04	.900e-04	.153e-03	.540e-04	.540e-04	.990e-04	.900e-03
980.00	2	0.	0.	0.	0.	0.	0.	0.	0.	.263e-10	.185e-07	.112e-06	.131e-06
985.00	1	.135e-03	.126e-03	.720e-04	.450e-04	.450e-04	.270e-04	.900e-04	.153e-03	.540e-04	.540e-04	.990e-04	.900e-03
985.00	2	0.	0.	0.	0.	0.	0.	0.	0.	.261e-10	.184e-07	.111e-06	.130e-06
990.00	1	.135e-03	.126e-03	.720e-04	.450e-04	.450e-04	.270e-04	.900e-04	.153e-03	.540e-04	.540e-04	.990e-04	.900e-03
990.00	2	0.	0.	0.	0.	0.	0.	0.	0.	.259e-10	.182e-07	.110e-06	.130e-06
995.00	1	.135e-03	.126e-03	.720e-04	.450e-04	.450e-04	.270e-04	.900e-04	.153e-03	.540e-04	.540e-04	.990e-04	.900e-03
995.00	2	0.	0.	0.	0.	0.	0.	0.	0.	.258e-10	.181e-07	.109e-06	.129e-06

REFERENCES

1. K. H. Duerre, R. W. Andrae, and W. S. Gregory, "TVENT, A Computer Program for Analysis of Tornado-Induced Transients in Ventilation Systems," Los Alamos Scientific Laboratory report LA-7397-M (July 1978).

2. W. S. Gregory, R. W. Andrae, J. W. Bolstad, R. A. Martin, and P. K. Tang, "TORAC User's Manual: A Computer Code for Analysis of Tornado-Induced Flow and Material Transport in Nuclear Facilities," Los Alamos National Laboratory report LA-10435-M, NUREG/CR-4260 (May 1985).

3. P. K. Tang, R. W. Andrae, J. W. Bolstad, R. A. Martin, W. S. Gregory, and B. D. Nichols, "EXPAC User's Manual: A Computer Code for Analysis of Explosion-Induced Flow and Material Transport in Nuclear Facilities," Los Alamos National Laboratory report in preparation.

4. M. K. Chan, M. Y. Ballinger, P. C. Owczarski, and S. L. Sutter, "User's Manual for FIRIN1: A Computer Code to Characterize Accidental Fire and Radioactive Source Terms in Nuclear Fuel Cycle Facilities," Battelle Pacific Northwest Laboratory report PNL-4532, NUREG/CR-3037 (December 1982).

5. R. W. Andrae, R. A. Martin, and W. S. Gregory, "Analysis of Nuclear Facilities for Tornado-Induced Flow and Reentrainment," Los Alamos Scientific Laboratory report LA-7571-MS, NUREG/CR-0521 (January 1979).

6. P. K. Tang, "A New Numerical Method for the Transient Gas Dynamic Code EVENT," Los Alamos National Laboratory report LA-9594-MS (December 1982).

7. A. I. Brown and S. M. Marco, Introduction to Heat Transfer (McGraw-Hill Book Company, Inc., New York, 1958), p. 126.

8. W. M. Kays and H. C. Perkins, "Forced Convection, Internal Flow in Ducts," in Handbook of Heat Transfer, W. M. Rohsenow and J. P. Hartnett, Eds. (McGraw-Hill Book Company, Inc., New York, 1973), Chap. 7.

9. M. Jakob, Heat Transfer (John Wiley and Sons, Inc., New York, 1959), Vol. 1, p. 547.

10. H. C. Hottel, "Radiant-Heat Transmission," in Heat Transmission, E. H. McAdams, Ed. (McGraw-Hill Book Co., Inc., New York, 1954), Chap. 4, p. 82.

11. R. Siegel and J. R. Howell, Thermal Radiation Heat Transfer (McGraw-Hill Book Company, Inc., New York, 1972), p. 570.

12. S. V. Patankar, Numerical Heat Transfer and Fluid Flow (McGraw-Hill Book Company, Inc., New York, 1980), Chap. 4.

13. W. H. McAdams, Heat Transmission (McGraw-Hill Book Co., Inc., New York, 1954) p. 176.

14. R. B. Bird, W. E. Stewart, and E. N. Lightfoot, Transport Phenomena (John Wiley and Sons, Inc., New York, 1960), pp. 445-448.

15. J. D. Stockham and E. G. Fochtman, Eds., Particle Size Analysis (Ann Arbor Science, Ann Arbor, Michigan, 1978).

16. T. T. Mercer, Aerosol Filtration in Hazard Evaluation (Academic Press, New York, 1973).

17. "Accident Analysis Handbook," Los Alamos National Laboratory report LA-9180-M in preparation.

18. J. Mishima and L. C. Schwendiman, "Some Experimental Measurements of Airborne Uranium (Representing Plutonium) in Transportation Accidents," Battelle Pacific Northwest Laboratory report BNWL-1732 (1973).

19. S. L. Sutter, "Accident Generated Particulate Materials and their Characteristics—A Review of Background Information," Battelle Pacific Northwest Laboratory report PNL-4154 (1981).

20. J. W. Healy, "Surface Contamination: Decision Levels," Los Alamos Scientific Laboratory report LA-4558-MS (September 1971).

21. J. M. Singer, E. E. Cook, and J. Grumer, "Dispersal of Coal and Rock-Dust Deposits," US Bureau of Mines report BM-RI-7642 (1972).

22. J. M. Singer, M. E. Harris, J. Grumer, "Dust Dispersal by Explosion-Induced Airflow, Entrainment by Air Blast," US Bureau of Mines report BM-RI-8130 (1976).

23. G. A. Sehmel and F. D. LLoyd, "Particle Resuspension Rates" in Atmosphere-Surface Exchange of Particulate and Gaseous Pollutants (1974), R. J. Englemann and G. A. Sehmel, Coordinators, Energy Research and Development Administration Symposium Series report CONF-740921 (1974), pp. 846-858.

24. J. R. Travis, "A Model for Predicting the Redistribution of Particulate Contaminants from Soil Surfaces," Los Alamos Scientific Laboratory report LA-6035-MS (August 1975).

25. J. D. Iversen, J. B. Pollack, R. Greeley, and B. R. White, "Saltation Threshold on Mars: The Effect of Interparticle Force, Surface Roughness, and Low Atmospheric Density," ICARUS 29, 381-393 (1976).

26. S. H. Friedlander, Smoke Dust and Haze (John Wiley and Sons, New York, 1977).

27. J. D. Iversen, R. Greeley, and J. B. Pollack, "Windblown Dust on Earth, Mars, and Venus," J. Atm. Sci. 33(12), 2425-2429 (1976).

28. J. D. Iversen, R. Greeley, B. R. White, and J. B. Pollack, "The Effect of Vertical Distortion in the Modeling of Sedimentation Phenomena: Martian Crater Wake Streaks," J. Geophys. Res. 81(26), 4846-4856 (1976).

29. S. L. Soo, Fluid Dynamics of Multiphase Systems (Blaisdell Publishing Company, Waltham, Massachusetts, 1967).

30. G. B. Wallis, One-Dimensional Two-Phase Flow (McGraw-Hill Book Company, Inc., New York, 1969).

31. F. A. Williams, Combustion Theory (Addison-Wesley Publishing Company, Inc., Reading, Massachusetts, 1965).

32. C. N. Davies, Ed., Aerosol Science (Academic Press, New York, 1966).

33. W. S. Gregory, H. L. Horak, P. R. Smith, C. I. Ricketts, and W. Gill, "Investigation of HEPA Filters Subjected to Tornado Pressure Pulses," Los Alamos Scientific Laboratory report LA-7202-MS (April 1978).

34. H. D'Arcy, Les Fontaines Publiques de la Ville de Dijon (Victor Dalmont, Paris, 1856).

35. H. Schlichting, Boundary Layer Theory, 4th Ed. (McGraw-Hill Book Company, Inc., New York, 1960).

36. J. Kozeny, "Uber Kapillare Leitung des Wassers in Boden," Akad. Wiss. Wien, Math.-Naturw. Klasses, Sitzber (Abt. IIa) 136, 271-306 (1927).

37. P. C. Carman, "Flow Through Granular Beds," Transactions of the Institution of Chemical Engineers 15, 150-166 (1937).

38. A. E. Sheidegger, The Physics of Flow Through Porous Media, 3rd Ed. (University of Toronto Press, Toronto, 1972), pp. 146-148.

39. S. P. Burke and W. B. Plummer, "Gas Flow Through Packed Columns," Industrial and Engineering Chemistry 20, 1196-1200 (1928).

40. S. Ergun, "Fluid Flow through Packed Columns," Chemical Engineering Progress 48, 89-94 (1952).

41. O. Reynolds, Papers on Mechanical and Physical Subjects (Cambridge University Press, Cambridge, Massachusetts, 1900).

42. J. Pich, "Theory of Aerosal Filtration," in Aerosol Science, C. N. Davies, Ed., (Academic Press, New York, 1966), pp. 223-285.

43. W. Bergman, H. Hebard, R. Taylor, and B. Lum, "Electrostatic Filters Generated by Electric Fields," Lawrence Livermore National Laboratory report UCRL-81926 (1979).

44. Fan Engineering, Robert Jorgensen, Ed. (Buffalo Forge Co., Buffalo, New York, 1970) Chap. 8.

45. "Flow of Fluids," Crane Co. Technical Paper No. 410 (1977).

DISTRIBUTION

	Copies
Nuclear Regulatory Commission,	
Technical Information Center, Oak Ridge, Tennessee	2
Los Alamos National Laboratory, Los Alamos, New Mexico	50

M 335

U S NUCLEAR REGULATORY COMMISSION

BIBLIOGRAPHIC DATA SHEET

1 REPORT NUMBER (Assigned by TIDC, add Vol No, if any)

NUREG/CR-4561
LA-10678-M

2 Leave blank

AND SUBTITLE

AC User's Manual: A Computer Code to Simulate
e Accidents in Nuclear Facilities

4 RECIPIENT'S ACCESSION NUMBER

5 DATE REPORT COMPLETED

MONTH	YEAR
February	1986

OR(S)

D. Nichols and W. S. Gregory

7 DATE REPORT ISSUED

MONTH	YEAR
April	1986

9 PROJECT/TASK/WORK UNIT NUMBER

ORMING ORGANIZATION NAME AND MAILING ADDRESS (Include Zip Code)

Los Alamos National Laboratory
Los Alamos, NM 87545

10 FIN NUMBER

A7152

NSORING ORGANIZATION NAME AND MAILING ADDRESS (Include Zip Code)

vision of Fuel Cycle and Material Safety
fice of Nuclear Material Safety and Safeguards
S. Nuclear Regulatory Commission
shington, DC 20555

12a TYPE OF REPORT

Manual

12b PERIOD COVERED (Inclusive dates)

PPLEMENTARY NOTES

STRACT (200 words or less)

This user's manual supports the fire accident analysis computer code FIRAC. FIRAC is signed to estimate radioactive and nonradioactive source terms and to predict fire-duced flows and thermal and material transport within the ventilation systems of nuclear el cycle facilities. FIRAC has been expanded and modified to include the capabilities the zone-type compartment fire model computer code FIRIN developed by Battelle Pacific rthwest Laboratories. The two codes have been coupled to provide an improved simulation a fire-induced transient within a facility. The basic material transport capability FIRAC has been retained and includes estimates of entrainment, convection, deposition, d filtration of material. Also, the interrelated effects of filter plugging, heat ansfer, gas dynamics, material transport, and fire and radioactive source terms are mulated.

This report summarizes the physical models that describe the gas dynamic, material ansport, heat transfer, and source term processes and illustrates how a typical cility is modeled using the code. The modifications required to couple the code to RIN also are presented. Finally, the input and code-calculated output for several mple problems that illustrate some of the capabilities of the code are described.

EY WORDS AND DOCUMENT ANALYSIS

IRAC computer code
IRIN computer code
ire accident
ource term

15b DESCRIPTORS

VAILABILITY STATEMENT

Unlimited

17 SECURITY CLASSIFICATION (This report)

Unclassified

18 NUMBER OF PAGES

19 SECURITY CLASSIFICATION (This page)

Unclassified

20 PRICE

$

UNITED STATES
NUCLEAR REGULATORY COMMISSION
WASHINGTON, D.C. 20555

OFFICIAL BUSINESS
PENALTY FOR PRIVATE USE, $300

SPECIAL FOURTH